Copper-mediated living radical polymerisation of acrylates and acrylamides; Utilising light as an external stimuli

Vasiliki Nikolaou

A thesis submitted in partial fulfilment of the requirements of the degree of Doctor of Philosophy in Chemistry

Department of Chemistry

University of Warwick

October 2015

Table of contents

List of figures

List of tables

List of schemes

Abbreviations

AIBN	Azobisisobutyronitrile
AMPS	2-Acrylamido-2-methylpropane sulfonic acid
AN	Acrylonitrile
ARGET	Activators regenerated by electron transfer
ATRP	Atom transfer radical polymerisation
***n*-BA**	*n*-Butyl acrylate
$(BiBOE)_2S_2$	Ethylene bis(2-bromoisobutyrate)
$CDCl_3$	Deuterated chloroform
CLRP	Controlled living radical polymerisation
CRP	Controlled radical polymerisation
CTA	Chain transfer agent
DCTB	trans-2-[3-(4-tert-Butylphenyl)-2-methyl-2-propenylidene]malononitrile
DEGEEA	Di(ethylene glycol) ethyl ether acrylate
DMF	Dimethyl formamide
DMSO	Dimethyl sulfoxide
DNA	Deoxyribonucleic acid
DP	Degree of polymerisation
DRI	Differential refractive index
EA	Ethyl acrylate
EBiB	Ethyl-2-bromoisobutyrate
EbBiB	Ethylene bis(2-bromoisobutyrate)
EGA	Ethylene glycol methyl ether acrylate
ESI-MS	Electrospray ionisation mass spectroscopy
FRP	Free radical polymerisation
SI-ATRP	Surface initiated atom transfer radical polymerisation
HEA	Hydroxyethyl acrylate
HEAm	Hydroxyethyl acrylamide
HPA	Hydroxypropyl acrylate
I	Initiator
ICAR ATRP	Initiators for continuous activator regeneration atom transfer

	radical polymerisation
IPA	Isopropyl alcohol
ISET	Inner sphere electron transfer
k_i	Rate constant of initiation
k_p	Rate constant of propagation
k_t	Rate constant of termination
LA	Lauryl acrylate
LAM	Less activated monomers
LCST	Low critical solution temperature
LRP	Living radical polymerisation
$[M]_0$	Concentration of monomer at t = 0
$[M]_t$	Concentration of monomer at t = t
MA	Methyl acrylate
MALDI	Matrix assisted laser desorption ionisation
MAM	More activated monomers
MEK	Methyl ethyl ketone
Me_6TREN	*N,N,N',N'',N''*-Hexamethyl-[tris(aminoethyl)amine]
MeCN	Acetonitrile
MeOH	Methanol
MS	Mass spectroscopy
MMA	Methyl methacrylate
MW	Molecular weight
MWD	Molecular weight distribution
NaBr	Sodium bromide
NMR	Nuclear magnetic resonance
NMP	Nitroxide mediated polymerisation
ODA	Octadecyl acrylate
OSET	Outer sphere electron transfer
PEG	Poly(ethylene glycol)
$PEGA_{480}$	Poly(ethylene glycol) methyl ether acrylate
PE	Polyethylene
PHC	Principle of halogen conservation
PMDETA	*N,N,N',N'',N''*-pentamethyldiethylenetriamine

PMMA	Poly(methyl methacrylate)
PMR	Principle of microscopic reversibility
PFOA	1,1,2,2-Perfluorooctyl acrylate
PRE	Persistent radical effect
PTFE	Poly(tetrafluoroethylene)
PS	Poly(styrene)
PVC	Poly(vinyl chloride)
RAFT	Reversible addition fragmentation chain transfer
RDRP	Reversible deactivation radical polymerisation
SA	Solketal acrylate
SARA ATRP	Supplemental activator and reducing agent atom transfer radical polymerisation
SEC	Size exclusion chromatography
SET-LRP	Single electron transfer living radical polymerisation
SFRP	Stable free radical polymerisation
***t*-BA**	*tert*-Butyl acrylate
TEA	Triethylamine
TEMPO	(2,2,6,6-Tetramethyl-piperidin-1-yl)oxyl
TFE	2,2,2-Trifluoroethanol
TFEA	2,2,2-Trifluoroethyl acrylate
TMM- LRP	Transition metal mediated living radical polymerisation
ToF	Time of flight
Tol	Toluene
Tren	Tris(2-aminoethyl)amine
UV	Ultraviolet
VAc	Vinyl acetate
VP	Vinyl pyrrolidone
VS	Viscometry
WSI	Water soluble initiator

Acknowledgements

I would like to thank Professor Haddleton for giving me the opportunity to pursue my PhD studies under his supervision. Among all the professors I have ever worked with, he is the only one that cares more about his students than their research. He actually asked me once if I feel happy here! I cannot thank him enough for all the opportunities he gave me during these 3 years including the freedom to carry out various projects, participate in many conferences where I was able to meet many famous academics and advertise my chemistry. I would also like to thank my industrial supervisors (Dr. Aydin Aykanat, Dr. Roger Day, Dr. Margaret Pafford) for being so patient with me (CPVC cannot be grafted from but I can make beautiful fluorinated polymers!). Having also worked with Prof. Percec for a couple of months, I learned what discipline looks like (Athina resembles a lamb after him!). I gained a lot through his experience and guidance. Special thanks go to Shampa Samanta for being so supportive and spending her "free" time to show me all the beauties of Philadelphia.

During my first year I was lucky enough to meet and collaborate with Athina. She was and still is the person that I will go with any kind of question that I have (even if it is not chemistry related!) and she will ALWAYS come up with an answer. I cannot thank her enough for all the help and the support throughout these years and especially for teaching me not to quit even when everything goes very wrong. I will miss our discussions on everything from chemistry to SET (Dave still wonders what this means!) at 6 am waking up everyone in the first bus. Good team never changes. (Apart from the national Greek team that NEEDS a change after Euro 2004!)

I would also like to thank Alex for the endless pizza we have consumed around midnight (calories don't count after 10 pm!), for being a brilliant co-cleaner

and help me mop the floor (from 5 inches of water, thanks Sam!) and for sharing our worse fears (will I ever get a PhD? Does she/he love me?). I also want to apologise that he has seen me crying so many times and thank him for being so patient with me and always giving me a reason to carry on (usually it contained chocolate!).

Working in the Haddleton group has been a great experience and I would like to thank all members, past and present. But there are always some people that won my heart. That includes 1) Fehaid (Alex you have an amazing tongue, Chris are you ill?, Athina your face looks ok today) but also for our endless discussions about various topics (He knows what I mean!) 2) Gabit for being a faithful robot and always helping me when Word was encouraging me to commit suicide! 3) George for always eating my biscuits (with or without permission) and for always stealing my fluorinated polymers for his batteries! 4) Nick (typically referred to as amoeba) for his kind coffee donations, his constant support (Athina she is crying, do something!) and our meaningful discussions. 5) Richard for being continuously happy and for making me happy as well (proposed purification method: sonication!) 6) Glen for being a perfect English teacher when helping Athina to proof read my thesis and for secretly love social discussions! 7) Paul for offering me precious NMR insight!

I would also like to thank my family (parents/sisters/Lucy/relatives) for always being there for me although they were having a rough time with their own problems. Last but not least, I am afraid the word thank you is not enough to express my love and gratitude for my partner and best friend Chris for always finding the way to calm me down (Wii, LOL, SET, gossip). I will now have more time to spend with him, I promise!!! (I also promise to start cooking again for us, no more cans!).

Declaration

Experimental work contained in this thesis is original research carried out by the author, unless otherwise stated, in the Department of Chemistry at the University of Warwick, October 2012 and October 2015. No material contained herein has been submitted for any other degree, or at any other institution.

Results from other authors are referenced in the usual manner throughout the text.

Date:

_____

Vasiliki Nikolaou

Abstract

The main focus of this thesis is to expand the scope of the newly developed copper-mediated photo-induced reversible deactivation radical polymerisation (RDRP) system. The synthesis of *α,ω*-telechelic multiblock copolymers will be attempted utilising a wide range of bi-functional initiators and acrylic monomers targeting different chain lengths. The compatibility of this system with special solvents and catalysts will also be investigated. Moreover, the limitations of this technique will be highlighted including the necessity to employ various components that require multiple optimisation studies and the challenge in efficiently storing many reactants (*e.g.* ligands, copper catalyst). Two novel discrete complexes that incorporate both precatalyst and ligand will be synthesised to address the aforementioned issues while advanced characteristics and advantages over the previous approach will be demonstrated.

In the second part the polymerisation of acrylamides will be demonstrated utilising aqueous Cu(0)-mediated RDRP since the light system is not applicable for the controlled polymerisation of this monomeric family. The high end-group fidelity of the resulted polyacrylamides will also be exemplified *via* sequential monomer addition with both acrylamide and acrylate monomers, yielding well-defined hydrophilic materials.

In the last chapter the synthesis of semifluorinated triblock copolymers in a multigram scale utilising the photo-induced RDRP will be demonstrated. This is an ongoing work with the Lubrizol Corporation and constitutes only a few initial studies towards developing materials with interesting properties or applications and basically sets the scene for future work.

Introduction

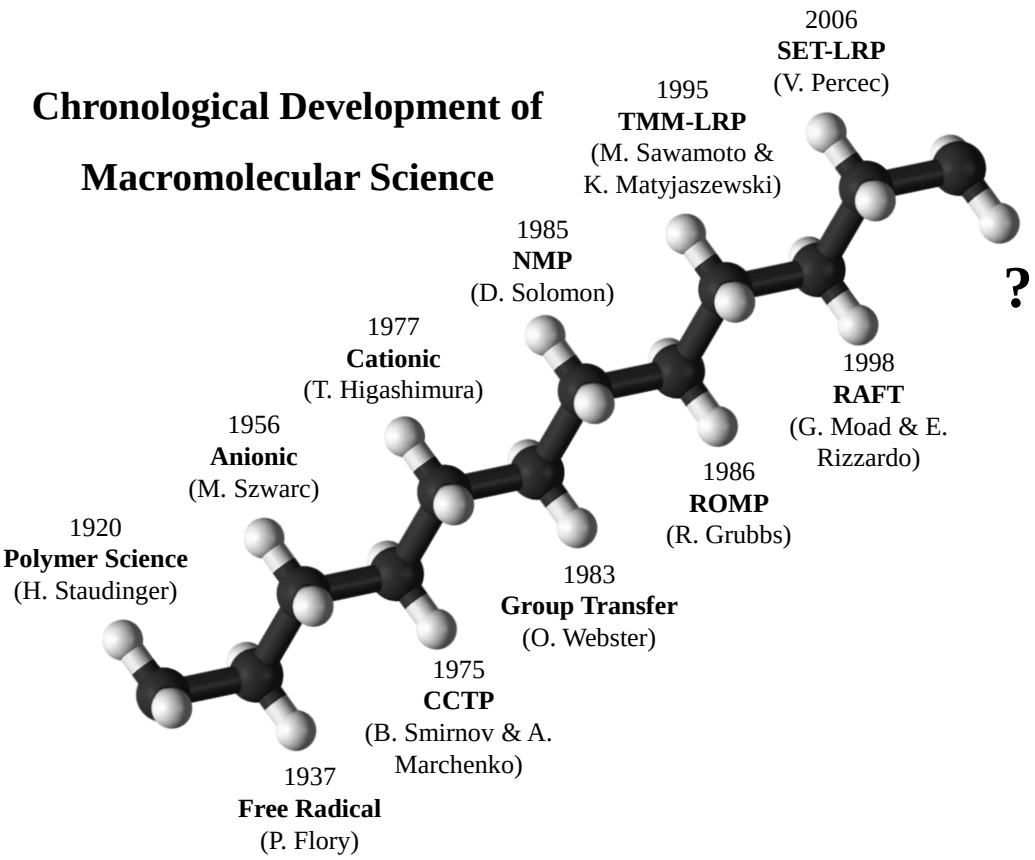

1.1. The concept of the "macromolecule"

The word "polymer" derives from the Greek ("poly" meaning many and "meros" meaning part) and denotes a molecule produced by the repetition of a simpler unit which is termed as "monomer". However, historically the concept of polymers was originally applied to molecules that had identical empirical formula but different chemical and physical properties (*e.g.* benzene (C_6H_6) was considered to be the polymer of acetylene (C_2H_2) since they both had the same empirical formula (CH)). Therefore the term "polymer" can be found in old organic textbooks but not with the current meaning. It was not until 1920s that Hermann Staudinger coined the concept of the "macromolecule", another Greek word that literally means "large molecule". In his classic paper entitled "Über polymerisation",[1] he describes that during some reactions, which he called "polymerisations", individual repeating units are joined together by covalent bonds forming high molecular weight molecules. This concept, even though it was not initially well received from the scientific community, heralded a decade of intense research and set the foundations of the modern polymer science. For his contribution in the field, Staudinger was awarded the Nobel Prize for chemistry in 1953.

1.2. History of common polymers

Polymers, natural or synthetic, have numerous applications and can be found in hundreds of different products. Indeed most of the materials used in the everyday life, including plastics, fibers, paints, coatings, adhesives *etc.* are based on polymers (Figure 1.1). Mayans are assumed to be one of the first to find an application for polymers in 1500 BC. They produced rubber balls by coagulating the latex obtained from puncturing the bark of local rubber trees. Thousands of years later, in 1839 Charles Goodyear discovered vulcanisation by mixing natural rubber with sulphur at high temperatures. The product was a stable material that could be used from raincoats and boots to tires for the carriages. Nevertheless, this procedure was used extensively in automobile industry and even today 70% of all types of rubbers are used in tires or in other automotive applications.

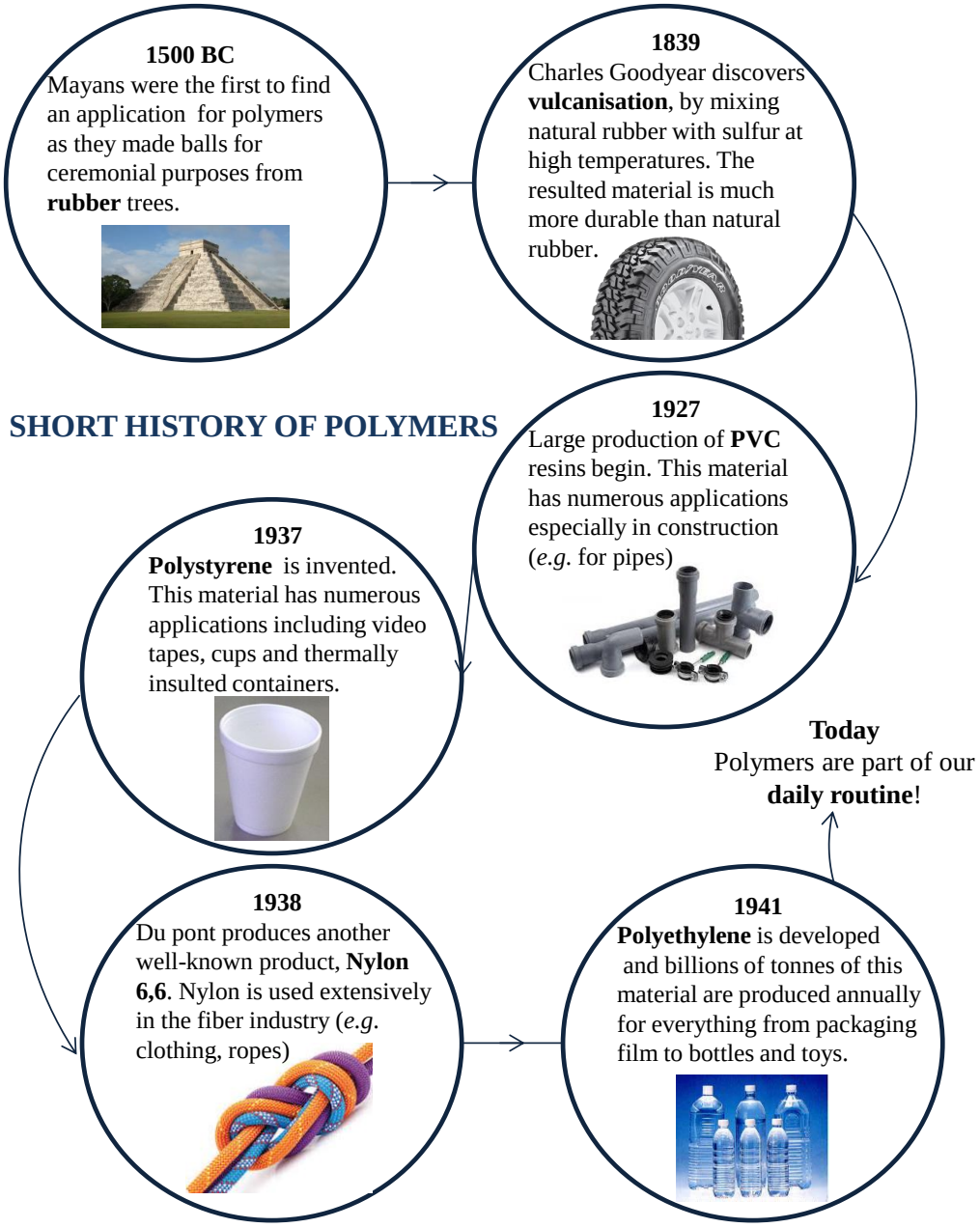

Figure 1.1: Short history of the development of some common polymeric materials.

In 1927 polyvinyl chloride (PVC) resin was produced in large scales and, even today, is the third most important polymer with the other two being polyethylene (PE) and polypropylene (PP). PVC comes in two different forms: rigid and flexible. The rigid form is mainly used in construction for pipes, window panels and synthetic floor tiles, but it is also used for credit cards, vinyl records and

banners. The addition of plasticisers produces the flexible form that has applications in plumbing, electrical cable insulation, imitation leather and so on. PE was discovered in 1941 and it is considered to be the most common plastic with an estimated annual global production around 80 million tonnes. Its primary use includes packaging, bottles and plastic bags. Polystyrene (PS) is another extensively used material that can be found in many different forms. Plastic cutlery, DVD cases, the outside housing of computers, model cars, cups, toys, rulers, and hair combs are all made from PS.

The discovery of Nylon 6,6 from the Du Pont company, USA in 1938 was also a significant breakthrough for the fiber world. Different types of nylon were synthesised since then and the majority of them are generally very tough materials with good thermal and chemical resistance. The different types give a wide range of properties with specific gravity, melting point and moisture content tending to reduce as the nylon number increases. Nylon fibres are used in textiles, fishing line and carpets. They can also be used as films for food packaging, offering toughness and low gas permeability, and coupled with its temperature resistance, for boil-in-the-bag food packaging.

Regardless the application and the type of polymer, different polymerisation protocols can be employed as efficient tools, many of which are presented in the following sections.

1.3. Free radical polymerisation (FRP)

Perhaps the most widely used polymerisation protocol is the (conventional) free radical polymerisation (FRP) which was introduced by Flory in 1937.[2] This technique proceeds under relatively undemanding conditions since it exhibits a tolerance of trace impurities. As a result high molecular weight polymers can be synthesised without removal of the stabilisers present in most commercial monomers, in the presence of trace amounts of oxygen or in solvents that have not been purified. Its apparent simplicity has led to this technique being dominant in the industrial field. Even today, the bulk production of commercial polymers usually involves FRP as the main synthetic route. FRP typically consists of three events: initiation (which involves two main reactions), propagation and termination.

1.3.1 Sequence of events

The first step during the initiation phase is the production of the free radicals (R·) from the initiating species (I) as shown in Eq. 1.1, where k_d is the rate constant for the initiator dissociation. Since there are several types of initiators, the dissociation can be achieved in many different ways but the usual case is either heat or light (photo-initiation). Once produced, the free radical reacts rapidly with a monomer (M) to yield a new species that is still free radical (M·) as shown in Eq. 1.2, where k_i is the rate constant for the initiation step.

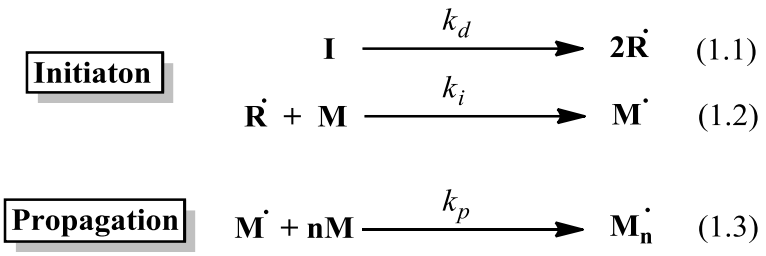

The series of reactions in which the free radical at the end of the growing chain reacts with monomer to further increase the length is termed as propagation. Generally it can it be described as shown in Eq. 1.3, where k_p is the rate constant of propagation. Propagation with growth of the chain to high polymer proportions takes place very rapidly and the value of k_p normally lies in the range 10^2-10^4 L mol^{-1} s^{-1}.[3]

Polymerisation does not continue until all the monomer is consumed mainly due to the reactive nature of the radicals that can lead to the loss of their radical activity. The two mechanisms of termination during FRP are combination and disproportionation. Combination occurs when two radical species react with each other as indicated in Eq. 1.4. Alternatively, two radicals can interact *via* hydrogen abstraction, leading to the formation of two new radicals; one saturated and one unsaturated (Eq. 1.5). However, it is relatively unnecessary to distinguish between these two mechanisms and therefore the rate constants (k_{tc} and k_{td}) are generally combined into a single rate constant k_t and the termination step can be also expressed by Eq. 1.6.[4] The term "dead polymer" describes the cessation of the growth for the propagating radical. Typically the termination rate constants are in the range of 10^6-10^8 L mol^{-1} s^{-1}.[3]

Termination

Combination $\mathbf{M_n^{\cdot}} + \mathbf{M_m^{\cdot}} \xrightarrow{k_{tc}} \mathbf{M_{n+m}}$ (1.4)

Disproportionation $\mathbf{M_n^{\cdot}} + \mathbf{M_m^{\cdot}} \xrightarrow{k_{td}} \mathbf{M_n} + \mathbf{M_m}$ (1.5)

General Expression $\mathbf{M_n^{\cdot}} + \mathbf{M_m^{\cdot}} \xrightarrow{k_t}$ **dead polymer** (1.6)

1.3.2 Kinetic expression of FRP

Generally very small radicals are more reactive than propagating radicals, however, the effect of the size can be neglected because it does not apply at the dimer or trimer size.[5] Having this in mind, it is safe to assume that k_p and k_t are independent of the size of the radical.

During the initiation and propagation steps the monomer is being consumed, so the rate of the monomer disappearance is given by Eq. 1.7, where R_i and R_p are the rates of the initiation and propagation respectively. However, since more monomer species react during the propagation step than the initiation, we can simplify the equation by neglecting the R_i (Eq.1.8).

$$-\frac{\boldsymbol{d}[\mathbf{M}]}{\boldsymbol{dt}} = \boldsymbol{R_i} + \boldsymbol{R_p} \quad (1.7)$$

$$-\frac{\boldsymbol{d}[\mathbf{M}]}{\boldsymbol{dt}} = \boldsymbol{R_p} \quad (1.8)$$

The rate of propagation is the state that involves the major consumption of the monomer and is considered to be the sum of all the individual propagation steps. The rate of propagation is given by Eq. 1.9, where [M] and [M·] are the monomer and the total radical concentration respectively.

$$\boldsymbol{R_p = k_p\,[M\cdot][M]} \quad (1.9)$$

Radical concentration is difficult to measure as it remains very low during the polymerisation (~10^{-8} M) thus the term of the radical concentration [M·] needs to be eliminated from the Eq. 1.9. Consequently the steady state assumption can be applied.[6] According to this theory, the concentration of the radicals increases initially but reaches a constant value almost instantaneously. As a result, the rate of change of the radical concentration becomes and remains zero throughout the polymerisation. This is equivalent to stating that the rates of initiation and termination are equal (Eq. 1.10). It is should be noted that the rate of termination can also be expressed by Eq. 1.10 and it applies for both termination mechanisms (combination and disproportionation). The use of factor 2 in the termination rate follows the generally accepted convention for reactions destroying radicals in pairs.

$$\boldsymbol{R_i = R_t = 2k_t[M\cdot]^2} \quad (1.10)$$

If we combine Eq. 1.9 and Eq. 1.10 and solve for [M·] we have Eq. 1.11 as following:

$$[M\cdot] = \left(\frac{R_i}{2k_t}\right)^{\frac{1}{2}} \quad (1.11)$$

Finally if we substitute Eq. 1.9 into Eq.1.11, then rate of polymerisation is given by the Eq. 1.12 which signifies the dependence of the rate of polymerisation from the square root of the initiation rate.

$$\boldsymbol{R_p = k_p\,[M]\left(\frac{R_i}{2k_t}\right)^{\frac{1}{2}}} \quad (1.12)$$

The rate of producing radicals by thermal homolysis of an initiator is given by the Eq. 1.13, where [I] is the concentration of the initiator and *f* is the initiator efficiency. As mentioned earlier in Eq. 1.1 & 1.2 the initiation reaction consists of two main steps with the second step to be much faster than the first. As a result, the rate determining step is the homolysis of the initiator and thus $R_d = R_i$ (Eq. 1.14).

$$\boldsymbol{R_d = 2fk_d\,[I]} \quad (1.13)$$

$$\boldsymbol{R_i = R_d = 2fk_d[I]} \quad (1.14)$$

If we substitute Eq. 1.14 into Eq. 1.12 yields Eq.1.15:

$$\boldsymbol{R_p = k_p\left(\frac{fk_d[I]}{k_t}\right)^{\frac{1}{2}}\,[M]} \quad (1.15)$$

The above equation shows that in the early stages of the polymerisation the rate of the reaction is proportional to the square root of the initiator concentration, assuming *f* is independent of monomer concentration (this assumption is acceptable for high initiator efficiencies). This dependence has been confirmed for many different monomer-initiator combinations.[7-9]

1.4. Living anionic polymerisation

Anionic polymerisation was first reported by Szwarc[10-12] and co-workers in 1956 who demonstrated the controlled polymerisation of styrene initiated by aromatic radical-anions such as sodium naphthalene.[10] The initiation step in an anionic polymerisation is fast compared to propagation and therefore each initiator should start only one polymer chain. As a result all chains initiate at time zero and grow equally fast giving access to well-defined materials. The high reactivity of the propagating species (carbanions) with oxygen and moisture or any other protic or carbanion-sensitive impurities indicates that they have to be rigorously removed. Under these conditions, termination is virtually absent and, for this reason, anionic polymerisation is also considered a living polymerisation.[13] A typical example is the polymerisation of styrene with butyl lithium as initiator (Scheme 1.1).

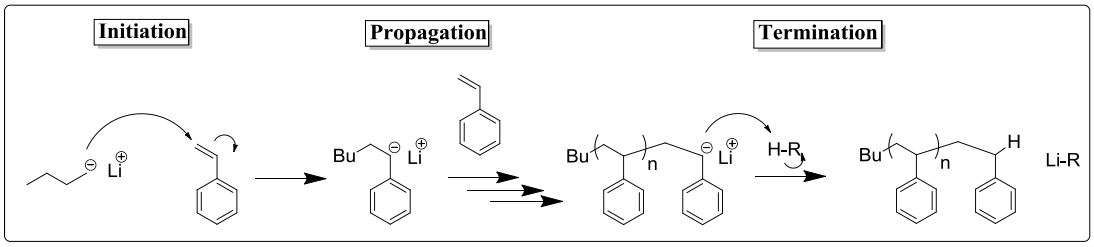

Scheme 1.1: Anionic polymerisation of styrene with butyl lithium as initiator.

This technique has been widely exploited mainly for the synthesis of well-defined polystyrene. Additionally, most of the elastomeric block copolymers are produced commercially by anionic living polymerisation. However, the extensive purification of the reagents (*e.g.* initiator, monomer), solvents, in addition to the low temperatures commonly employed (-78°C) make the technique less attractive.

1.5. "Living" radical polymerisation (LRP)

As mentioned in the previous section, Szwarc was the first to develop a truly living polymerisation system. However, the process is limited in a narrow pool of monomers (*e.g.* styrene, isoprene). On the other hand conventional FRP is employed to produce millions tonnes of polymers, with thousands of different compositions. Yet, the architectural control utilising this technique is very limited. Therefore the advent of living radical polymerisation (LRP) or according to IUPAC reversible deactivation radical polymerisation (RDRP)[14] paved the way for the synthesis of advanced materials with precisely controlled molecular architecture. Although RDRP is theoretically restricted due to the reactive nature of the radicals, the concept of the dynamic equilibrium revolutionised the field giving access to well-defined polymers with various functionalities and architectures.[15] The dynamic equilibria in RDRP can be accomplished either by employing reversible deactivation of the propagating radical to form the dormant species or by employing "degenerate transfer" between the propagating radicals and the dormant species (*e.g.* reversible addition-fragmentation chain transfer polymerisation (RAFT)).[16] In the first scenario the dormant species can be intermittently reactivated either in a catalytic manner, as in the case of transition metal mediated living radical polymerisation (TMM-LRP), or spontaneously as in stable free-radical polymerisation (SFRP). In most polymerisations bimolecular termination will still occur and one can argue the "livingness" of the system. To avoid confusion, Quirk and Lee proposed a list of criteria for a living polymerisation[17]: (1) Polymerisation proceeds until all of the monomer has been consumed. (2) The number average MW (M_n), is a linear function of conversion. (3) The number of the active centers isa constant, which is sensibly

independent of conversion. (4) The MW can be controlled by the stoichiometry of the reaction. (5) Narrow MWDs are produced. (6) Block copolymers can be prepared by sequential monomer addition and (7) Chain-end functionalised polymers can be prepared in quantitative yield.

1.5.1. Nitroxide-mediated polymerisation (NMP)

SFRP was one of the earliest living radical technique to be discovered and can utilise a wide range of stable free radicals, including nitroxide,[18] (arylazo)oxy,[19] substituted triphenyls,[20] triazolinyl,[21] verzadyl,[22] *etc.* as the mediating species (or persistent radical) in the polymerisation. Nitroxides and their associated alkylated derivates (alkoxyamines) are certainly the most widely studied class of stable radicals. The exploitation of alkoxyamines as polymerisation initiators, and the use of NMP as a RDRP technique was first reported by Solomon, Rizzardo and Cacioli in 1985.[23] In this initial approach, Solomon and co-workers utilised 2,2,6,6-tetramethylpiperidinyl-1-oxy (TEMPO), a stable, persistent free radical capable of radical trapping. However the method received significant attention when Georges *et al.* demonstrated the controlled polymerisation of styrene in 1993.[24]

The proposed mechanism for the NMP polymerisation is described in Scheme 1.2. The reactive radical initiates the polymerisation while the stable radical mediates the reaction by reacting with propagating radical. Thus the propagating radical concentration is much lower than the dormant species which results in RDRP with control of the molecular weight and dispersity.

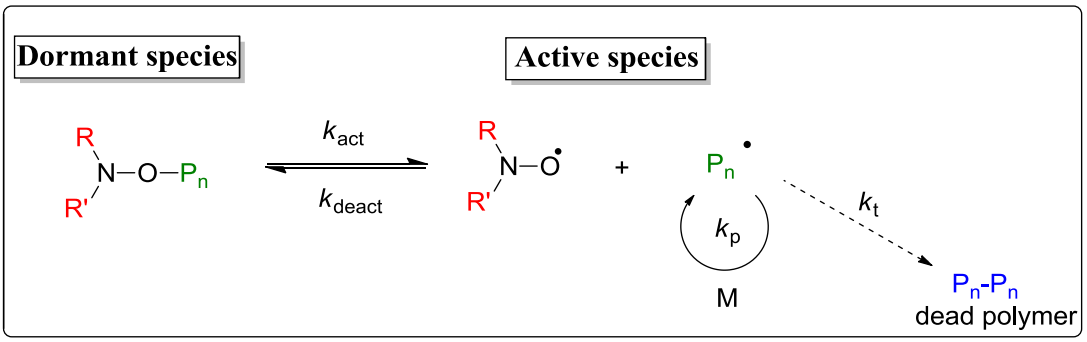

Scheme 1.2: Proposed mechanism of NMP.[23]

A drawback of the NMP with TEMPO is the high temperatures (125 - 140 ^{o}C) required along with the long reaction times (1 - 3 days). Moreover, relatively narrow MWDs can be achieved only for a narrow pool of monomers (*e.g.* styrene and its derivatives or 4-vinylpyridine).[3]

1.5.2. Reversible addition-fragmentation chain transfer polymerisation (RAFT)

RAFT was first reported by Moad, Rizzardo and Thang at the Commonwealth Scientific and Industrial Research Organisation (CSIRO) of Australia in 1998.[25] Although the term "RAFT" is sometimes used in a more general sense, it was coined to describe and it is most associated with reactions that utilise thiocarbonylthio compounds (RSC(Z)=S) as chain transfer agents (CTAs). The RAFT process normally involves a conventional radical initiator (*e.g.* AIBN), monomer, CTA (also referred to as RAFT agent) and it can be carried out in bulk, solution, emulsion or suspension. The appropriate choice of reagents and reaction conditions is crucial for the success of the polymerisation. A wide variety of monomers is compatible with this technique including more activated monomers (MAM) such as (meth)acrylic monomers and styrene or less activated monomers

(LAM) such as vinyl acetate (VAc), *N*-vinyl pyrrolidone (VP) or *N*-vinylcarbazole (NVC) merely by matching the activity of the monomer with an appropriate RAFT agent.[26, 27]

The proposed mechanism for the RAFT polymerisation is described in Scheme 1.3. Initiation occurs by the decomposition of a conventional free radical initiator to form the propagating species ($P_n\cdot$). In the next step, addition of the propagating radical to the thiocarbonylthio compound followed by fragmentation of the intermediate radical results to a polymeric thiocarbonylthio compound and a new radical ($R\cdot$). Subsequently, the new radical reacts with another monomer species to form a new propagating radical ($P_m\cdot$). The key feature of the RAFT mechanism is the rapid equilibrium between the propagating species and the dormant polymeric thiocarbonylthio compounds that allows for equal chain growth providing access to well-defined polymers.[28]

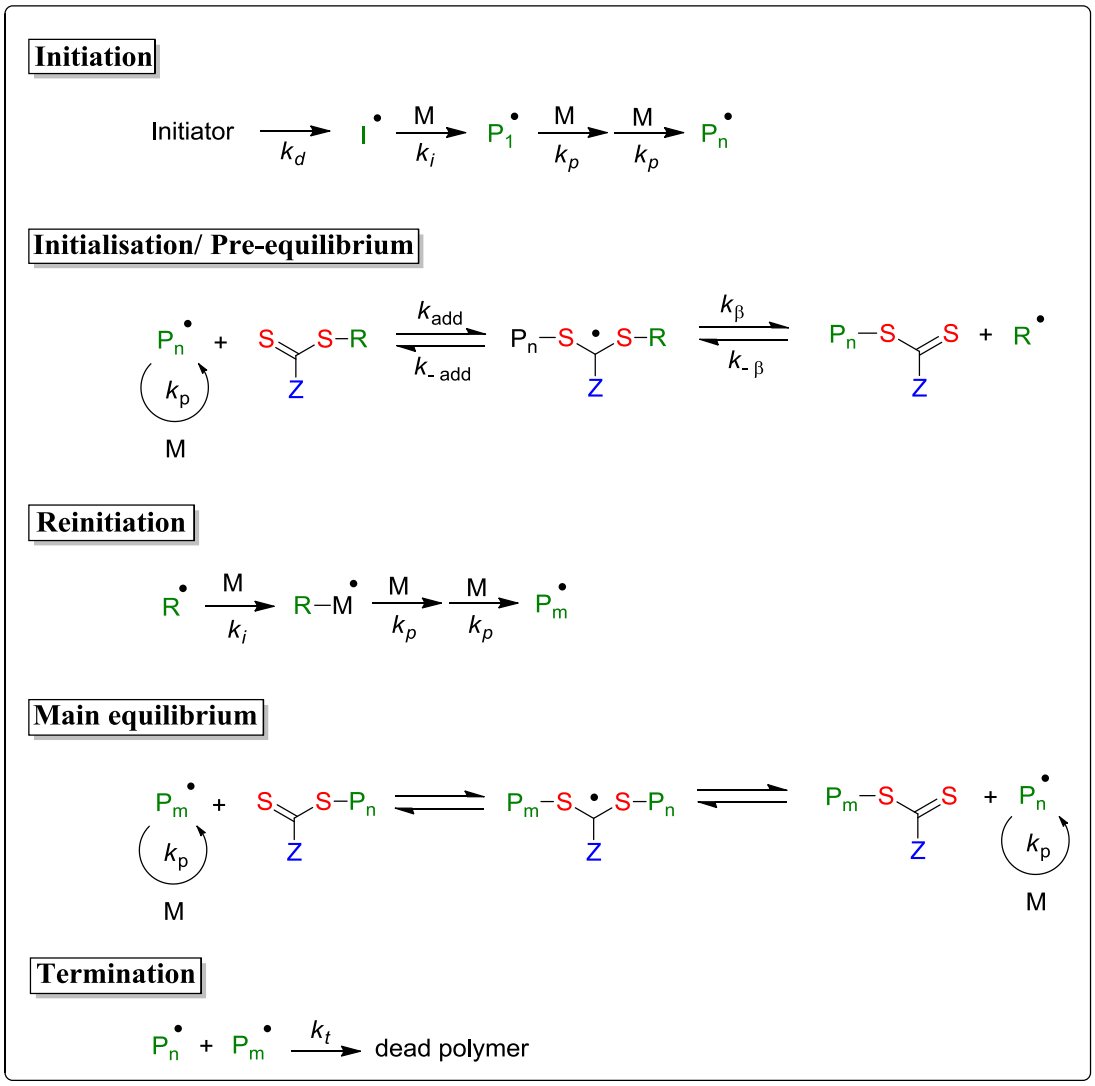

Scheme 1.3: Proposed mechanism of RAFT polymerisation.[28]

Undoubtedly, RAFT is a versatile system and one of the most widely used polymerisation processes since it is easy to perform, it does not employ metal catalysts and it can operate efficiently in a wide range of chemical environments, functionalities and reaction conditions. On the down side, many RAFT agents are not commercially available and their synthesis requires multistep synthetic procedures. Moreover RAFT agents are highly coloured (pink/ red to yellow) and have unpleasant odours due to gradual decomposition of the dithioester moiety to

yield small sulfur compounds which is undesirable for potential applications (*e.g.* personal care).

1.5.3. Atom Transfer Radical Polymerisation (ATRP)

Another popular technique is the so-called TMM-LRP which was introduced by Sawamoto[29] and Matyjaszewski.[30] Radical generation in TMM-LRP usually involves an alkyl halide undergoing a reversible redox process catalysed by a transition metal complex such as copper halide. Among other transition metals, both ruthenium and copper have been successfully utilised as the catalyst source, although copper remains, to date, the most studied transition metal, mainly due to its large availability, low costs and ease of handling. When copper, rather than ruthenium, is utilised the process is typically termed ATRP. ATRP is dominated by an equilibrium between propagating radicals and dormant species, predominately in the form of initiating alkyl halides/macromolecular species (P_nX).[16] The dormant species periodically react with a rate constant of activation (k_{act}) with transition metal complexes in their lower oxidation state, [Mt^m(L)X], (Mt^m represents the transition metal species in oxidation state m and L is a ligand); to intermittently form growing radicals (P_n^*), and deactivators-transition metal complexes in their higher oxidation state, coordinated by an additional, abstracted halide ligand [Mt^m(L)X]**X** (Scheme 1.4).

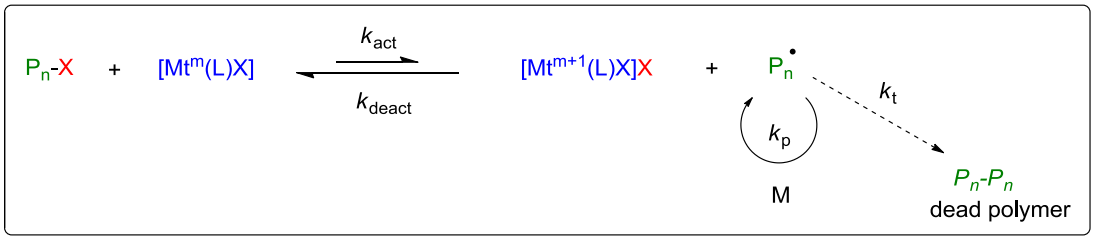

Scheme 1.4: ATRP equilibrium.[16]

In all RDRP methods, irreversible radical termination always occurs to some extent. However, in ATRP the small amount of bimolecular termination present at the initial stage of the reaction is beneficial for the polymerisation as it provides further control over the MWDs. This is because propagating radicals are irreversibly terminated *via* any other method than the end-capping reaction with CuX_2 (*i.e.* bimolecular termination), resulting in a slight excess of deactivating species in the system which will provide more control over the radical propagation, by shifting the equilibrium towards the dormant species. This phenomenon is known as the persistent radical effect (PRE).[31-33]

With respect to the mechanism ATRP is considered to proceed *via* an inner sphere electron transfer mechanism (ISET), where the radical and the deactivating species are formed through the concerted homolytic atom transfer of the halogen radical from the dormant species (P_nX) to the activating species (Mt^m/L). ISET mechanism is more likely to happen in comparison with outer sphere electron transfer (OSET), as it is energetically favoured.[34]

As in many fields, polymer synthesis has seen a substantial drive toward environmentally friendly synthesis, resulting in the development of so-called "green chemistry" techniques. Of particular relevance in ATRP is the a conscious effort to

reduce the catalyst loading to ppm levels[35] which led to the development of activator (re)generated by electron transfer ATRP (A(R)GET-ATRP)[36] and initiators for continuous activator regeneration ATRP (ICAR-ATRP).[37] In A(R)GET-ATRP a reducing agent is utilised to (re)generate the active catalyst from the deactivating species that accumulate *via* unavoidable termination reactions. A wide range of reducing agents have been successfully employed, including FDA-approved tin(II) 2-ethylhexanoate ($Sn(EH)_2$),[38] glucose,[36, 39, 40] ascorbic acid,[41] phenol,[42] hydrazine, phenylhydrazine[36] and nitrogen containing ligands[43] and monomers.[44] In a similar vein to A(R)GET-ATRP, ICAR-ATRP can also be considered as a "reverse" ATRP where a source of organic free radicals (*e.g.* AIBN) is typically employed to continuously regenerate the CuBr activator which would otherwise be consumed *via* termination reactions, particularly when the metal is used in ppm concentrations. Both A(R)GET and ICAR-ATRP can provide access to well-defined polymers ($Đ$ < 1.2) while the low concentration of metal reduces the need for extensive purification, at least for some applications. Nevertheless, both A(R)GET-ATRP and ICAR-ATRP do have a number of limitations, such as relatively long reaction times (typically 24 – 48 h), moderate conversions (typically 10 - 80%) and the need to purify the macroinitiators prior to block copolymerisation.[45]

1.5.4. Single Electron Transfer Living Radical Polymerisation (SET-LRP)

The concept of SET-LRP (or Cu(0) mediated RDRP) was initially introduced by Percec and co-workers in 2002[46] and attracted more attention in 2006, when the "*ultrafast synthesis of ultrahigh molecular weight polymers*" at ambient temperature or below from functional monomers containing electron withdrawing groups such as acrylates and methacrylates was reported.[47] Polar solvents, such as H_2O, dimethyl sulfoxide (DMSO), alcohols and ionic liquids were reported to encourage the rapid disproportionation of CuBr into Cu(0) and $CuBr_2$ species in the presence of disproportionating ligands (*e.g.* tris[2-(dimethylamino)ethyl]amine (Me_6-Tren), *N*,*N*,*N*′,*N*′′,*N*′′-pentamethyldiethylenetriamine (PMDETA) *etc.*). The initial activation step was proposed to occur *via* Cu(0), either in the form of copper wire or copper powder, *via* single electron transfer (SET) to the electron acceptor alkyl halide. Without any purification step the synthesis of high molecular weight polymers (M_n ~ 1400000 $g.mol^{-1}$) was demonstrated in less than 3 h.

According to the proposed mechanism Cu(0) (or "nascent" Cu(0) particles) is the major activator of alkyl halides[47-49] and CuBr is "inactive" under "SET-LRP conditions" (polar solvents and *N*-containing ligands) due to rapid or even instantaneous disproportionation[50, 51] into Cu(0) and $CuBr_2$. The activation step is proposed to occur *via* an outer sphere electron transfer process (OSET) through the formation and decomposition of a radical anion intermediate (Scheme 1.5).

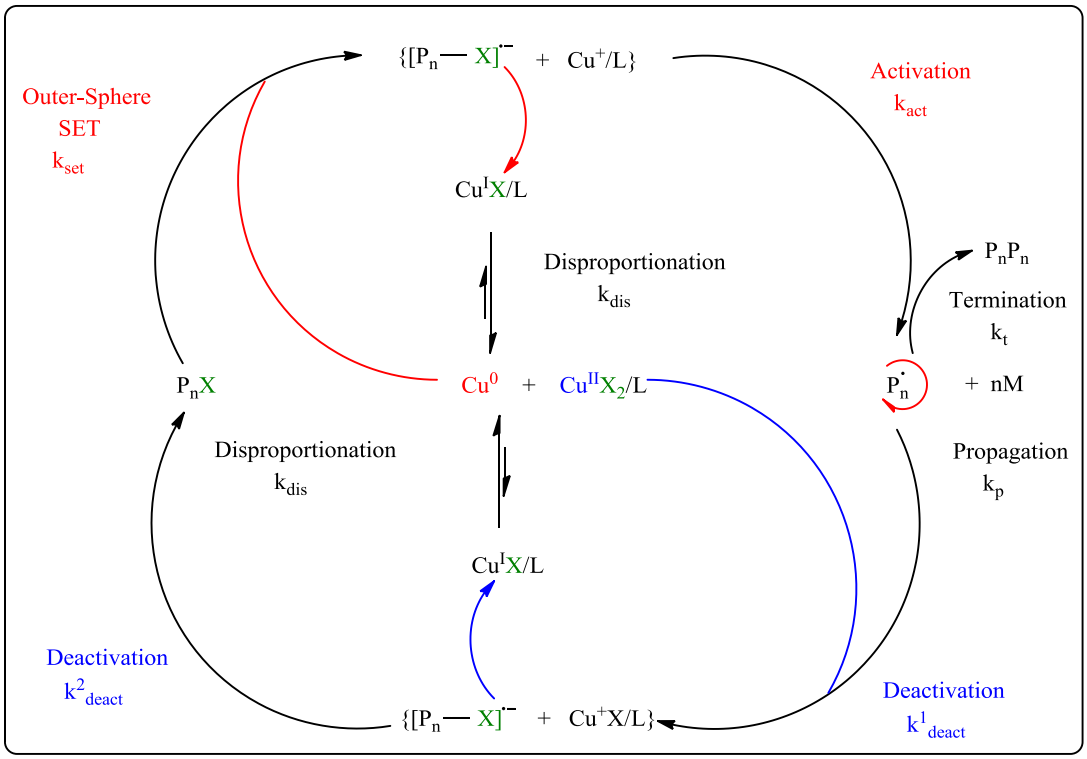

Scheme 1.5: Proposed mechanism for the SET-LRP.[47]

Cu(0), either in the form of powder or wire, is a very efficient method for polymer synthesis when organic solvents are employed. For applications where water is the required solvent, the polymerisation of acrylates has proved to be compatible with the copper wire system, resulting in full conversion within 6 h and low dispersities.[52] An excess of external $CuBr_2$ is required to provide good control over the MWDs in most cases.

Conversely, TMM-LRP of acrylamide monomers has been traditionally proven to be problematic, either due to lack of control[53] or the necessity to employ a high ratio of Cu(II) salts to facilitate effective deactivation and thus retain good control.[54] Furthermore, the vast majority of acrylamide polymerisations are conducted in organic solvents or in mixtures of water/organic solvents and the synthesis of block copolymers is limited.[55-64] Thus, NMP and RAFT protocols have

been routinely employed for the synthesis and copolymerisation of these monomers.[65-68]

In 2013, Haddleton and co-workers introduced a new method to perform Cu(0)- mediated RDRP in water.[69] It was emphasised that the key step in the process is to allow full disproportionation of CuBr/Me_6-Tren to Cu(0) powder and $CuBr_2$/Me_6-Tren in water prior to addition of both monomer and initiator. Strictly following this reaction protocol, provides access to a wide range of functional water-soluble polymers with controlled chain length and narrow MWDs ($Đ$ ~ 1.10), including poly(*N*-isopropylacrylamide) (PNIPAM), poly(*N*,*N*-dimethylacrylamide) (PDMA), poly(oligopoly(ethylene glycol) methyl ether acrylate (PPEGA), poly(hydroxyethyl acrylate) (PHEA) and even a polymer derived from an acrylamide glycomonomer.[69] Moreover, the use of aqueous Cu(0)- mediated RDRP has enabled the preparation of poly(*N*-acryloylmorpholine (NAM)),[70] the controlled synthesis of which has previously been limited to RAFT. All the polymerisations have been performed at, or below, ambient temperature with quantitative conversions attained in minutes. Moreover, polymers obtained have high end-group fidelity and are capable of undergoing *in situ* chain extensions to full conversion or multiblock copolymerisation *via* iterative monomer addition, with each step proceeding to full conversion. The Cu(0)- mediated RDRP of NIPAM was thoroughly investigated and careful selection of the catalyst ratio and the reaction temperature provided access to a range of molecular weights (DP = 8 - 320). Full characterisation of low molecular weight PNIPAM resulted in identification of the end-group functionality. Although a significant amount of hydrolysis of the ω-Br chain-end (premature termination) was detected at ambient temperature, adequate suppression could be achieved by decreasing the reaction temperature (ice bath).[69]

Aqueous Cu(0)- mediated RDRP was also performed in more complex solvents, including blood (sheep) serum, resulting in the formation of highly active Cu(0) particles.[71] Subsequently, the addition of monomer and initiator allowed the homogenous polymerisation ($Đ$ ~ 1.09 - 1.25) of various hydrophilic monomers including NIPAM, DMA, PEGA and HEA. The controlled nature of the polymerisations in this medium was exemplified by *in situ* copolymerisation of PNIPAM and PDMA macroinitiators with DMA and NIPAM respectively.[71] Although following a relatively slower rate than in pure water, disproportionation of CuBr/Me_6-Tren in phosphate-buffered saline (PBS) buffer was also conducted with the final polymers presenting slightly higher dispersity values ($Đ$ ~ 1.21 - 1.29).[69] To further illustrate the versatility of the system, the controlled polymerisation of NIPAM has also been reported in a range of international commercial alcoholic beverages/solvents (*e.g.* beers, wines, spirits *etc.*) utilising Cu(0)- mediated RDRP. Impressively, the chemical diversity in these solvents (*e.g.* phenols, sugars, alpha acids *etc.*) was well tolerated, yielding well-defined polymers with narrow MWDs ($Đ$ ~ 1.10). Thus, it was concluded that Cu(0)- mediated RDRP can operate efficiently in a wide range of chemical environments.[72] Disproportionation of CuBr/Me_6-Tren in ionic liquids has also been reported.[47] When Cu(0)- mediated RDRP was conducted in the presence of ionic liquids, first order kinetics with respect to the monomer concentration and low dispersity polymers were obtained, further illustrating the robust nature of the technique.[73]

Perhaps the most significant limitation of the technique, relative to RAFT, is that it cannot, to date, mediate the polymerisation of less activated monomers such as vinyl pyrrolidone (VP) and vinyl acetate (VA) (although vinyl chloride has been successfully polymerised[47]). Polymerisation of styrene and methacrylamides has also

not been well studied. Moreover, Cu(0)- mediated RDRP cannot be conducted in the presence of significant amounts of acids (*e.g.* acetic acid) as the catalyst would be contaminated/complexed, although small amounts of acid (10%) can be tolerated.[74] In addition, efficient stirring is required for an effective polymerisation, especially for the case of the copper wire system as a consequence of a surface catalysed polymerisation. Although a diversity of solvents have been utilised for Cu(0)-mediated RDRP, DMSO and H_2O represent by far the most studied solvents.

1.6. External regulation of controlled polymerisations

The development of the RDRP techniques has revolutionized the field of polymer science, providing access to well-defined polymers with pre-determined molecular weight, high end-group fidelity,[75-80] various functionalities[45, 81-83] and complex architectures.[84-90] However, one of the major challenges that still remain is the spatial and temporal control of the polymerisation. Recently, the use of external stimuli to control the polymerisation "on demand" has attracted considerable interest. Mimicking nature's ability to reversibly turn reactions "on" and "off" utilising specific stimulus provides dynamic control of material synthesis and paves the way for new applications. Controlled polymerisations can be regulated by a wide range of stimuli including added reagents, applied voltage, mechanical force or light (Figure 1.2).[91]

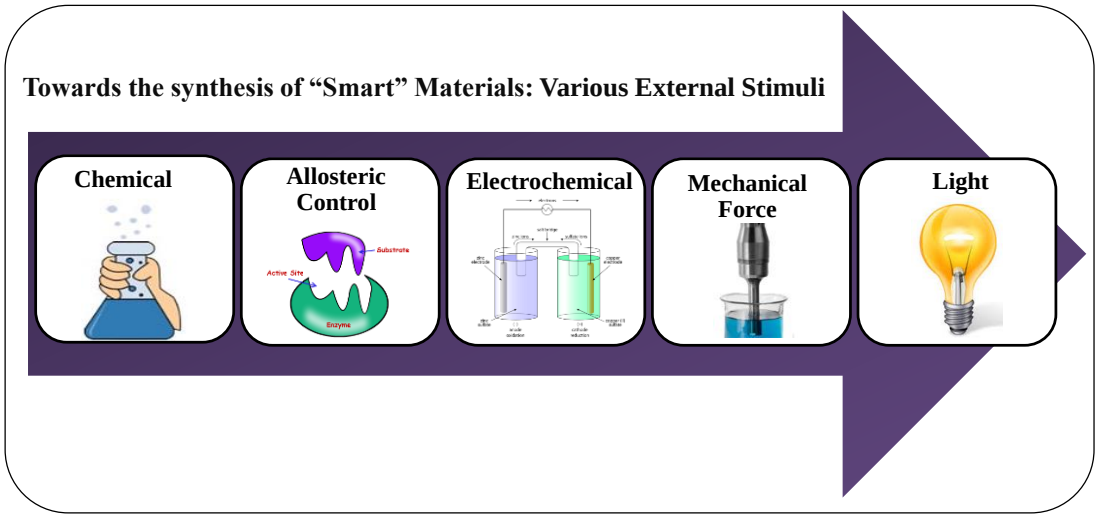

Figure 1.2: Various external stimuli.

1.6.1. Various external stimuli

One of nature's main enzyme regulation mechanism is the allosteric control. The word "allosteric" is derived from the Greek words "allos" (meaning other) and "stereos", (meaning site). Allosteric control of the catalytic activity can be achieved by the reversible binding of a small molecule (effector) to a location other than the active site. The addition of the effector, changes the shape of the enzyme so as to affect the formation of the usual complex at the active site between the enzyme and its substrate (the compound upon which it acts to form a product). As a result, the ability of the enzyme to catalyse a reaction is modified. Mirkin and co-workers were the first to report allosteric control of a polymerisation in 2010.[92] Other prominent examples of allosteric systems are based on bimetallic catalysts where binding of the effector changes the distance between the two metal sites, affecting the rate of the polymerisation.[93-95]Similar results can be obtained with other chemical transformations during the polymerisation, also known as chemical control. A common example is the addition of a redox-active system that can afford temporal

control over polymerisation. During the reaction, catalyst can reversibly switch between two stable oxidation states that have different catalytic efficiencies.[96-98]

In 2011 Matyjaszewski and co-workers introduced the first electrochemically-mediated atom transfer radical polymerisation (eATRP).[99] According to the proposed mechanism the $CuBr_2$/Me_6-Tren deactivator is reduced to CuBr/Me_6-Tren activator electrochemically to invoke or trigger polymerisation. Reoxidising the compex *via* an anodic current yields again the catalytically inactive Cu(II) species. Temporal control can be demonstrated by switching of polymerisation "on" and "off" in response to applied voltage. In a subsequent report the same system was applied under purely aqueous conditions providing excellent control over MW and MWDs, accompanied by a fast polymerisation rate and low charge consumption.[100] Thus, eATRP was proven to be an attractive system that provides for the synthesis of well-defined materials with novel applications.

The concept of applying mechanical force to create stress-responsive materials *via* altering the molecular or the supramolecular structure of polymers has been recently reported.[101] At the intersection of mechanics and chemistry, mechano-chemistry is a subject that embraces many daily phenomena including wear and abrasion, friction and lubrication, and stress-accelerated degradation of materials. During these processes, mechanical stress can be translated in various chemical transformations and the resulted polymers are known as mechanophores.[102-107] Sonication is one of the most famous examples to apply mechanical force in solution with strong shear forces being created changing the distribution of products or even cause the formation of new substances.[108] Mechanochemically controlled polymerisation allows for dynamic control of the reaction and future applications include self-healing of materials or diagnostic reporting of damage.

1.6.2. Utilising light as an external stimulus

Light combines several advantages since it is widely available, non-invasive and environmentally benign, thus is considered to be one of the most prominent among the external stimuli available.[91] Apart from the ability to switch "on" and "off" the polymerisation, light allows further and more precise control over the reaction rate by modifying the intensity of irradiation. Oster and Yang were the first to employ light as an external stimulus for the polymerisation of vinyl monomers in 1968.[109] Subsequently, three main strategies have been developed employing light for the activation of a) the monomer,[110, 111] b) initiator (also known as photo-initiators)[112-115] or c) catalyst.[116-119] Despite the strategy employed, the field of photo-polymerisation encompass a wide range of applications (*e.g.* photoresist materials,[120] photolithography,[121-123] printing plates,[124] dental filling materials[125] *etc.*) and thus attracts more and more scientific interest.

Monomer activation

Manners and co-workers reported the photo-controlled living anionic polymerisation of silicon-bridged ferrocenophane monomers.[110, 111]Exposure of these monomers to sunlight or to pyrex-filtered light (λ > 310 nm) in the presence of an anionic initiator resulted in controlled polymerisation which depends upon the irradiation time. In most cases the polymerisation proceeded to near-quantitative conversions resulting in well-defined polymers with narrow MWDs ($Đ$ < 1.1). In terms of the mechanism, UV-irradiation weakens the Fe-cyclopentadienyl (Cp) bond of the monomer and induces an excited state which allows for the displacement of a

Cp ligand by a weak nucleophilic initiator (*e.g.* NaCp) (initiation). The resulted anionic Cp chain-end can subsequently undergo chain propagation by reacting with additional excited monomers (Scheme 1.6). Since the propagation relies on the continued irradiation, the synthesis of block copolymers was also targeted. Sequence controlled polymers were achieved by the addition of monomers by switching the light "on" and "off". This system provides unprecedented, photo-controlled access to new types of functional materials. However, the main drawback is the use of specialised ferrocene monomers that limits the potentials of this strategy.

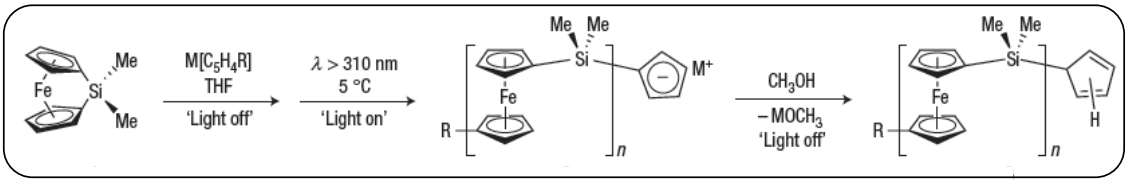

Scheme 1.6: Photo-controlled living polymerisation of ferrocenophanes.[111]

Photo-initiators

Photo-initiators are classified as cleavage (Type I) and H-abstraction type (Type II).[126, 127] Specifically, Type I initiators undergo unimolecular fragmentation upon light absorption forming two initiating radicals (Scheme 1.7a). Examples of this type of photo-initiators include mostly benzoin compounds along with its derivatives.[128-132]The formation of initiating species in Type II initiators occurs through electron transfer reactions or hydrogen abstraction or through a combination of both mechanisms (Scheme 1.7b). Ketones are considered to be the most important Type II photo-initiators including benzophenone, thioxanthone, camphorquinone *etc.*[133-137]The selection of the photoinitiator depends on the requirement of a

particular system or application, however, Type I photo-initiators require more energy to undergo bond cleavage and therefore they considered to be less advantageous than Type II.

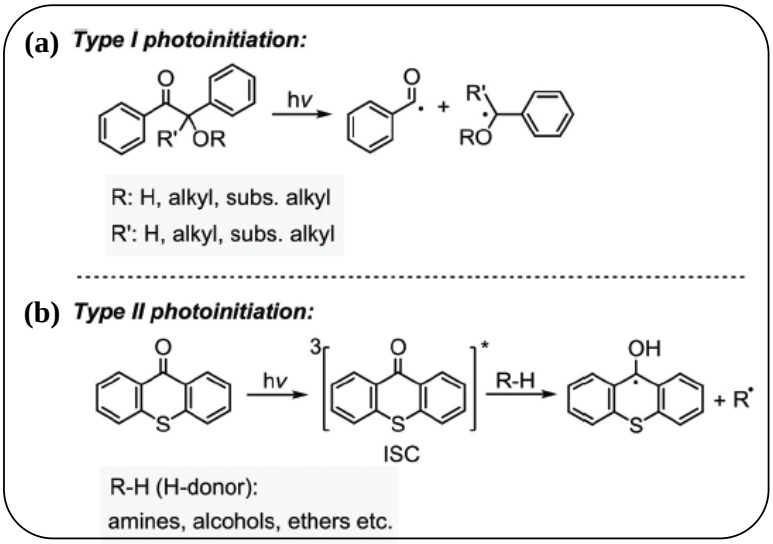

Scheme 1.7: Photolysis of the two types of photo-initiators.[113]

Catalyst photo-activation

The direct photo-activation of the catalyst is probably the best strategy for regulating controlled polymerisations since the catalytic species are employed only in small amounts (usually ppm levels). Hawker and co-workers investigated the polymerisation of methacrylates by employing previously well-established photoredox catalysts.[116, 138] By utilising Ir-based catalysts they developed a novel living radical system that displays an unprecedented response to activation and deactivation of polymerisation through external visible light stimulation. The proposed mechanism for this system is given in Scheme 1.8.

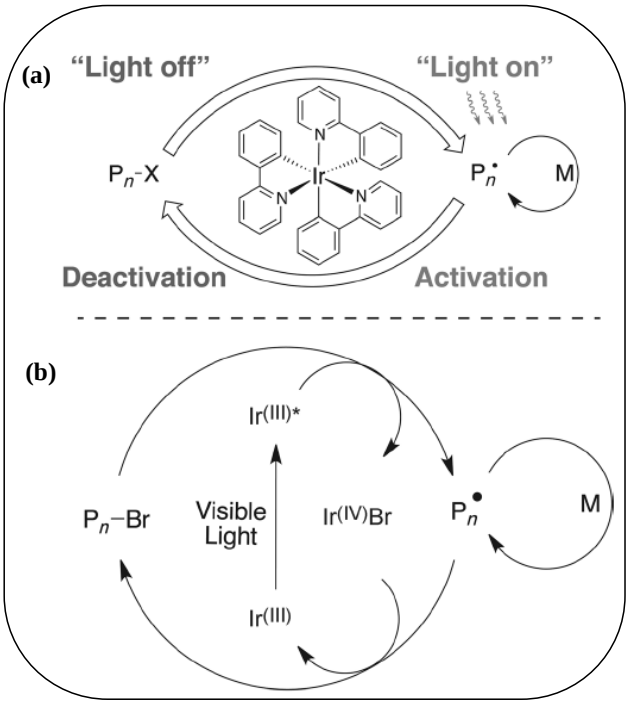

Scheme 1.8: (a) Schematic illustration of the photoredox radical polymerisation concept and (b) proposed mechanism.[91]

The Ir-based catalyst has been shown to absorb light to form the Ir^{III}*. The excited species (Ir^{III}*) can reduce an alkyl bromide initiator and thus form the initiating radical. The resulting Ir^{IV} can then oxidise the alkyl radical chain-end to form the dormant species and the process can be repeated with an additional photon of light. Although the resulted materials were low dispersed, the conversions were relatively moderate and reached only 70% in some cases. In a subsequent report the same system was applied for the polymerisation of acrylates generating similar results.[119] Boyer *et al.* employed the same iridium based catalyst for the development of photo-induced electron transfer reversible addition−fragmentation chain transfer (PET-RAFT).[139, 140]

Since Hawker's initial report, several groups have investigated alternative metal complexes as redox catalytic sources including copper (Cu) (see section 1.5.3),

cobalt (Co),[141, 142] ruthenium (Ru),[140, 143] zinc (Zn)[144] and iron (Fe)[145] to achieve photochemically mediated synthesis of well-controlled macromolecular architectures. For instance, Fe is a highly attractive metal as it is inexpensive, nontoxic, abundant and environmentally benign, biocompatible and easy to remove. Recently, Matyjaszewski and co-workers reported the Fe-mediated photo-induced polymerisation of methacrylates.[145] Narrow MWDs were obtained without any addition of ligands or reducing agents. Nevertheless, the reaction times were very long (> 24 h) and the conversions did not reach quantitative or near-quantitative levels (41-86%) for most of the monomers employed.

In an attempt to circumvent the metal contamination issues present in most RDRP systems, Hawker and co-workers employed an organic-based photoredox catalyst for the polymerisation of vinyl monomers under UV irradiation.[146] The metal-free ATRP gave rise to well-defined materials with accurate control over the molecular weights, low dispersity and high retention of chain end-groups. Further exploiting the high end-group fidelity, block copolymers were synthesised while the technique was also combined successfully with other processes (traditional Cu-catalysed and photo-mediated Ir-based systems).

Inspired by Hawker's metal free system, many other groups employed organic-based catalysts. Boyer and co-worker investigated a series of organo-dyes, including methylene blue, fluorescein, rhodamine 6G, Nile red and eosin Y, to perform a visible light-mediated RDRP of methacrylates.[117] Specifically, eosin Y and fluorescein were efficient catalysts to activate the PET-RAFT) mechanism. This system yielded well-defined (co)polymers with good control over the molecular weights ranging from 10000 to 100000 g.mol^{-1} and low dispersities ($Đ$ < 1.30). A

variety of functional monomers, including *N*,*N*-dimethylaminoethyl methacrylate, hydroxyl ethyl methacrylate, pentafluorophenyl methacrylate, glycidyl methacrylate, oligoethylene glycol methyl ether methacrylate (OEGMA), and methacrylic acid, were also successfully polymerised.

The same group subsequently reported the efficient photo-induced RDRP process that involves the use of chlorophyll as the photoredox biocatalyst.[118] Chlorophyll A (the most abundant chlorophyll in plants) activated successfully the PET-RAFT process under blue and red LED light (λ_{max} = 461 and 635 nm, respectively). A wide range of monomers, including (meth)acrylamide and (meth)acrylates containing a large variety of functional groups, such as carboxylic acid, amine, alcohol, and glycidyl groups, were polymerised within a few hours showing excellent control over molecular weight and dispersity.

Photo-induced metal-free atom transfer radical polymerisation has also been investigated by Matyjaszewski and co-workers where the synthesis of polyacrylonitrile (PAN) with predictable molecular weights and low dispersities was achieved.[147] Chen *et al.*[148] employed 10-phenylphenothiazine as an organic photoredox catalyst providing polymers from a variety of acrylate and acrylamide monomers with good molecular weight control, narrow molar mass distributions, and excellent end-group fidelity.

Indeed all the aforementioned systems utilise organic-based redox catalysts and thus avoid the potential toxicity of the "heavy metals" employed in most living radical techniques. However, in most cases exotic catalysts have to be employed while long reaction times and low conversions are compromising the appeal of these techniques.

1.6.3. Copper mediated photo-induced RDRP

Many copper(II)/ligand (Cu(II)/L) complexes are known to be light sensitive and undergo photoredox reactions during UV-irradiation.[149] Specifically, some ligands (amines) have been employed as outer-sphere electron donors and photoelectron donors in a range of reactions (*e.g.* dehalogenation, cyclisation).[150-154] Hence, the development of copper-mediated photo-regulated approaches that control both the initiation and all of the subsequent activation/ propagation steps would pave the way for the synthesis of "smart" materials with novel applications.

Yagci and co-workers were the first to develop a copper mediated photo-induced system investigating the (co)polymerisation of methacrylates.[155] MMA was employed as the model monomer and the polymerisation was initiated by *in situ* photochemical generation of Cu(I) complex from air-stable Cu(II) species in the presence of PMDETA, without any additional reducing agents. The controlled living character of this polymerisation was confirmed by both the linear tendency of molecular weight evolution with conversion and a chain extension experiment. However, since this study was conducted in bulk, the poor solubility of the Cu(II) complexes in the monomer solution gave rise to heterogeneous polymerisation and low conversions (~50%). In a subsequent report, the same group employed MeOH in an attempt to circumvent these issues.[156] Although MeOH facilitated the homogeneous polymerisation of MMA and allowed for better control over the molecular weights, conversions remained low (~40%).

Matyjaszewski and co-workers have also reported visible/sunlight photo-induced ATRP employing Cu(II)(TPMA)Br_2 complexes with subtle differences to Yagci's proposed mechanism.[157] Both acrylic and methacrylic monomers (MA and

MMA) were investigated utilising a variety of wavelengths. Well-defined polymers were obtained in most cases with the best result being obtained in sunlight (80%, $Đ$=1.09). In a joint report both Matyjaszewski's and Yagci's group implemented the photoinitiated ATRP in inverse microemulsion polymerisation of oligo(ethylene glycol) monomethyl ether methacrylate in an attempt to facilitate the process control of water-soluble monomers.[158] The polymers obtained molecular weight values close to the theoretical and relatively narrow MWDs ($Đ$ = 1.20-1.40). However, in all these reports low polymerisation rates and limited range of monomer compatibility (MA and MMA) were reported while high end-group fidelity was not demonstrated.

In 2014 Haddleton and co-workers reported the photo-induced RDRP of acrylates in the presence of precursor Cu(II)(Me_6-Tren)Br_2 complexes and excess of aliphatic tertiary amines (*e.g.* Me_6-Tren).[159] For the first time quantitative conversions and high end-group fidelity were reported for a light-mediated system for a wide range of molecular weights (*DP* = 25-800). Reactions times for the polymerisation of MA in DMSO, were generally 15 h under sunlight following an initial induction period of approximately 3 h. However, accelerated reaction rates were observed (~80 min) under UV irradiation (λ = 365 nm) as evidenced by kinetic experiments. Additionally, temporal control during polymerisation was also demonstrated *via* consecutive light and dark exposure resulting in PMA (93%, $Đ$ = 1.07) in the final cycle which is directly comparable with the result obtained during uninterrupted UV irradiation.

The scope of the technique was subsequently expanded to include a wide range of monomers such as hydrophilic, hydrophobic, functional acrylates and monomers bearing sugar moieties.[160] In all cases near-quantitative conversions and

narrow MWDs were observed further demonstrating the versatility of the technique. Solvent screening was also performed (MA was employed as the model monomer) to ascertain their compatibility with the system including alcohols, fluorinated solvents, solvent that induce phase separation,[161, 162] toluene, dioxane, anisole. Although in most cases the rate was significantly slower (~ 24 h) full conversion was obtained along with low dispersities. Toluene, dioxane and anisole gave rise to uncontrolled polymers ($Đ$ > 1.46) due to limited solubility of the Cu(II) complexes. Finally, water was also utilised as the solvent for the photo-induced polymerisation of PEGA. Interestingly, poor control over the MWDs was observed ($Đ$ > 1.45) probably due to the increased stability of the Cu(II) amine complexes in water. Nevertheless, mixture of water with DMSO gave rise to well-defined polymers ($Đ$ < 1.20).

The high end-group fidelity of the system was further exploited for the synthesis of multiblock copolymers in a one pot process.[163] A wide range of molecular weights (*DP* = 3-100 per block) were also targeted to demonstrate the versatility of the technique. The amine employed (Me_6-Tren) is considered to be consumed by a photo reduction during the irradiation and therefore polymerisation requires replenishing through a feed process in order to maintain the polymerisation rates. Under these optimised conditions, very high conversions were attained in each cycle yielding well-defined block (co)polymers with narrow MWDs ($Đ$ <1.20) at ambient temperatures. However, telechelic multiblock copolymers and higher amount of blocks (> 11 chain extensions) could not be obtained.

Haddleton's protocol has since been readily translated into a continuous flow process, reported by Junkers and co-workers, whereby poly(MA) homopolymers and poly-(MA)-*b*-(*n*-BA) block copolymers were prepared in the micro and milli flow reactors.[164] The same group utilised this procedure for the synthesis of

monodispersed sequence defined acrylate oligomers *via* consecutive single unit monomer insertion reactions. Nevertheless, intermediate purification of the compounds was essential to overcome the statistical nature of the radical insertion process.[165] Finally, the photo-induced copper mediated polymerisation was employed for the synthesis of methacrylate-acrylate block copolymers by alternating the ligand from Me_6-Tren to PMDETA.[166] However, successful synthesis of block copolymers is only observed when the PMMA block is polymerised first and if all the PMDETA ligand and residual monomer are completely removed prior to addition of the acrylate.

A mechanistic insight for the Cu(II)-mediated photo-induced polymerisation was initially conducted by Haddleton's group. According to the proposed mechanism (Scheme 1.9a), the initial photo-activation occurs in the free ligand (ligand is used in excess in respect to copper) and subsequently outer-sphere electron transfer (OSET) occurs from the excited state of the ligand to the alkyl halide initiator leading to the scission of the C-Br bond. In this stage an initiating radical, a ligand radical cation along with a Br^- as a counterion are formed. The initiating radical mediates the propagation step based on the deactivation reaction imposed by the presence of the deactivating species (Cu(II)(Me_6-Tren)Br_2). Deactivation results in the formation of the dormant species (P_n-Br) and Cu(I)(Me_6-Tren)Br_2 complex which is oxidised back to (Cu(II)(Me_6-Tren)Br_2) upon reaction with the Me_6-Tren radical cation. However, since the deactivation process in the only pathway to form the activating species, one would expect very low polymerisation rates to be observed which is contradictory with the experimental data obtained.

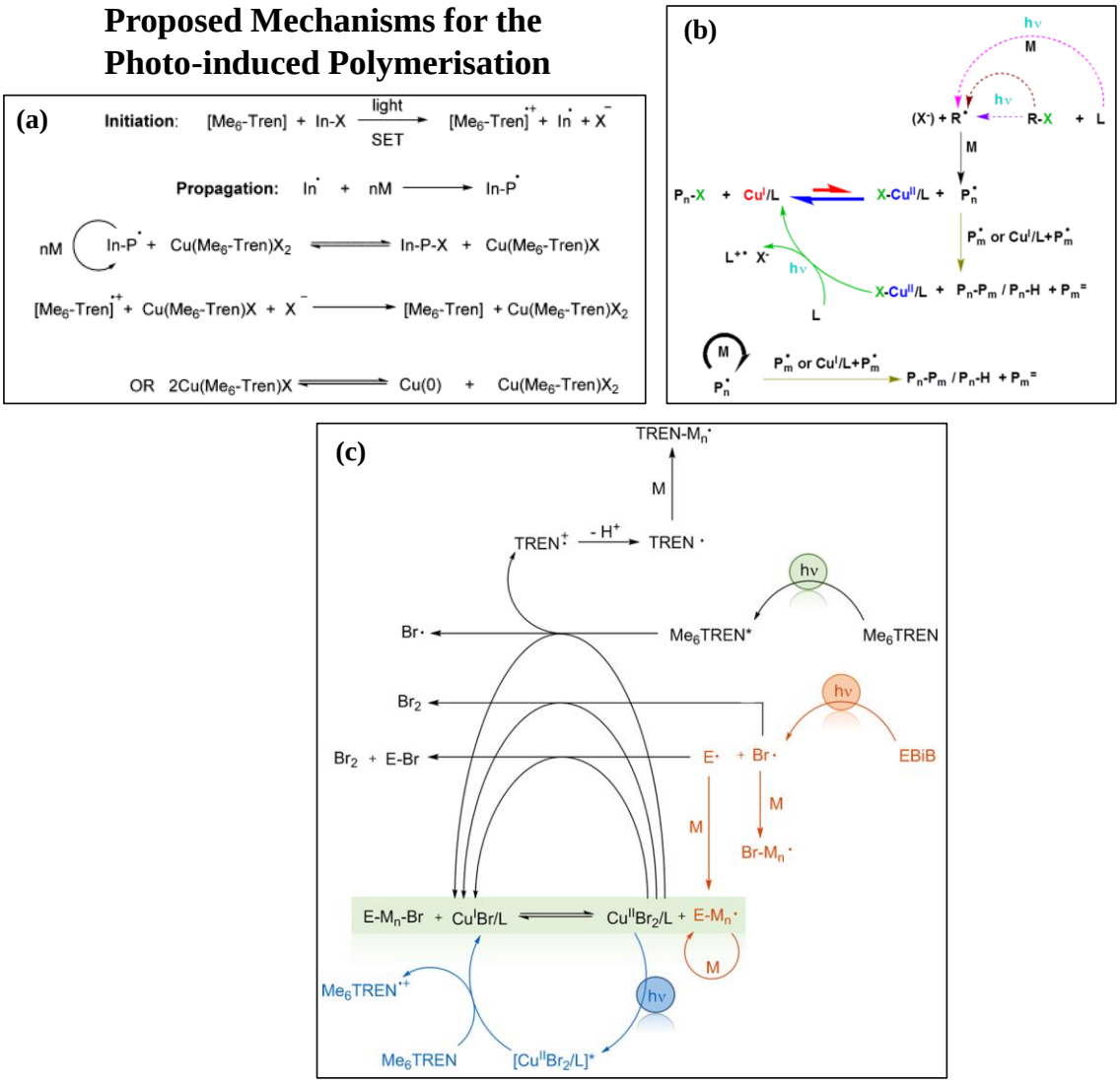

Scheme 1.9: Proposed mechanistic pathways from (a) Haddleton's,[167] (b) Matyjaszewski's[168] and (c) Barner-Kowollik's in collaboration with Haddleton's group.[169]

Matyjaszewski and co-workers subsequently employed the same system and carried out both experimental and kinetic simulations in an attempt to unravel this complex mechanism (Scheme 1.9b).[168] The dominant mode of activator (re)generation is the photochemically mediated reduction of Cu(II) complexes by an excess of amine groups. This was proposed to be a photochemical ARGET ATRP process, with the amine becoming oxidised to the corresponding radical cation, which can initiate a new chain after proton transfer. The second step was reported to

be the synergistic radical generation between alkyl halide species and the ligand, in a similar vein to a photochemical ICAR ATRP. However, since the ICAR process occurs approximately 1 order of magnitude slower than the ARGET, its contribution is significantly lower. Additionally, other processes involved such as direct photochemical cleavage of the alkyl halide, photochemical radical generation from the ligand, or ligand with monomer are minor reactions that were also shown to have a minor role. It is noted, that it was not sufficiently demonstrated how an adequate amount of initiator radicals can be generated under irradiation to rapidly start the polymerisation.

Both the aforementioned proposed mechanistic studies were based on kinetic experiments without employing any other characterisation techniques (*e.g.* mass spectrometry) and thus not sufficient evidence is given. Barner-Kowollik and co-workers in collaboration with the Haddleton group, presented a thorough mechanistic study based on pulsed-laser polymerisation (PLP)[170-172] and electrospray-ionisation mass spectrometry (ESI-MS)[173] offering a comprehensive understanding of the mechanism (Scheme 1.9c).[169] Interestingly, their findings indicated that the initiation of the polymerisation occurs *via* the photo-induced C-Br bond scission of the initiator (note that EBiB is not considered to be a photo-initiator) which can either react with the initially present Cu(II) species or it can mediate the propagation step. The generation of the activating species Cu(I) occurs *via* the electron transfer reaction between the excited amine ligand and the Cu(II) species. Additionally, the ligand is also proposed to act as a reducing agent quenching the excited Cu(II) species and forming the corresponding Cu(I) complex and the amine radical cation. However, apart from the ligand, other species were also shown to promote the generation of the activating species including alkyl and

bromine radical as demonstrated by mass spectrometry. Regardless of the mechanism, Cu(II)-mediated polymerisation allows for the controlled synthesis of novel materials with additional applications arising from the precise spatiotemporal control.

In this work, the main focus is to expand the scope of this newly developed photo-induced Cu(II)-mediated polymerisation. The synthesis of *α,ω*-telechelic multiblock copolymers employing various bi-functional initiators will be attempted targeting various chain lengths at below ambient temperature. The symmetrical nature of these telechelic materials will be demonstrated by cleaving the S-S bond of a tridecablock copolymer (initiated by a disulphide initiator). The compatibility of this system with special solvents and catalysts will also be investigated. Importantly, in an attempt to overcome the main limitations of this technique (*e.g.* ligand degradation), two novel discrete complexes will be synthesised demonstrating advanced characteristics and advantages over the previous approach.

In the second part the polymerisation of acrylamides will be investigated utilising a different polymerisation protocol, aqueous Cu(0)-mediated RDRP, since the light mediated system is not compatible with these monomers. A wide range of molecular weights will be targeted and the end-group fidelity will be exploited by *in situ* chain extensions and block copolymerisations.

In the final chapter, the synthesis of semifluorinated triblock copolymers in a multigram scale capable to afford subsequent industrial testing will be described utilising the photo-induced RDRP. This is an ongoing project funded from Lubrizol and thus only a few initial studies will be presented which basically set the scene for future work.

1.7. References

1. H. Staudinger, *Ber. Dtsch. Chem. Ges.*, 1920, **53**, 1073-1085.

2. P. J. Flory, *J. Am. Chem. Soc.*, 1937, **59**, 241-253.

3. G. Odian, *Principles of Polymerisation, 4th Edition*, Wiley, 2004.

4. J. W. Nicholson, *The Chemistry of Polymers, 2nd Edition*, RSC Paperbacks, 1997.

5. A. A. Gridnev and S. D. Ittel, *Macromolecules*, 1996, **29**, 5864-5874.

6. V. N. Kondratiev, *Chain Reactions,Comprehensive Chemical Kinetics*, Elsevier, 1969.

7. M. Kamachi, J. Satoh and S. I. Nozakura, *J. Polym. Sci. Part A: Polym. Chem.*, 1978, **16**, 1789-1800.

8. G. F. Santee, R. H. Marchessault, H. G. Clark, J. J. Kearny and V. Stannett, *Macromol. Chem. Phys.*, 1964, **73**, 177-187.

9. G. V. Schulz and F. Blaschke, *Z. Phys. Chem*, 1942, **51**, 75.

10. M. Szwarc, M. Levy and R. Milkovich, *J. Am. Chem. Soc.*, 1956, **78**, 2656-2657.

11. M. Szwarc, *J. Polym. Sci. Part A: Polym. Chem.*, 1998, **36**, ix-xv.

12. M. Szwarc, *J. Polym. Sci. Part A: Polym. Chem.*, 1998, **36**, v-xiii.

13. M. Szwarc, *Nature*, 1956, **178**, 1168-1169.

14. A. D. Jenkins, R. G. Jones and G. Moad, *Pure Appl. Chem.*, 2009, **82**, 483-491.

15. B. B. Wayland, G. Poszmik, S. L. Mukerjee and M. Fryd, *J. Am. Chem. Soc.*, 1994, **116**, 7943-7944.

16. K. Matyjaszewski, *Macromolecules*, 2012, **45**, 4015-4039.

17. R. P. Quirk and B. Lee, *Polym. Int.*, 1992, **27**, 359-367.

18. R. D. Puts and D. Y. Sogah, *Macromolecules*, 1996, **29**, 3323-3325.

19. J. D. Druliner, *Macromolecules*, 1991, **24**, 6079-6082.

20. E. De León-Sáenz, G. Morales, R. Guerrero-Santos and Y. Gnanou, *Macromol. Chem. Phys.*, 2000, **201**, 74-83.

21. M. Steenbock, M. Klapper and K. Müllen, *Macromol. Chem. Phys.*, 1998, **199**, 763-769.

22. B. Yamada, Y. Nobukane and Y. Miura, *Polym. Bull.*, 1998, **41**, 539-544.

23. D. H. Solomon, E. Rizzardo, P. Cacioli, US 4581429, 1986.

24. M. K. Georges, R. P. N. Veregin, P. M. Kazmaier and G. K. Hamer, *Macromolecules*, 1993, **26**, 2987-2988.

25. J. Chiefari, Y. K. Chong, F. Ercole, J. Krstina, J. Jeffery, T. P. T. Le, R. T. A. Mayadunne, G. F. Meijs, C. L. Moad and G. Moad, *Macromolecules*, 1998, **31**, 5559-5562.

26. G. Moad, E. Rizzardo and S. H. Thang, *Aust. J. Chem.*, 2009, **62**, 1402-1472.

27. D. J. Keddie, *Chem. Soc. Rev.*, 2014, **43**, 496-505.

28. G. Moad, E. Rizzardo and S. H. Thang, *Aust. J. Chem.*, 2005, **58**, 379-410.

29. M. Kato, M. Kamigaito, M. Sawamoto and T. Higashimura, *Macromolecules*, 1995, **28**, 1721-1723.

30. J.-S. Wang and K. Matyjaszewski, *J. Am. Chem. Soc.*, 1995, **117**, 5614-5615.

31. H. Fischer, *Macromolecules*, 1997, **30**, 5666-5672.

32. H. Fischer, *J. Polym. Sci. Part A: Polym. Chem.*, 1999, **37**, 1885-1901.

33. H. Fischer, *Chem. Rev.*, 2001, **101**, 3581-3610.

34. C. Y. Lin, M. L. Coote, A. Gennaro and K. Matyjaszewski, *J. Am. Chem. Soc.*, 2008, **130**, 12762-12774.

35. Y. Wang, N. Soerensen, M. Zhong, H. Schroeder, M. Buback and K. Matyjaszewski, *Macromolecules*, 2013, **46**, 683-691.

36. K. Matyjaszewski, W. Jakubowski, K. Min, W. Tang, J. Huang, W. A. Braunecker and N. V. Tsarevsky, *Proc. Natl. Acad. Sci. U.S.A.*, 2006, **103**, 15309-15314.

37. H. Dong, W. Tang and K. Matyjaszewski, *Macromolecules*, 2007, **40**, 2974-2977.

38. W. Jakubowski and K. Matyjaszewski, *Macromolecules*, 2005, **38**, 4139-4146.

39. A. de Vries, B. Klumperman, D. de Wet-Roos and R. D. Sanderson, *Macromol. Chem. Phys.*, 2001, **202**, 1645-1648.

40. W. Jakubowski and K. Matyjaszewski, *Angew. Chem., Int. Ed.*, 2006, **45**, 4482-4486.

41. K. Min, H. Gao and K. Matyjaszewski, *Macromolecules*, 2007, **40**, 1789-1791.

42. Y. Gnanou and G. Hizal, *J. Polym. Sci. Part A: Polym. Chem.*, 2004, **42**, 351-359.

43. Y. Kwak, A. J. D. Magenau and K. Matyjaszewski, *Macromolecules*, 2011, **44**, 811-819.

44. H. Dong and K. Matyjaszewski, *Macromolecules*, 2008, **41**, 6868-6870.

45. A. Anastasaki, V. Nikolaou, G. Nurumbetov, P. Wilson, K. Kempe, J. F. Quinn, T. P. Davis, M. R. Whittaker and D. M. Haddleton, *Chem. Rev.*, 2015.

46. V. Percec, A. V. Popov, E. Ramirez-Castillo, M. Monteiro, B. Barboiu, O. Weichold, A. D. Asandei and C. M. Mitchell, *J. Am. Chem. Soc.*, 2002, **124**, 4940-4941.

47. V. Percec, T. Guliashvili, J. S. Ladislaw, A. Wistrand, A. Stjerndahl, M. J. Sienkowska, M. J. Monteiro and S. Sahoo, *J. Am. Chem. Soc.*, 2006, **128**, 14156-14165.

48. G. Lligadas, B. M. Rosen, C. A. Bell, M. J. Monteiro and V. Percec, *Macromolecules*, 2008, **41**, 8365-8371.

49. N. H. Nguyen, H.-J. Sun, M. E. Levere, S. Fleischmann and V. Percec, *Polym. Chem.*, 2013, **4**, 1328-1332.

50. M. E. Levere, N. H. Nguyen, X. Leng and V. Percec, *Polym. Chem.*, 2013, **4**, 1635-1647.

51. B. M. Rosen, X. Jiang, C. J. Wilson, N. H. Nguyen, M. J. Monteiro and V. Percec, *J. Polym. Sci. Part A: Polym. Chem.*, 2009, **47**, 5606-5628.

52. N. H. Nguyen, J. Kulis, H.-J. Sun, Z. Jia, B. van Beusekom, M. E. Levere, D. A. Wilson, M. J. Monteiro and V. Percec, *Polym. Chem.*, 2013, **4**, 144-155.

53. J. T. Rademacher, M. Baum, M. E. Pallack, W. J. Brittain and W. J. Simonsick, *Macromolecules*, 1999, **33**, 284-288.

54. M. Pierre-Eric, C. M. Nathalie, B. Alexander and H. E. M. Axel, in *Controlled/Living Radical Polymerisation: Progress in ATRP*, ACS, 2009, vol. 1023, 127-137.

55. G. Masci, L. Giacomelli and V. Crescenzi, *Macromol. Rapid Commun.*, 2004, **25**, 559-564.

56. Y. Xia, X. Yin, N. A. D. Burke and H. D. H. Stöver, *Macromolecules*, 2005, **38**, 5937-5943.

57. Y. Xia, N. A. D. Burke and H. D. H. Stöver, *Macromolecules*, 2006, **39**, 2275-2283.

58. Q. Duan, Y. Miura, A. Narumi, X. Shen, S.-I. Sato, T. Satoh and T. Kakuchi, *J. Polym. Sci. Part A: Polym. Chem.*, 2006, **44**, 1117-1124.

59. H. Akiyama and N. Tamaoki, *Macromolecules*, 2007, **40**, 5129-5132.

60. E. A. Appel, J. del Barrio, X. J. Loh, J. Dyson and O. A. Scherman, *J. Polym. Sci. Part A: Polym. Chem.*, 2012, **50**, 181-186.

61. D. Bontempo, R. C. Li, T. Ly, C. E. Brubaker and H. D. Maynard, *Chem. Commun.*, 2005, **37**, 4702-4704.

62. C. Feng, Z. Shen, Y. Li, L. Gu, Y. Zhang, G. Lu and X. Huang, *J. Polym. Sci. Part A: Polym. Chem.*, 2009, **47**, 1811-1824.

63. X. Tang, X. Liang, Q. Yang, X. Fan, Z. Shen and Q. Zhou, *J. Polym. Sci. Part A: Polym. Chem.*, 2009, **47**, 4420-4427.

64. M. Vachaudez, D. R. D'hooge, M. Socka, J. Libiszowski, O. Coulembier, M. F. Reyniers, A. Duda, G. B. Marin and P. Dubois, *React. Funct. Polym.*, 2013, **73**, 484-491.

65. A. W. Bosman, R. Vestberg, A. Heumann, J. M. J. Fréchet and C. J. Hawker, *J. Am. Chem. Soc.*, 2002, **125**, 715-728.

66. E. N. Savariar and S. Thayumanavan, *J. Polym. Sci. Part A: Polym. Chem.*, 2004, **42**, 6340-6345.

67. A. O. Moughton, J. P. Patterson and R. K. O'Reilly, *Chem. Commun.*, 2011, **47**, 355-357.

68. A. O. Moughton and R. K. O'Reilly, *Chem. Commun.*, 2010, **46**, 1091-1093.

69. Q. Zhang, P. Wilson, Z. Li, R. McHale, J. Godfrey, A. Anastasaki, C. Waldron and D. M. Haddleton, *J. Am. Chem. Soc.*, 2013, **135**, 7355-7363.

70. A. Anastasaki, A. J. Haddleton, Q. Zhang, A. Simula, M. Droesbeke, P. Wilson and D. M. Haddleton, *Macromol. Rapid Commun.*, 2014, **35**, 965-970.

71. Q. Zhang, Z. Li, P. Wilson and D. M. Haddleton, *Chem. Commun.*, 2013, **49**, 6608-6610.

72. C. Waldron, Q. Zhang, Z. Li, V. Nikolaou, G. Nurumbetov, J. Godfrey, R. McHale, G. Yilmaz, R. K. Randev, M. Girault, K. McEwan, D. M. Haddleton, M. Droesbeke, A. J. Haddleton, P. Wilson, A. Simula, J. Collins, D. J. Lloyd, J. A. Burns, C. Summers, C.

Houben, A. Anastasaki, M. Li, C. R. Becer, J. K. Ki*via*ho and N. Risangud, *Polym. Chem.*, 2014, **5**, 57-61.

73. J. Ma, H. Chen, M. Zhang and M. Yu, *J. Polym. Sci. Part A: Polym. Chem.*, 2012, **50**, 609-613.

74. S. Fleischmann and V. Percec, *J. Polym. Sci. Part A: Polym. Chem.*, 2010, **48**, 4889-4893.

75. A. H. Soeriyadi, C. Boyer, F. Nyström, P. B. Zetterlund and M. R. Whittaker, *J. Am. Chem. Soc.*, 2011, **133**, 11128-11131.

76. A. Anastasaki, C. Waldron, P. Wilson, C. Boyer, P. B. Zetterlund, M. R. Whittaker and D. Haddleton, *ACS Macro Lett.*, 2013, **2**, 896-900.

77. G. Gody, T. Maschmeyer, P. B. Zetterlund and S. Perrier, *Nat. Commun.*, 2013, **4**.

78. G. Gody, M. Danial, R. Barbey and S. Perrier, *Polym. Chem.*, 2015, **6**, 1502-1511.

79. F. Alsubaie, A. Anastasaki, P. Wilson and D. M. Haddleton, *Polym. Chem.*, 2015, **6**, 406-417.

80. K. A. Davis and K. Matyjaszewski, *Macromolecules*, 2001, **34**, 2101-2107.

81. C. L. McCormick and A. B. Lowe, *Acc. Chem. Res.*, 2004, **37**, 312-325.

82. K. Matyjaszewski and N. V. Tsarevsky, *Nat.Chem.*, 2009, **1**, 276-288.

83. Q. Zhang, L. Su, J. Collins, G. Chen, R. Wallis, D. A. Mitchell, D. M. Haddleton and C. R. Becer, *J. Am. Chem. Soc.*, 2014, **136**, 4325-4332.

84. C. Boyer, A. Derveaux, P. B. Zetterlund and M. R. Whittaker, *Polym. Chem.*, 2012, **3**, 117-123.

85. A. Blencowe, J. F. Tan, T. K. Goh and G. G. Qiao, *Polymer*, 2009, **50**, 5-32.

86. B. M. Rosen, G. Lligadas, C. Hahn and V. Percec, *J. Polym. Sci. Part A: Polym. Chem.*, 2009, **47**, 3931-3939.

87. B. I. Voit and A. Lederer, *Chem. Rev.*, 2009, **109**, 5924-5973.

88. Z. Jia, D. E. Lonsdale, J. Kulis and M. J. Monteiro, *ACS Macro Lett.*, 2012, **1**, 780-783.

89. J. Rosselgong, E. G. L. Williams, T. P. Le, F. Grusche, T. M. Hinton, M. Tizard, P. Gunatillake and S. H. Thang, *Macromolecules*, 2013, **46**, 9181-9188.

90. H. Gao and K. Matyjaszewski, *Macromolecules*, 2008, **41**, 1118-1125.

91. F. A. Leibfarth, K. M. Mattson, B. P. Fors, H. A. Collins and C. J. Hawker, *Angew. Chem., Int. Ed.*, 2013, **52**, 199-210.

92. H. J. Yoon, J. Kuwabara, J.-H. Kim and C. A. Mirkin, *Science*, 2010, **330**, 66-69.

93. N. C. Gianneschi, P. A. Bertin, S. T. Nguyen, C. A. Mirkin, L. N. Zakharov and A. L. Rheingold, *J. Am. Chem. Soc.*, 2003, **125**, 10508-10509.

94. N. C. Gianneschi, S.-H. Cho, S. T. Nguyen and C. A. Mirkin, *Angew. Chem., Int. Ed.*, 2004, **116**, 5619-5623.

95. C. G. Oliveri, P. A. Ulmann, M. J. Wiester and C. A. Mirkin, *Acc. Chem. Res.*, 2008, **41**, 1618-1629.

96. C. K. A. Gregson, V. C. Gibson, N. J. Long, E. L. Marshall, P. J. Oxford and A. J. P. White, *J. Am. Chem. Soc.*, 2006, **128**, 7410-7411.

97. E. M. Broderick, N. Guo, C. S. Vogel, C. Xu, J. Sutter, J. T. Miller, K. Meyer, P. Mehrkhodavandi and P. L. Diaconescu, *J. Am. Chem. Soc.*, 2011, **133**, 9278-9281.

98. E. M. Broderick, N. Guo, T. Wu, C. S. Vogel, C. Xu, J. Sutter, J. T. Miller, K. Meyer, T. Cantat and P. L. Diaconescu, *Chem. Commun.*, 2011, **47**, 9897-9899.

99. A. J. D. Magenau, N. C. Strandwitz, A. Gennaro and K. Matyjaszewski, *Science*, 2011, **332**, 81-84.

100. N. Bortolamei, A. A. Isse, A. J. D. Magenau, A. Gennaro and K. Matyjaszewski, *Angew. Chem., Int. Ed.*, 2011, **123**, 11593-11596.

101. M. M. Caruso, D. A. Davis, Q. Shen, S. A. Odom, N. R. Sottos, S. R. White and J. S. Moore, *Chem. Rev.*, 2009, **109**, 5755-5798.

102. M. J. Kryger, M. T. Ong, S. A. Odom, N. R. Sottos, S. R. White, T. J. Martinez and J. S. Moore, *J. Am. Chem. Soc.*, 2010, **132**, 4558-4559.

103. K. L. Berkowski, S. L. Potisek, C. R. Hickenboth and J. S. Moore, *Macromolecules*, 2005, **38**, 8975-8978.

104. K. M. Wiggins, J. A. Syrett, D. M. Haddleton and C. W. Bielawski, *J. Am. Chem. Soc.*, 2011, **133**, 7180-7189.

105. J. N. Brantley, K. M. Wiggins and C. W. Bielawski, *Science*, 2011, **333**, 1606-1609.

106. C. R. Hickenboth, J. S. Moore, S. R. White, N. R. Sottos, J. Baudry and S. R. Wilson, *Nature*, 2007, **446**, 423-427.

107. J. M. Lenhardt, M. T. Ong, R. Choe, C. R. Evenhuis, T. J. Martinez and S. L. Craig, *Science*, 2010, **329**, 1057-1060.

108. G. Cravotto and P. Cintas, *Angew. Chem., Int. Ed.*, 2007, **46**, 5476-5478.

109. G. Oster and N.-L. Yang, *Chem. Rev.*, 1968, **68**, 125-151.

110. M. Tanabe and I. Manners, *J. Am. Chem. Soc.*, 2004, **126**, 11434-11435.

111. M. Tanabe, G. W. M. Vandermeulen, W. Y. Chan, P. W. Cyr, L. Vanderark, D. A. Rider and I. Manners, *Nat. Mater.*, 2006, **5**, 467-470.

112. X. Zheng, M. Yue, P. Yang, Q. Li and W. Yang, *Polym. Chem.*, 2012, **3**, 1982-1986.

113. S. Dadashi-Silab, C. Aydogan and Y. Yagci, *Polym. Chem.*, 2015, **6**, 6595-6615.

114. Y. Yagci, S. Jockusch and N. J. Turro, *Macromolecules*, 2010, **43**, 6245-6260.

115. T. Gong, B. J. Adzima and C. N. Bowman, *Chem. Commun.*, 2013, **49**, 7950-7952.

116. B. P. Fors and C. J. Hawker, *Angew. Chem., Int. Ed.*, 2012, **51**, 8850-8853.

117. J. Xu, S. Shanmugam, H. T. Duong and C. Boyer, *Polym. Chem.*, 2015.

118. S. Shanmugam, J. Xu and C. Boyer, *Chem. Sci.*, 2015, **6**, 1341-1349.

119. N. J. Treat, B. P. Fors, J. W. Kramer, M. Christianson, C.-Y. Chiu, J. R. d. Alaniz and C. J. Hawker, *ACS Macro Lett.*, 2014, **3**, 580-584.

120. J. H. Moon, J. Ford and S. Yang, *Departmental Papers (MSE)*, 2006, 100.

121. M. Husemann, M. Morrison, D. Benoit, J. Frommer, C. M. Mate, W. D. Hinsberg, J. L. Hedrick and C. J. Hawker, *J. Am. Chem. Soc.*, 2000, **122**, 1844-1845.

122. L. A. Connal, R. Vestberg, C. J. Hawker and G. G. Qiao, *Adv. Funct. Mater.*, 2008, **18**, 3315-3322.

123. L. A. Connal and G. G. Qiao, *Adv. Mater.*, 2006, **18**, 3024-3028.

124. J. A. Hiller, J. D. Mendelsohn and M. F. Rubner, *Nat.Matter.*, 2002, **1**, 59-63.

125. N. Moszner, U. Salz and J. Zimmermann, *Dent. Mater.*, 2005, **21**, 895-910.

126. H. J. Hageman, *Prog. Org. Coat.*, 1985, **13**, 123-150.

127. H. F. Gruber, *Prog. Polym. Sci.*, 1992, **17**, 953-1044.

128. J. P. Fouassier, D. J. Lougnot, A. Paverne and F. Wieder, *Chem. Phys. Lett.*, 1987, **135**, 30-34.

129. A. Borer, R. Kirchmayr and G. Rist, *Helv. Chim. Acta.*, 1978, **61**, 305-324.

130. D. Leopold and H. Fischer, *J. Chem. Soc., Perkin Trans.* 1992, **2**, 513-517.

131. N. Arsu and R. S. Davidson, *J. Photochem. Photobiol. A*, 1994, **84**, 291-297.

132. J. P. Fouassier and D. J. Lougnot, *J. Appl. Polym. Sci.*, 1987, **34**, 477-488.

133. A. Ledwith and M. D. Purbrick, *Polymer*, 1973, **14**, 521-522.

134. A. Ledwith, J. A. Bosley and M. D. Purbrick, *J. Oil Colour Chem. As.*, 1978, **61**, 95-104.

135. M. J. Davis, J. Doherty, A. A. Godfrey, P. N. Green, J. R. A. Young and M. A. Parrish, *J. Oil Colour Chem. As.*, 1978, **61**, 256-263.

136. J. Jakubiak, X. Allonas, J. P. Fouassier, A. Sionkowska, E. Andrzejewska, L. Linden and J. F. Rabek, *Polymer*, 2003, **44**, 5219-5226.

137. H. Ma, R. H. Davis and C. N. Bowman, *Macromolecules*, 2000, **33**, 331-335.

138. J. M. R. Narayanam and C. R. J. Stephenson, *Chem. Soc. Rev.*, 2011, **40**, 102-113.

139. S. Shanmugam, J. Xu and C. Boyer, *Macromolecules*, 2014, **47**, 4930-4942.

140. S. Shanmugam and C. Boyer, *J. Am. Chem. Soc.*, 2015, **137**, 9988-9999.

141. X. Miao, W. Zhu, Z. Zhang, W. Zhang, X. Zhu and J. Zhu, *Polym. Chem.*, 2014, **5**, 551-557.

142. A. Kermagoret, B. Wenn, A. Debuigne, C. Jérôme, T. Junkers and C. Detrembleur, *Polym. Chem.*, 2015, **6**, 3847-3857.

143. J. Yeow, J. Xu and C. Boyer, *ACS Macro Lett.*, 2015, **4**, 984-990.

144. S. Shanmugam, J. Xu and C. Boyer, *J. Am. Chem. Soc.*, 2015, **137**, 9174-9185.

145. X. Pan, N. Malhotra, J. Zhang and K. Matyjaszewski, *Macromolecules*, 2015.

146. N. J. Treat, H. Sprafke, J. W. Kramer, P. G. Clark, B. E. Barton, J. Read de Alaniz, B. P. Fors and C. J. Hawker, *J. Am. Chem. Soc.*, 2014, **136**, 16096-16101.

147. X. Pan, M. Lamson, J. Yan and K. Matyjaszewski, *ACS Macro Lett.*, 2015, **4**, 192-196.

148. M. Chen, M. J. MacLeod and J. A. Johnson, *ACS Macro Lett.*, 2015, **4**, 566-569.

149. P. Natarajan and G. Ferraudi, *Inorg. Chem.*, 1981, **20**, 3708-3712.

150. J. L. Kurz, R. Hutton and F. H. Westheimer, *J. Am. Chem. Soc.*, 1961, **83**, 584-588.

151. W. J. Lautenberger, E. N. Jones and J. G. Miller, *J. Am. Chem. Soc.*, 1968, **90**, 1110-1115.

152. H. Ishibashi, S. Haruki, M. Uchiyama, O. Tamura and J.-i. Matsuo, *Tetrahedron Lett.*, 2006, **47**, 6263-6266.

153. A. J. Clark, S. R. Coles, A. Collis, D. R. Fullaway, N. P. Murphy and P. Wilson, *Tetrahedron Lett.*, 2009, **50**, 6311-6314.

154. H. Ishibashi, M. Sasaki and T. Taniguchi, *Tetrahedron*, 2008, **64**, 7771-7773.

155. M. A. Tasdelen, M. Uygun and Y. Yagci, *Macromol. Rapid Commun.*, 2011, **32**, 58-62.

156. M. A. Tasdelen, M. Uygun and Y. Yagci, *Macromol. Chem. Phys.*, 2010, **211**, 2271-2275.

157. D. Konkolewicz, K. Schröder, J. Buback, S. Bernhard and K. Matyjaszewski, *ACS Macro Lett.*, 2012, **1**, 1219-1223.

158. M. Ciftci, M. A. Tasdelen, W. Li, K. Matyjaszewski and Y. Yagci, *Macromolecules*, 2013, **46**, 9537-9543.

159. A. Anastasaki, V. Nikolaou, Q. Zhang, J. Burns, S. R. Samanta, C. Waldron, A. J. Haddleton, R. McHale, D. Fox, V. Percec, P. Wilson and D. M. Haddleton, *J. Am. Chem. Soc.*, 2013, **136**, 1141-1149.

160. A. Anastasaki, V. Nikolaou, A. Simula, J. Godfrey, M. Li, G. Nurumbetov, P. Wilson and D. M. Haddleton, *Macromolecules*, 2014, **47**, 3852-3859.

161. A. Anastasaki, C. Waldron, V. Nikolaou, P. Wilson, R. McHale, T. Smith and D. M. Haddleton, *Polym. Chem.*, 2013, **4**, 4113-4119.

162. C. Boyer, A. Atme, C. Waldron, A. Anastasaki, P. Wilson, P. B. Zetterlund, D. Haddleton and M. R. Whittaker, *Polym. Chem.*, 2013, **4**, 106-112.

163. A. Anastasaki, V. Nikolaou, G. S. Pappas, Q. Zhang, C. Wan, P. Wilson, T. P. Davis, M. R. Whittaker and D. M. Haddleton, *Chem. Sci.*, 2014, **5**, 3536-3542.

164. B. Wenn, M. Conradi, A. D. Carreiras, D. M. Haddleton and T. Junkers, *Polym. Chem.*, 2014, **5**, 3053-3060.

165. J. Vandenbergh, G. Reekmans, P. Adriaensens and T. Junkers, *Chem. Sci.*, 2015, **6**, 5753-5761.

166. Y.-M. Chuang, B. Wenn, S. Gielen, A. Ethirajan and T. Junkers, *Polym. Chem.*, 2015, **6**, 6488-6497.

167. A. Anastasaki, V. Nikolaou, N. W. McCaul, A. Simula, J. Godfrey, C. Waldron, P. Wilson, K. Kempe and D. M. Haddleton, *Macromolecules*, 2015, **48**, 1404-1411.

168. T. G. Ribelli, D. Konkolewicz, S. Bernhard and K. Matyjaszewski, *J. Am. Chem. Soc.*, 2014, **136**, 13303-13312.

169. E. Frick, A. Anastasaki, D. M. Haddleton and C. Barner-Kowollik, *J. Am. Chem. Soc.*, 2015, **137**, 6889-6896.

170. O. F. Olaj, I. Bitai and F. Hinkelmann, *Angew. Chem., Int. Ed.*, 1987, **188**, 1689-1702.

171. D. Voll, T. Junkers and C. Barner-Kowollik, *J. Polym. Sci. Part A: Polym. Chem.*, 2012, **50**, 2739-2757.

172. E. Frick, H. A. Ernst, D. Voll, T. J. A. Wolf, A.-N. Unterreiner and C. Barner-Kowollik, *Polym. Chem.*, 2014, **5**, 5053-5068.

173. C. Barner-Kowollik, T. Gruendling, J. Falkenhagen and S. Weidner, *Mass spectrometry in Polym. Chem.*, John Wiley & Sons, 2012.

Photo-induced synthesis of α,ω-telechelic sequence-controlled multiblock copolymers

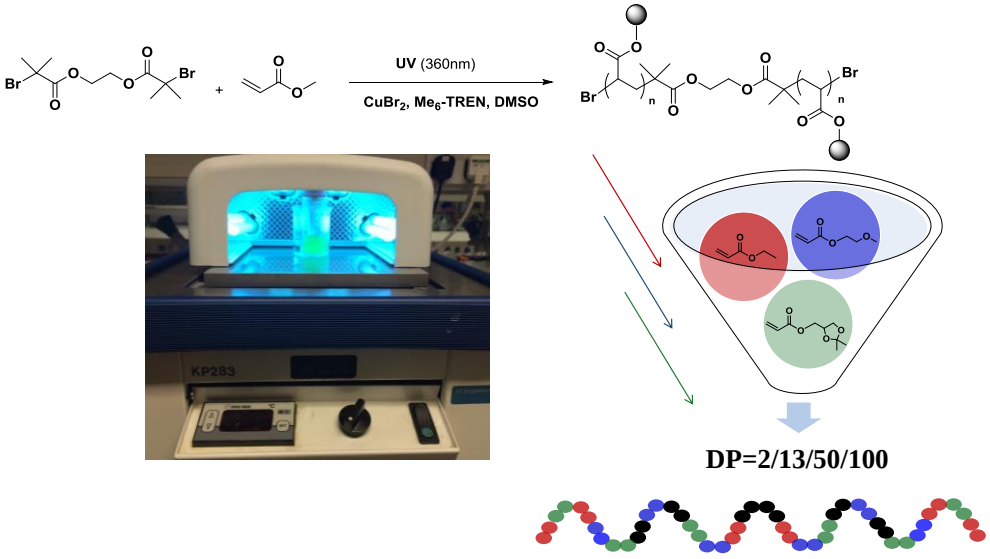

In this chapter, the photo-induced RDRP has been employed to synthesise α,ω-telechelic multiblock copolymers of a range of acrylic monomers. Under carefully optimised conditions, a well-defined tricosablock (23 blocks) copolymer was obtained (Đ = 1.18) with high conversion (98%) achieved throughout all the iterative monomer additions. Crucially, a reduced temperature (15 °C) was found to result in an observed decrease in the dispersities (1.14 vs 1.45) as opposed to when higher temperatures (50 °C) were employed. A number of bi-functional initiators were employed, including ethylene bis(2-bromoisobutyrate) (EbBiB), a PEG initiator (av. M_w = 1000 g.mol^{-1}) and bis[2-(2'-bromoisobutyryloxy)ethyl]disulphide ((BiBOE)$_2$S$_2$) resulting in low dispersed multiblock copolymers in various molecular weights (DP_n ~ 2/13/50/100 per block). Impressively, a high molecular weight undecablock (11 blocks) copolymer, of M_n = 150000 g.mol^{-1} and Đ = 1.22 was also synthesised. In order to demonstrate the symmetry of the resulting telechelic materials, a well-defined tridecablock (13 blocks, Đ = 1.18, M_n = 25000 g.mol^{-1}) was synthesised utilising a bi-functional disulfide initiator which was cleaved post polymerisation, yielding a polymer with narrow MWD at half the molecular weight of the parent polymer (Đ = 1.10, M_n = 12400 g.mol^{-1}).

2.1 Introduction

A major challenge for polymer chemistry is to mimic the complexity of biological macromolecules *via* synthetic methods. Natural polymers such as peptides and proteins are sophisticated complex structures that exhibit perfect monomer sequence in order to fulfil a predefined function. However, synthetic analogues of these domains have not yet been realised, although notable progress has been made over the past few years to achieve better control over the polymer primary sequence.[1, 2] Various approaches have been explored to precisely control the monomer sequence including single monomer addition,[3, 4] tandem monomer addition and modification,[5, 6] kinetic control,[7-9] as well as solution[10-15] and segregated[16] templating.

The implementation of single monomer addition *via* radical chain growth polymerisation techniques is challenging, if not impossible, given the reactive nature of the radical. However, the ability to control the sequence of multiple discrete regions within a macromolecular structure allows the introduction of functional domains along the polymer backbone. Thus, many RDRP techniques[17-20] have been developed for the synthesis of multiblock copolymers in an attempt to satisfy four major requirements i) quantitative or near-quantitative conversion for each block, ii) no purification step involved between each monomer addition, iii) low dispersities for all the blocks and iv) high end-group functionality.

These criteria were initially introduced by Whittaker and his co-workers utilising Cu(0)-mediated RDRP to synthesise a well-defined ($Đ$ ~ 1.20) acrylic hexablock copolymer (*DP* ~ 2 per block) in a very high yield.[18, 21, 22] When larger *DP* blocks were targeted (*DP* ~ 100 per block) triblocks and quasi-pentablock

copolymers could be prepared, however, a limitation was reached as full monomer conversion could not be achieved throughout the monomer additions.[23] The same technique was subsequently utilised by Haddleton and co-workers for the synthesis of multiblock glycopolymers with a good degree of monomer sequence control.[24, 25] The same group also demonstrated applicability of acrylamides reporting various acrylamide multiblock copolymers in < 5 h [26, 27] employing aqueous Cu(0)-mediated RDRP.[27]

An alternative approach utilising RAFT has also been developed recently by Perrier and co-workers synthesising an icosablock copolymer comprising of acrylamides in both organic and aqueous media.[19, 28-31] However, the high temperature (~70 °C) employed is the main limitation of this approach. High temperatures are disadvantageous for the polymerisation of monomers that possess an LCST upon polymerisation (*e.g.* NIPAM) while unavoidable termination and side reactions (*e.g.* backbiting, chain transfer) are also more likely to occur as the temperature is increased.[32]

Recently, Haddleton and co-workers reported the photo-induced RDRP of acrylates in the presence of ppm concentration of $CuBr_2$ and Me_6-Tren.[33, 34] A family of four acrylic monomers was employed including: methyl acrylate (MA), ethyl acrylate (EA), ethylene glycol methyl ether acrylate (EGA) and solketal acrylate (SA). The high end-group fidelity of the obtained polymers was subsequently exploited for the synthesis of acrylic multiblock copolymers without any need for purification between the iterative monomer additions. However, a limitation of this work was reached as "only" 12 blocks (11 chain extensions) could be achieved when utilising a mono-functional initiator before accumulated termination had a

detrimental effect on the dispersity. Moreover, a pentablock copolymer (*DP* ~ 100 per block, final M_n = 80000 g.mol^{-1}, $Đ$ = 1.21) was found to be the upper limitation of this system and higher molecular weight multiblock copolymers were not obtained[20]. Therefore the synthesis of *a,ω*-telechelic materials would be able to circumvent these issues as the same number of chain extensions would result in a higher number of blocks (2n-1 blocks for n chain extensions) and thus less termination and side reactions. Furthermore, telechelic materials are of high interest due to the ability to functionalise both ends post polymerisation and further enhance their properties.[35] Moreover, the utility of bi-functional macroinitiators (*e.g.* PEG) allows for the incorporation of additional properties alongside the polymer backbone[36].

In this chapter, the synthesis of *α,ω*-telechelic multiblock copolymers utilising various bi-functional initiators, including EbBiB, ($(BiBOE)_2S_2$) and a PEG initiator is investigated. The photo-induced one pot multi-step sequential polymerisation process was employed to yield a well-defined tricosablock copolymer (23 blocks, 12 chain extensions, $Đ$ ~ 1.18). Importantly, the reaction temperature was discovered to have a significant effect on the control over the molecular distributions as a dispersity of 1.45 was obtained for the nonadecablock copolymer at 50 °C (*vs* 1.14 when the polymerisation was performed at 15 °C). Subsequently, the effect of chain length was investigated allowing for higher molecular weight blocks to be obtained. Remarkably, an undecablock (11 blocks) copolymer, of M_n = 150000 g.mol^{-1}, $Đ$ = 1.22 could be attained, which represents the highest molecular weight multiblock copolymer reported to date. Finally, when a disulfide initiator was employed, the final tridecablock (13 blocks, M_n = 25000 g.mol^{-1}, $Đ$ = 1.18) copolymer was subsequently cleaved yielding an impressively

well-defined polymer at exactly half of the molecular weight (M_n = 12400 g.mol^{-1}, $Đ$ = 1.10), thus illustrating the symmetrical nature of the materials prepared.

2.2 Results and Discussion

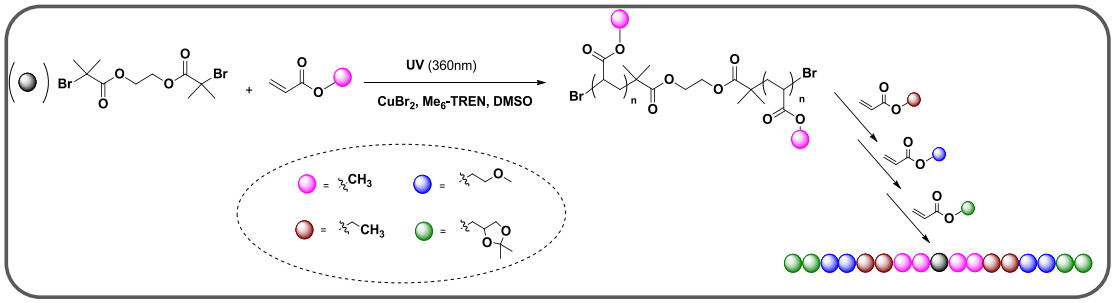

Scheme 2.1: General scheme for the synthesis of *α,ω*-telechelic multiblock copolymers *via* photo-induced RDRP utilising EbBiB.

Initially, the ability of the bi-functional initiator (EbBiB) to afford multiblock copolymers was investigated utilising previously employed conditions (Scheme 2.1).[33] A feed ratio of [I]:[$CuBr_2$]:[Me_6-Tren] = [1]:[0.04]:[0.24] was employed in DMSO (50% *v/v* with respect to monomer) while an additional amount of [$CuBr_2$]:[Me_6-Tren] in DMSO ([0.04]:[0.24] in respect to initiator) was injected in the reaction mixture upon every third monomer addition, following previously optimised conditions.[20] Upon sampling the conversions were determined by ^{1}H NMR analysis (Section 2.4.4, Figure 2.13), using the signals at 5.5-6.5 ppm and at 3.5 ppm which are attributed to the acrylic and OCH_3 groups, respectively. After 10 h, full monomer conversion was attained ($Đ$ = 1.40) and a deoxygenated solution of EA and DMSO (2:1) was subsequently injected in the reaction mixture. A relatively high dispersity of the first block was measured with addition of the second aliquot of monomer giving a relative reduction in the dispersity ($Đ$ = 1.29), which was maintained for all of the following monomer additions ($Đ$ = 1.25-1.35, Table 2.1,

Section 2.4.4, Table 2.4). In particular, the final nonadecablock (10 chain extensions) copolymer presented a bimodal molecular weight distribution (*Đ* = 1.45, Figure 2.1 and 2.3), thus suggesting considerable termination events and/or side reactions under these conditions. A greater extent of termination for a telechelic initiator (in comparison with a mono-functional analogue) is not surprising given the increase in the number of initiating sides (2-fold).

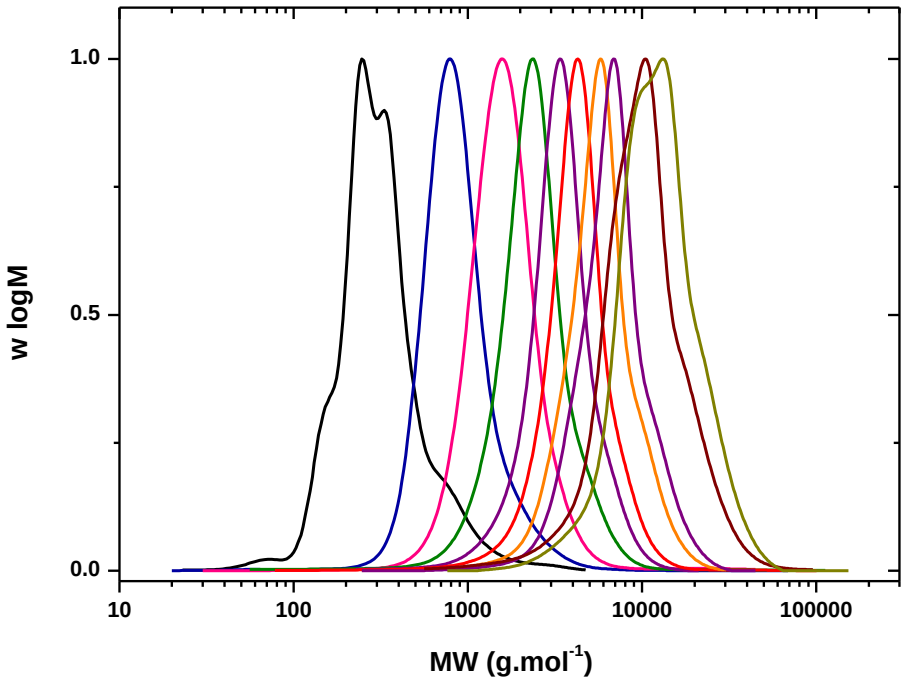

Figure 2.1: Molecular weight distributions for successive cycles during synthesis of the nonadecablock copolymer (*DP* = 4 per chain extension or *DP* = 2 per block) in DMSO at 50 ^{o}C.

In an attempt to optimise the conditions, it was speculated that a lower reaction temperature might suppress the unwanted termination events and/or side reactions. It should be noted that in the initial work no difference in the rate (or the control) between a typical UV experiment (~50 °C) and the one carried out at lower

temperature (~25 °C) was observed for the synthesis of a homopolymer.[20] However, since bi-functional multiblock copolymers are more complex structures (and the system is forced to reach full conversion multiple times, thus termination is more likely to accumulate) any termination would be highlighted in such a system. In order to verify this hypothesis the effect of temperature was investigated using a cold plate (Section 2.4.4, Figure 2.14) to maintain the temperature at ~15 °C. Kinetic experiments for the polymerisation of MA at 50 °C and 15 °C utilising typical conditions (*DP* = 50) revealed similar rates (4 h *vs* 5 h respectively) and $\ln[M]_o/[M]_t$ increased linearly with time in both cases demonstrating a constant radical concentration (Figure 2.2, Section 2.4.4, Figures 2.15 & 2.16).

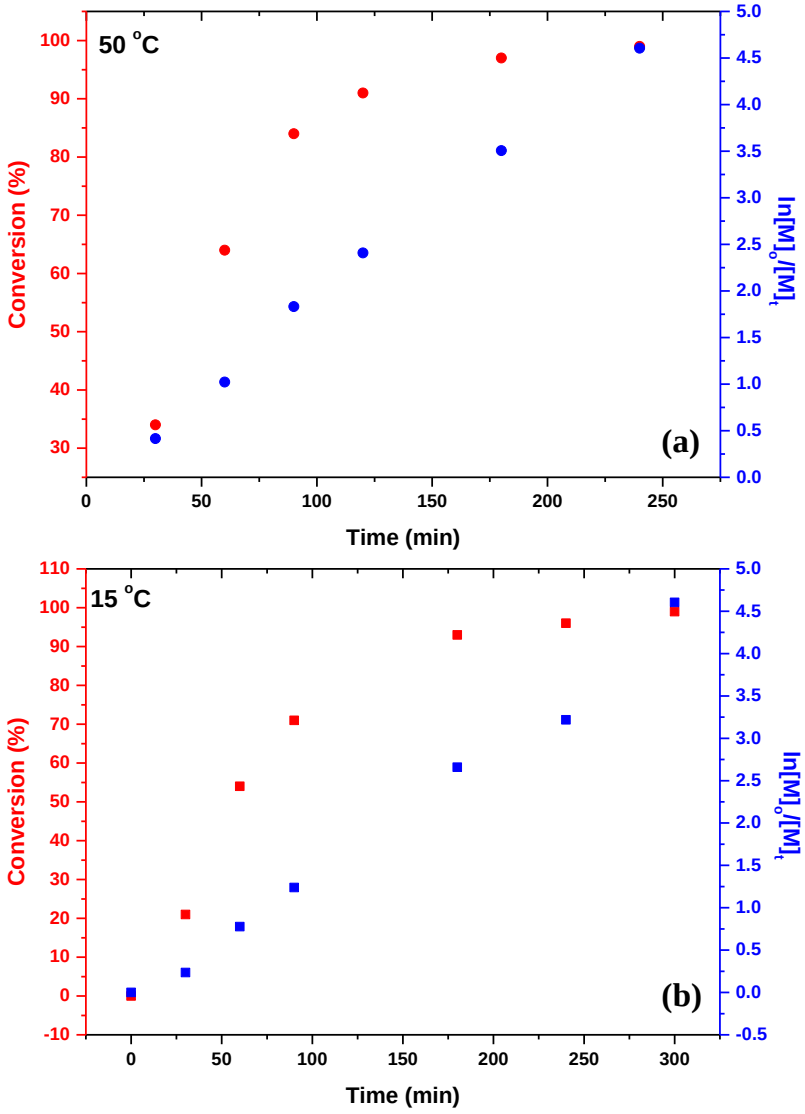

Figure 2.2: Kinetic data for the photo-induced polymerisation of MA at (a) 50 °C and (b) 15 °C utilising EbBiB.

Encouragingly, the homopolymerisation of MA furnished polymers with lower final dispersity ($Đ$ = 1.20 *vs* $Đ$ = 1.40 for the typical UV experiment). Following several monomer additions, a nonadecablock copolymer (10 chain extensions) was obtained and the low dispersity was retained ($Đ$ = 1.14 *vs* $Đ$ = 1.45 for the typical UV experiment, Figure 2.3, Table 2.1).

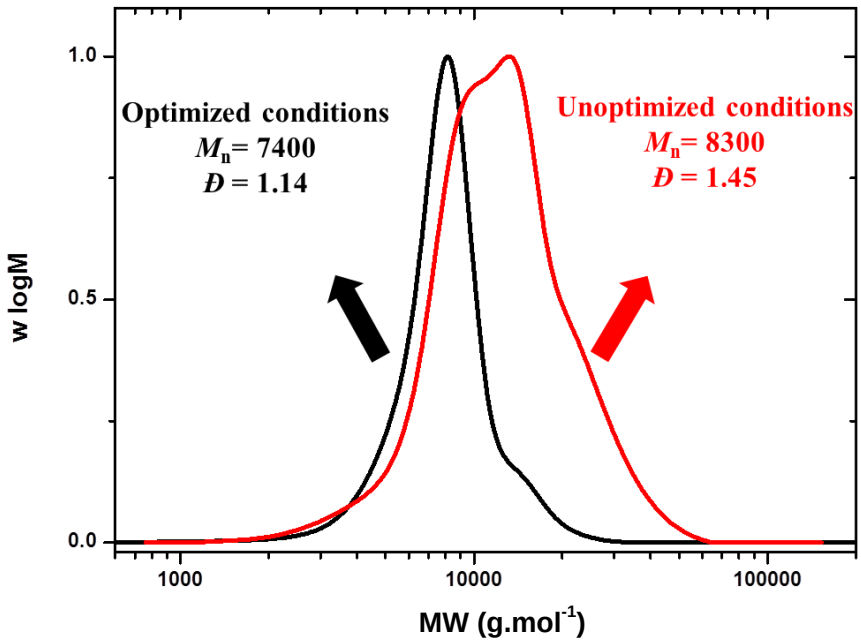

Figure 2.3: Comparison of final molecular weight distributions (nonadecablock copolymer) obtained under optimised conditions ("cooling" plate) and unoptimised conditions *via* photo-induced RDRP.

Table 2.1: Comparison of multiblock copolymers obtained under optimised conditions ("cooling" plate) and unoptimised conditions *via* photo-induced RDRP.

Cycle	Un-optimised conditions				Optimised Conditions			
	Conv. (%)	$M_{n,th}$ (g.mol^{-1})	$M_{n,SEC}$ (g.mol^{-1})	$Đ$	**Conv. (%)**	$M_{n,th}$ (g.mol^{-1})	$M_{n,SEC}$ (g.mol^{-1})	$Đ$
1	100	700	265	1.40	100	700	400	1.20
2	99	1100	750	1.29	99	1100	950	1.20
3	99	1600	1400	1.27	99	1600	1500	1.19
4	99	2400	2000	1.26	99	2400	2200	1.16
5	98	2700	2900	1.26	98	2700	3000	1.14
6	99	3100	3800	1.25	99	3100	3600	1.14
7	98	3400	5000	1.26	98	3400	4700	1.13
8	99	4100	6000	1.28	99	4100	5500	1.14
9	99	4600	8000	1.35	99	4600	6500	1.15
10	99	5000	8300	1.45	98	5000	7400	1.14
11	-		-	-	99	5700	8200	1.19
12	-		-	-	98	6100	9600	1.18
13	-		-	-	100	6400	13000	1.28

Remarkably, under the optimised "cooling" conditions the nonablock copolymer could be further chain extended to yield a tricosablock copolymer, poly(EA_2-*b*-SA_2-*b*-EA_2-*b*-EGA_2-*b*-SA_2-*b*-MA_2-*b*-EGA_2-*b*-MA_2-*b*-SA_2-*b*-EGA_2-*b*-EA_2-*b*-MA_2-I-MA_2-*b*-EA_2-*b*-EGA_2-*b*-SA_2-*b*-MA_2-*b*-EGA_2-*b*-MA_2-*b*-SA_2-*b*-EGA_2-*b*-EA_2-*b*-SA_2-*b*-EA_2) (or poly(MA_2-*b*-EA_2-*b*-EGA_2-*b*-SA_2-*b*-MA_2-*b*-EGA_2-*b*-MA_2-*b*-SA_2-*b*-EGA_2-*b*-EA_2-*b*-SA_2-*b*-EA_2)$_2$ ($Đ$ = 1.18, M_n = 9600 g.mol^{-1}). Beyond this,

further chain extensions resulted in broader molecular weight distributions (Figure 2.4). Nevertheless, a pentacosablock copolymer (25 blocks, 13 chain extensions) was attained in a quantitative manner (100% conversion, $Đ$ = 1.28, M_n = 13000 g.mol^{-1}), which represents the largest number of blocks reported in the literature to date (Section 2.4.4, Figures 2.17 & 2.18, Table 2.5).

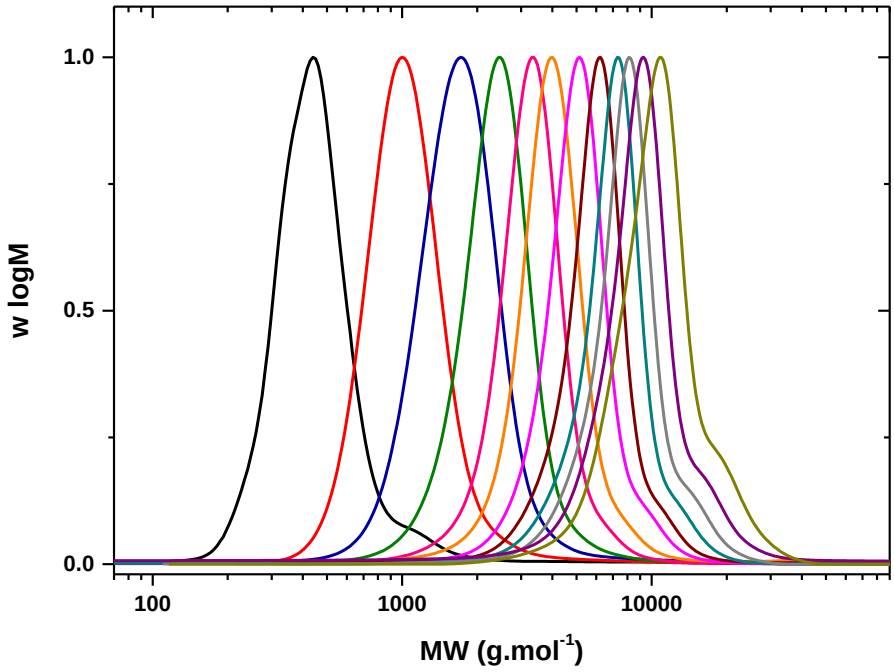

Figure 2.4: Molecular weight distributions for successive cycles during synthesis of the tricosablock copolymer (*DP* = 4 per chain extension or *DP* = 2 per block) in DMSO at 15 ^{o}C.

Higher molecular weight block lengths were also targeted as an attempt to further investigate this system. Thus, a multiblock copolymer comprised of 13 repeat units per block (or 26 repeat units per chain extension) was attempted. Excellent end-group fidelity was confirmed by MALDI-ToF-MS for the initial homopolymer with the main polymer peak distribution corresponding to PMA initiated by the EbBiB and terminated by two bromine atoms (Figure 2.5c,d). Pleasingly, upon 6 chain

extensions, this photo-induced polymerisation protocol afforded a well-defined undecablock copolymer (11 blocks, 6 chain extensions, $Đ$ = 1.17, M_n = 22000 g.mol^{-1} (Figure 2.5a,b, Table 2.2, Section 2.4.4, Table 2.6). A small high molecular weight shoulder can be observed in SEC which could be attributed to bimolecular coupling as indicated by the M_p value of the shoulder being at double the molecular weight as opposed to the main polymer peak distribution. However, it is important to note that for bi-functional initiators (and resulting telechelic polymers) termination by bimolecular coupling still maintains a near perfect bi-functional polymer with bromine chain ends.

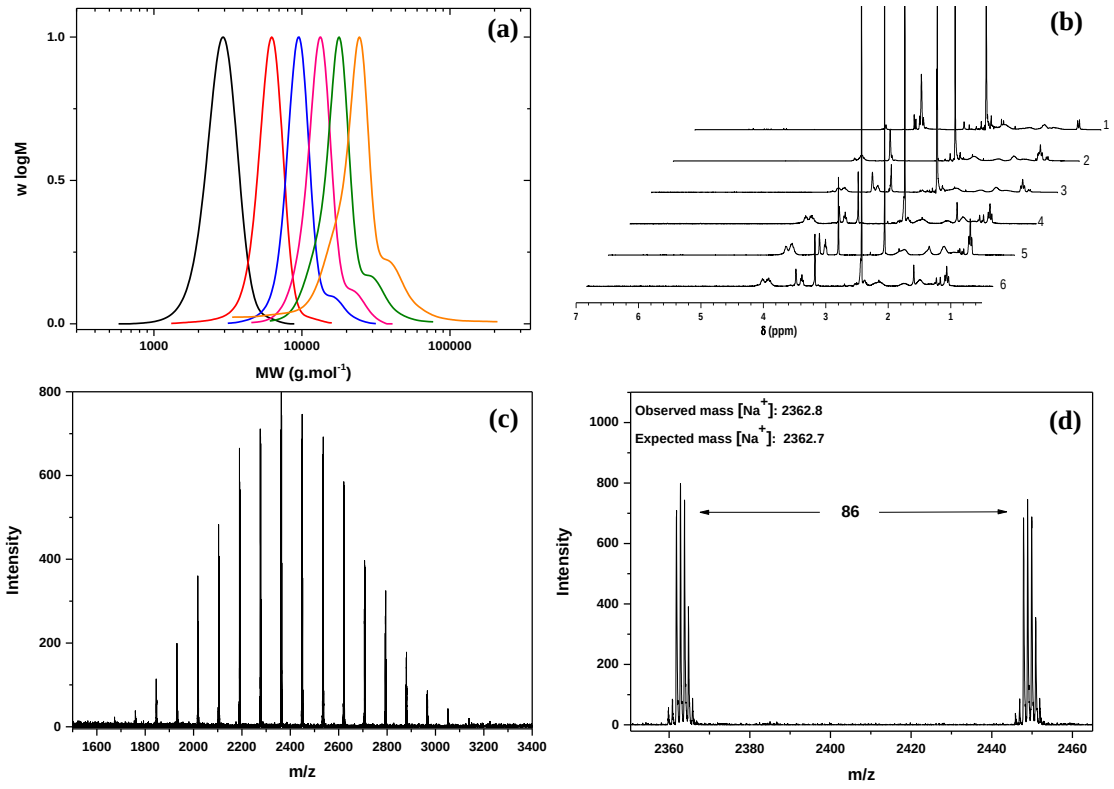

Figure 2.5: (a) Molecular weight distributions, (b) ^{1}H NMR for the successive cycles during synthesis of the undecablock copolymer (*DP* = 26 per chain extension or *DP* = 13 per block) in DMSO at 15 ^{o}C and (c), (d) MALDI-ToF-MS of the first chain extension.

The livingness of a system is strongly correlated with the *DP* targeted. Thus, the next target was to assess if multiblock copolymers exhibiting longer blocks could also result in well-defined polymers under our conditions. High molecular weight blocks are of great interest due to their ability to self-assemble and phase-separate forming higher ordered structures.[37-39]When each block was composed by 50 repeat units (100 repeat units per chain extension) the one pot, multistep sequential photo-induced polymerisation furnished a nonablock copolymer (5 chain extensions) with a low final dispersity ($Đ$ = 1.18) (Figure 2.6, Table 2.2) and quantitative or near-quantitative (> 98%) conversions maintained throughout the sequential monomer additions (Section 2.4.4, Figure 2.19, Table 2.7). It should be noted that quantitative conversions are important to ensure the structural integrity of the multiblocks and the high yield of the final material. Moreover, when the polymerisations are carried out to complete or high conversions, the monomer concentration decreases significantly and thus the propagation process is slow, whereas bimolecular termination, being second order with respect to radical concentration, becomes more prominent. Thus, pushing this system to reach full conversion upon each monomer addition further demonstrates the robustness and the versatility of the technique.

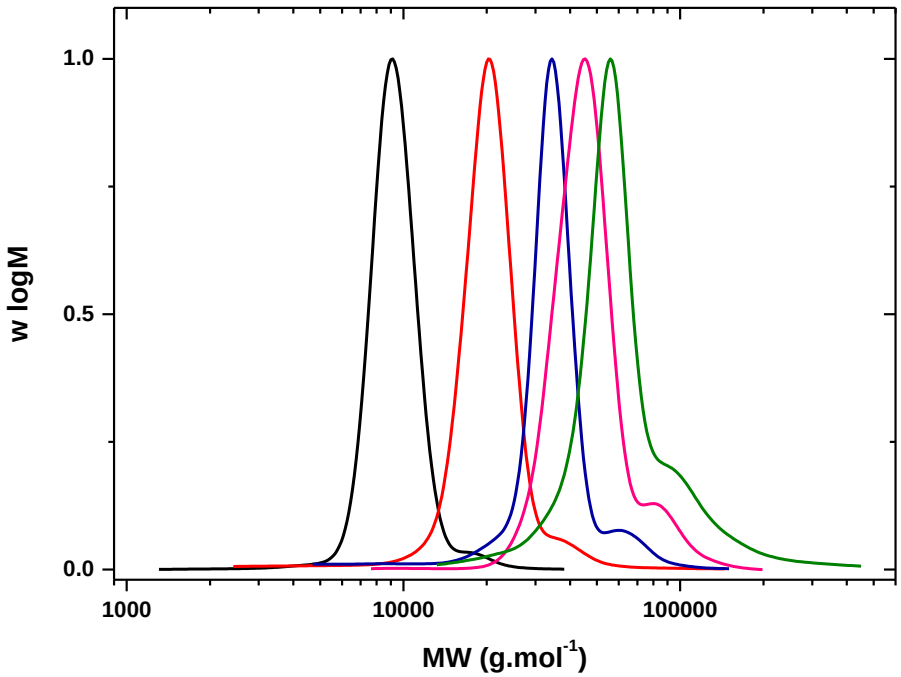

Figure 2.6: Molecular weight distributions for the successive cycles during synthesis of the nonablock copolymer (*DP* = 100 per chain extension or *DP* = 50 per block) in DMSO at 15 ^{o}C.

Table 2.2: Summary of multiblock copolymers prepared utilising EbBiB.

Multiblock Copolymer	No. of blocks	Conversion (%)	$M_{n,th}$ (g.mol^{-1})	$M_{n,SEC}$ (g.mol^{-1})	$Đ$
***DP* = 2** 	23	99	6400	9600	1.18
***DP* = 13** 	11	99	19000	22000	1.17
***DP* = 50** 	9	98	58000	56000	1.18
***DP* = 100** 	9	99	117000	107000	1.19

Identical conditions were subsequently applied for a multiblock copolymerisation with even higher chain length (*DP* = 200 per addition or 100 per block). The first 3 chain extensions proceeded as expected, with a final dispersity = 1.09 while good correlation between the theoretical and the experimental values further confirms the controlled/living character of the polymerisation. However, during the polymerisation of the heptablock copolymer, cessation of the stirring was observed (Figure 2.7a) due to the increased viscosity. Unfortunately, the addition of the fourth aliquot of monomer did not restore the stirring and two layers were formed in the reaction vial (upper layer: monomer, bottom layer: macroinitiator), disturbing the efficient mixing of the monomer with the macroinitiator. However, with the use of a vortex mixer (2 min) the mixture became homogeneous again and subsequently the vial was re-exposed to UV irradiation. Although stirring ceased again after a few hours, the polymerisation surprisingly reached quantitative conversion and the MWDs of the nonablock copolymer remained narrow (*Đ* = 1.19). The procedure was repeated yielding a well-defined undecablock copolymer (13 blocks, 6 chain extensions, *Đ* = 1.22, M_n = 150000 g.mol^{-1} (Figure 2.7b, Table 2.2, Section 2.4.4, Figure 2.20, Table 2.8).

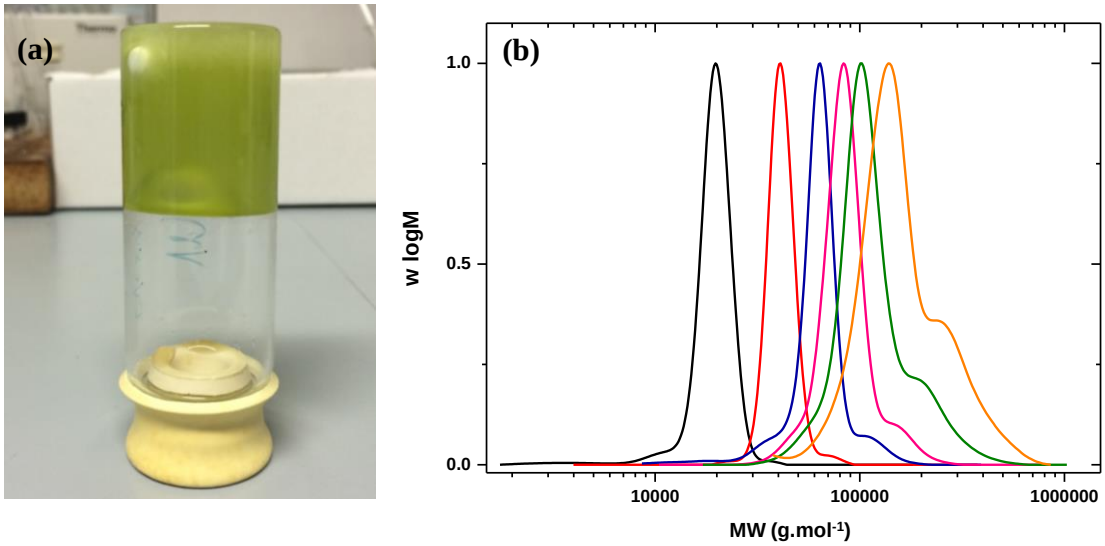

Figure 2.7: (a) Photo of the undecablock copolymer (*DP* = 200 per chain extension or *DP* = 100 per block) obtained upon cessation of the stirring in DMSO at 15 °C and (b) molecular weight distributions for the successive cycles during synthesis of the nonablock copolymer (*DP* = 200 per chain extension or *DP* = 100 per block) in DMSO at 15 °C.

It should be noted that in RDRP techniques (ATRP, SET-LRP, RAFT *etc.*) which involve radicals, termination will always occur despite the best efforts to suppress this. Termination events and side reactions are best highlighted by plotting the evolution of molecular weight with each addition of monomer (Figure 2.8). In the absence of termination, M_n should increase linearly, with little deviation from $M_{n,th}$. This is indeed the case for *DP* = 13/50/100 (Figure 2.8b, c, d), where the good correlation between theoretical and experimental values confirms the controlled/living character of the polymerisations. However, a deviation in the final molecular weight is observed for lower targeted *DP*, (Figure 2.8a) where good agreement is maintained only up to the 6th chain extension. After this point, an upward shift in M_n was observed which can be attributed to coupling reactions that occur as a result of the increased reaction times. Nevertheless, such highly complex

structures can be obtained in very high yields with very narrow MWDs for all the *DP* targeted.

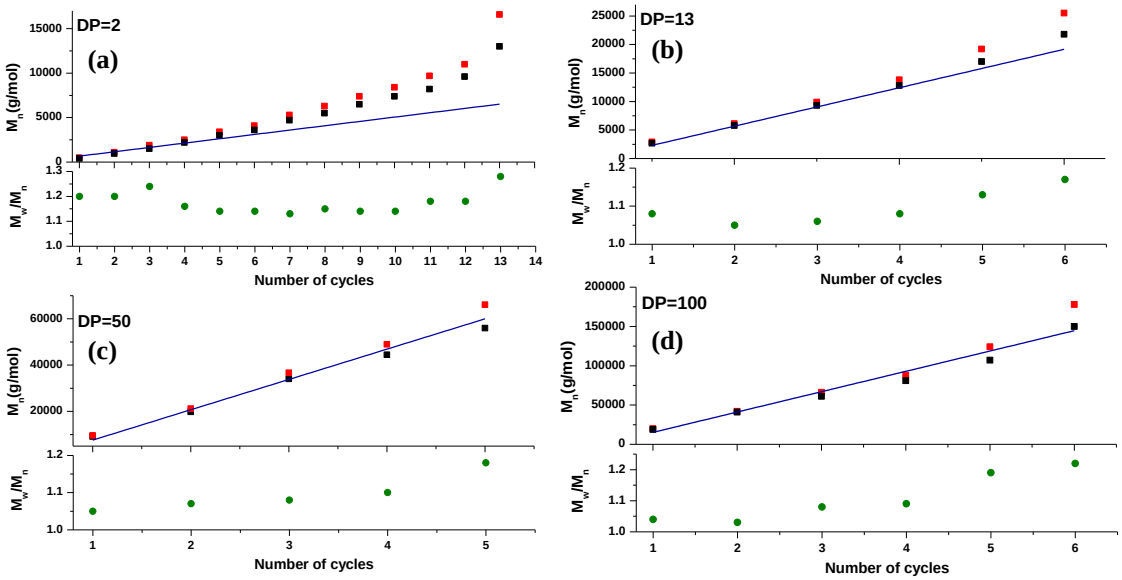

Figure 2.8: Evolution of number average molecular weights and dispersity with the number of blocks or the preparation of (a) tricosablock copolymer (*DP* = 2), (b) undecablock copolymer (*DP* = 13), (c) nonablock copolymer (*DP* = 50) and (d) undecablock copolymer copolymer (*DP* = 100). The blue line represents the theoretical molecular weight, black and red squares represent the experimental M_n and M_w from SEC, green cycles represent the dispersity from SEC.

The use of PEG macroinitiators (both mono-functional and bi-functional) is common in the synthesis of block copolymer and has attracted considerable interest for various applications.[36] Thus, we were interested to test the versatility of this technique utilising a bi-functional PEG initiator, which was synthesised according to a literature protocol (Section 2.4.4, Figures 2.21-2.23).[40] From the perspective of multiblock preparation it should be noted that the incorporation of a PEG macroinitiator would result in 2n + 1 blocks for n chain extensions. Pleasingly, a well-defined tridecablock copolymer was attained (*DP* = 26 per addition, *DP* = 13

per block, $Đ$ = 1.15, M_n = 24600 g.mol^{-1} (Figure 2.9). Further chain extensions resulted in broader MWDs. Nevertheless, a pentadecablock copolymer could be obtained in a quantitative manner with M_n = 29000 g.mol^{-1} and $Đ$ = 1.24 (Table 2.3, Section 2.4.4, Figures 2.24 & 2.25, Table 2.9). Thus, macroinitiators were proved to be compatible with the optimised polymerisation conditions.

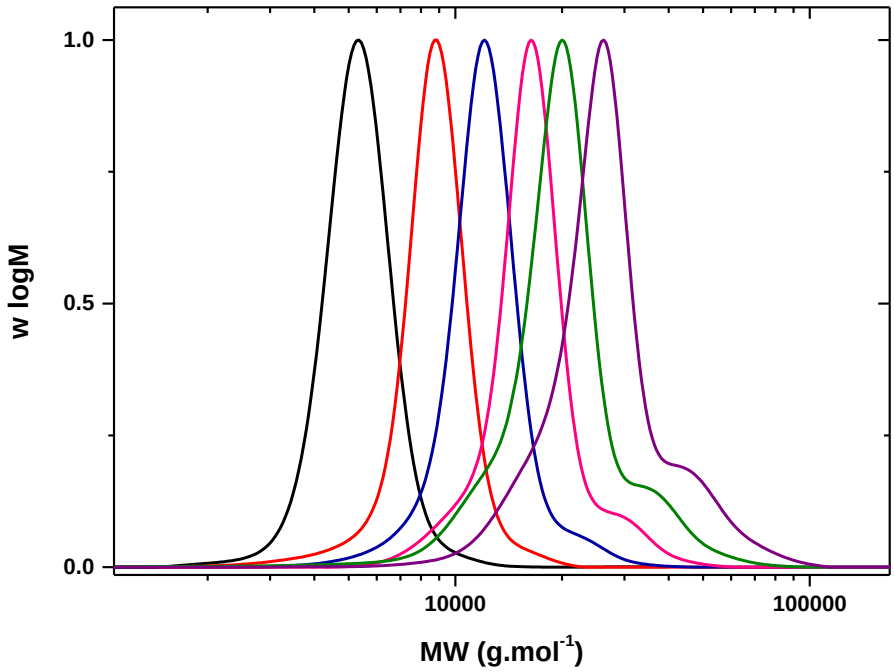

Figure 2.9: Molecular weight distributions for the successive cycles during synthesis of the tridecablock copolymer (*DP* = 26 per chain extension or *DP* = 13 per block) utilising a PEG bi-functional initiator in DMSO at 15 ^{o}C.

Table 2.3: Summary of multiblock copolymers obtained utilising a PEG and a disulphide bi-functional initiator respectively.

Multiblock Copolymer	Conv. (%)	$M_{n,th}$ (g.mol^{-1})	$M_{n,SEC}$ (g.mol^{-1})	$Đ$
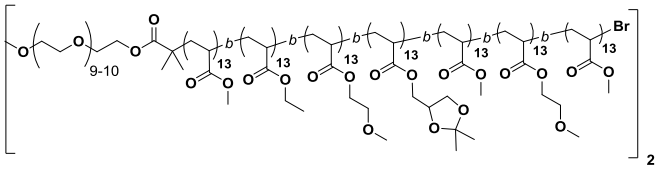	98	22000	29000	1.24
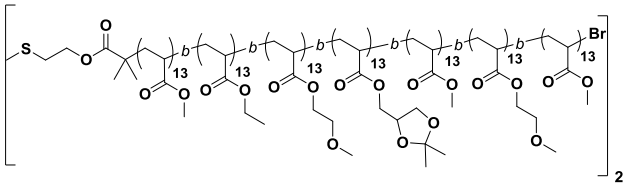	99	21000	25000	1.18

Typically, the synthesis of near perfect bi-functional polymers can be demonstrated experimentally by post polymerisation modification, halogen exchange experiments and chain extension.[41] Chain extension verifies the functionality of the prepared poly(acrylates) by demonstrating that at least one chain end has active bromine end-groups. However, it does not confirm that polymerisation is initiated from both *α,ω*-chain ends. In order to assess the retention of both chain ends, a disulphide initiator was employed for the preparation of a multiblock copolymer. MALDI-ToF-MS of the initial homopolymer confirmed the existence of the *α,ω*-bromine functional polymer chains and the presence of the initiator (and thus the S-S moieties, Figure 2.9c,d) in the polymer backbone. This high end-group fidelity was subsequently exemplified by one pot sequential additions, yielding a tridecablock copolymer with narrow molecular weight distribution ($Đ$ = 1.18) and final M_n of 25000 g.mol^{-1} (Figure 2.9a,b, Table 2.3, Section 2.4.4, Table 2.10).

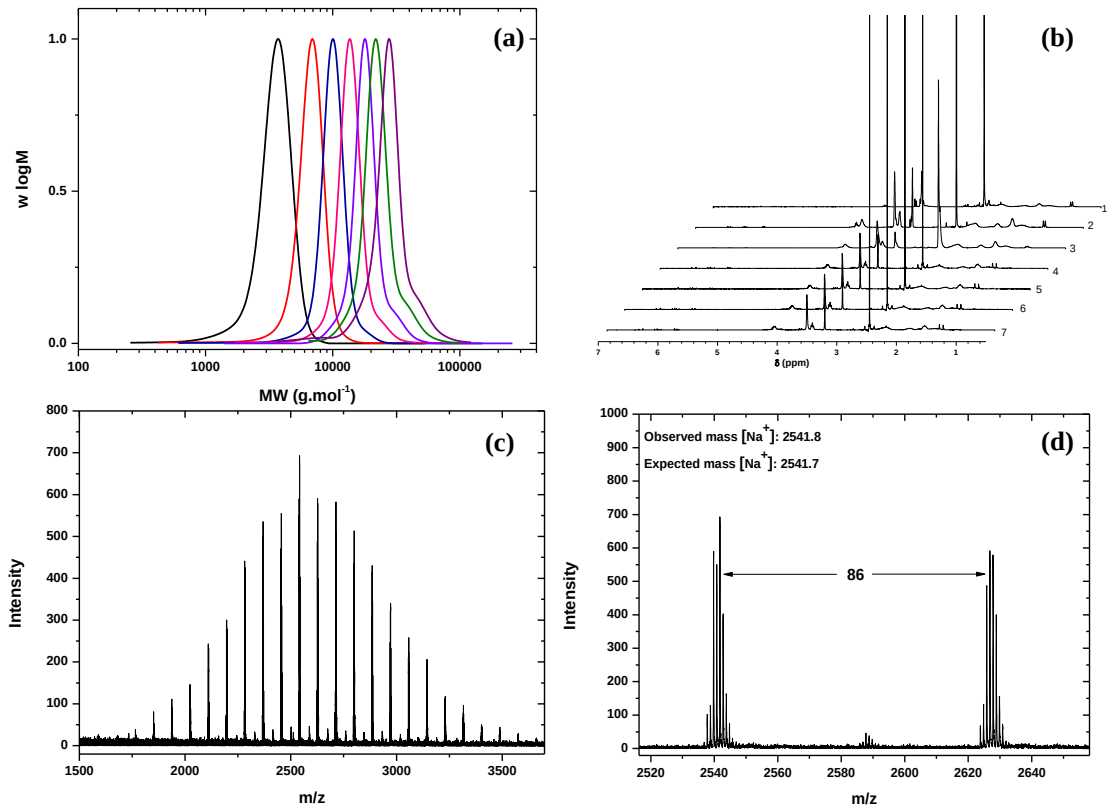

Figure 2.10: (a) Molecular weight distributions, (b) ^{1}H NMR for the successive cycles during synthesis of the tridecablock copolymer (*DP* = 26 per chain extension or *DP* = 13 per block) in DMSO at 15 ^{o}C utilising $(BiBOE)_2S_2$ and (c), (d) MALDI-ToF-MS of the first chain extension.

Subsequently, an excess of tributylphosphine was added in order to reduce the disulphide bond. Within 2 h quantitative reduction was observed as indicated by the complete shift of the molecular peak distribution from M_n = 25000 g.mol^{-1} ($Đ$ = 1.18) to M_n = 12400 while maintaining low dispersity ($Đ$ = 1.10, Figure 2.11 & 2.12). Despite the high complexity of these multiblocks structures, this is indicative of a telechelic polymerisation proceeding throughout the multi-step additions.

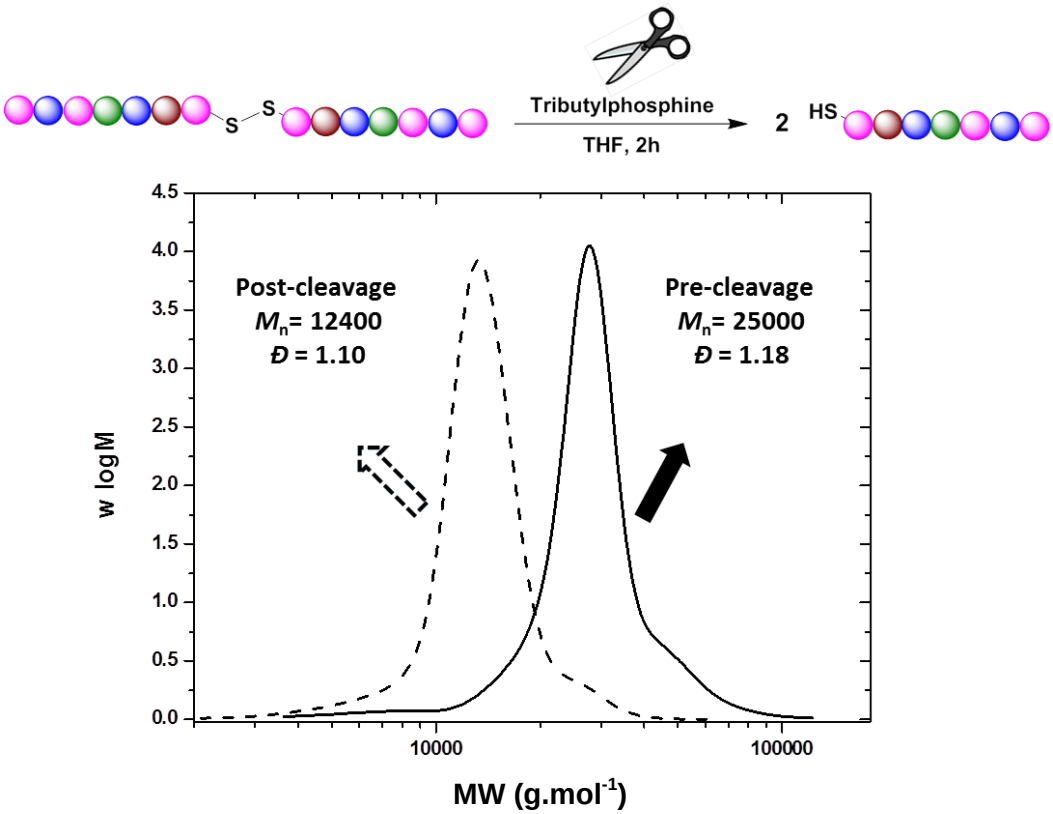

Figure 2.11: Complete reduction of the tridecablock copolymer utilising tributylphosphine.

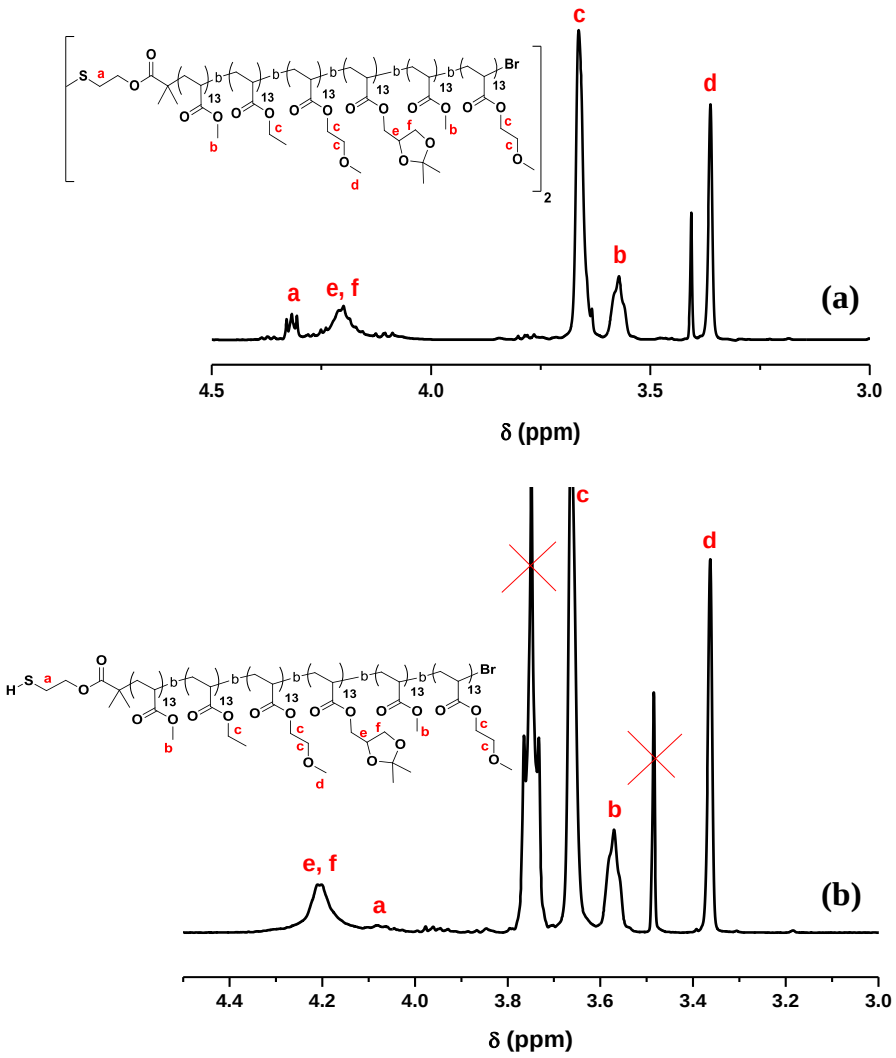

Figure 2.12: ^{1}H NMR of the (a) tridecablock copolymer (*DP* = 26 per chain extension or *DP* = 13 per block) in DMSO at 15 ^{o}C, utilising $(BiBOE)_2S_2$ and (b) ^{1}H NMR of the reduced tridecablock copolymer.

2.3 Conclusions

In this chapter, the synthesis of *α,ω*-telechelic multiblock copolymers *via* photo-induced RDRP of acrylic monomers was presented. Various bi-functional initiators were successfully employed to yield well-defined multiblock copolymers in high yields, exhibiting narrow MWDs (*Đ* < 1.19) with different chain lengths (*DP* ~ 4/26/100/200 per chain extension or *DP* ~ 2/13/50/100 per block). Crucially, low temperatures were found to decrease the dispersity values from 1.45 (50 °C) to 1.14 (15 °C), suggesting increased termination and side reactions at elevated temperatures. Under these optimised conditions, a well-defined tricosablock copolymer (*Đ* = 1.18, M_n = 9500 g.mol^{-1}, *DP* ~ 2 per block) and a high molecular weight undecablock copolymer (*Đ* = 1.22, M_n = 150000 g.mol^{-1}) were obtained which represent the highest number of blocks and the highest molecular weight multiblock respectively to date. Finally, the symmetrical nature of the telechelic materials was demonstrated by cleaving the S-S bond of a tridecablock copolymer (initiated by a disulphide initiator), furnishing a low dispersed multiblock copolymer at half of the molecular weight of the telechelic starting material.

2.4 Experimental

2.4.1 Materials and Methods

All materials were purchased from Sigma Aldrich or Fischer Scientific unless otherwise stated. Copper(II) bromide ($CuBr_2$) and tributylphosphine were used as received. All monomers were passed through a basic Al_2O_3 chromatographic column prior to use to remove the inhibitor. Tris-(2-(dimethylamino)ethyl)amine (Me_6-Tren)

was synthesised according to previously reported literature.[42] Solketal acrylate was synthesised according to a reported procedure[43] and distilled under reduced pressure (45 °C, 10^{-1} mbar) to yield a colourless liquid. EbBiB, PEG (*av.* M_w = 1000 g.mol^{-1}) and ($(BiBOE)_2S_2$) were also synthesised according to literature protocols.[40, 44]

2.4.2 Instrumentation

^{1}H NMR spectra were recorded on Bruker DPX-250 and DPX-300 spectrometers using deuterated chloroform ($CDCl_3$) obtained from Aldrich. Chemical shifts are given in ppm downfield from the internal standard tetramethylsilane. Size exclusion chromatography (SEC) measurements were conducted using an Agilent 1260 GPC-MDS fitted with differential refractive index (DRI), light scattering (LS) and viscometry (VS) detectors equipped with 2 × PLgel 5 mm mixed-D columns (300 × 7.5 mm), 1 × PLgel 5 mm guard column (50 × 7.5 mm) and autosampler. Narrow linear poly(methyl methacrylate) standards in range of 200 to 1.0 × 10^6 g.mol^{-1} were used to calibrate the system. All samples were passed through 0.45 μm PTFE filter before analysis. The mobile phase was chloroform with 2% triethylamine at a flow rate of 1.0 mL/min. SEC data was analysed using Cirrus v3.3. Matrix assisted laser desorption ionization mass spectrometry (MALDI-ToF-MS) was conducted using a Bruker Daltonics Ultraflex II MALDI-ToF-MS mass spectrometer, equipped with a nitrogen laser delivering 2 ns laser pulses at 337 nm with positive ion ToF detection performed using an accelerating voltage of 25 kV. Solutions in tetrahydrofuran (50 μL) of trans-2-[3-(4-tert-butylphenyl)-2-methyl-2-propylidene] malonitrile (DCTB) as matrix (saturated solution), sodium iodide as cationisation agent (1.0 mg/mL) and sample (1.0 mg/mL)

were mixed, and 0.7 μL of the mixture was applied to the target plate. Spectra were recorded in reflector mode calibrating PEG-Me 1100 kDa. The source of UV light was a UV nail gel curing lamp (available online from a range of suppliers) (λ_{max} ~ 360 nm) equipped with four 9W bulbs. The "cooling" plate utilised for this study was from CAMLAB (KP283).

2.4.3 General procedures

(a) Typical procedure for the preparation of multiblock copolymers by photo-induced living radical polymerisation without purification.

Filtered monomer (*DP* equiv.), EbBiB (1 equiv.), $CuBr_2$ (0.04 equiv.), Me_6-Tren (0.24 equiv.) and DMSO (2 mL) were added to a septum sealed vial and degassed by purging with nitrogen for 15 min. Polymerisation commenced upon placement of the degassed reaction vessel under UV lamp. Samples were taken periodically (0.05 ml) and conversions were measured using ^{1}H NMR and SEC analysis.

For the iterative chain extensions, an aliquot of a degassed monomer (*DP* equiv.), in DMSO (50% *v/v*) was added *via* a nitrogen-purged syringe and again the solution was allowed to polymerise in the lamp. When required, a fresh solution of $CuBr_2$ (0.04 equiv.), Me_6-Tren (0.24 equiv.) in DMSO was fed together with the monomer *via* a nitrogen-purged syringe. The above polymerisation-extension procedure was repeated as required.

(b) Disulfide reduction

The reduction of the disulphide bond is adapted from a reported procedure[44]. A 50 mL round bottom flask was charged with the final multiblock copolymer (0.1 g obtained *via* precipitation in methanol), tributylphosphine (100 equiv.) and THF (10 mL). The reaction was allowed to stir for 2 h at ambient temperature. The volatiles were removed by rotary evaporation to yield the reduced product, which was subsequently characterised by ^{1}H NMR and SEC.

2.4.4 Additional Characterisation

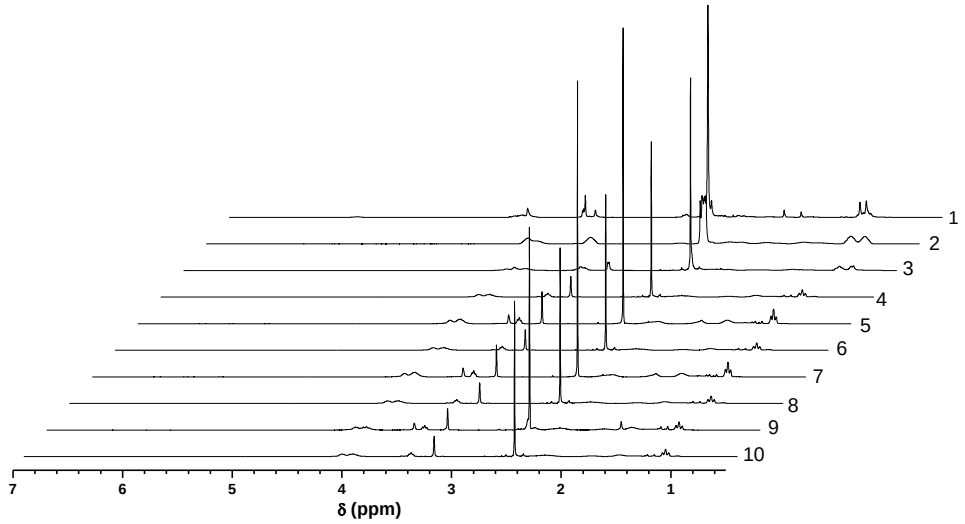

Figure 2.13: ^{1}H NMR for the successive cycles during synthesis of the nonadecablock copolymer (*DP*=4 per chain extension or *DP*=2 per block) in DMSO at 50 ^{o}C.

Table 2.4: Characterisation data for the synthesis of the nonadecablock copolymer (*DP*=4 per chain extension or *DP*=2 per block) obtained from UV experiment: [MA]:[EbBiB]:[$CuBr_2$]:[Me_6-Tren] = [4]:[1]:[0.04]:[0.24] in DMSO at 50 °C.

Cycle	Multiblock copolymer composition	Time (h)	Monomer conversion (%)	$M_{n,th}$ (g.mol^{-1})	$M_{n,SEC}$ (g.mol^{-1})	$Đ$
1	poly(MA_2)$_2$	10	100	700	265	1.40
2	poly(MA_2-*b*-EA_2)$_2$	10	99	1100	750	1.29
3	poly(MA_2-*b*-EA_2-*b*-EGA_2)$_2$	11	99	1600	1400	1.27
4	poly(MA_2-*b*-EA_2-*b*-EGA_2-*b*-SA_2)$_2$	11	99	2400	2000	1.26
5	poly(MA_2-*b*-EA_2-*b*-EGA_2-*b*-SA_2-*b*-MA_2)$_2$	12	98	2700	2900	1.26
6	poly(MA_2-*b*-EA_2-*b*-EGA_2-*b*-SA_2-*b*-MA_2-*b*-EGA_2)$_2$	12	99	3100	3800	1.25
7	poly(MA_2-*b*-EA_2-*b*-EGA_2-*b*-SA_2-*b*-MA_2-*b*-EGA_2-*b*-MA_2)$_2$	14	98	3400	5000	1.26
8	poly(MA_2-*b*-EA_2-*b*-EGA_2-*b*-SA_2-*b*-MA_2-*b*-EGA_2-*b*-MA_2-*b*-SA_2)$_2$	18	99	4100	6000	1.28
9	poly(MA_2-*b*-EA_2-*b*-EGA_2-*b*-SA_2-*b*-MA_2-*b*-EGA_2-*b*-MA_2-*b*-SA_2-*b*-EGA_2)$_2$	24	99	4600	8000	1.35
10	poly(MA_2-*b*-EA_2-*b*-EGA_2-*b*-SA_2-*b*-MA_2-*b*-EGA_2-*b*-MA_2-*b*-SA_2-*b*-EGA_2-*b*-EA_2)$_2$	24	99	5000	8300	1.45

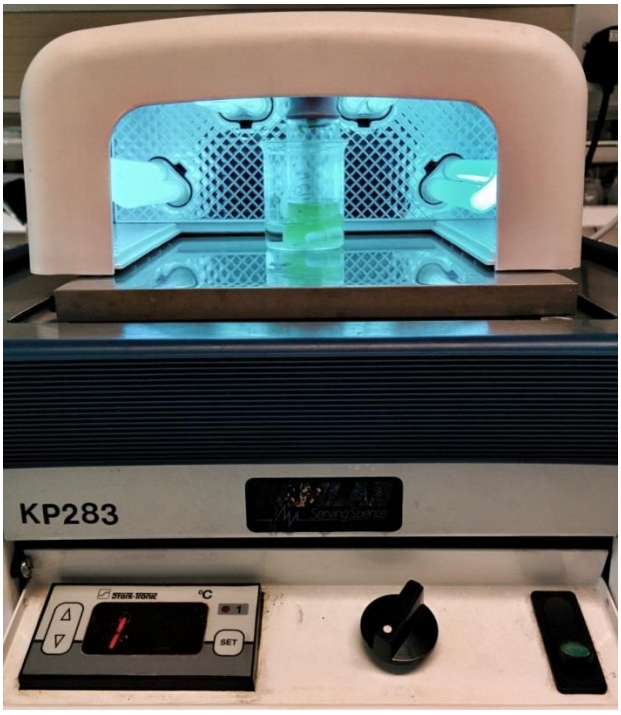

Figure 2.14: Typical set up for the photo-induced RDRP, utilising a "cooling" plate.

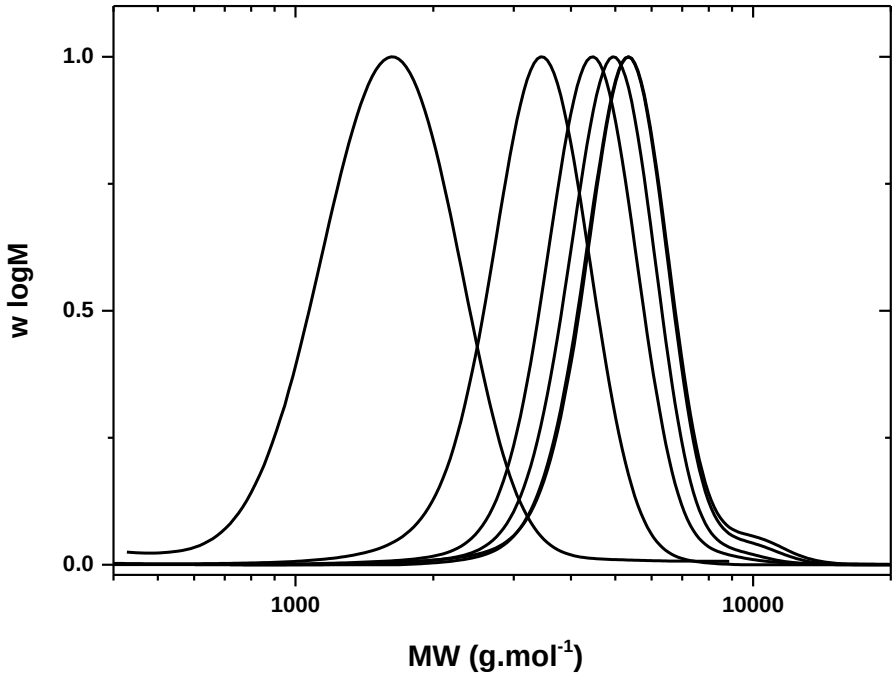

Figure 2.15: SEC analysis showing the molecular weight evolution during the kinetic experiment of photo-induced polymerisation of MA at 50 °C utilising EbBiB.

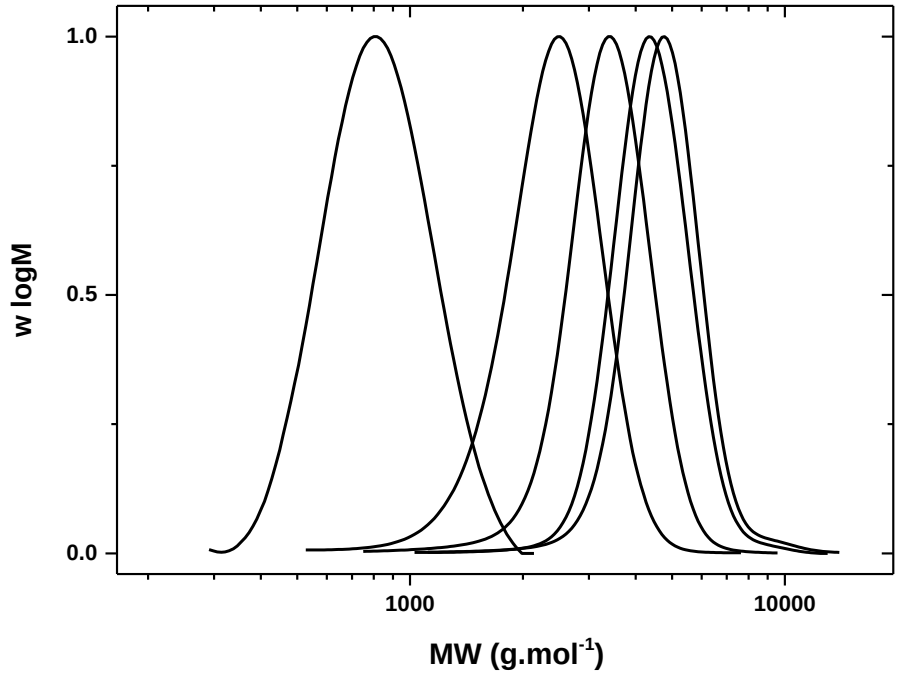

Figure 2.16: SEC analysis showing the molecular weight evolution during the kinetic experiment of photo-induced polymerisation of MA at 15 °C utilising EbBiB.

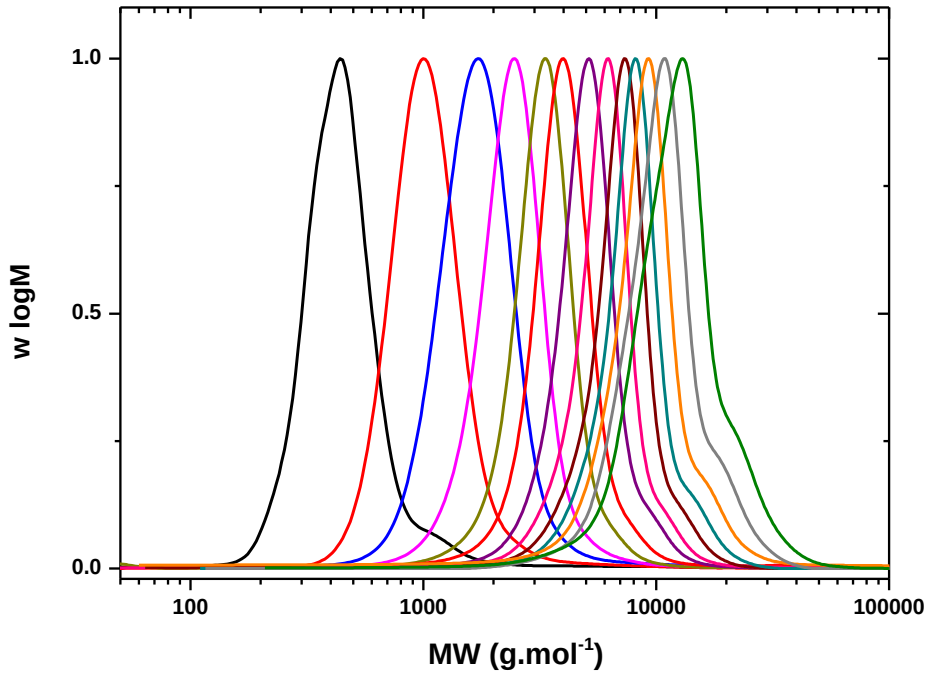

Figure 2.17: Molecular weight distributions for successive cycles during synthesis of the pentacosablock copolymer (*DP* = 4 per chain extension or *DP* = 2 per block) in DMSO at 15 ^{o}C.

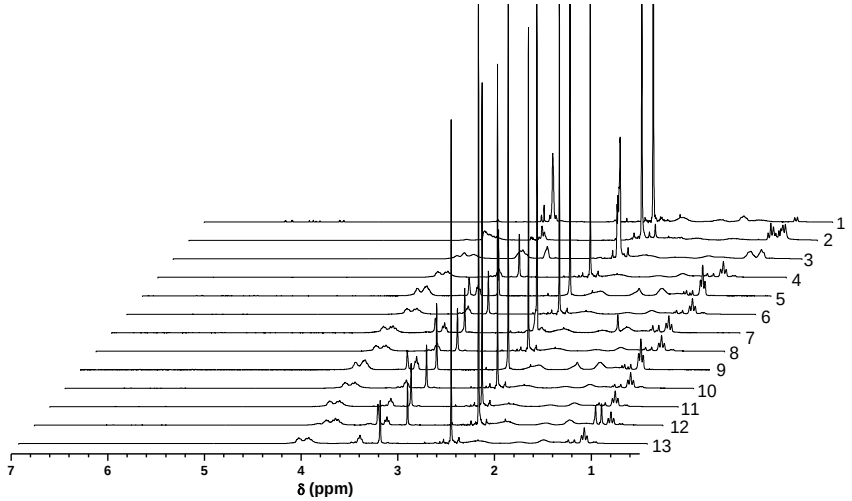

Figure 2.18: ^{1}H NMR for the successive cycles during synthesis of the pentacosablock copolymer (*DP* = 4 per chain extension or *DP* = 2 per block) in DMSO at 15 ^{o}C.

Table 2.5: Characterisation data for the synthesis of the pentacosablock copolymer (*DP* = 4 per chain extension or *DP* = 2 per block) obtained from UV experiment: [MA]:[EbBiB]:[$CuBr_2$]:[Me_6-Tren] = [4]:[1]:[0.04]:[0.24] in DMSO at 15 °C.

Cycle	Multiblock copolymer composition	Time (h)	Monomer conversion (%)	$M_{n,th}$ (g.mol^{-1})	$M_{n,SEC}$ (g.mol^{-1})	$Đ$
1	poly(MA_2)$_2$	12	100	700	400	1.20
2	poly(MA_2-*b*-EA_2)$_2$	12	99	1100	950	1.20
3	poly(MA_2-*b*-EA_2-*b*-EGA_2)$_2$	12	99	1600	1500	1.21
4	poly(MA_2-*b*-EA_2-*b*-EGA_2-*b*-SA_2)$_2$	12	99	2400	2200	1.16
5	poly(MA_2-*b*-EA_2-*b*-EGA_2-*b*-SA_2-*b*-MA_2)$_2$	14	98	2700	3000	1.14
6	poly(MA_2-*b*-EA_2-*b*-EGA_2-*b*-SA_2-*b*-MA_2-*b*-EGA_2)$_2$	14	99	3100	3600	1.14
7	poly(MA_2-*b*-EA_2-*b*-EGA_2-*b*-SA_2-*b*-MA_2-*b*-EGA_2-*b*-MA_2)$_2$	14	98	3400	4700	1.13
8	poly(MA_2-*b*-EA_2-*b*-EGA_2-*b*-SA_2-*b*-MA_2-*b*-EGA_2-*b*-MA_2-*b*-SA_2)$_2$	14	99	4100	5500	1.14
9	poly(MA_2-*b*-EA_2-*b*-EGA_2-*b*-SA_2-*b*-MA_2-*b*-EGA_2-*b*-MA_2-*b*-SA_2-*b*-EGA_2)$_2$	20	99	4600	6500	1.15
10	poly(MA_2-*b*-EA_2-*b*-EGA_2-*b*-SA_2-*b*-MA_2-*b*-EGA_2-*b*-MA_2-*b*-SA_2-*b*-EGA_2-*b*-EA_2)$_2$	24	98	5000	7400	1.14
11	poly(MA_2-*b*-EA_2-*b*-EGA_2-*b*-SA_2-*b*-MA_2-*b*-EGA_2-*b*-MA_2-*b*-SA_2-*b*-EGA_2-*b*-EA_2-*b*-SA_2)$_2$	24	99	5700	8200	1.19
12	poly(MA_2-*b*-EA_2-*b*-EGA_2-*b*-SA_2-*b*-MA_2-*b*-EGA_2-*b*-MA_2-*b*-SA_2-*b*-EGA_2-*b*-EA_2-*b*-SA_2-*b*-EA_2)$_2$	32	99	6100	9600	1.18
13	poly(MA_2-*b*-EA_2-*b*-EGA_2-*b*-SA_2-*b*-MA_2-*b*-EGA_2-*b*-MA_2-*b*-SA_2-*b*-EGA_2-*b*-EA_2-*b*-SA_2-*b*-EA_2- MA_2)$_2$	48	100	6400	13000	1.28

Table 2.6: Characterisation data for the synthesis of the undecablock copolymer (*DP* = 26 per chain extension or *DP* = 13 per block) obtained from UV experiment: [MA]:[EbBiB]:[$CuBr_2$]:[Me_6-Tren] = [26]:[1]:[0.04]:[0.24] in DMSO at 15 °C.

Cycle	Multiblock copolymer composition	Time (h)	Monomer conversion (%)	$M_{n,th}$ (g.mol^{-1})	$M_{n,SEC}$ (g.mol^{-1})	$Đ$
1	poly(MA_2)$_2$	4	99	2600	2700	1.08
2	poly(MA_2-*b*-EA_2)$_2$	6	99	5200	5800	1.05
3	poly(MA_2-*b*-EA_2-*b*-EGA_2)$_2$	8	98	8600	9300	1.06
4	poly(MA_2-*b*-EA_2-*b*-EGA_2-*b*-SA_2)$_2$	12	99	13400	12800	1.08
5	poly(MA_2-*b*-EA_2-*b*-EGA_2-*b*-SA_2-*b*-MA_2)$_2$	24	98	15600	17000	1.13
6	poly(MA_2-*b*-EA_2-*b*-EGA_2-*b*-SA_2-*b*-MA_2-*b*-EGA_2)$_2$	48	99	19000	22000	1.17

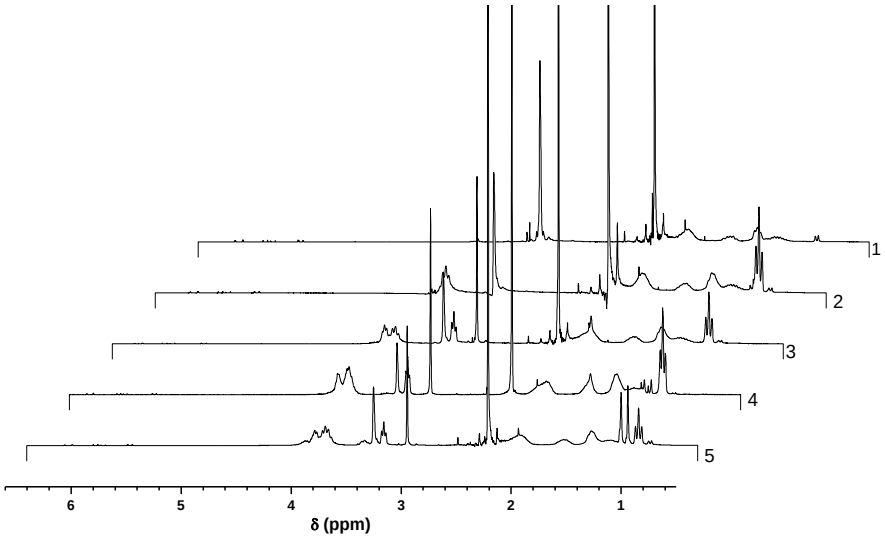

Figure 2.19: ^{1}H NMR for the successive cycles during synthesis of the nonablock copolymer (*DP* = 100 per chain extension or *DP* = 50 per block) in DMSO at 15 °C.

Table 2.7: Characterisation data for the synthesis of the nonablock copolymer (*DP* = 100 per chain extension or *DP* = 50 per block) obtained from UV experiment: [MA]:[EbBiB]:[$CuBr_2$]:[Me_6-Tren] = [100]:[1]:[0.04]:[0.24] in DMSO at 15 °C.

Cycle	Multiblock copolymer composition	Time (h)	Monomer conversion (%)	$M_{n,th}$ (g.mol^{-1})	$M_{n,SEC}$ (g.mol^{-1})	$Đ$
1	poly(MA_2)$_2$	3	99	9000	9100	1.05
2	poly(MA_2-*b*-EA_2)$_2$	8	99	19000	19800	1.07
3	poly(MA_2-*b*-EA_2-*b*-EGA_2)$_2$	12	99	32000	34000	1.08
4	poly(MA_2-*b*-EA_2-*b*-EGA_2-*b*-SA_2)$_2$	24	98	50000	44500	1.10
5	poly(MA_2-*b*-EA_2-*b*-EGA_2-*b*-SA_2-*b*-MA_2)$_2$	48	97	59000	56000	1.18

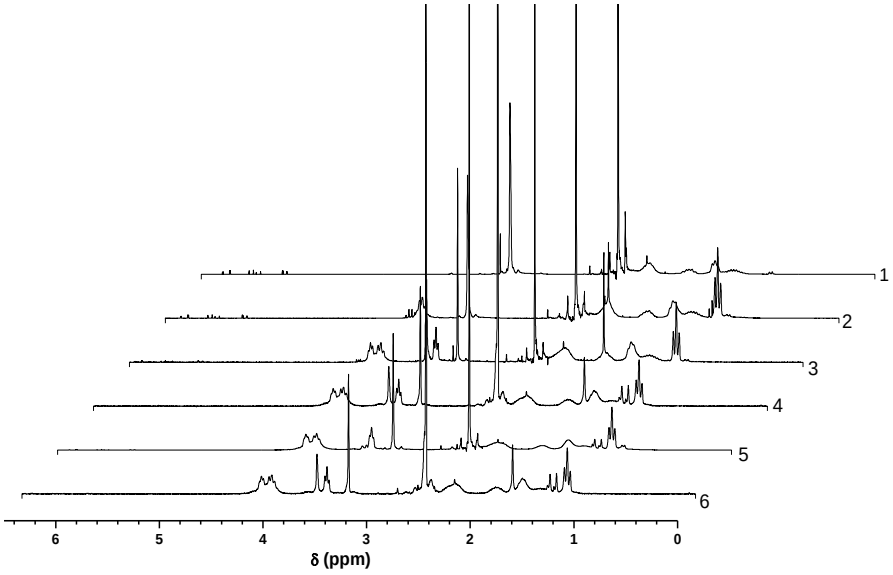

Figure 2.20: ^{1}H NMR for the successive cycles during synthesis of the undecablock copolymer (*DP* = 200 per chain extension or *DP* = 100 per block) in DMSO at 15 °C.

Table 2.8: Characterisation data for the synthesis of the undecablock copolymer (*DP* = 200 per chain extension or *DP* = 100 per block) obtained from UV experiment: [MA]:[EbBiB]:[$CuBr_2$]:[Me_6-Tren] = [200]:[1]:[0.04]:[0.24] in DMSO at 15 °C.

Cycle	Multiblock copolymer composition	Time (h)	Monomer conversion (%)	$M_{n,th}$ (g.mol^{-1})	$M_{n,SEC}$ (g.mol^{-1})	$Đ$
1	poly(MA_2)$_2$	3	98	18000	19000	1.04
2	poly(MA_2-*b*-EA_2)$_2$	8	99	38000	41000	1.03
3	poly(MA_2-*b*-EA_2-*b*-EGA_2)$_2$	12	98	64000	61000	1.08
4	poly(MA_2-*b*-EA_2-*b*-EGA_2-*b*-SA_2)$_2$	24	98	101000	81000	1.09
5	poly(MA_2-*b*-EA_2-*b*-EGA_2-*b*-SA_2-*b*-MA_2)$_2$	32	99	118000	107000	1.19
6	poly(MA_2-*b*-EA_2-*b*-EGA_2-*b*-SA_2-*b*-MA_2-*b*-EGA_2)$_2$	48	99	144000	150000	1.22

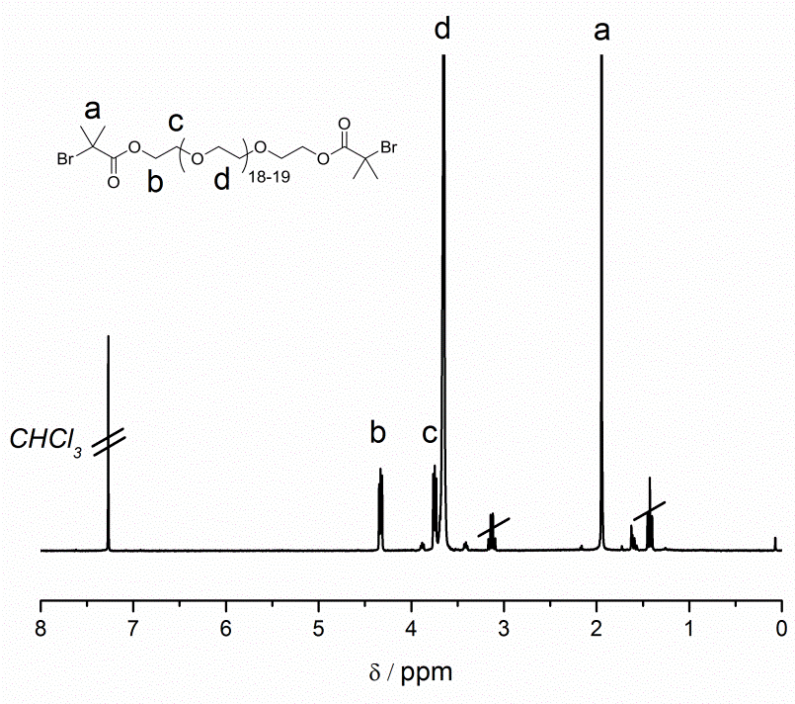

Figure 2.21: ^{1}H NMR spectrum of poly(ethylene glycol) bis(2-bromoisobutyrate) (PEG initiator, *av*. M_w=1000 g.mol^{-1}).

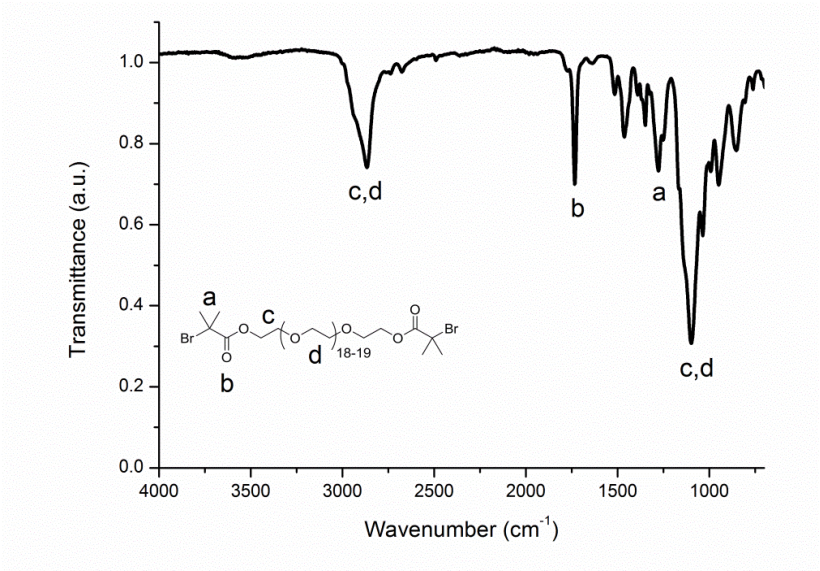

Figure 2.22: FT-IR spectrum of PEG initiator, *av.* M_w=1000 g.mol^{-1}.

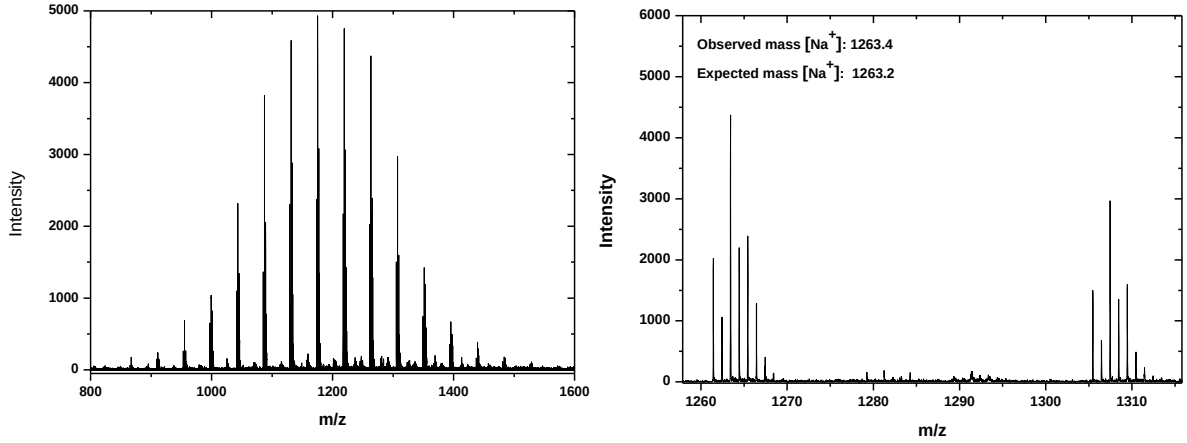

Figure 2.23: MALDI-ToF-MS spectrum of PEG initiator, *av.* M_w=1000 g.mol^{-1}.

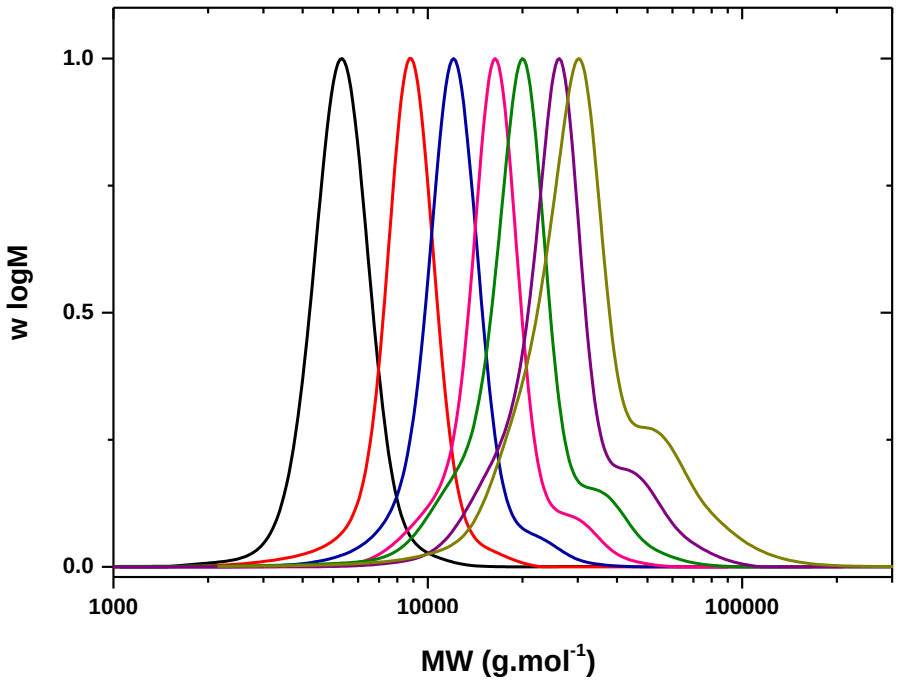

Figure 2.24: Molecular weight distributions for the successive cycles during synthesis of the of the pentadecablock copolymer, utilising PEG initiator (*av.* M_w=1000 g.mol^{-1}) (*DP* = 26 per chain extension or *DP* = 13 per block) in DMSO at 15 ^{o}C.

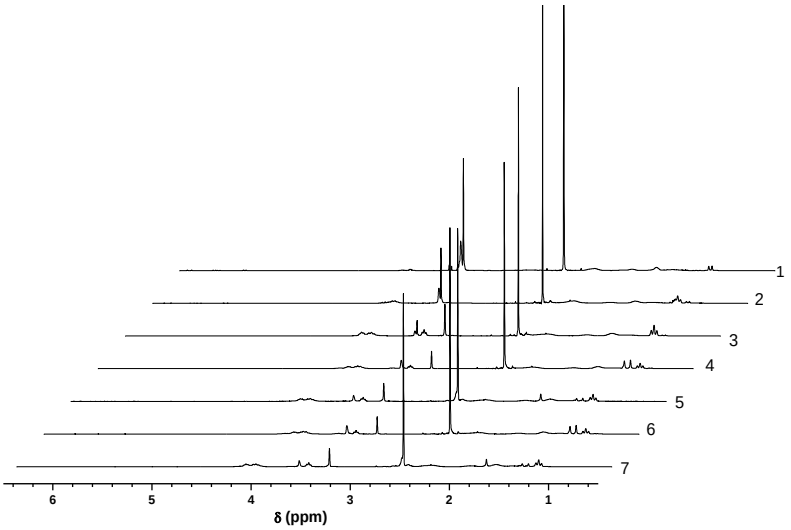

Figure 2.25: ^{1}H NMR for the successive cycles during synthesis of the of the pentadecablock copolymer, utilising PEG initiator (*av.* M_w=1000 g.mol^{-1}) (*DP* = 26 per chain extension or *DP* = 13 per block) in DMSO at 15 ^{o}C.

Table 2.9: Characterisation data for the synthesis of the pentadecablock copolymer (*DP* = 26 per chain extension or *DP* = 13 per block) obtained from UV experiment: [MA]:[Bi-functional PEG]:[$CuBr_2$]:[Me_6-Tren] = [26]:[1]:[0.04]:[0.24] in DMSO at 15 °C.

Cycle	Multiblock copolymer composition	Time (h)	Monomer conversion (%)	$M_{n,th}$ (g.mol^{-1})	$M_{n,SEC}$ (g.mol^{-1})	$Đ$
1	poly(MA_2)$_2$	3	99	3500	5100	1.06
2	poly(MA_2-*b*-EA_2)$_2$	6	99	6100	8300	1.07
3	poly(MA_2-*b*-EA_2-*b*-EGA_2)$_2$	8	98	9500	11600	1.08
4	poly(MA_2-*b*-EA_2-*b*-EGA_2-*b*-SA_2)$_2$	11	99	14000	16000	1.09
5	poly(MA_2-*b*-EA_2-*b*-EGA_2-*b*-SA_2-*b*-MA_2)$_2$	16	98	16500	18600	1.14
6	poly(MA_2-*b*-EA_2-*b*-EGA_2-*b*-SA_2-*b*-MA_2-*b*-EGA_2)$_2$	24	98	20000	24600	1.15
7	poly(MA_2-*b*-EA_2-*b*-EGA_2-*b*-SA_2-*b*-MA_2-*b*-EGA_2-*b*-MA_2)$_2$	48	99	22000	29000	1.24

Table 2.10: Characterisation data for the synthesis of the tridecablock copolymer (*DP* = 26 per chain extension or *DP* = 13 per block) obtained from UV experiment: [MA]:[Disulphide initiator]:[$CuBr_2$]:[Me_6-Tren] = [26]:[1]:[0.04]:[0.24] in DMSO at 15 ^oC, utilising $(BiBOE)_2S_2$.

Cycle	Multiblock copolymer composition	Time (h)	Monomer conversion (%)	$M_{n,th}$ (g.mol^{-1})	$M_{n,SEC}$ (g.mol^{-1})	$Đ$
1	poly(MA_2)$_2$	3	99	2700	3200	1.12
2	poly(MA_2-*b*-EA_2)$_2$	6	99	5300	6300	1.08
3	poly(MA_2-*b*-EA_2-*b*-EGA_2)$_2$	8	98	8700	9600	1.06
4	poly(MA_2-*b*-EA_2-*b*-EGA_2-*b*-SA_2)$_2$	12	99	13500	13600	1.07
5	poly(MA_2-*b*-EA_2-*b*-EGA_2-*b*-SA_2-*b*-MA_2)$_2$	18	98	15700	17500	1.08
6	poly(MA_2-*b*-EA_2-*b*-EGA_2-*b*-SA_2-*b*-MA_2-*b*-EGA_2)$_2$	24	99	19000	21000	1.11
7	poly(MA_2-*b*-EA_2-*b*-EGA_2-*b*-SA_2-*b*-MA_2-*b*-EGA_2-*b*-MA_2)$_2$	48	98	21000	25000	1.18

2.5 References

1. N. Badi and J.-F. Lutz, *Chem.Rev.*, 2009, **38**, 3383-3390.

2. M. Ouchi, N. Badi, J.-F. Lutz and M. Sawamoto, *Nat. Chem.*, 2011, **3**, 917-924.

3. J. Vandenbergh, G. Reekmans, P. Adriaensens and T. Junkers, *Chem. Commun.*, 2013, **49**, 10358-10360.

4. J. Vandenbergh, G. Reekmans, P. Adriaensens and T. Junkers, *Chem. Sci.*, 2015, **6**, 5753-5761.

5. K. Nakatani, T. Terashima and M. Sawamoto, *J. Am. Chem. Soc.*, 2009, **131**, 13600-13601.

6. K. Nakatani, Y. Ogura, Y. Koda, T. Terashima and M. Sawamoto, *J. Am. Chem. Soc.*, 2012, **134**, 4373-4383.

7. S. Pfeifer, Z. Zarafshani, N. Badi and J.-F. Lutz, *J. Am. Chem. Soc.*, 2009, **131**, 9195-9197.

8. M. Zamfir and J.-F. Lutz, *Nat. Commun.*, 2012, **1138**.

9. D. Moatsou, C. F. Hansell and R. K. O'Reilly, *Chem. Sci.*, 2014, **5**, 2246-2250.

10. A. Marsh, A. Khan, D. M. Haddleton and M. J. Hannon, *Macromolecules*, 1999, **32**, 8725-8731.

11. P. J. Milnes, M. L. McKee, J. Bath, L. Song, E. Stulz, A. J. Turberfield and R. K. O'Reilly, *Chem. Commun.*, 2012, **48**, 5614-5616.

12. A. Khan, D. M. Haddleton, M. J. Hannon, D. Kukulj and A. Marsh, *Macromolecules*, 1999, **32**, 6560-6564.

13. S. Ida, T. Terashima, M. Ouchi and M. Sawamoto, *J. Am. Chem. Soc.*, 2009, **131**, 10808-10809.

14. Y. Hibi, M. Ouchi and M. Sawamoto, *Angew. Chem., Int. Ed.*, 2011, **50**, 7434-7437.

15. Y. Hibi, S. Tokuoka, T. Terashima, M. Ouchi and M. Sawamoto, *Polym. Chem.*, 2011, **2**, 341-347.

16. R. McHale, J. P. Patterson, P. B. Zetterlund and R. K. O'Reilly, *Nat. Chem.*, 2012, **4**, 491-497.

17. K. A. Davis and K. Matyjaszewski, *Macromolecules*, 2001, **34**, 2101-2107.

18. A. H. Soeriyadi, C. Boyer, F. Nyström, P. B. Zetterlund and M. R. Whittaker, *J. Am. Chem. Soc.*, 2011, **133**, 11128-11131.

19. G. Gody, T. Maschmeyer, P. B. Zetterlund and S. Perrier, *Nat. Commun.*, 2013, **4**.

20. A. Anastasaki, V. Nikolaou, G. S. Pappas, Q. Zhang, C. Wan, P. Wilson, T. P. Davis, M. R. Whittaker and D. M. Haddleton, *Chem. Sci.*, 2014, **5**, 3536-3542.

21. C. Boyer, A. Derveaux, P. B. Zetterlund and M. R. Whittaker, *Polym. Chem.*, 2012, **3**, 117-123.

22. C. Boyer, A. H. Soeriyadi, P. B. Zetterlund and M. R. Whittaker, *Macromolecules*, 2011, **44**, 8028-8033.

23. A. Anastasaki, C. Waldron, P. Wilson, C. Boyer, P. B. Zetterlund, M. R. Whittaker and D. Haddleton, *ACS Macro Lett.*, 2013, **2**, 896-900.

24. Q. Zhang, J. Collins, A. Anastasaki, R. Wallis, D. A. Mitchell, C. R. Becer and D. M. Haddleton, *Angew. Chem., Int. Ed.*, 2013, **52**, 4435-4439.

25. Q. Zhang, A. Anastasaki, G.-Z. Li, A. J. Haddleton, P. Wilson and D. M. Haddleton, *Polym. Chem.*, 2014, **5**, 3876-3883.

26. F. Alsubaie, A. Anastasaki, P. Wilson and D. M. Haddleton, *Polym. Chem.*, 2015, **6**, 406-417.

27. Q. Zhang, P. Wilson, Z. Li, R. McHale, J. Godfrey, A. Anastasaki, C. Waldron and D. M. Haddleton, *J. Am. Chem. Soc.*, 2013, **135**, 7355-7363.

28. G. Gody, T. Maschmeyer, P. B. Zetterlund and S. Perrier, *Macromolecules*, 2014, **47**, 639-649.

29. G. Gody, T. Maschmeyer, P. B. Zetterlund and S. Perrier, *Macromolecules*, 2014, **47**, 3451-3460.

30. P. B. Zetterlund, G. Gody and S. Perrier, *Macromol. Theory Simul.*, 2014, **23**, 331-339.

31. G. Gody, M. Danial, R. Barbey and S. Perrier, *Polym. Chem.*, 2015, **6**, 1502-1511.

32. J. Chiefari, J. Jeffery, R. T. A. Mayadunne, G. Moad, E. Rizzardo and S. H. Thang, *Macromolecules*, 1999, **32**, 7700-7702.

33. A. Anastasaki, V. Nikolaou, Q. Zhang, J. Burns, S. R. Samanta, C. Waldron, A. J. Haddleton, R. McHale, D. Fox, V. Percec, P. Wilson and D. M. Haddleton, *J. Am. Chem. Soc.*, 2013, **136**, 1141-1149.

34. B. Wenn, M. Conradi, A. D. Carreiras, D. M. Haddleton and T. Junkers, *Polym. Chem.*, 2014, **5**, 3053-3060.

35. M. A. Tasdelen, M. U. Kahveci and Y. Yagci, *Prog. Polym. Sci.*, 2011, **36**, 455-567.

36. L. Ayres, M. R. J. Vos, P. J. H. M. Adams, I. O. Shklyarevskiy and J. C. M. van Hest, *Macromolecules*, 2003, **36**, 5967-5973.

37. A. O. Moughton, M. A. Hillmyer and T. P. Lodge, *Macromolecules*, 2011, **45**, 2-19.

38. G. Pasparakis, N. Krasnogor, L. Cronin, B. G. Davis and C. Alexander, *Chem. Soc. Rev.*, 2010, **39**, 286-300.

39. J. Rodríguez-Hernández, F. Chécot, Y. Gnanou and S. Lecommandoux, *Prog. Polym. Sci.*, 2005, **30**, 691-724.

40. A. Simula, G. Nurumbetov, A. Anastasaki, P. Wilson and D. M. Haddleton, *Eur. Polym. J.*, 2015, **62**, 294-303.

41. G. Lligadas and V. Percec, *J. Polym. Sci. Part A: Polym. Chem.*, 2007, **45**, 4684-4695.

42. M. Ciampolini and N. Nardi, *Inorg. Chem.* , 1966, **5**, 41-44.

43. K. Oguchi, K. Sanui, N. Ogata, Y. Takahashi and T. Nakada, *Polym. Eng. Sci.* , 1990, **30**, 449-452.

44. J. A. Syrett, M. W. Jones and D. M. Haddleton, *Chem. Commun.*, 2010, **46**, 7181-7183.

Synthesis of well-defined poly(acrylates) in ionic liquids *via* copper(II) mediated photo-induced RDRP

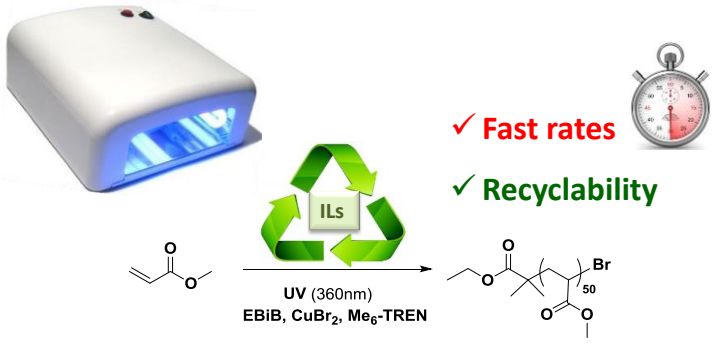

In this chapter, the photo-induced RDRP of acrylates in a variety of ionic liquids (ILs) has been investigated. 1-Ethyl-3-methylimidazolium ethyl sulphate [emim][EtSO$_4$], 1-heptyl-3-methylimidazolium bromide [C$_7$mim][Br], 1-hexyl-3-methylimidazolium tetrafluoroborate [C$_6$mim][BF$_4$], 1-hexyl-3-methylimidazolium hexafluorophosphate [C$_6$mim][PF$_6$] and 1-octyl-3-methylimidazolium hexafluorophosphate [C$_8$mim][PF$_6$] were employed as solvents for the homopolymerisation of a variety of acrylates. Polymerisation proceeded in a controlled manner in most cases, as evidenced by kinetic studies, narrow molecular weight distributions (Đ ~ 1.1) and quantitative conversions (> 99%) within 30 min. MALDI-ToF-MS and ^{1}H NMR confirmed very high end-group fidelity, which was further exemplified by in situ chain extensions and block copolymerisations, yielding well-defined block copolymers in a quantitative manner. Interestingly, all polymerisations in ILs experienced a significant acceleration on the rate of polymerisation without compromising the end-group fidelity, as opposed to the slower rates observed when DMSO was used as the solvent. The versatility of the approach was also demonstrated by polymerisation of MA to a number of chain lengths (M_n ~ 4500 – 40000 g.mol^{-1}) furnishing poly(acrylates) with low dispersities in all cases (Đ ~ 1.1). Importantly, extraction of the obtained polymer with toluene allowed the IL/catalyst solution to be reused as the solvent for further polymerisations without affecting the living nature of the polymerisation. Moreover, the polymer extracted into the toluene (copper-free) can be used directly for post polymerisation modifications (e.g. click reactions).

3.1 Introduction

Ionic liquids (ILs) are organic salts that are liquid at ambient temperature and are usually composed of large organic cations and small inorganic or organic anions. Over the past few years significant attention has been directed towards ILs due to their unique properties including low volatility, chemical stability, high conductivity and wide electrochemical window.[1, 2] ILs are of considerable interest to synthetic chemists as replacement solvents for chemical reactions, including hydrogenation, alkylation, Diels-Alder coupling,[3, 4] *etc.* One key advantage of using ILs for the synthesis of low molecular weight compounds, is that the products can be separated simply by evaporation, thus enabling the IL solution to be reused for subsequent reaction cycles.[5, 6]Aside from the obvious environmental benefits of such an approach, the large number of cations and anions that can be used in an IL provide for a wide range of physical and chemical characteristics allowing control over the reaction processing and solvent-solvent interactions to be tailored for the specific situation.[2]

To date, ILs have been applied to various RDRP systems, including RAFT (introduced for the first time by Davis and co-workers)[7, 8] and NMP (developed by Mays, Aldabbagh, Zetterlund, Yamada and co-workers).[9, 10] In the case of TMM-LRP, the use of ILs was pioneered by Haddleton and co-workers[11] who utilised 1-butyl-3-methyl-imidazolium hexafluorophosphate [bmim][PF_6] as the solvent for the CuBr mediated RDRP of methyl methacrylate (MMA) which demonstrated narrow MWDs ($Đ$ ~ 1.3) and relatively fast polymerisation rates, as observed in other polar solvents (solvent-induced acceleration was also obtained during the free radical polymerisation of MMA in ILs).[12] Although the polymer was recovered with only

ppm levels of copper *via* a simple solvent wash, the recycling of the ionic liquid/catalyst mixture was not attempted.[11] Matyjaszewski and co-workers subsequently reported the ATRP of MMA in the presence of ILs that could interact with the transition metal, thus providing an ATRP system that could operate in the absence of additional organic ligands.[13] Percec *et al.* also reported the RDRP of MMA in ILs catalysed by the self-regulated Cu_2O/2,2'– bipyridine system, demonstrating 100% initiator efficiency and yielding polymers with narrow MWDs.[14] However, in all the aforementioned reports only methacrylates have been studied and relatively fast polymerisation rates (fastest achieved = 82% conversion in 1 h, $Đ$ ~ 1.36) were realised only at relatively high temperatures (~ 70 ºC), with substantial decrease in the rate observed at lower temperatures (~ 22 ºC). Moreover, chain extensions and block copolymerisations were not reported and thus high end-group fidelity was not demonstrated. On a different note, Kubisa and co-workers investigated the ATRP of acrylates in ILs, though narrow MWDs were only observed for relatively low molecular weight polymers (M_n ~ 1000-4000 g.mol^{-1}) and block formation could be achieved only upon purification of the macroinitiators.[15, 16]

In this chapter the photo-induced RDRP[17] of acrylates in ILs, in the presence of low concentration of $CuBr_2$ and Me_6-Tren under UV irradiation is investigated. The homopolymerisation of a diverse range of acrylates including methyl acrylate (MA), *n*-butyl acrylate (*n*-BA), ethylene glycol methyl ether acrylate (EGA) and poly(ethylene glycol) methyl ether acrylate (PEGA, M_n ~ 480) was attempted in five different ILs. Among them, [C_6mim][BF_4], [C_6mim][PF_6] and [C_8mim][PF_6] facilitate the rapid polymerisation of acrylates achieving full monomer conversion (> 99%) in less than 30 min while maintaining narrow MWDs ($Đ$ ~ 1.1) and very high end-group fidelity (by ^{1}H NMR and MALDI-ToF-MS) for a range of molecular

weights. The excellent degree of control was confirmed by demonstrating first order reaction kinetics, which indicated a constant concentration of propagating radicals and good agreement between the theoretical and experimental molecular weights. The exceptional end-group fidelity was further demonstrated *via in situ* chain extensions and block copolymerisation upon sequential monomer addition, furnishing higher molecular weight monomers with low dispersities ($Đ$ ~ 1.1). Remarkably, the IL/catalyst solution could be reused several times after extraction of the homopolymer with toluene, proving true recyclability of the catalyst without any effect on the control over the MWDs or polymerisation rate.

3.2 Results and Discussion

The photo-induced RDRP of acrylates in ILs (Scheme 3.1) was carried out using EBiB as initiator, $CuBr_2$ (0.02 equiv. with respect to initiator) and Me_6-Tren (0.12 equiv. with respect to initiator) at 50% *v/v* at ambient temperature. A selection of ILs was used in order to investigate variations in polymerisations arising from changes in the properties of the reaction medium.

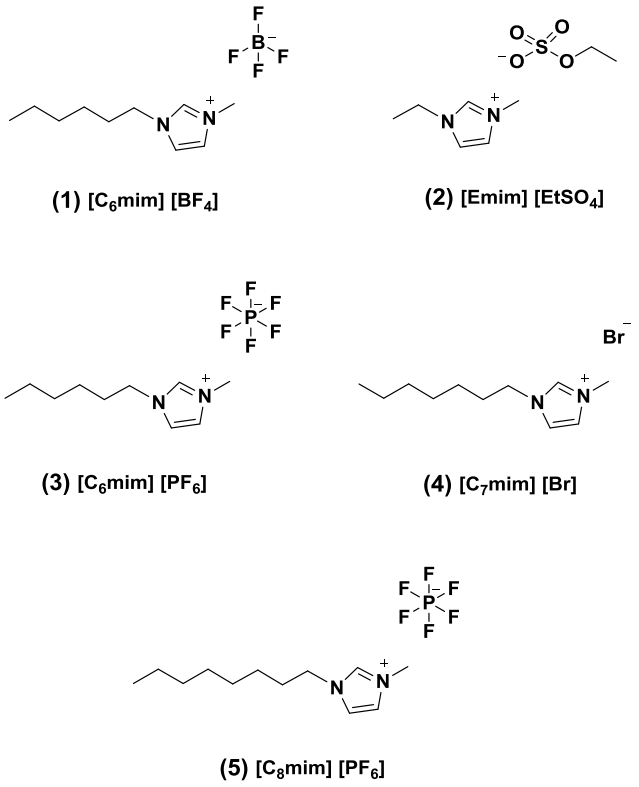

Scheme 3.1: Ionic liquids utilised as solvents for the photo-induced RDRP of acrylates.

Initially the homopolymerisation of MA in $[C_6mim][BF_4]$ was attempted. The polymerisation proceeded rapidly with full monomer conversion obtained in less than 30 min, as determined by ^{1}H NMR (Section 3.4.4, Figure 3.12). Kinetic studies revealed that the polymerisation fulfils the criteria of a controlled/living radical polymerisation with $\ln[M]_0/[M]_t$ increasing linearly with time demonstrating a constant radical concentration (Figure 3.1). The good agreement between the experimental molecular weights and the theoretical values also confirms the controlled character of the polymerisation. It should be noted that the polymerisation in IL proceeded with an enhanced polymerisation rate compared with that observed in DMSO under otherwise identical conditions[17] (> 95% conversion in 30 min *vs* 90 min for DMSO). Moreover, SEC indicated a mono-modal molecular weight distribution which shifts to higher molecular weight with increasing conversion

(Section 3.4.4, Figure 3.13), as would be anticipated for a living system with good control. Finally, the dispersity values remained low throughout the polymerisation.

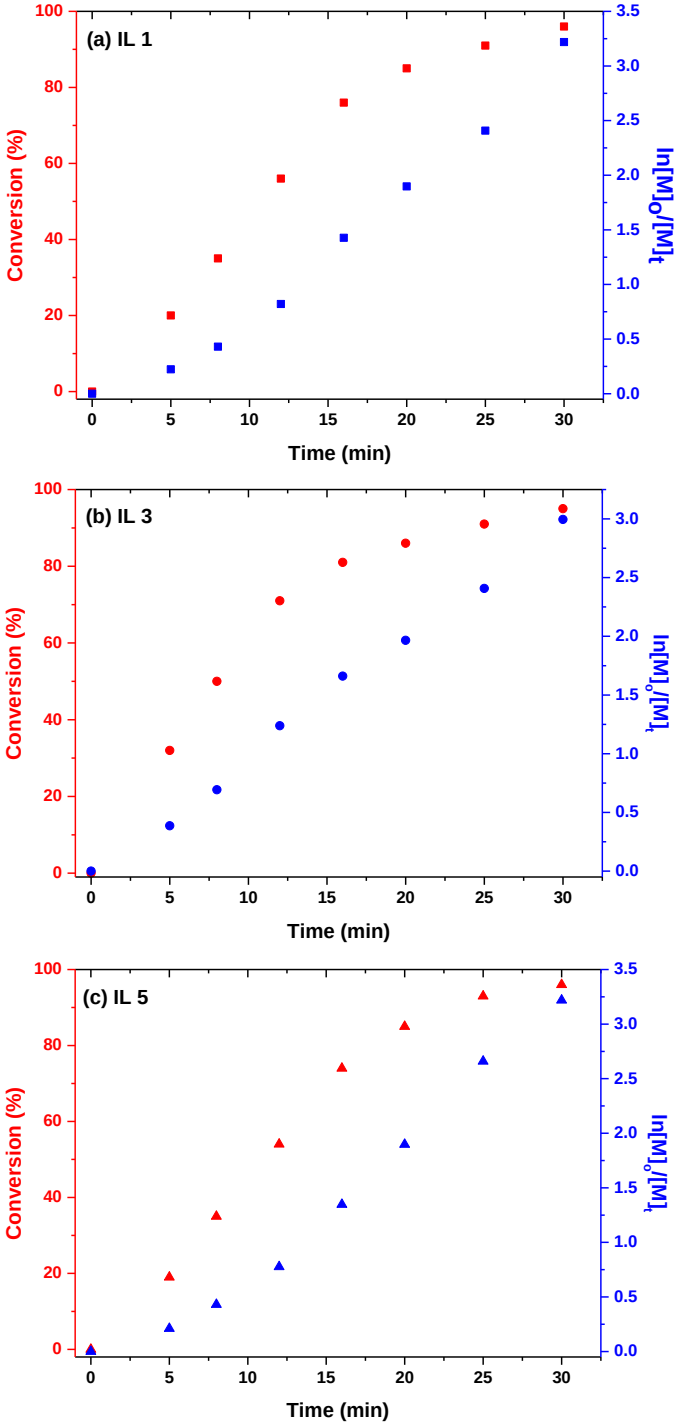

Figure 3.1: Kinetic data for the photo-induced polymerisation of MA in (a) $[C_6mim][BF_4]$, (b) $[C_6mim][PF_6]$ and (c) $[C_8mim][PF_6]$.

The high degree of control attained in the polymerisation was also confirmed utilising MALDI-ToF-MS analysis of the final polymer obtained directly from the reaction mixture (> 99% conversion). A single polymer peak distribution was observed corresponding to PMA initiated by the EBiB fragment and terminated by a bromine atom (Figures 3.2a,b). In addition, ^{1}H NMR also indicated excellent end-group fidelity (> 99%), as evaluated by comparison of the signals from the $–CH_3$ groups of the isobutyrate group of EBiB (~ 1.0 ppm) with the ω-terminal methine signal from the polymer backbone (~ 4.3 ppm). This high end-group fidelity was verified by *in situ* chain extension of the PMA (99% conversion in 30 min, $Đ$ ~ 1.10) after addition of a second aliquot of MA without the requirement to purify the macroinitiator (Section 3.4.4, Figure 3.14). SEC analysis revealed a complete shift to higher molecular weights while the molecular weight distributions remained narrow ($Đ$ ~ 1.10) (Figure 3.2c). Addition of a second aliquot of a different acrylic monomer (EGA or PEGA) resulted in a one-pot block copolymerisation, furnishing a well-defined block copolymers with low dispersity values ($Đ$ ~ 1.12), even at high monomer conversion (> 99%) (Figures 3.2d & Section 3.4.4, Figure 3.14, Figure 3.15).

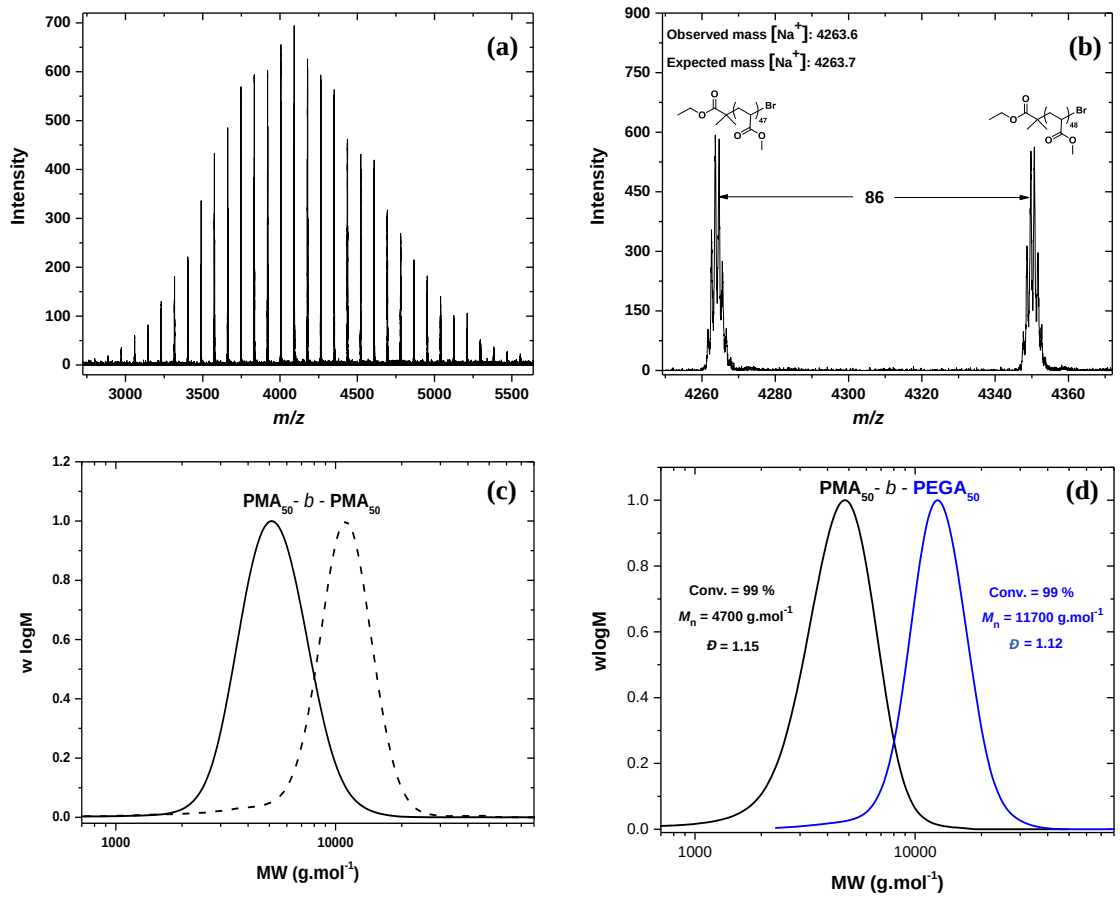

Figure 3.2: (a) and (b) MALDI-ToF-MS analysis of PMA, (c) *in situ* chain extension and (d) block copolymerisation from a PMA macroinitiator. Initial conditions [MA]:[EBiB]:[$CuBr_2$]:[Me_6-Tren] = [50]:[1]:[0.02]:[0.12], [C_6mim][BF_4] (50% *v/v*).

Higher molecular weight poly(acrylates) were subsequently targeted. A well-defined PMA (*DP* = 200) with a narrow MWDs was obtained within 30 min (M_n = 15100 g.mol^{-1}, *Đ* ~ 1.10). In addition, when the chain length was extended to *DP* = 400, control of the polymerisation was retained with good agreement between theoretical and experimental molecular weight and low dispersity (*Đ* ~ 1.11). In both cases the polymerisation was allowed to reach near-quantitative conversion (98%) prior to SEC analysis. Thus, it was demonstrated that good control over the MWDs was not just limited to polymers with a low targeted molecular weight (Figure 3.3, Table 3.2).

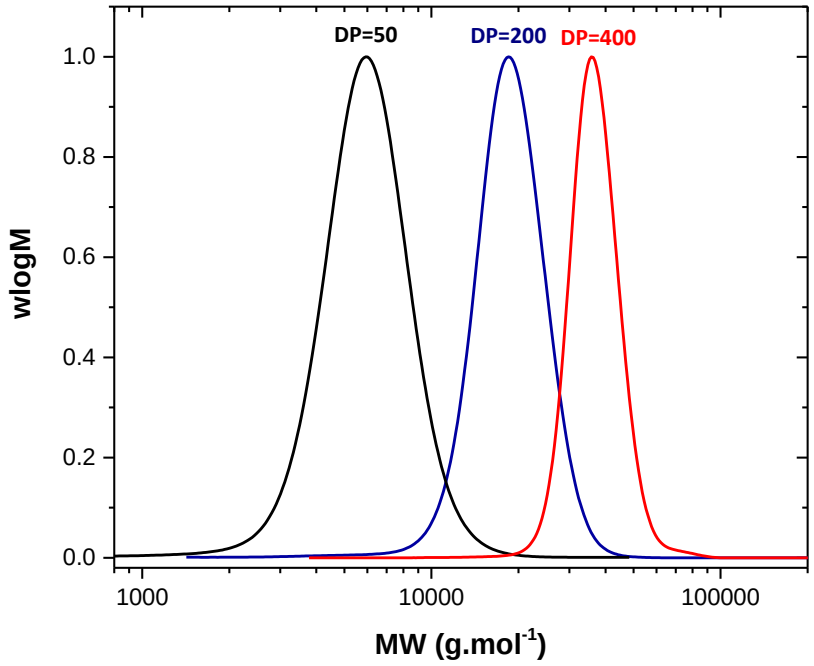

Figure 3.3: SEC analysis of PMA with various *DP* prepared by photo-induced RDRP in [C_6mim][BF_4].

The scope of the polymerisation in [C_6mim][BF_4] was subsequently expanded utilising a number of acrylic monomers including *n*-BA, EGA and PEGA (Table 3.1). Both EGA and PEGA were polymerised successfully, exhibiting fast polymerisation rates (~ 30 min for the reaction to reach full conversion) and low dispersity values ($Đ$ < 1.19) for the resulting polymer at quantitative or near-quantitative conversions, illustrating the robustness of the technique (Figure 3.4). Unfortunately, *n*-BA could not be successfully polymerised in a controlled manner using [C_6mim][BF_4], possibly due to the limited solubility, with the SEC revealing bimodality (Section 3.4.4, Figure 3.16).

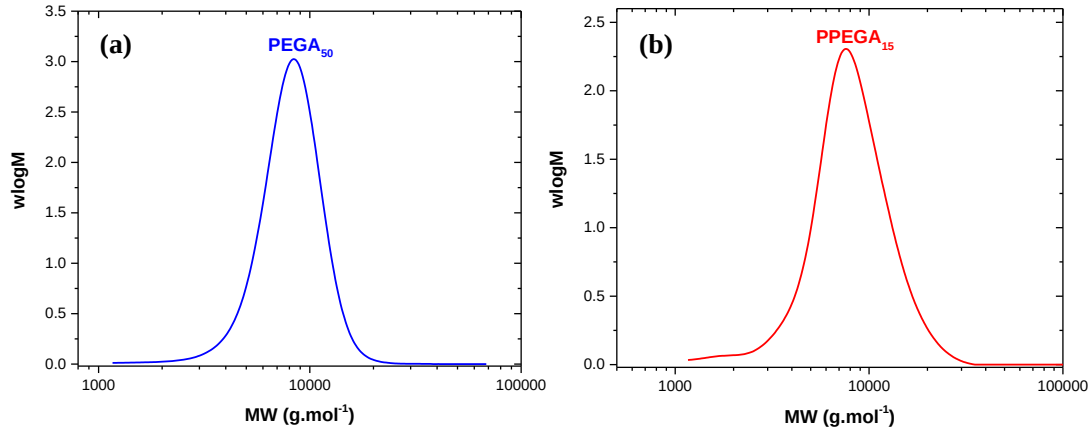

Figure 3.4: SEC analysis for the synthesis of (a) PEGA, initial conditions: [EGA]:[EBiB]:[$CuBr_2$]:[Me_6-Tren] = [50]:[1]:[0.02]:[0.12] and (b) PPEGA in initial conditions: [PEGA]:[EBiB]:[$CuBr_2$]:[Me_6-Tren] = [15]:[1]:[0.02]:[0.12] [C_6mim][BF_4] (50:50 *v/v* monomer/ionic liquid).

Table 3.1: Summary of photo-induced RDRP of various acrylates in ionic liquids.

Monomer	IL	t (min)	Conv. (%)	$M_{n,th}$ (g.mol^{-1})	$M_{n,SEC}$ (g.mol^{-1})	$Đ$
MA *DP* = 50	**1**	35	> 99	4500	4900	1.14
	2	960	0	-	-	-
	3	35	> 99	4500	4800	1.16
	4	960	11	500	1700	Bimodal
	5	35	99	4500	5100	1.07
EGA *DP* = 50	**1**	35	99	6700	7600	1.12
	2	960	0	-	-	-
	3	35	99	6700	7300	1.17
	4	960	45	3000	6000	Bimodal
	5	35	> 99	6700	6600	1.10
***n*-BA** *DP* = 50	**1**	960	90	5900	6200	Bimodal
	2	960	0	-	-	-
	3	960	93	6100	6900	Bimodal
	4	960	85	5600	53000	Bimodal
	5	35	97	6500	6400	1.22
PEGA *DP* = 15	**1**	35	> 99	7300	6900	1.18
	2	960	99	7300	8200	5.40
	3	35	99	7300	6800	1.17
	4	960	0	-	-	-
	5	35	98	7200	8700	1.19

The polymerisation of acrylates in [C_6mim][PF_6] was also investigated. Again homopolymerisation of MA proceeded quickly at ambient temperature,

attaining high conversion (> 99%) in 30 min with SEC analysis revealing a linear increase in number average molecular weight (M_n) with increasing conversion, excellent agreement with theoretical M_n and low dispersity ($Đ$ ~ 1.16) (Figure 3.5). Kinetic analysis confirmed a largely first order reaction kinetics with monomer and propagating radical concentration (Figure 3.1b & Section 3.4.4, Figure 3.17). To further explore the degree of control obtained in this polymerisation, final polymer samples were analysed by MALDI-ToF-MS (Figure 3.5). Only one major polymer peak distribution was detected which corresponds to ω-bromo-terminated PMA, thus indicating high bromo end-group fidelity and minimal side reactions (*i.e.* chain transfer).[18]

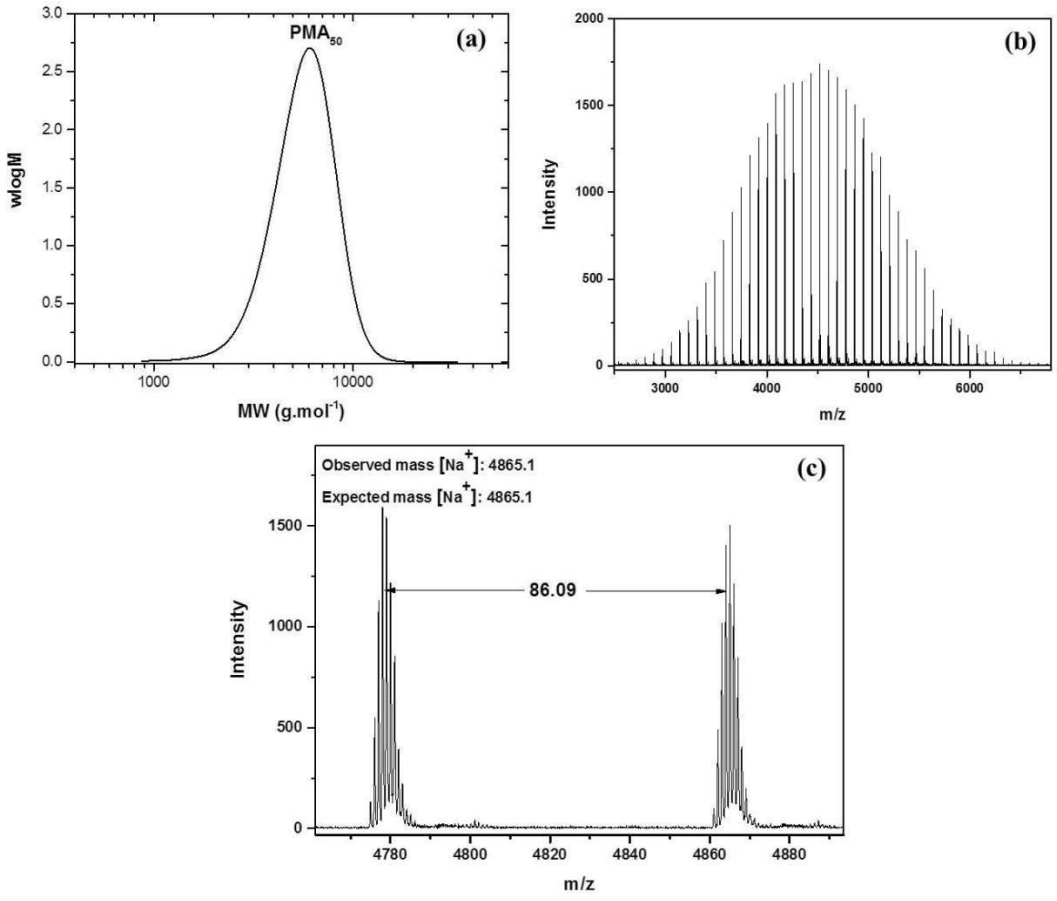

Figure 3.5: (a) SEC and (b),(c) MALDI-ToF-MS analyses for the synthesis of PMA in [C_6mim][PF_6] (50:50 *v/v* monomer/ionic liquid). Initial conditions: [MA]:[EBiB]:[$CuBr_2$]:[Me_6-Tren] = [50]:[1]:[0.02]:[0.12].

The livingness/controlled character of the system was further supported by chain extension (with a second aliquot of MA) and block copolymerisation with either EGA or PEGA. In all cases, a clear shift to higher molecular weights was evident by SEC and no low or high molecular weight shoulder could be observed, despite the *in situ* addition at full conversion of the macroinitiator (PMA > 99% conversion) (Section 3.4.4, Figure 3.18). Well-defined diblock homo/block copolymers (*Đ* ~ 1.14) could be obtained without compromising the initial fast rate of polymerisation, as > 97% conversion could be achieved in 1 h of reaction time (Table 3.2, Figure 3.6, Section 3.4.4, Figure 3.19).

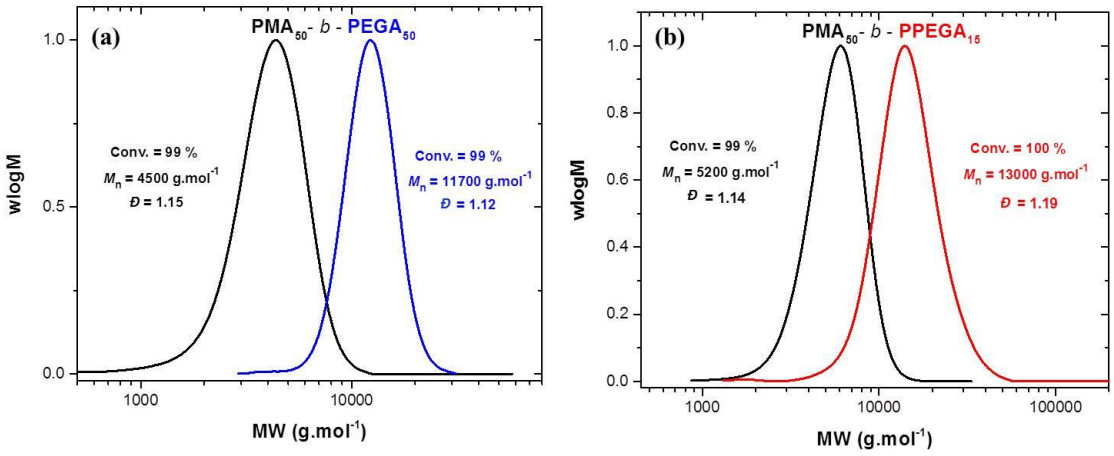

Figure 3.6: SEC analysis for block copolymerisation of (a) EGA and (b) PEGA from a PMA macroinitiator in [C_6mim][PF_6] (50:50 *v/v* monomer/ionic liquid). Initial conditions: [MA]:[EBiB]:[$CuBr_2$]:[Me_6-Tren] = [50]:[1]:[0.02]:[0.12]. Chain extension achieved upon addition of an aliquot of EGA (50 equiv.) or PEGA (15 equiv.) in [C_6mim][PF_6] (33% *v/v*).

Subsequently, in order to probe the potential of this IL in the synthesis of higher molecular weight polymers, higher degrees of polymerisation were targeted (*DP* = 200 and 400). The ratio of [$CuBr_2$]:[Me_6-Tren] = [1]:[6] was maintained for these polymerisations, resulting in high conversions within 30 min (~ 97%) and narrow molecular weight distributions (*Đ* ~ 1.10) (Table 3.2, Figure 3.7). Different acrylic monomers, including EGA and PEGA (Section 3.4.4, Figure 3.20-3.21), were also polymerised furnishing well-defined homopolymers with good agreement between theoretical and experimental values and low dispersity (*Đ* < 1.17 in both cases). Similarly to [C_6mim][BF_4], [C_6mim][PF_6] was not suitable for the controlled polymerisation of *n*-BA (Table 3.1, Section 3.4.4, Figure 3.22).

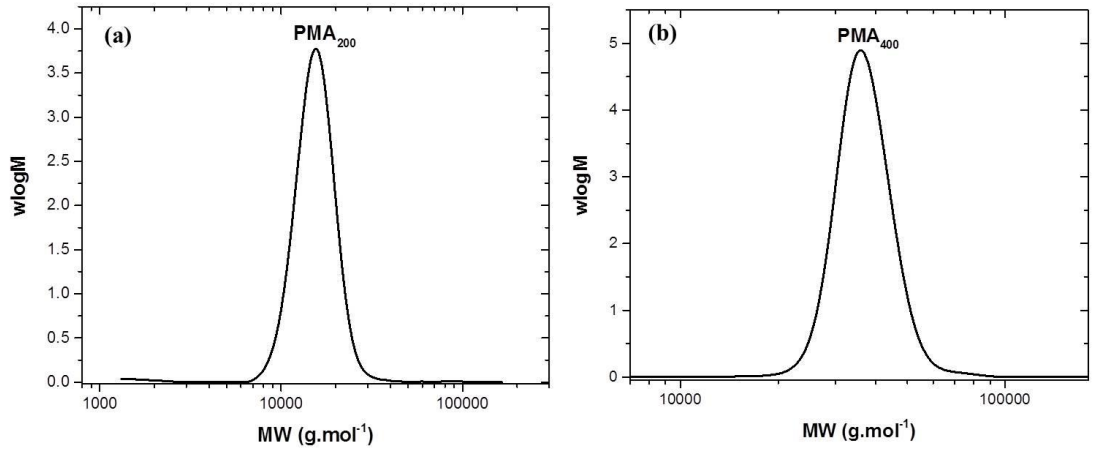

Figure 3.7: SEC analysis for the synthesis of (a) PMA_{200} and (b) PMA_{400} in [C_6mim][PF_6] (50:50 *v/v* monomer/ionic liquid).

In order to successfully catalyse the polymerisation of *n*-BA, it was hypothesised that a more hydrophobic IL would be required. Hence, [C_8mim][PF_6] was selected for the polymerisation of *n*-BA. Indeed, utilising this more

hydrophobic reaction medium the polymer retained solubility with no phase separation observed throughout the polymerisation.

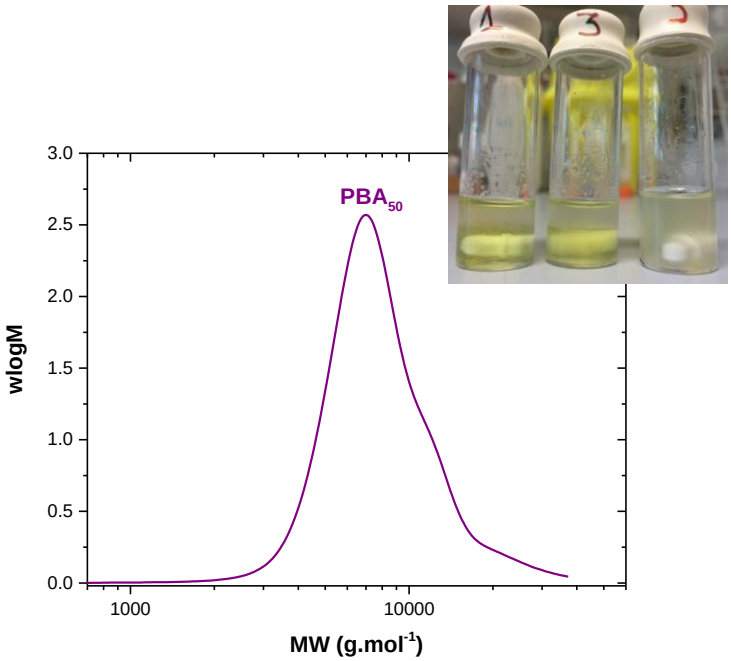

Figure 3.8: SEC analysis for the synthesis of PBA in [C_8mim][PF_6] (50:50 *v/v* monomer/ionic liquid). Initial conditions: [*n*-BA]:[EBiB]:[$CuBr_2$]:[Me_6-Tren] = [50]:[1]:[0.02]:[0.12].

SEC revealed a mono-modal peak distribution with low dispersity ($Đ$ ~ 1.22) (Table 3.1, Figure 3.8). Similarly, other acrylates (MA, EGA, PEGA) also presented narrow MWDs at quantitative or near-quantitative conversions (Section 3.4.4, Figure 3.23) while the rate of the polymerisation was rapid, achieving very high conversions within 30 min (Figure 3.1c, Section 3.4.4, Figure 3.24). Higher molecular weight polymers and block copolymerisations (Figure 3.9, Section 3.4.4, Figure 3.23) were also successfully performed, evident of the high retention of end-group functionality during this polymerisation (Table 3.2). However, when the polymerisation of MA

was attempted in [emim][$EtSO_4$], no conversion was observed by ^{1}H NMR, even when the reaction was left to proceed overnight (16 h). Similar results were obtained for *n*-BA (no conversion) while the polymerisation of PEGA was uncontrolled (*Đ* ~ 4) and finally EGA showed poor solubility in the reaction medium. Polymerisation of the aforementioned monomers in [C_7mim][Br] was also unsuccessful with limited conversions and/or broad MWDs (Section 3.4.4, Figures 3.25-3.28). Thus, it was concluded that both [emim][$EtSO_4$] and [C_7mim][Br] are unsuitable for the controlled polymerisation of acrylates under the conditions employed perhaps due to the more coordinating nature of the anion.

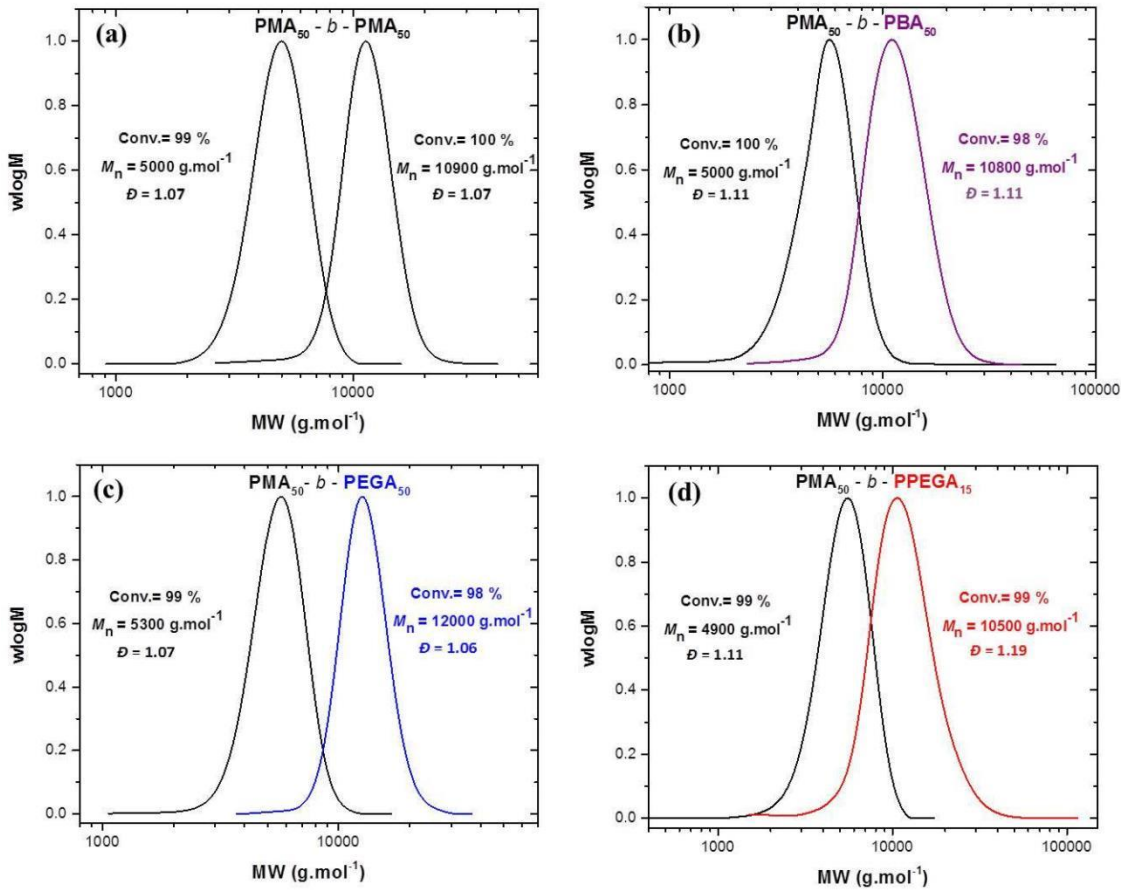

Figure 3.9: SEC analysis for the (a) *in situ* chain extension and block copolymerisations of (b) *n*-BA (c) EGA and (d) PEGA from a PMA macroinitiator in [C_8mim][PF_6] (50:50 *v/v*

monomer/ionic liquid). Initial conditions: [MA]:[EBiB]:[$CuBr_2$]:[Me_6-Tren] = [50]:[1]:[0.02]:[0.12]. Chain extension achieved upon addition of an aliquot of *n*-BA (50 equiv.), EGA (50 equiv.) or PEGA (15 equiv.) in [C_8mim][PF_6] (33% *v/v*).

Table 3.2: *In situ* chain extensions and block copolymerisations of PMA in ionic liquids.

IL	Block copolymer	t (min)	Conv. (%)	$M_{n,th}$ (g.mol^{-1})	$M_{n,SEC}$ (g.mol^{-1})	$Đ$
1	PMA_{50}-*b*-PMA_{50}	60	98	8600	10000	1.12
	PMA_{50}-*b*-$PEGA_{50}$	60	100	11000	11700	1.12
	PMA_{50}-*b*-$PPEGA_{15}$	60	100	11700	12900	1.14
	PMA_{200}	30	98	16000	15100	1.09
	PMA_{400}	30	98	34000	32600	1.07
3	PMA_{50}-*b*-PMA_{50}	60	100	8800	9800	1.14
	PMA_{50}-*b*-$PEGA_{50}$	60	99	10900	11700	1.12
	PMA_{50}-*b*-$PPEGA_{15}$	60	100	11700	13000	1.19
	PMA_{200}	30	98	16000	14800	1.10
	PMA_{400}	30	99	34000	32800	1.09
5	PMA_{50}-*b*-PMA_{50}	60	100	8800	10900	1.07
	PMA_{50}-*b*-$PEGA_{50}$	60	98	11000	12000	1.06
	PMA_{50}-*b*-$PPEGA_{15}$	60	99	11500	10500	1.19
	PMA_{50}-*b*-PBA_{50}	60	98	10700	10800	1.11
	PMA_{200}	30	97	16800	16000	1.06
	PMA_{400}	30	96	32900	27000	1.07

Importantly, ILs have attracted considerable interest as potential environmentally friendly solvents as they can be reused for organic reactions by evaporating the low molecular weight compounds while maintaining the catalyst in the IL reaction mixture given their low vapour pressure. However, in polymer science, this convenient reaction methodology cannot be employed due to the non-volatile nature of the polymers. In order to circumvent this, organic solvents must be used to isolate the polymer from the IL solution and thus it can be argued that the advantage of using this environmentally friendly reaction medium is partly lost. However, in TMM-LRP systems, the extraction of the polymer with an organic solvent can potentially maintain the catalyst in the IL solution and thus allow for the recycling of the catalytic system ($CuBr_2$/Me_6-Tren). This is of considerable

importance as *N*-containing ligands are typically the most expensive reagents in the polymerisation. Thus, potential re-use of these compounds could be highly desirable. A further advantage of extracting the polymer with toluene (copper-free) is the possibility of subsequent post polymerisation modifications directly in the toluene solution without the need to remove the organic solvent (*e.g.* click reaction).[19] In order to explore the possibility of reusing the IL solution, PMA was extracted from the polymerisation solution ([C_6mim][BF_4] or [C_6mim][PF_6]) using toluene until ^{1}H-NMR of both phases confirmed complete extraction of the polymer into the toluene phase (*i.e.* no polymer was detected in the IL solution) (Figure 3.10).

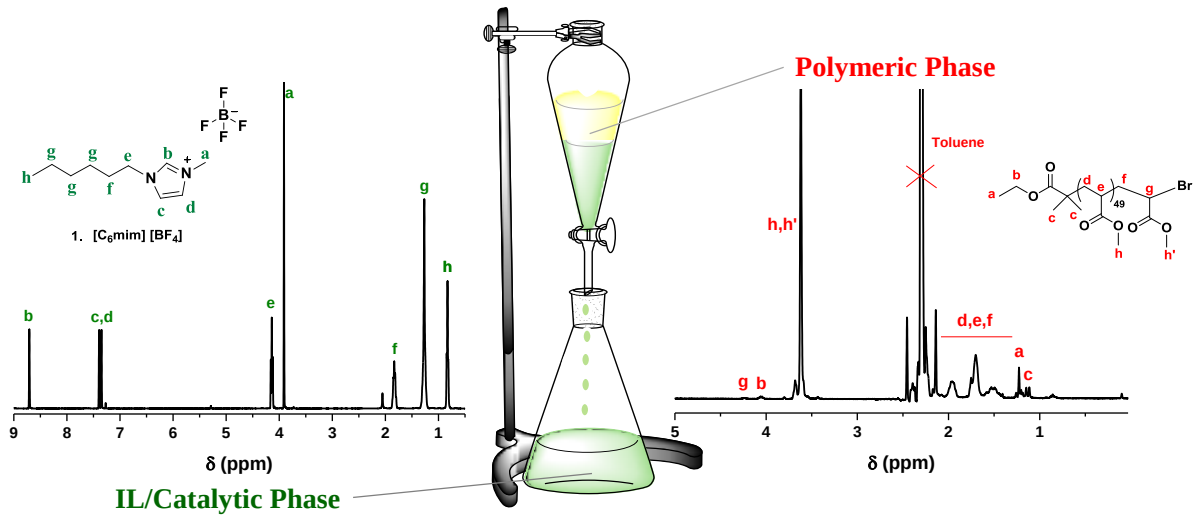

Figure 3.10: ^{1}H NMR of the extracted polymer in toluene (right) and the polymer free IL/catalytic phase (left).

The IL solution (which contains $CuBr_2$/Me_6-Tren) was subsequently charged with additional initiator and monomer and deoxygenated, resulting in a well-defined homopolymer, which exhibited similar polymerisation rate, control over the MWD and molecular weight predictability as in the initial polymerisation. This procedure

(extraction/charging with new monomer-initiator) was repeated three times. In all cases, quantitative conversion was achieved within 1 h while dispersity values remained as low as 1.12 (Figure 3.11). When the process was repeated for the fourth time, the polymerisation rate was slightly decreased, requiring 2 h to reach full conversion. Nevertheless, it was clearly demonstrated that with appropriate selection of the IL it was possible for the IL/catalyst to be recovered and reused several times without compromising the controlled/living features of the polymerisations.

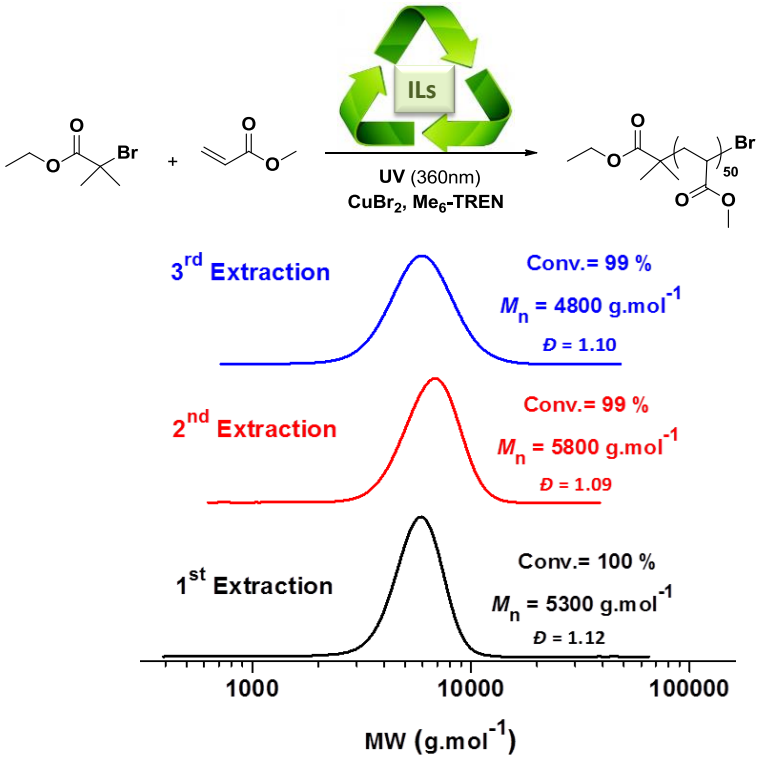

Figure 3.11: SEC analysis of PMA obtained from the recycling cycles of $[C_6mim][BF_4]$.

3.3 Conclusions

The synthesis of well-defined poly(acrylates) in ILs *via* photo-induced RDRP has been investigated. Five different ILs, including [emim][$EtSO_4$], [C_7mim][Br], [C_8mim][PF_6], [C_6mim][BF_4] and [C_6mim][PF_6], were employed for the homopolymerisation of MA, *n*-BA, EGA and PEGA. The use of [$EtSO_4$] and [Br] as counter ions failed to mediate the controlled polymerisation of acrylates under our reaction conditions while the use of the larger and less coordinating [BF_4] and [PF_6] allowed for the RDRP of all monomers (with the exception of *n*-BA in [C_6mim][BF_4] and [C_6mim][PF_6]), presenting fast polymerisation rates, quantitative conversions (> 98% in 30 min) good control over the MWDs ($Đ$ <1.15) and high end-group fidelity, as evidenced by both ^{1}H NMR and MALDI-ToF-MS analysis. This high end-group fidelity was exemplified by sequential *in situ* chain extensions and block copolymerisations which lead to the synthesis of well-defined materials in a facile manner. Higher molecular weight polymers (M_n ~ 40000 g.mol^{-1}) were also targeted, maintaining high conversions and low dispersity. Importantly, the combination of ppm concentrations of catalyst *via* this photo-induced polymerisation protocol with the recyclability of the IL/catalyst solution significantly contributes to the reduction of polymerisation cost and thus paves the way for the inexpensive synthesis of well-defined materials.

3.4 Experimental

3.4.1 Materials and Methods

All materials were purchased from Sigma-Aldrich or Fischer Scientific and used as received unless otherwise stated. All monomers were passed through a basic Al_2O_3 chromatographic column prior to use to remove the inhibitor. Tris-(2-(dimethylamino)ethyl)amine (Me_6-Tren)[20] and all ionic liquids employed in this study were synthesised according to previously reported literature.[21]

3.4.2 Instrumentation

^{1}H NMR spectra were recorded on Bruker DPX-250 and DPX-400 spectrometers using deuterated chloroform ($CDCl_3$) obtained from Aldrich. Chemical shifts are given in ppm downfield from the internal standard tetramethylsilane. Size exclusion chromatography (SEC) measurements were conducted using an Agilent 1260 GPC-MDS fitted with differential refractive index (DRI), light scattering (LS) and viscometry (VS) detectors equipped with 2 × PLgel 5 mm mixed-D columns (300 × 7.5 mm), 1 × PLgel 5 mm guard column (50 × 7.5 mm) and an autosampler. Narrow linear poly (methyl methacrylate) standards in the range of 200 to 1.0×10^6 g·mol^{-1} were used to calibrate the system. All samples were passed through 0.45 μm PTFE filter before analysis. The mobile phase was chloroform with 2% triethylamine at a flow rate of 1.0 mL/min. SEC data was analysed using Cirrus v3.3 software. Matrix Assisted Laser Desorption Ionisation Mass Spectrometry (MALDI-ToF-MS) was conducted using a Bruker Daltonics Ultraflex II MALDI-ToF-MS mass spectrometer, equipped with a nitrogen laser delivering 2 ns laser pulses at 337 nm

with positive ion ToF detection performed using an accelerating voltage of 25 kV. Solutions of trans-2-[3-(4-tert-butylphenyl)-2-methyl-2-propylidene] malonitrile (DCTB) as matrix (saturated solution) in tetrahydrofuran (50 μL), sodium iodide as cationisation agent (1.0 mg/mL) and sample (1.0 mg/mL) were mixed, and 0.7 μL of the mixture was applied to the target plate. Spectra were recorded in reflector mode calibrated with PEG-Me 1100 kDa. The source of UV light was a UV "nail gel curing lamp" (available online from a range of ad hoc suppliers) (λ_{max} ~ 360 nm) equipped with four 9Watt bulbs.

3.4.3 General procedures

(a) Typical conditions for the photo-induced polymerisation of MA in ionic liquids

Filtered monomer (*DP* equiv., 2 mL), ethyl bromoisobutyrate (EBiB) (1 equiv.), $CuBr_2$ (0.02 equiv.), Me_6-Tren (0.12 equiv.) and IL (2 mL) were added to a septum sealed vial and purged with nitrogen for 15 min. Polymerisation commenced upon placement of the deoxygenated reaction vessel under the UV lamp. Samples were taken periodically and conversions were measured using ^{1}H NMR and SEC analysis.

For the chain extensions / block copolymerisations, a deoxygenated solution of MA (50 equiv.), EGA (50 equiv.), *n*-BA (50 equiv.) or $PEGA_{480}$ (15 equiv.) in IL (50% *v/v* with respect to monomer) was added *via* a nitrogen-purged syringe and again the solution was allowed to polymerise under the lamp. Samples were taken periodically and conversions were measured using ^{1}H NMR and SEC analysis.

(b) Typical procedure for the recycling experiment

The crude polymerisation mixture (PMA in IL) was extracted with toluene (2 ml). This procedure was repeated three times and ^{1}H NMR was utilised for the characterisation of both phases. Once extraction was complete as observed by ^{1}H NMR, the (polymer free) IL phase was reused as the solvent for the homopolymerisation of MA without adding further $CuBr_2$/Me_6-Tren.

3.4.4 Additional characterisation

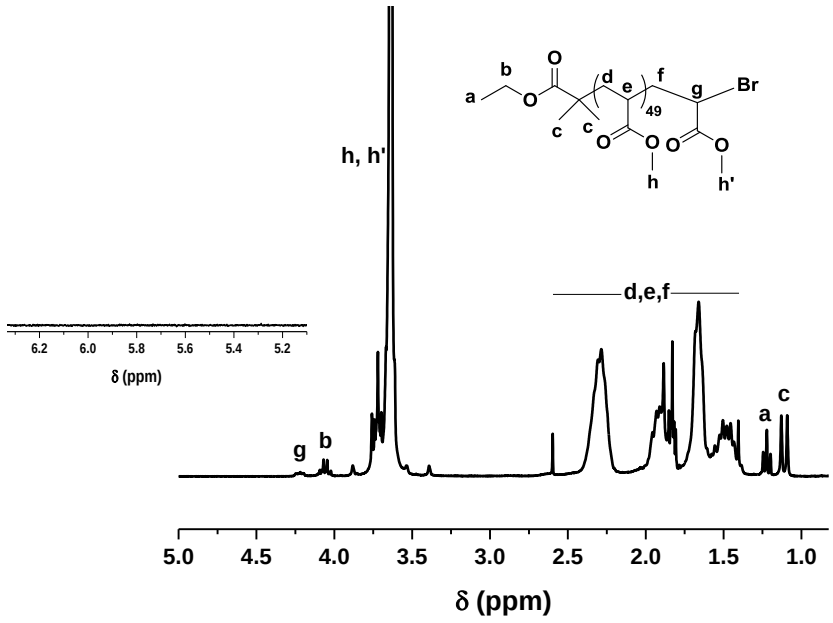

Figure 3.12: ^{1}H NMR spectrum of PMA in [C_6mim][BF_4] (50:50 *v/v* monomer/ionic liquid) [MA]:[EBiB]:[$CuBr_2$]:[Me_6-Tren] = [50]:[1]:[0.02]:[0.12], integrated ratio of g : c = 0.99 : 6.00.

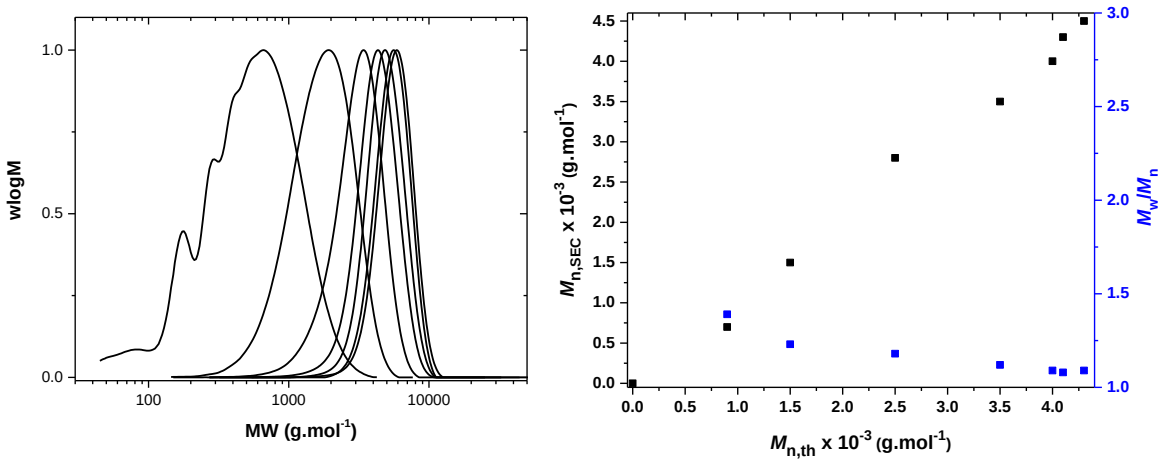

Figure 3.13: SEC analysis showing the molecular weight evolution during the kinetic experiment of photo-induced polymerisation of MA in [C_6mim][BF_4] (left) and $M_{n,SEC}$ and M_w/M_n *vs.* theoretical molecular weight $M_{n,th}$ (right).

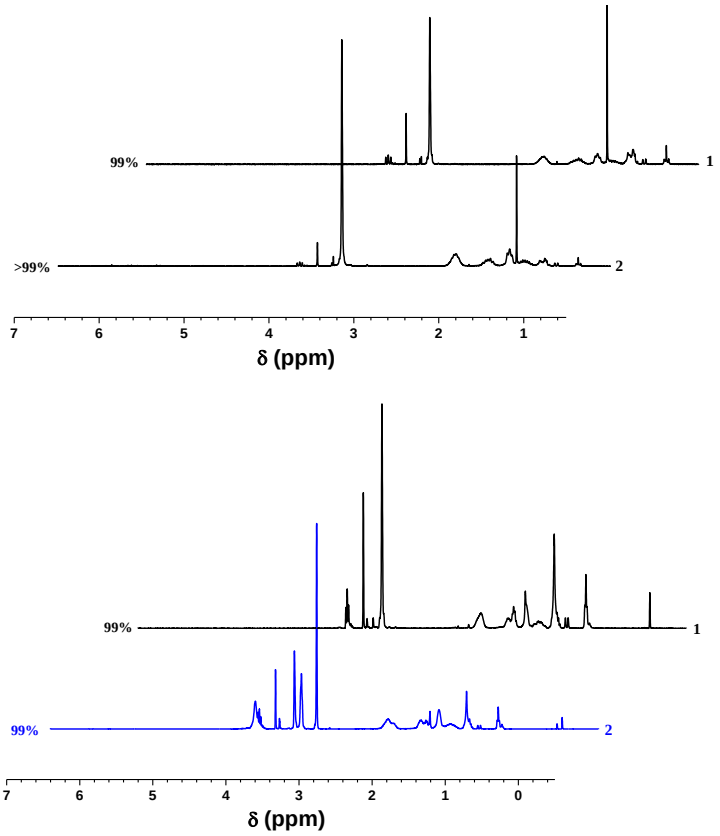

Figure 3.14: ^{1}H NMR for the *in situ* chain extension (up) and for the block copolymerisation (down) from a PMA macroinitiator in [C_6mim][BF_4] (50:50 *v/v* monomer/ionic liquid). Initial conditions: [MA]:[EBiB]:[$CuBr_2$]:[Me_6-Tren] = [50]:[1]:[0.02]:[0.12]. Chain

extension achieved upon addition of an aliquot of MA (50 equiv.) or EGA (50 equiv.) in [C_6mim][BF_4] (33% *v/v*).

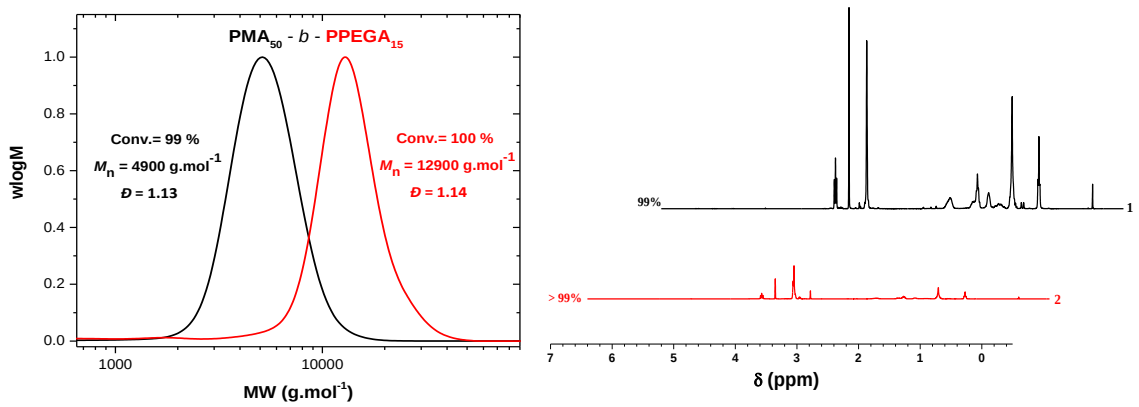

Figure 3.15: SEC and ^{1}H NMR analysis for the block copolymerisation from a PMA macroinitiator in [C_6mim][BF_4] (50:50 *v/v* monomer/ionic liquid). Initial conditions: [MA]:[EBiB]:[$CuBr_2$]:[Me_6-Tren] = [50]:[1]:[0.02]:[0.12]. Chain extension achieved upon addition of an aliquot of PEGA (15 equiv.) in [C_6mim][BF_4] (33% *v/v*).

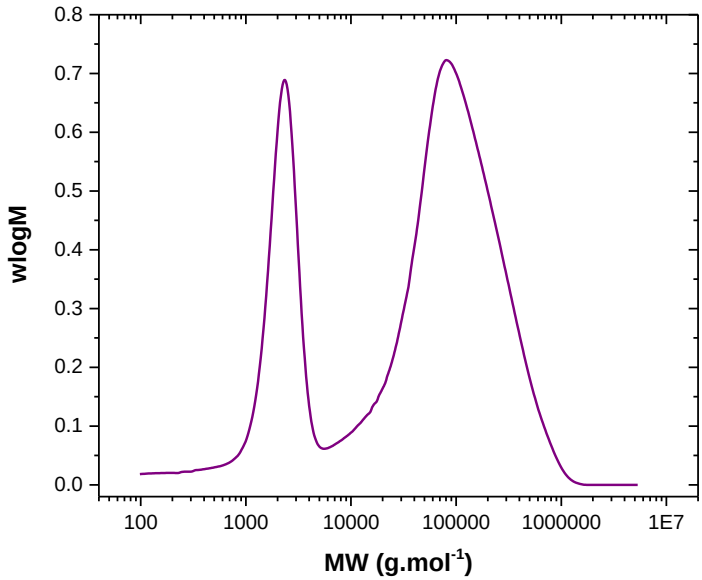

Figure 3.16: SEC analysis for the synthesis of PBA in [C_6mim][BF_4] (50:50 *v/v* monomer/ionic liquid). Initial conditions: [*n*-BA]:[EBiB]:[$CuBr_2$]:[Me_6-Tren] = [50]:[1]:[0.02]:[0.12].

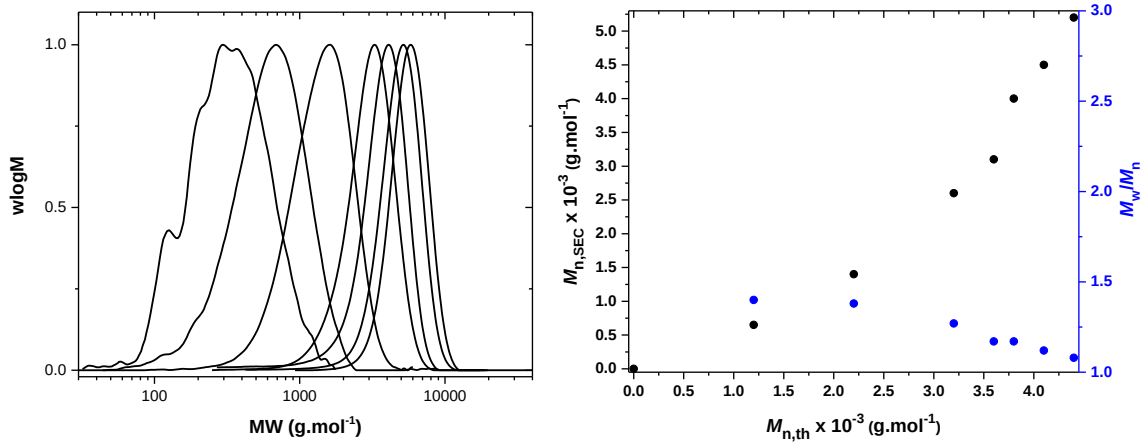

Figure 3.17: SEC analysis showing the molecular weight evolution during the kinetic experiment of photo-induced polymerisation of MA in $[C_6mim][PF_6]$ (up) and $M_{n,SEC}$ and M_w/M_n *vs.* theoretical molecular weight $M_{n,th}$ (down).

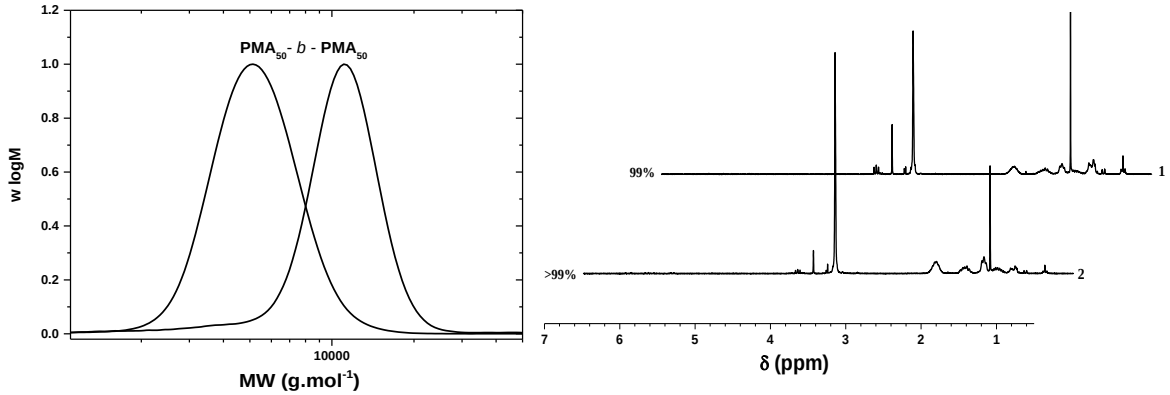

Figure 3.18: SEC and ^1H NMR analysis for the *in situ* chain extension from a PMA macroinitiator in $[C_6mim][PF_6]$ (50:50 *v/v* monomer/ionic liquid). Initial conditions: [MA]:[EBiB]:[$CuBr_2$]:[Me_6-Tren] = [50]:[1]:[0.02]:[0.12]. Chain extension achieved upon addition of an aliquot of MA (50 equiv.) in $[C_6mim][PF_6]$ (33% *v/v*).

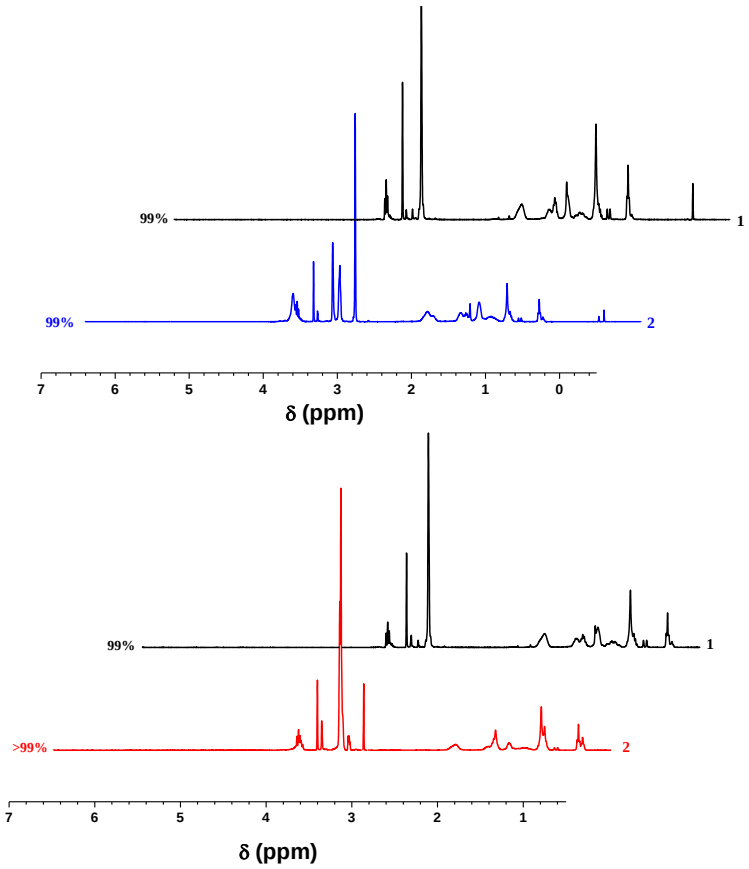

Figure 3.19: SEC and ^{1}H NMR analysis for block copolymerisation from a PMA macroinitiator in [C_6mim][PF_6] (50:50 *v/v* monomer/ionic liquid). Initial conditions: [MA]:[EBiB]:[$CuBr_2$]:[Me_6-Tren] = [50]:[1]:[0.02]:[0.12]. Chain extension achieved upon addition of an aliquot of EGA (50 equiv.) or PEGA (15 equiv.) in [C_6mim][PF_6] (33% *v/v*).

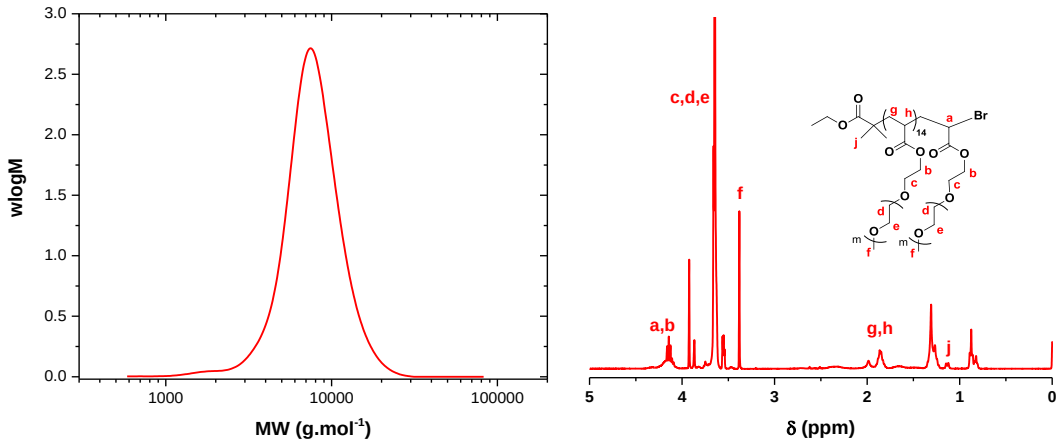

Figure 3.20: SEC and ^{1}H NMR analysis for the synthesis of PEGA in [C_6mim][PF_6] (50:50 *v/v* monomer/ionic liquid). Initial conditions [EGA]:[EBiB]:[$CuBr_2$]:[Me_6-Tren] = [50]:[1]:[0.02]:[0.12].

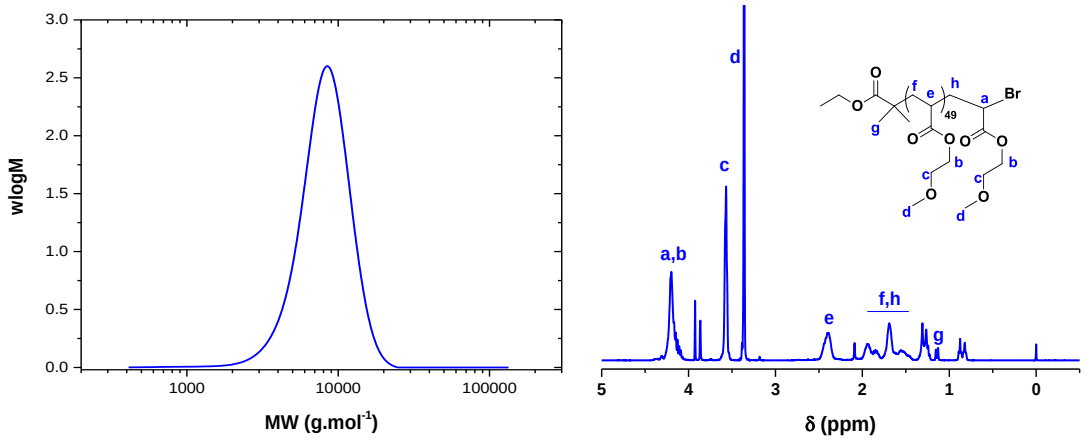

Figure 3.21: SEC and ^{1}H NMR analysis for the synthesis of PPEGA in [C_6mim][PF_6] (50:50 *v/v* monomer/ionic liquid). Initial conditions [PEGA]:[EBiB]:[$CuBr_2$]:[Me_6-Tren] = [15]:[1]:[0.02]:[0.12].

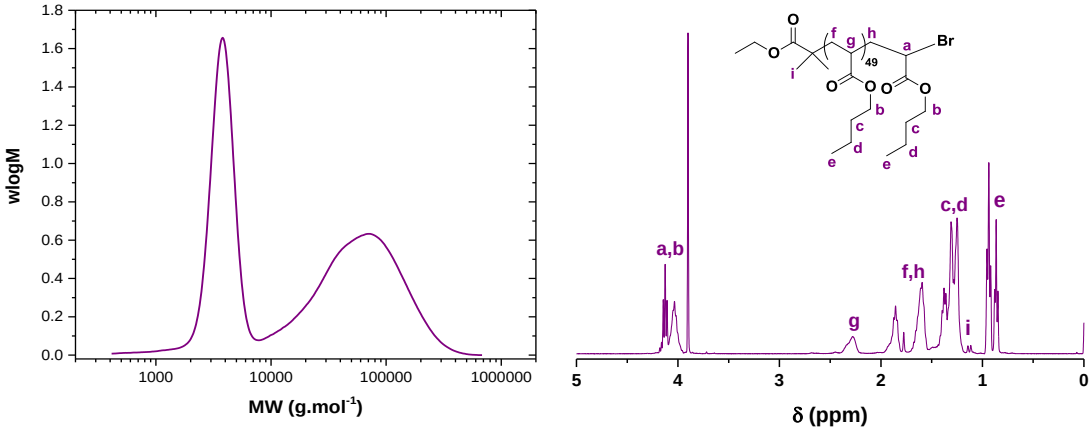

Figure 3.22: SEC and ^{1}H NMR analysis for the synthesis of PBA in [C_6mim][PF_6] (50:50 *v/v* monomer/ionic liquid). Initial conditions [*n*-BA]:[EBiB]:[$CuBr_2$]:[Me_6-Tren] = [50]:[1]:[0.02]:[0.12].

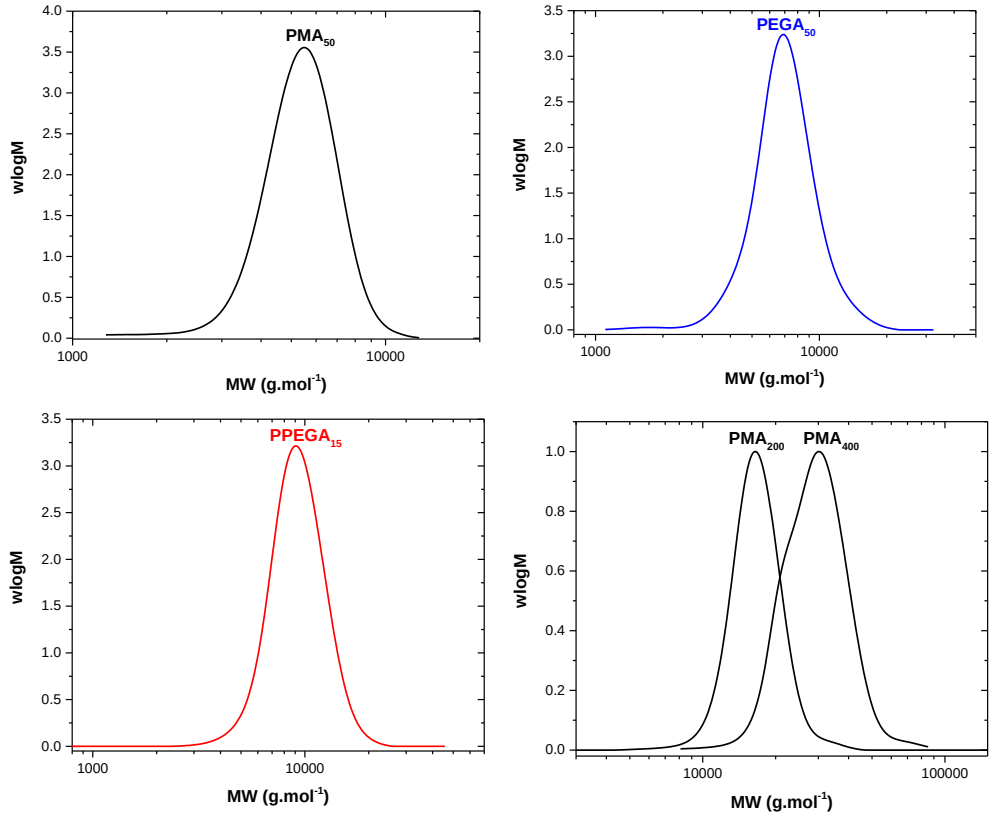

Figure 3.23: SEC analysis for the synthesis of PMA (up left), PEGA (up right), PPEGA (down left) and high molecular weight PMA_{200} and PMA_{400} (down right) in [C_8mim][PF_6] (50:50 *v/v* monomer/ionic liquid). Initial conditions: [EBiB]:[$CuBr_2$]:[Me_6-Tren] = [1]:[0.02]:[0.12].

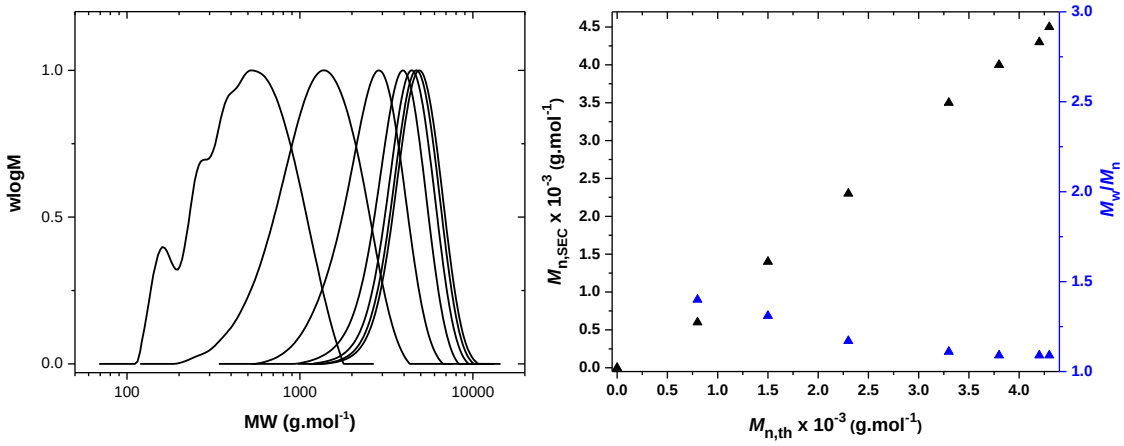

Figure 3.24: SEC analysis showing the molecular weight evolution during the kinetic experiment of photo-induced polymerisation of MA in [C_8mim][PF_6] (left) and $M_{n,SEC}$ and M_w/M_n *vs.* theoretical molecular weight $M_{n,th}$ (right).

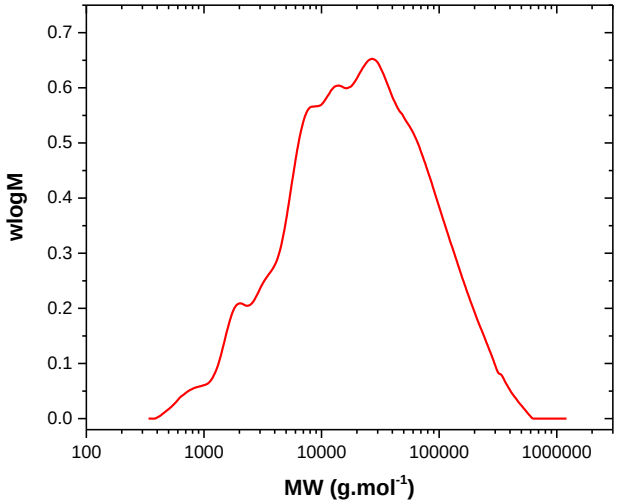

Figure 3.25: SEC analysis for the synthesis of PPEGA in [emim][$EtSO_4$] (50:50 *v/v* monomer/ionic liquid). Initial conditions: [PEGA]:[EBiB]:[$CuBr_2$]:[Me_6-Tren] = [15]:[1]:[0.02]:[0.12].

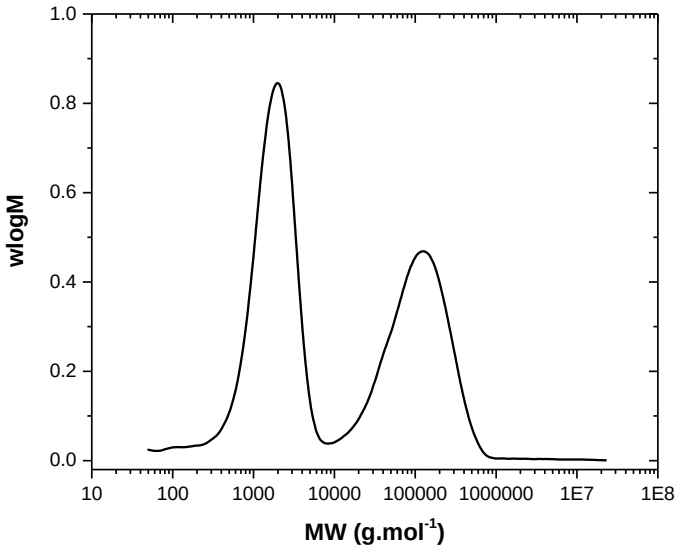

Figure 3.26: SEC analysis for the synthesis of PMA in [C_7mim][Br] (50:50 *v/v* monomer/ionic liquid). Initial conditions: [MA]:[EBiB]:[$CuBr_2$]:[Me_6-Tren] = [50]:[1]:[0.02]:[0.12].

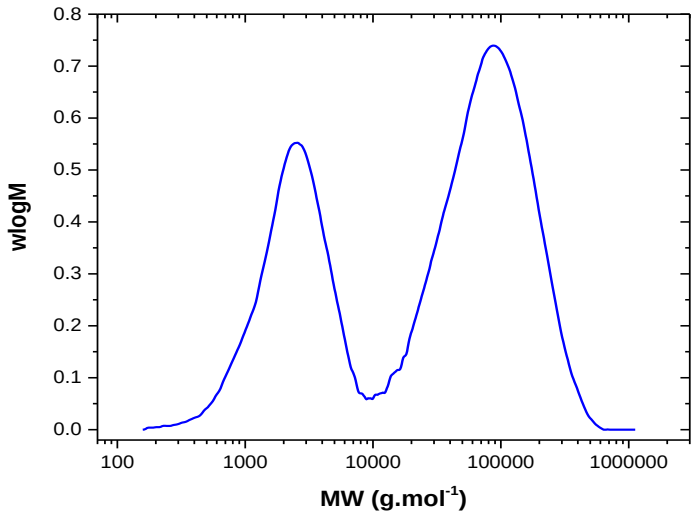

Figure 3.27: SEC analysis for the synthesis of PEGA in [C_7mim][Br] (50:50 *v/v* monomer/ionic liquid). Initial conditions: [EGA]:[EBiB]:[$CuBr_2$]:[Me_6-Tren] = [50]:[1]:[0.02]:[0.12].

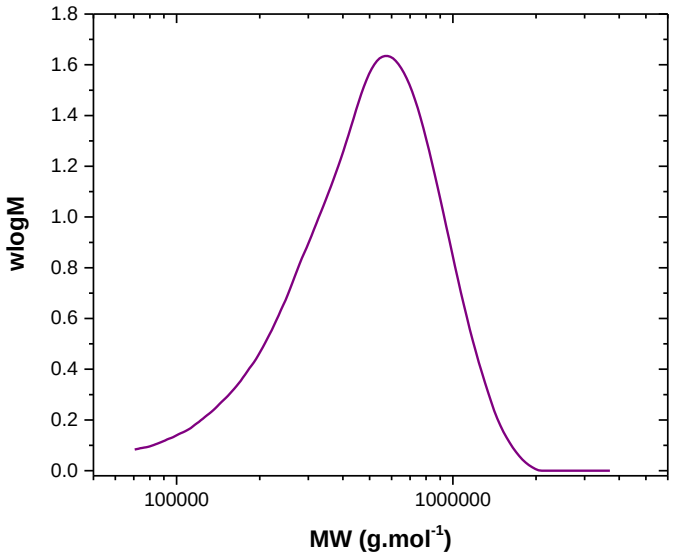

Figure 3.28: SEC analysis for the synthesis of PBA in [C_7mim][Br] (50:50 *v/v* monomer/ionic liquid). Initial conditions: [*n*-BA]:[EBiB]:[$CuBr_2$]:[Me_6-Tren] = [50]:[1]:[0.02]:[0.12].

3.5 References

1. T. Ueki and M. Watanabe, *Macromolecules*, 2008, **41**, 3739-3749.

2. V. I. Pârvulescu and C. Hardacre, *Chem. Rev.*, 2007, **107**, 2615-2665.

3. M. J. Earle, P. B. McCormac and K. R. Seddon, *Green Chem.*, 1999, **1**, 23-25.

4. M. J. Earle, P. B. McCormac and K. R. Seddon, *Chem. Commun.*, 1998, **20**, 2245-2246.

5. P. Kubisa, *Prog. Polym. Sci.*, 2004, **29**, 3-12.

6. P. Kubisa, *Prog. Polym. Sci.*, 2009, **34**, 1333-1347.

7. S. Perrier, T. P. Davis, A. J. Carmichael and D. M. Haddleton, *Chem. Commun.*, 2002, **19**,2226-2227.

8. S. Perrier, T. P. Davis, A. J. Carmichael and D. M. Haddleton, *Eur. Polym. J.*, 2003, **39**, 417-422.

9. J. Ryan, F. Aldabbagh, P. B. Zetterlund and B. Yamada, *Macromol. Rapid Commun.*, 2004, **25**, 930-934.

10. H. Zhang, K. Hong and J. Mays, *Polym. Bull.*, 2004, **52**, 9-16.

11. A. J. Carmichael, D. M. Haddleton, S. A. F. Bon and K. R. Seddon, *Chem. Commun.*, 2000, **14**, 1237-1238.

12. S. Harrisson, S. R. Mackenzie and D. M. Haddleton, *Chem. Commun.*, 2002, **23**, 2850-2851.

13. T. Sarbu and K. Matyjaszewski, *Macromol. Chem. Phys.*, 2001, **202**, 3379-3391.

14. V. Percec and C. Grigoras, *J. Polym. Sci. Part A: Polym. Chem.*, 2005, **43**, 5609-5619.

15. T. Biedroń and P. Kubisa, *Macromol. Rapid Commun.*, 2001, **22**, 1237-1242.

16. T. Biedroń and P. Kubisa, *J. Polym. Sci. Part A: Polym. Chem.*, 2002, **40**, 2799-2809.

17. A. Anastasaki, V. Nikolaou, Q. Zhang, J. Burns, S. R. Samanta, C. Waldron, A. J. Haddleton, R. McHale, D. Fox, V. Percec, P. Wilson and D. M. Haddleton, *J. Am. Chem. Soc.*, 2013, **136**, 1141-1149.

18. A. Anastasaki, C. Waldron, P. Wilson, R. McHale and D. M. Haddleton, *Polym. Chem.*, 2013, **4**, 2672-2675.

19. C. A. Bell, Z. Jia, J. Kulis and M. J. Monteiro, *Macromolecules*, 2011, **44**, 4814-4827.

20. M. Ciampolini and N. Nardi, *Inorg. Chem.*, 1966, **5**, 41-44.

21. J. D. Holbrey and K. R. Seddon, *Dalton Trans.*, 1999, **13**, 2133-2140.

Chapter 4

Copper(II) gluconate (a non-toxic food supplement/dietary aid) as a precursor catalyst for effective photo-induced living radical polymerisation of acrylates

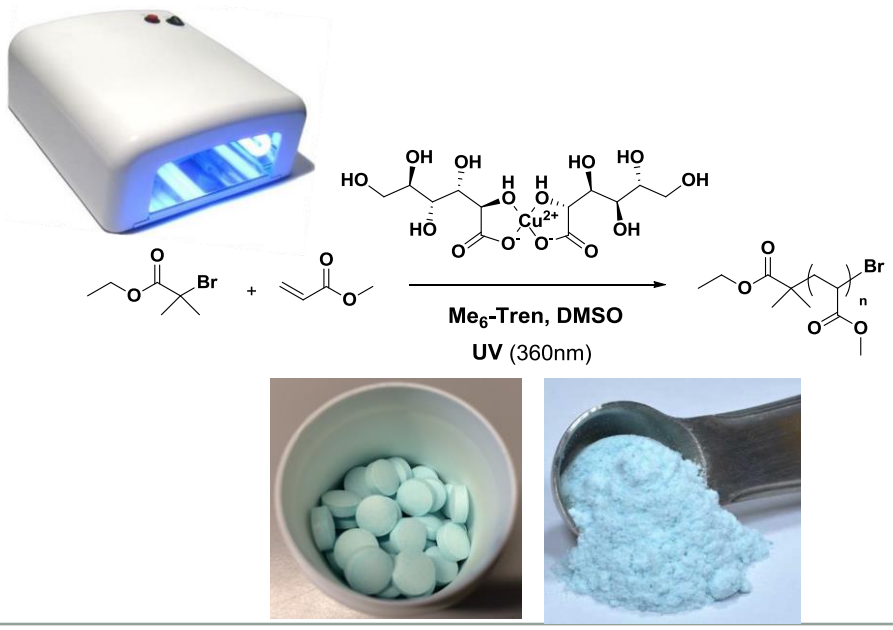

Copper gluconate, is a widely used commercially available dietary supplement that can be exploited to metabolise copper and treat copper deficiency. In this chapter, copper gluconate is employed as a precursor catalyst for the photo-induced living radical polymerisation of acrylates. Optimised reaction conditions for efficient ligand transfer leads to well-defined polymers within 2 h with near-quantitative conversions (> 95%), low dispersities (Đ ~ 1.16) and high end-group fidelity, as demonstrated by MALDI-ToF-MS and in situ block copolymerisation. Additionally, in the presence of ppm concentrations of NaBr, similar degree of control could also be attained by facilitating ligand exchange, furnishing low dispersed polymers (Đ < 1.12).

4.1 Introduction

One of the main perceived drawbacks of the RDRP techniques, is considered to be copper contamination of the products.[1] The presence of trace metal, is often heralded as a weakness, due to potential toxicity of "*heavy metals*", whilst one would argue that organic ligands and residual monomers should be of more concern. It is noted that this concern is not restricted to polymerisation and the use of "*copper-free click*" reactions are also prevalent as a way of carrying out less toxic reactions.[2] A wide range of different protocols have been established with primary focus to minimise the catalyst loadings and to remove residual metals.[3-5] A diverse array of external stimuli,[6] including photochemical,[7-14] pressure[15] and electrochemical,[16] have been developed, with photochemical control exhibiting excellent results when combined with copper-mediated polymerisation.[17-25]

Although some heavy metals are indeed very toxic and poisonous, they are often essential for human life (*e.g.* Fe (haemoglobin), Co (vitamin B_{12}), Cu *etc.*).[26-29] Copper, is involved in various biological processes (haemoglobin formation, carbohydrate metabolism, the cross-linking of collagen, hair keratin and the antioxidant defence mechanism *etc.*) while being incorporated into a number of metalloenzymes. Copper deficiency in humans, although relatively rare, is a known cause of hypochromic anaemia, leukopenia and various neurological manifestations.[30] Interestingly, the World Health Organisation recommends a daily requirement of 0.6 mg per day with an estimated lethal dose in human adults of 10-20 g.[31, 32]

Generally, there is a misconception regarding copper toxicity and depending on the application and levels of impurities it is often desirable to copper residues

from products prior to use. Thus, the main focus of this chapter is the use of a commercially available, non-toxic food supplement (Cu(II) gluconate) as a precursor catalyst for the photo-induced polymerisation of acrylates. Under carefully optimised conditions the gluconate is allowed to exchange with Me_6-Tren to form the active catalyst. This ligand was chosen as it has been shown to be very effective in this photo-mediated reaction.

4.2 Results and Discussion

Initially, the solubility of copper gluconate in DMSO was investigated. The commercially available tablet was ground into a fine powder and the reaction vessel was subsequently charged with methyl acrylate (MA), DMSO, ethyl bromo isobutyrate (EBiB), 2% copper gluconate (approximately 200 mg tablet containing 1.1 mg Cu(II)) and 12% Me_6-Tren.[7] A dispersion was immediately formed, suggesting that the copper gluconate and/or additives (stated bulking agents include calcium phosphate, cellulose and magnesium stearate) had limited solubility in this particular solvent. As an attempt to demonstrate polymerisation in the presence of multiple functional groups and thus the presence and effect of the formulating agents was of interest.[33] Despite these solubility issues, the polymerisation was allowed to proceed under UV irradiation (λ = 365 nm) for 2 h yielding an uncontrolled polymer (96%, M_n = 5500 g.mol^{-1}, $Đ$ = 2.30) (Table 4.1, Figure 4.1). To further investigate this result, commercial copper gluconate was employed, giving rise to an equally broad dispersed polymer (98%, M_n = 5400 g.mol^{-1}, $Đ$ = 1.80 after 2 h), while remaining partly insoluble (Table 4.1, Figure 4.1).

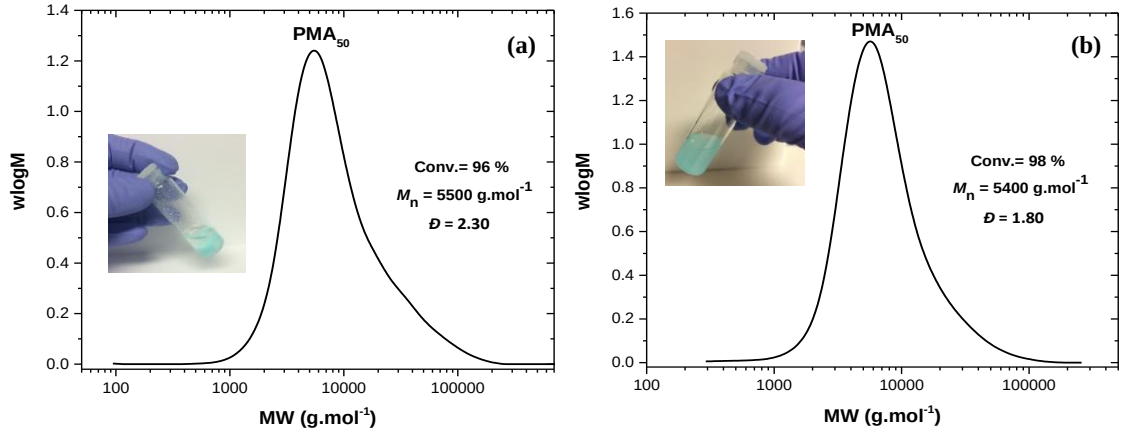

Figure 4.1: SEC analysis of PMA utilising (a) the dietary supplement and (b) pure Cu(II) gluconate. Initial conditions: [MA]:[EBiB]:[Cu(II) gluconate]:[Me_6-Tren] = [50]:[1]:[0.02]:[0.12] in DMSO 50% *v/v*.

There is a requirement for ligand exchange between the *O*-donor gluconate to *N*-donor ligands and a slow rate of the ligand exchange between the gluconate and Me_6-Tren could be responsible for the inefficient deactivation of the polymer chains. Upon stirring Me_6-Tren and copper gluconate for ~ 12 h, at ambient temperature, followed by the addition of both monomer and initiator and UV exposure for a further 2 h, 98% conversion was obtained with M_n = 5000 g.mol^{-1} and an encouragingly slight reduction in the observed dispersity ($Đ$ = 1.50) (Table 4.1, Section 4.4.4, Figure 4.8). Interestingly, when the pre-mixing took place for 2 weeks prior to polymerisation, a well-defined polymer (96%, M_n = 5500 g.mol^{-1}, $Đ$ = 1.19) was obtained (Table 4.1, Figure 4.2), implying that when Me_6-Tren replaces the gluconate entirely, an efficient deactivation can be mediated.

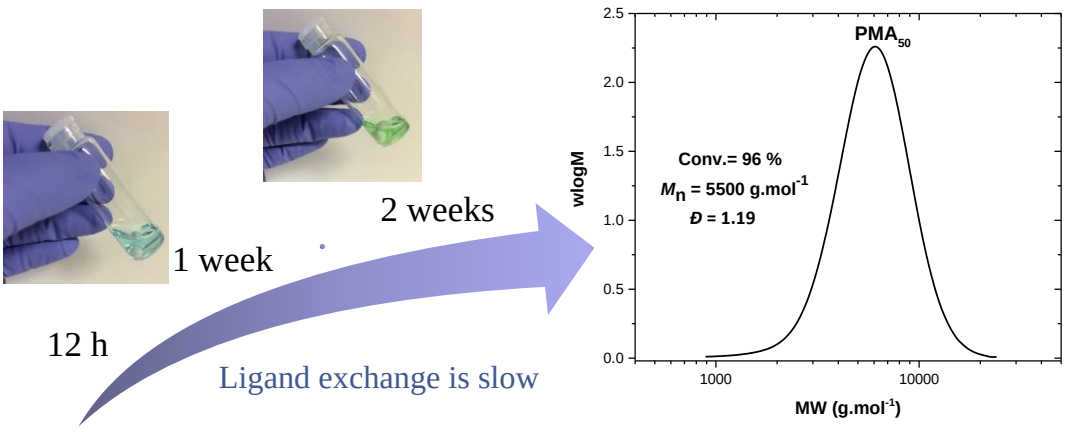

Figure 4.2: SEC analysis of PMA utilising Cu(II) gluconate (supplement) as the precursor catalyst. Initial conditions: [MA]:[EBiB]:[Cu(II) gluconate]:[Me_6-Tren] = [50]:[1]:[0.02]:[0.12] in DMSO 50% *v/v*, pre-mixing of the Cu(II) gluconate/Me_6-Tren complex for 2 weeks.

UV-Vis spectroscopy measurements were also performed. Upon addition of Me_6-Tren on the copper gluconate solution, an instantaneous change in the UV spectrum was observed, resulting in identical absorbance characteristic peaks when compared with Me_6-Tren/$CuBr_2$ complex. No further change was monitored by UV within 2 weeks, despite the observed reduction in the dispersity of the product (Figure 4.3). Nevertheless, reduction in pre-mixing time scale to 1 week resulted in broader MWDs (97%, M_n = 5400 g.mol^{-1}, $Đ$ = 1.38) as opposed to pre-mixing for 2 weeks (96%, M_n = 5500 g.mol^{-1}, $Đ$ = 1.19), suggesting that the substitution needed significant time in order to reach the desired equilibrium (Section 4.4.4, Figure 4.8).

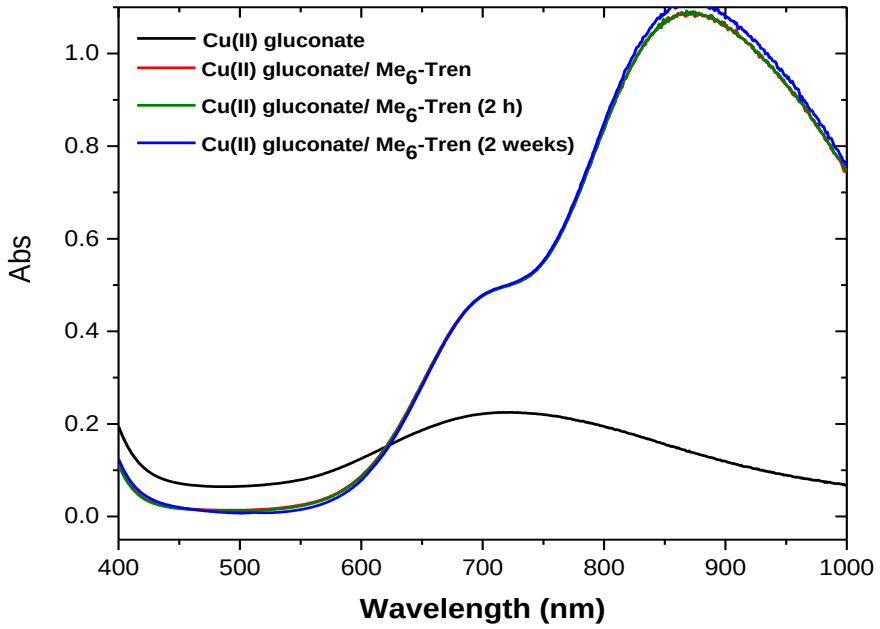

Figure 4.3: Monitoring effect of UV irradiation on Cu(II) gluconate/Me_6-Tren in DMSO complex as a function of time by UV−vis spectroscopy.

Table 4.1: Photo-induced polymerisation of MA utilising copper gluconate as the precursor catalyst.

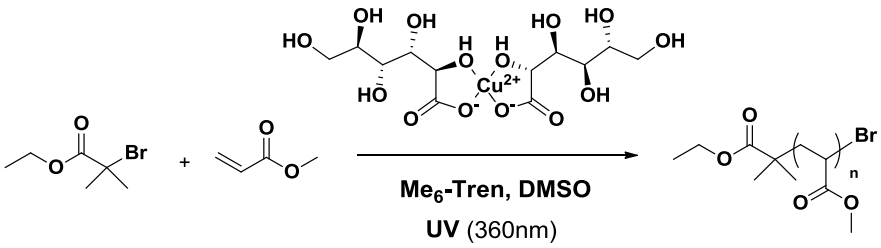

Entry	[M]:[I]:[Cu]:[L]	Conv. (%)	$M_{n,th}$ (g.mol^{-1})	$M_{n,SEC}$ (g.mol^{-1})	$Đ$
1	[50]:[1]:[0.02]:[0.12]	96	4300	5500	2.30
2[a]		98	4400	5400	1.80
3[b]		98	4400	5400	1.50
4[c]		96	4300	5500	1.19

[a]Utilising pure copper gluconate, [b,c]premixing for 12 h and 2 weeks respectively, prior to polymerisation

In order to accelerate the ligand exchange rate, a solution of the pure copper gluconate (1 equiv.) with Me_6-Tren (6 equiv.) in DMSO was left under UV

irradiation for ~ 2 h. Monomer and initiator were subsequently added in the polymerisation mixture yielding, within 2 h, a well-defined PMA (97%, M_n = 4900 g.mol^{-1}, $Đ$ = 1.15) (Table 4.2, Section 4.4.4, Figure 4.9). Similar results were obtained when the food supplement was employed (98%, M_n = 5600 g.mol^{-1}, $Đ$ = 1.16), highlighting the potential of this protocol to operate in the presence of various chemical environments/impurities (Table 4.2). The high end-group fidelity obtained during the polymerisation was confirmed by both ^{1}H NMR and MALDI-ToF unveiling a single mass distribution corresponding to bromo-terminated polymer chains (Figure 4.4).

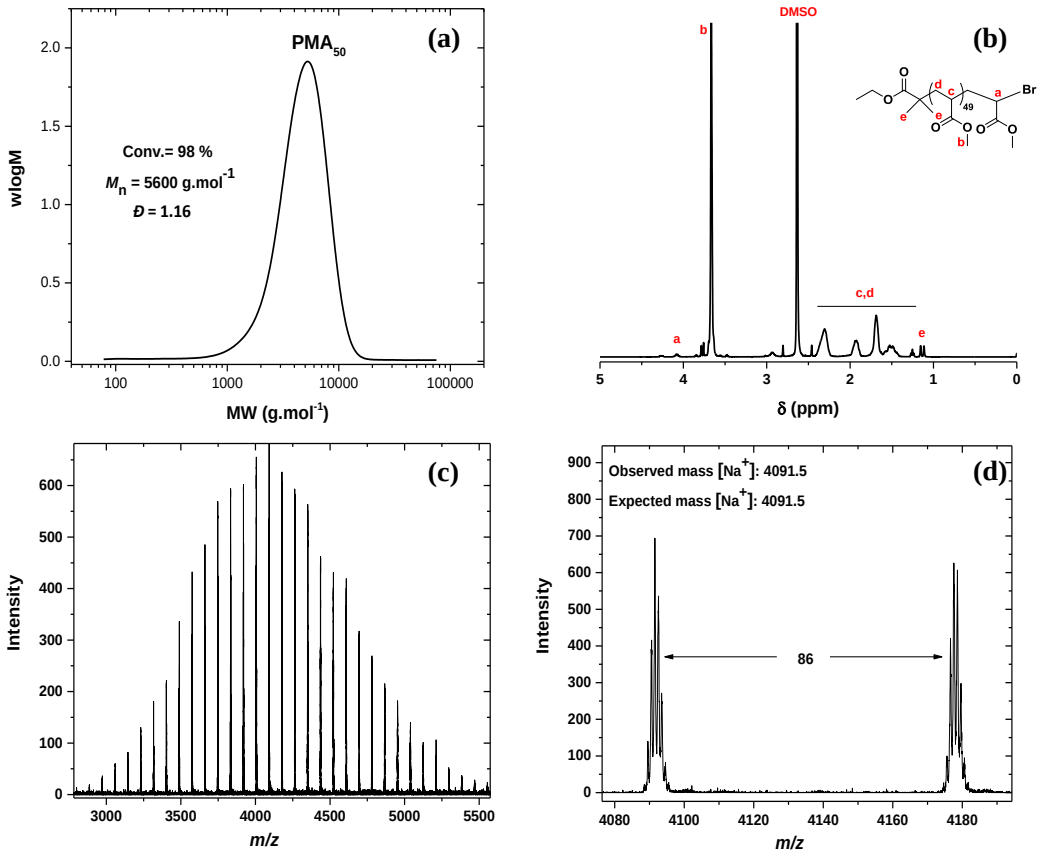

Figure 4.4: (a) SEC, (b) ^{1}H NMR, (c) and(d) MALDI-ToF-MS analyses of PMA obtained from the experiment [MA]:[EBiB]:[Cu(II) gluconate (supplement)]:[Me_6-Tren] =

[50]:[1]:[0.02]:[0.12] in DMSO (50% *v/v*). The pre-mixed Cu/L solution was left under UV irradiation for 2 h prior to polymerisation.

In previous studies it has already been demonstrated that the temperature throughout the reaction fluctuates between 55 and 60 ^{o}C.[7] Consequently, we repeated polymerisations under UV irradiation utilising a cooling plate to maintain lower temperatures (~ 15 ^{o} C). After identical reaction times (2 h) 70% (M_n = 3900 g.mol^{-1}, $Đ$ = 1.33), (Section 4.4.4, Figure 4.10) and 75% (M_n = 4200 g.mol^{-1}, $Đ$ = 1.40) (Figure 4.5 (a)) conversions were obtained for pure gluconate and the food supplement respectively (Table 2), indicating that light also mediates ligand exchange, however, not as effectively as when combined with heat. Conversely, under purely thermal conditions, (60^{o}C, no UV irradiation) well-defined polymers were attained in both cases (M_n = 4300 g.mol^{-1}, $Đ$ = 1.18 for pure gluconate and M_n = 5200 g.mol^{-1}, $Đ$ = 1.19) for the dietary supplement, (Table 4.2, Figure 4.5 (b), Section 4.4.4, Figure 4.10) demonstrating that increased temperatures allows effective ligand exchange.

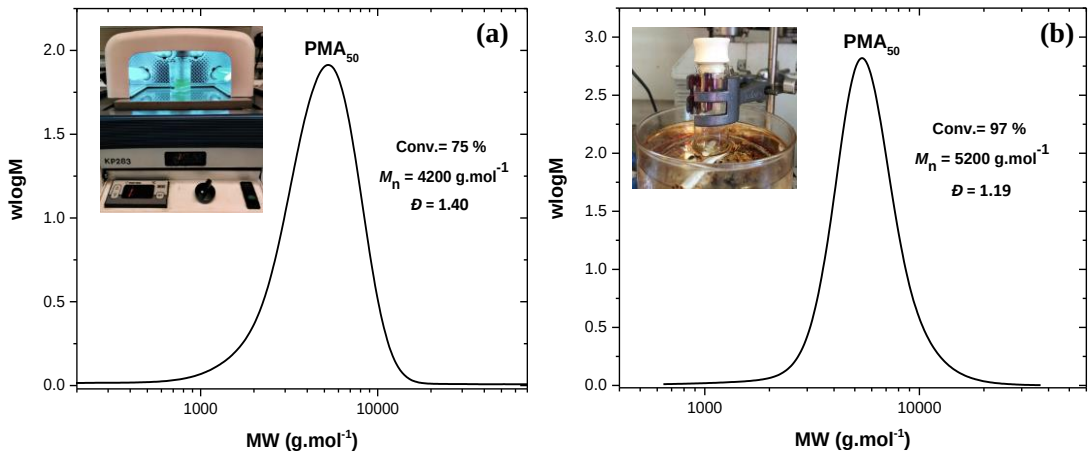

Figure 4.5: SEC analysis of PMA utilising Cu(II) gluconate (supplement) as the precursor catalyst. Initial conditions: [MA]:[EBiB]:[Cu(II) gluconate]:[Me_6-Tren] =

[50]:[1]:[0.02]:[0.12] in DMSO 50% *v/v*, pre-mixing of the Cu(II) gluconate/Me_6-Tren complex for 2 h under UV irradiation at (a) 15 °C and (b) 60 °C.

Table 4.2: Optimised reaction conditions for the photo-induced polymerisation of methyl acrylate. Both formulated tablet and pure copper(II) gluconate used as a precursor to Me_6-Tren exchange.

	Conditions	Conv. (%)	$M_{n,th}$ (g.mol^{-1})	$M_{n,SEC}$ (g.mol^{-1})	$Đ$
Tablet 	UV-Vis	98	4400	5600	1.16
	Cooling plate	75	3400	4200	1.40
	Heat 60 °C	97	4400	5200	1.19
	NaBr	99	4500	5400	1.15
Pure gluconate 	UV-Vis	97	4400	4900	1.15
	Cooling plate	70	3100	3900	1.33
	Heat 60 °C	95	4300	4300	1.18
	NaBr	98	4400	5100	1.12

For applications where elevated temperatures are undesirable, an alternative synthetic route was also explored. The addition of ppm concentrations of NaBr in the reaction mixture,[34] gave rise to well-defined polymers without the need for elevated temperatures and pre-mixing protocols (Table 4.2). Near identical results were obtained for both the tablet (99%, M_n = 5400 g.mol^{-1}, $Đ$ = 1.15) and the pure copper gluconate (98%, M_n = 5100 g.mol^{-1}, $Đ$ = 1.12), (Section 4.4.4, Figure 4.11) with good correlation between the theoretical/experimental molecular weights and narrow molecular weight distributions. The excess bromide anion is able to promote ligand exchange presumably by coordinating to copper causing dissociation of a gluconate ligand.

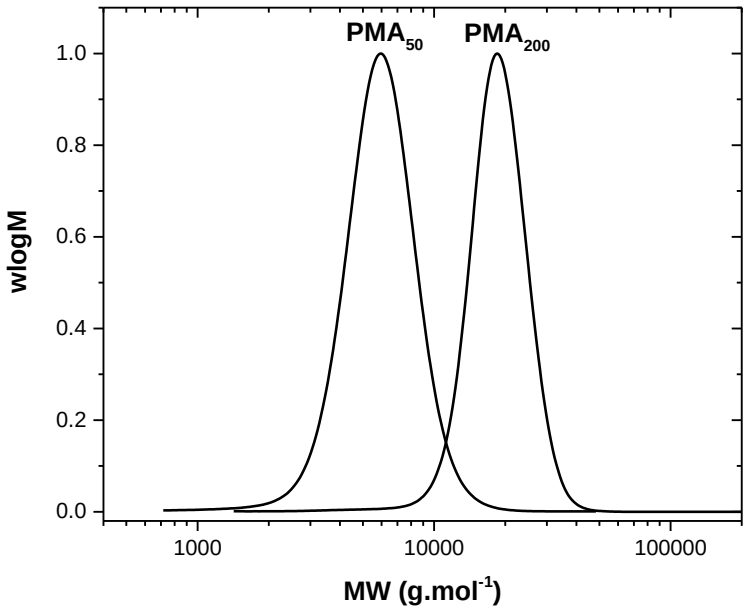

Figure 4.6: SEC analysis of PMA with *DP* = 50, 200 prepared by photo-induced polymerisation utilising copper gluconate (supplement). Initial conditions: [EBiB]:[Cu(II) (supplement)]:[Me_6-Tren]:[NaBr] = [1]:[0.02]:[0.12]:[0.04] in DMSO (50% *v/v*) at 50^{o}C.

We were interested to assess whether the copper gluconate tablet could also support the synthesis of higher molecular weight polymers. In order to verify this, a higher degree of polymerisation (*DP* = 200) was targeted. High conversions and low dispersity were attained within 2 h (95%, M_n = 20000 g.mol^{-1}, $Đ$ = 1.09) (Figure 4.6). To further demonstrate the high end-group fidelity, *in situ* block copolymerisation of PMA (*DP* = 50, 96% in 2 h, M_n= 4400 g.mol^{-1}, $Đ$ = 1.13) with PEGA was attempted. Upon addition of a second aliquot of PEGA, a complete shift to higher molecular weight was evident by SEC, while the dispersity remained as low as 1.10 (*DP* = 15, 98% in 10 h, M_n= 11000 g.mol^{-1}) (Figure 4.7, Section 4.4.4, Figure 4.12).

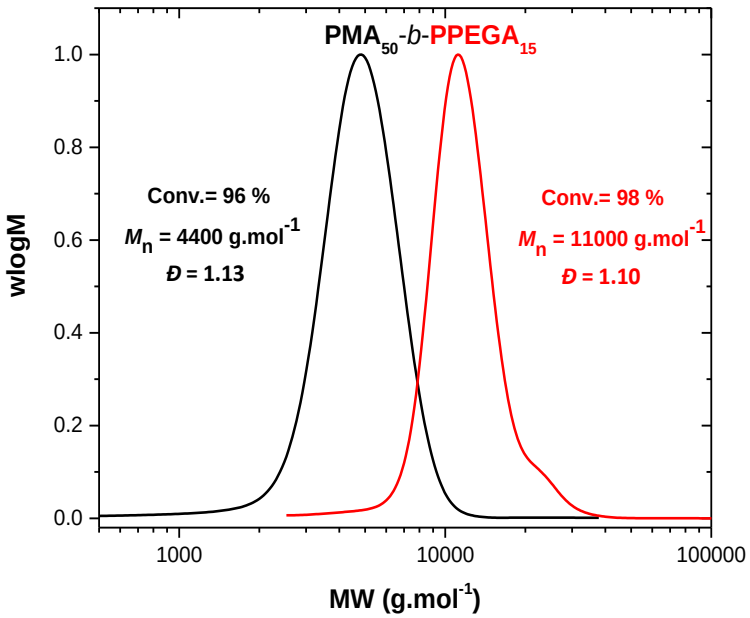

Figure 4.7: *In situ* block copolymerisation from a PMA macroinitiator with PEGA. Initial conditions: [MA]:[EBiB]:[Cu(II) (supplement)]:[Me_6-Tren]:[NaBr] = [50]:[1]:[0.02]:[0.12]:[0.04] in DMSO (50% *v/v*).

4.3 Conclusions

In summary, the photo-induced polymerisation of acrylates utilising Cu(II) gluconate as a precursor catalyst has been investigated. Upon optimised conditions, narrow MWDs and near-quantitative conversions were attained within 2 h, while the high-end-group fidelity was exemplified by MALDI-ToF-MS and *in situ* block copolymerisation. The need for product purification and removal of inorganic and organic catalysts as well as residual monomer must be taken on a case by case basis. Although some applications may preclude the use of copper or other metallic catalysts these catalysts should not be ruled out in favour of non-metallic catalysts just on the basis of being "*metal-free*".

4.4 Experimental

4.4.1 Materials and Methods

All materials were purchased from Sigma Aldrich or Fisher Scientific unless otherwise stated. The dietary supplement (purchased on the internet from "BioCare" with a stated 1.1 mg Cu per pill (110% RDA)), the analytical pure copper(II) gluconate and ethyl 2-bromoisobutyrate (EBiB) were used as received. Methyl acrylate was passed through a basic Al_2O_3 chromatographic column prior to use. Tris-(2-(dimethylamino)ethyl)amine (Me_6-Tren) was synthesised according to previously reported literature.[35]

4.4.2 Instrumentation

^{1}H NMR spectra were recorded on Bruker DPX-300 or DPX-400 spectrometers in $CDCl_3$ unless otherwise stated. Chemical shifts are given in ppm downfield from the internal standard tetramethylsilane. Size exclusion chromatography (SEC) measurements were conducted using an Agilent 1260 SEC-MDS fitted with differential refractive index (DRI), light scattering (LS) and viscometry (VS) detectors equipped with 2 × PLgel 5 mm mixed-D columns (300 × 7.5 mm), 1 × PLgel 5 mm guard column (50 × 7.5 mm) and autosampler. Narrow linear poly(methyl methacrylate) standards in the range of 200 to 1.0 × 10^6 g.mol^{-1} were used to calibrate the system. All samples were passed through 0.45 μm PTFE filter before analysis. The mobile phase was chloroform with 2% triethylamine eluent at a flow rate of 1.0 mL/min. SEC data was analysed using Cirrus v3.3 software with calibration curves produced using Varian Polymer laboratories Easi-Vials linear

poly(methyl methacrylate) standards (200 - 4.7×10^5 $g.mol^{-1}$). MALDI-ToF mass spectrometry was conducted using a Bruker Daltonics Ultraflex II MALDI-ToF mass spectrometer, equipped with a nitrogen laser delivering 2 ns laser pulses at 337 nm with positive ion ToF detection performed using an accelerating voltage of 25 kV. Solutions in tetrahydrofuran (50 μL) of trans-2-[3-(4-tert-butylphenyl)-2-methyl-2-propylidene] malonitrile (DCTB) as a matrix (saturated solution), sodium iodide as cationisation agent (1.0 mg/mL) and sample (1.0 mg/mL) were mixed, and 0.7 μL of the mixture was applied to the target plate. Spectra were recorded in reflector mode calibrating PEG-Me 1100 kDa. UV/Vis spectra were recorded on Agilent Technologies Cary 60 UV-Vis spectrophotometer in the range of 200-1100 nm using a cuvette with 10 mm path length. A nail lamp was purchased online (λ ~ 365 nm) and used as the main UV source.

4.4.3 General procedures

(a) Typical conditions for the photo-induced polymerisation of MA utilising Cu(II) gluconate as a precursor catalyst

Appropriate amounts of EBiB (1 equiv.), MA (*DP* eq), Cu(II) gluconate (0.02 equiv.), Me_6-Tren (0.12 equiv.) and DMSO (50% *v/v*) were placed in a polymerisation flask, which was equipped with a magnetic stir bar and fitted with a rubber septum. The reaction mixture was degassed *via* bubbling with nitrogen for 20 min. The polymerisation was allowed to proceed for 2 h under irradiation at λ~365 nm. Samples were taken periodically for conversion and molecular weight analyses. The polymerisation mixture was initially dissolved in THF and then passed through

a small basic Al_2O_3 chromatographic column to remove the copper salts. The resulting solution was precipitated in methanol.

(b) Typical conditions for the *in situ* block copolymerisations

Filtered MA (1 mL, 11.1 mmol, 50 eq), EBiB (32 μL, 0.22 mmol, 1 eq), Cu(II) gluconate (tablet) (1.0 mg, 4.4μmol, 0.02 eq), Me_6-Tren (7 μL, 22.0 μmol, 0.12 eq) and DMSO (1 mL) were added to a septum sealed vial and degassed by purging with nitrogen for 15 mins. Polymerisation commenced upon addition of the degassed reaction mixture to the UV lamp. After 90 min a 1: 0.5 mixture of degassed PEGA (15 eq) used for block copolymerisation and DMSO was added to the reaction mixture *via* degassed syringe. Samples were taken periodically and conversions were measured using ^{1}H NMR and SEC analysis.

4.4.4 Additional characterisation

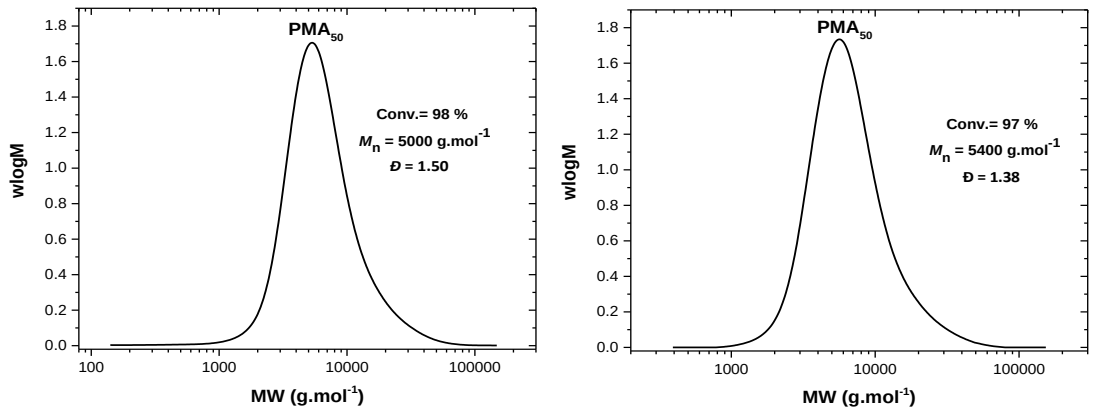

Figure 4.8: SEC analysis of PMA utilising Cu(II) gluconate (supplement) as the precursor catalyst. Initial conditions: [MA]:[EBiB]:[Cu(II) gluconate]:[Me_6-Tren] = [50]:[1]:[0.02]:[0.12] in DMSO 50% *v/v*, pre-mixing of the Cu(II) gluconate/Me_6-Tren complex for 12 h (left) and 1 week (right).

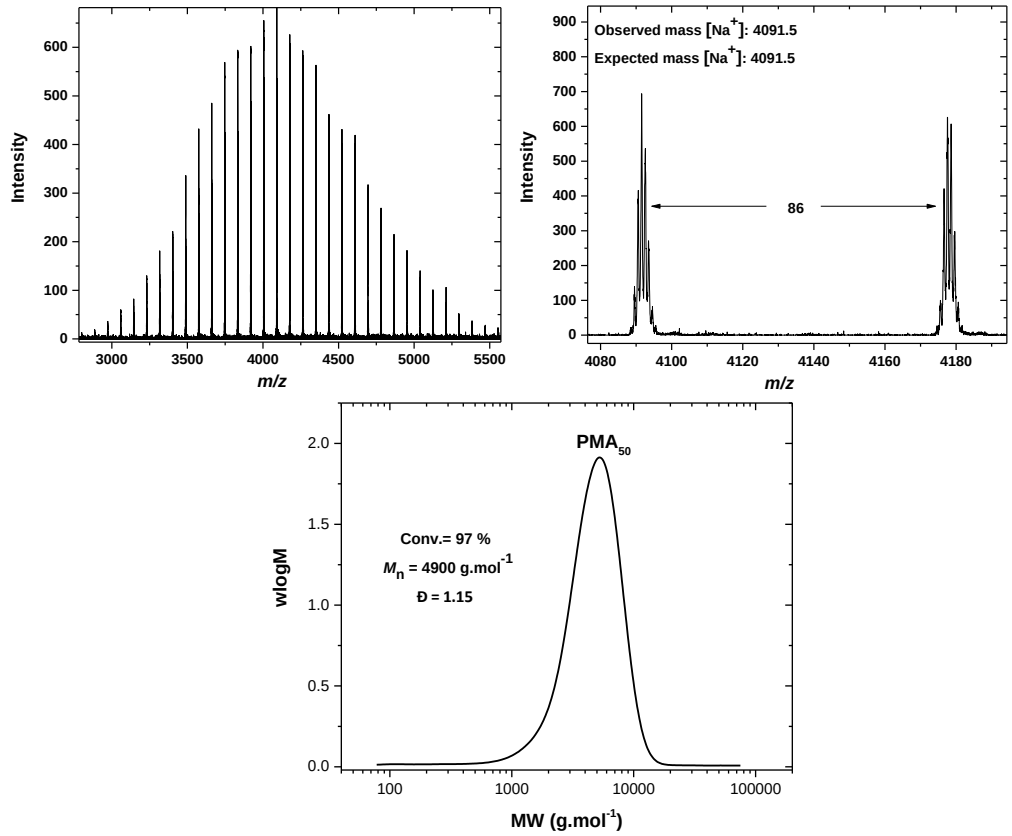

Figure 4.9: MALDI-ToF-MS (up) and SEC (down) analyses of PMA obtained from the experiment [MA]:[EBiB]:[Cu(II) gluconate (pure)]:[Me_6-Tren] = [50]:[1]:[0.02]:[0.12] in DMSO (50% *v/v*). The pre-mixed Cu/L solution was left under UV irradiation for 2 h prior to polymerisation.

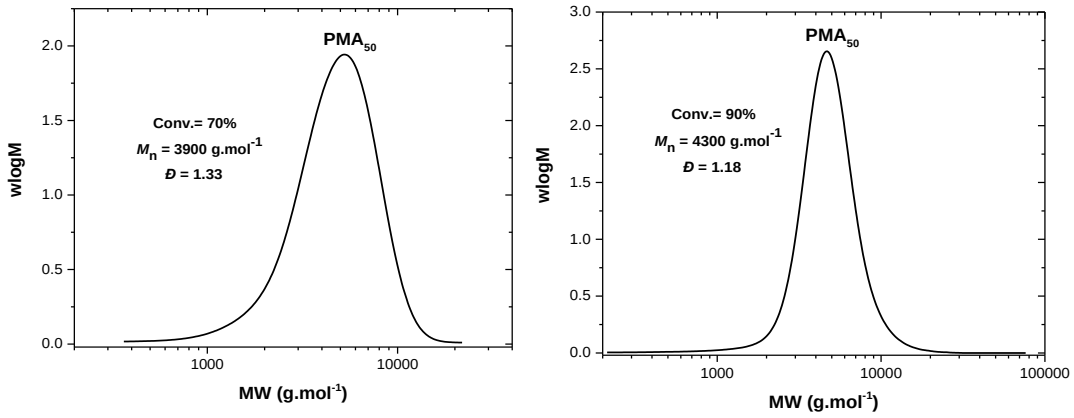

Figure 4.10: SEC analysis of PMA utilising Cu(II) gluconate (pure) as the precursor catalyst. Initial conditions: [MA]:[EBiB]:[Cu(II) gluconate]:[Me_6-Tren] = [50]:[1]:[0.02]:[0.12] in DMSO 50% *v/v*, pre-mixing of the Cu(II) gluconate/Me_6-Tren complex for 2 h under UV irradiation at 15 ^oC (left) and 60 ^oC (right).

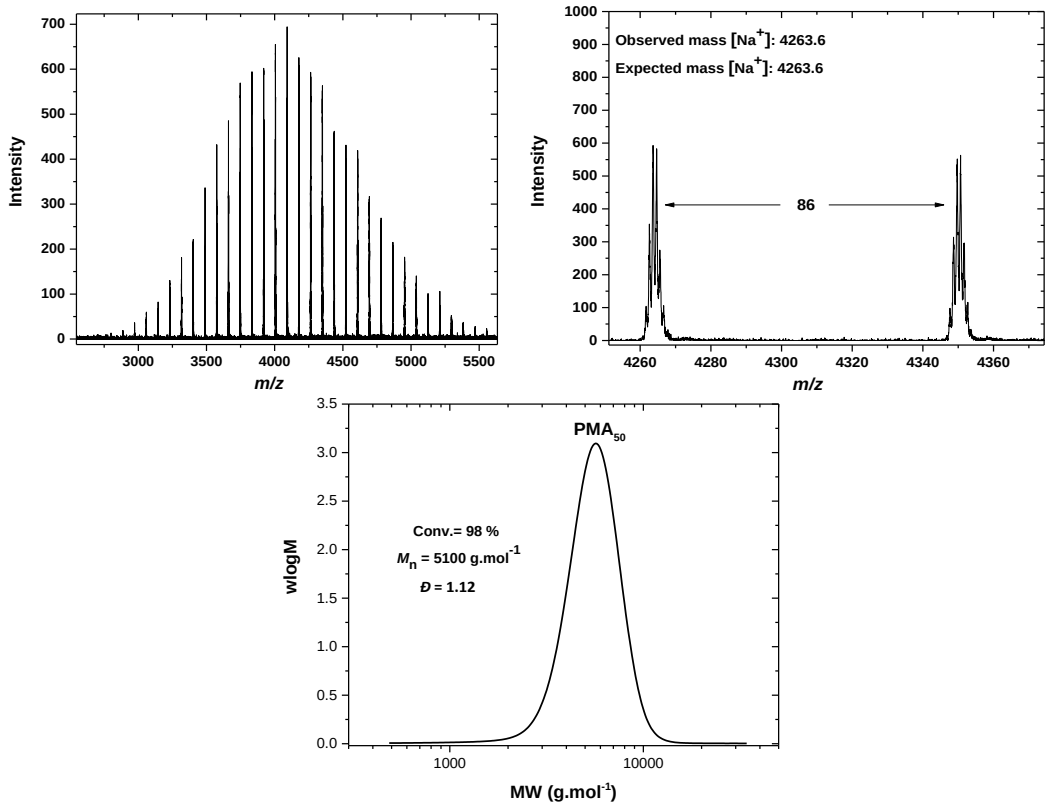

Figure 4.11: MALDI-ToF-MS (up) and SEC (down) of PMA prepared by photo-induced polymerisation utilising copper gluconate (pure). Initial conditions: [EBiB]:[Cu(II) gluconate]:[Me_6-Tren]:[NaBr] = [1]:[0.02]:[0.12]:[0.04] in DMSO (50% *v/v*).

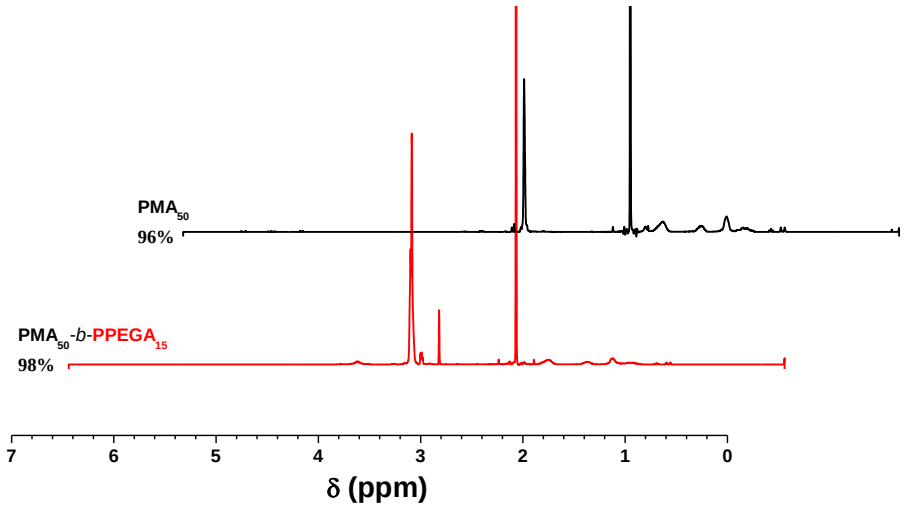

Figure 4.12: ^{1}H NMR for the block copolymerisation from a PMA macroinitiator. Initial conditions: [MA]:[EBiB]:[Cu(II) gluconate (supplement)]:[Me_6-Tren]:[NaBr] =

[50]:[1]:[0.02]:[0.12]:[0.04], DMSO (50%, *v/v*). Chain extension achieved upon addition of an aliquot of PEGA (15 equiv.) in DMSO (33%, *v/v*).

4.5 References

1. F. Perreault, A. Oukarroum, S. P. Melegari, W. G. Matias and R. Popovic, *Chemosphere*, 2012, **87**, 1388-1394.

2. J. M. Baskin, J. A. Prescher, S. T. Laughlin, N. J. Agard, P. V. Chang, I. A. Miller, A. Lo, J. A. Codelli and C. R. Bertozzi, *Proc. Natl. Acad. Sci. U.S.A.*, 2007, **104**, 16793-16797.

3. C. Boyer, A. Atme, C. Waldron, A. Anastasaki, P. Wilson, P. B. Zetterlund, D. Haddleton and M. R. Whittaker, *Polym. Chem.*, 2013, **4**, 106-112.

4. K. Matyjaszewski, W. Jakubowski, K. Min, W. Tang, J. Huang, W. A. Braunecker and N. V. Tsarevsky, *Proc. Natl. Acad. Sci. U.S.A.*, 2006, **103**, 15309-15314.

5. T. Pintauer and K. Matyjaszewski, *Chem. Soc. Rev.*, 2008, **37**, 1087-1097.

6. F. A. Leibfarth, K. M. Mattson, B. P. Fors, H. A. Collins and C. J. Hawker, *Angew. Chem., Int. Ed.*, 2013, **52**, 199-210.

7. A. Anastasaki, V. Nikolaou, Q. Zhang, J. Burns, S. R. Samanta, C. Waldron, A. J. Haddleton, R. McHale, D. Fox, V. Percec, P. Wilson and D. M. Haddleton, *J. Am. Chem. Soc.*, 2013, **136**, 1141-1149.

8. B. P. Fors and C. J. Hawker, *Angew. Chem., Int. Ed.*, 2012, **51**, 8850-8853.

9. S. Dadashi-Silab, M. Atilla Tasdelen and Y. Yagci, *J. Polym. Sci. Part A: Polym. Chem.*, 2014, **20**, 2878-2888.

10. J. Xu, K. Jung, A. Atme, S. Shanmugam and C. Boyer, *J. Am. Chem. Soc.*, 2014, **136**, 5508-5519.

11. Y.-M. Chuang, A. Ethirajan and T. Junkers, *ACS Macro Lett.*, 2014, **3**, 732-737.

12. N. J. Treat, B. P. Fors, J. W. Kramer, M. Christianson, C.-Y. Chiu, J. R. d. Alaniz and C. J. Hawker, *ACS Macro Lett.*, 2014, **3**, 580-584.

13. S. Shanmugam, J. Xu and C. Boyer, *Macromolecules*, 2014, **47**, 4930-4942.

14. J. Xu, A. Atme, A. F. Marques Martins, K. Jung and C. Boyer, *Polym. Chem.*, 2014, **5**, 3321-3325.

15. J. Rzayev and J. Penelle, *Macromolecules*, 2002, **35**, 1489-1490.

16. A. J. D. Magenau, N. C. Strandwitz, A. Gennaro and K. Matyjaszewski, *Science*, 2011, **332**, 81-84.

17. B. Wenn, M. Conradi, A. D. Carreiras, D. M. Haddleton and T. Junkers, *Polym. Chem.*, 2014, **5**, 3053-3060.

18. M. A. Tasdelen, M. Uygun and Y. Yagci, *Macromol. Chem. Phys.*, 2010, **211**, 2271-2275.

19. M. A. Tasdelen, M. Ciftci and Y. Yagci, *Macromol. Chem. Phys.*, 2012, **213**, 1391-1396.

20. Y. Yagci, S. Jockusch and N. J. Turro, *Macromolecules*, 2010, **43**, 6245-6260.

21. A. Anastasaki, V. Nikolaou, A. Simula, J. Godfrey, M. Li, G. Nurumbetov, P. Wilson and D. M. Haddleton, *Macromolecules*, 2014, **47**, 3852-3859.

22. A. Anastasaki, V. Nikolaou, G. S. Pappas, Q. Zhang, C. Wan, P. Wilson, T. P. Davis, M. R. Whittaker and D. M. Haddleton, *Chem. Sci.*, 2014, **5**, 3536-3542.

23. T. G. Ribelli, D. Konkolewicz, S. Bernhard and K. Matyjaszewski, *J. Am. Chem. Soc.*, 2014, **136**, 13303-13312.

24. D. Konkolewicz, K. Schröder, J. Buback, S. Bernhard and K. Matyjaszewski, *ACS Macro Lett.*, 2012, **1**, 1219-1223.

25. A. Anastasaki, V. Nikolaou, F. Brandford-Adams, G. Nurumbetov, Q. Zhang, G. J. Clarkson, D. J. Fox, P. Wilson, K. Kempe and D. M. Haddleton, *Chem. Commun.*, 2015, **51**, 5626-5629.

26. B. B. Wayland, G. Poszmik, S. L. Mukerjee and M. Fryd, *J. Am. Chem. Soc.*, 1994, **116**, 7943-7944.

27. D. C. Woska, Z. D. Xie, A. A. Gridnev, S. D. Ittel, M. Fryd and B. B. Wayland, *J. Am. Chem. Soc.*, 1996, **118**, 9102-9109.

28. T. Nakano, D. Tamada, J.-i. Miyazaki, K. Kakiuchi and Y. Okamoto, *Macromolecules*, 2000, **33**, 1489-1491.

29. T. Nakano, T. Yade and Y. Okamoto, *Macromolecules*, 2003, **36**, 3498-3504.

30. Agency for Toxic Substances and Disease Registry, *Toxicological Profile for Copper*, Atlanta, Georgia, 2004.

31. World Health Organization, Cu, Trace Elements in Human Nutrition and Health, Geneva, 1996, pp. 123–143.

32. Food and Drug Administration, *Copper Gluconate*, 1979.

33. C. Waldron, Q. Zhang, Z. Li, V. Nikolaou, G. Nurumbetov, J. Godfrey, R. McHale, G. Yilmaz, R. K. Randev, M. Girault, K. McEwan, D. M. Haddleton, M. Droesbeke, A. J. Haddleton, P. Wilson, A. Simula, J. Collins, D. J. Lloyd, J. A. Burns, C. Summers, C. Houben, A. Anastasaki, M. Li, C. R. Becer, J. K. Ki*via*ho and N. Risangud, *Polym. Chem.*, 2014, **5**, 57-61.

34. D. Konkolewicz, P. Krys, J. R. Góis, P. V. Mendonça, M. Zhong, Y. Wang, A. Gennaro, A. A. Isse, M. Fantin and K. Matyjaszewski, *Macromolecules*, 2014, **47**, 560-570.

35. M. Ciampolini and N. Nardi, *Inorg. Chem.*, 1966, **5**, 41-44.

Photo-induced living radical polymerisation of acrylates utilising a discrete copper(II)/formate complex

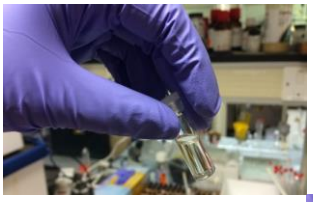

Freshly distilled Me_6-Tren

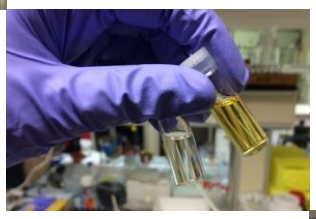

Degraded Me_6-Tren (~1 month)

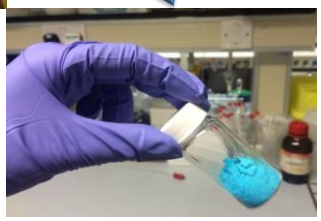

Stable complex: [Cu(Me_6-Tren)(O_2CH)] (ClO_4)

- ✓ Degradation of ATRP/SET-LRP ligands under air
- ✓ Too many variables (catalyst (Cu(0) or Cu(I), $CuBr_2$) induce error

A photo-polymerisation protocol, utilising a pre-formed and well-characterised Cu(II)/formate complex, [Cu(Me_6-Tren)(O_2CH)](ClO_4), mediated by UV light is described. In the absence of additional reducing agents and/or photosensitisers, ppm concentrations of the oxidatively stable [Cu(Me_6-Tren)(O_2CH)](ClO_4), furnish near-quantitative conversions(> 95%) within 2 h, yielding poly(acrylates) with low dispersities (~ 1.10). The exceptional end-group fidelity is confirmed by MALDI-ToF-MS and exemplified by in situ chain extension/block copolymerisations upon sequential monomer addition without any need for further purification. Additionally the facile and convenient storage potential of the complex provides for a new and versatile polymerisation protocol.

5.1 Introduction

RDRP methods have significantly evolved the last decades allowing access to narrow MWDs, efficient regulation of the molecular weight and the monomer sequence and complex architectures.[1, 2] Transition metal methods in particular, including atom transfer radical polymerisation (ATRP)[3, 4] and single electron transfer living radical polymerisation (SET-LRP)[5-7], have significantly contributed towards this direction exploiting the manipulation of the activation/deactivation equilibrium between active and dormant species.

Both polymerisation techniques utilise either Cu(I) or Cu(0) to facilitate the activation of alkyl halide initiators in order to generate carbon-based radicals and allow the propagation (activation and propagation have been reported to proceed *via* either an inner sphere or an outer sphere mechanism). Importantly, in both methods, the control over the polymerisation is inferred by the accumulation of the higher oxidation species, Cu(II) which has been reported to occur through either the persistent radical effect (PRE)[8, 9] or *via* the disproportionation mechanism.[10-12] Cu(II) will thus act as deactivating species by adjusting the polymerisation equilibrium towards the dormant species and limiting the termination events. The role of the deactivator is of outmost importance for copper-mediated polymerisations and external amounts of Cu(II) are often added when high end-group fidelity is required in both ATRP[13, 14] and SET-LRP protocols.[15, 16] Therefore, it is crucial to optimise the Cu(II) concentration in order to achieve narrow MWDs, high end-group fidelity as well as acceptable polymerisation rates. In some occasions, sodium bromide (NaBr) is also added to invoke further control over the molecular weight distributions and thus further adding to the complexity of the system.[17, 18]

The role of the ligand to form the copper/complexes is also very important for copper-mediated radical polymerisation not only to facilitate the solubility of the transition metal salt but also to adjust the redox potential and halogenophilicity of the metal center.[19-21] Unlike other parameters, such as deactivator concentration, no simple external rate-order can be determined and a minimal concentration is essential to achieve good control over the MWDs accompanied with an acceptable polymerisation rate.[22] Moreover, even minor changes in the ligand concentration can lead to significant loss of end-group fidelity and termination events and thus careful optimisation of the reaction conditions is required.[23, 24]

Thus, various components (*e.g.* type of activator, ligand and deactivator concentration *etc.*) have to be optimised for a successful copper-mediated radical polymerisation which is not only time consuming but also challenging.[25, 26] Furthermore, additional issues arise from the storage of these compounds. CuBr for example has to be stored under oxygen free conditions to avoid oxidation by air and in many occasions has to be purified prior to use as it contains a high level of Cu(II) contamination despite its commercially stated high purity (a typical bottle of Cu(I), even at >99% purity is green, although it should be colourless given its d^{10} state). Cu(0) also needs to be purified prior to use with either hydrazine[27] or acid[28-30] while in many occasions there is a general confusion of whether Cu(0) powder or Cu(0) wire should be preferred.[31] *N*-Containing ligands such as Me_6-Tren are also susceptible to oxidation and degradation[32] and have to be stored under dry, dark and inert conditions, although degradation will still occur in many cases which will require further purification methods prior to use (*e.g.* redistilling the ligand).

In order to circumvent the complexity of the polymerisations, various "alternative ATRP" techniques have been employed, including ARGET[33] and ICAR.[34] However, the presence of reducing agents or free radical initiators is further adding on the complexity of the system while the concentration between Cu(II) and ligand also requires careful optimisation. Recently, considerable attention has been drawn towards controlling the activation-deactivation step *via* external regulation.[35] Photochemical stimuli in particular have been extensively used to mediate the controlled polymerisation of various monomers, although still requiring photo-initiators, excess of ligands or exotic catalysts.[36-48]

In this chapter, a pre-formed, discrete Cu(II)/formate complex was prepared and characterised prior to being utilised as a facile route to perform photo-induced polymerisations whilst maintaining excellent control over the MWDs ($Đ$ ~ 1.10) at ambient temperature. Significantly, excellent temporal control is observed during intermittent light and dark reaction when MA is employed as the monomer.

5.2 Results and Discussion

The synthesis of the [Cu(Me_6-Tren)(O_2CH)](ClO_4) was conducted according to a literature procedure[49] (Figure 5.1) and was subsequently employed for the following photo-induced reactions.

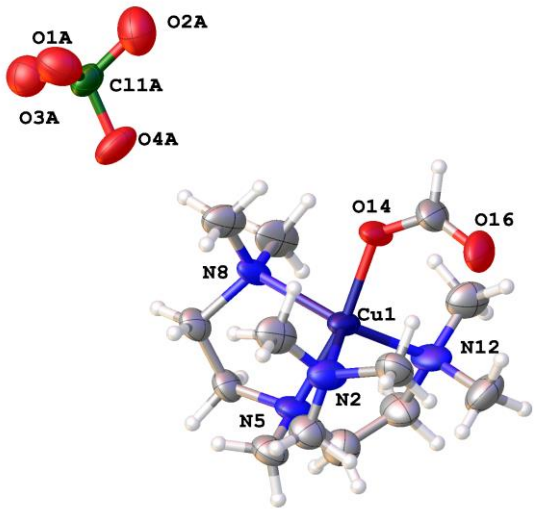

Figure 5.1: Solid state structure of [Cu(Me_6-Tren)(O_2CH)](ClO_4) with atom labeling.

A deoxygenated mixture containing methyl acrylate (MA), dimethyl sulfoxide (DMSO), ethyl bromo isobutyrate (EBiB) and 1% of the complex (with respect to initiator) was exposed to UV irradiation (320-390 nm, 200W, Section 5.4.4, Figure 5.9) for 2 h, yielding well-defined PMA (M_n = 3500 g.mol^{-1}, $Đ$ ~ 1.10) at 75% conversion (Table 5.1, Section 5.4.4, Figure 5.10). Under carefully optimised conditions ([EBiB] : [[Cu(Me_6-Tren)(O_2CH)](ClO_4)] = [1] : [0.08], acceleration of the polymerisation rate was achieved resulting in 97% conversion in 2 h while the MWDs remained narrow ($Đ$ < 1.10) (Table 5.1, Figure 5.2a,b).

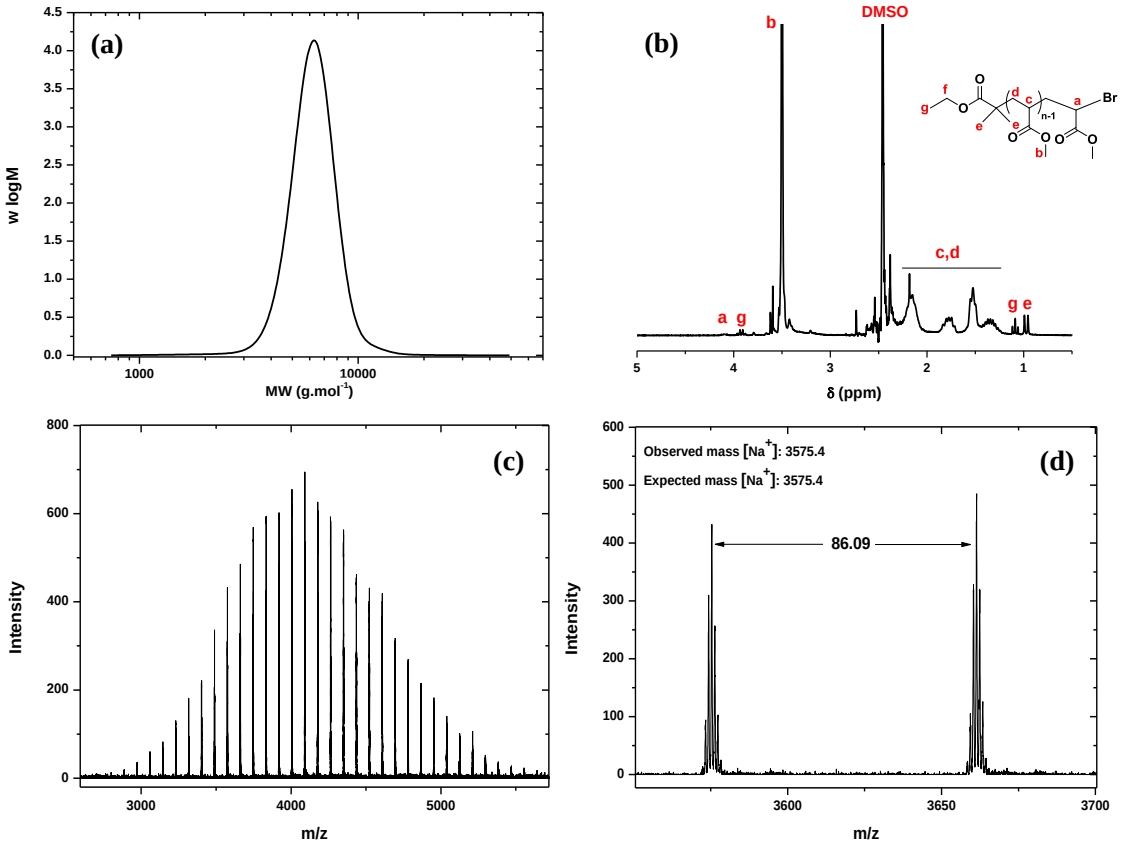

Figure 5.2: (a) SEC, (b) ^{1}H NMR, (c) and (d) MALDI-ToF-MS analyses obtained from the photo-induced polymerisation of MA catalysed by the Cu(II)/formate complex. Initial conditions: [MA] : [EBiB] : [[Cu(Me$_6$-Tren)(O$_2$CH)](ClO$_4$)] = [50] : [1] : [0.08] in DMSO 50% *v/v*.

Table 5.1: Photo-induced polymerisation of MA catalysed by the Cu(II)/formate complex.

DP		**t (h)**	**Conv. (%)**	$M_{n,th}$ **(g.mol^{-1})**	$M_{n,SEC}$ **(g.mol^{-1})**	***Đ***
50	1%	2	75	3700	3300	1.19
	2%	2	87	3900	4100	1.10
	4%	2	92	4100	2500	1.29
	6%	2	94	4200	1900	1.33
	8%	2	97	4400	5100	1.07
	Dark Conditions	24	0	-	-	-
100		2	96	8500	8700	1.08
200		2	95	16500	16400	1.05

Kinetic analysis revealed a linear increase of $\ln([M]_0/[M]_t)$ *vs* time as well as linear evolution of M_n with monomer conversion (Figure 5.3, Section 5.4.4, Figure 5.11) The good correlation between the theoretical and the experimental values further confirms the controlled character of the polymerisation. Additionally, both MALDI-ToF-MS and ^{1}H NMR analyses (Figure 5.2c,d), illustrated excellent end-group fidelity with the former revealing a single distribution corresponding to polymer chains initiated by the expected EBiB fragment and terminated by a bromine atom.

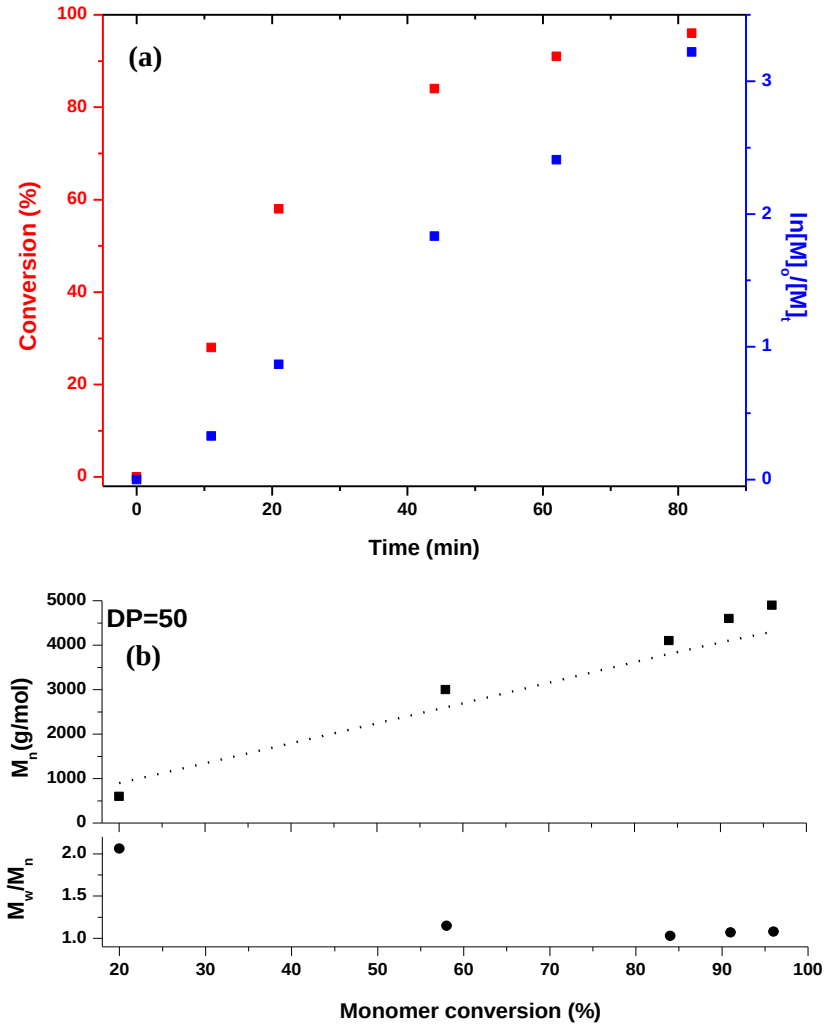

Figure 5.3: (a) Kinetic data and (b) molecular weight, dispersity data for the polymerisation of PMA under UV irradiation.

In order to demonstrate the potential and versatility of this system in maintaining control over higher molecular weights, a range of polymerisations were conducted, targeting higher degrees of polymerisation (*DP*= 50/100/200). Very high conversions (> 92%, 2 h) with good agreement between $M_{n,exp}$ and $M_{n.th}$ were attained while the dispersities remained low (*Đ* ~ 1.10) in all cases (Table 5.1, Figure 5.4).

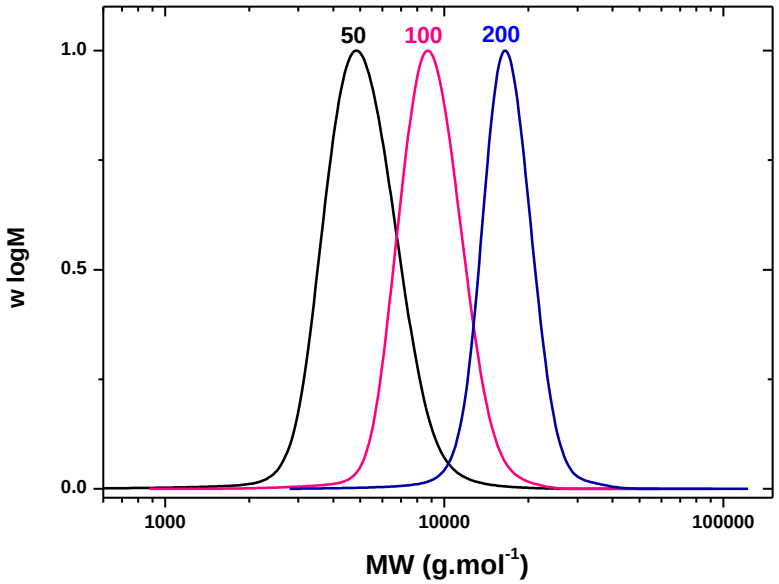

Figure 5.4: SEC analysis of PMA with various *DP*, prepared by photo-induced polymerisation.

High end-group fidelity was subsequently exemplified by *in situ* chain extension upon addition of a second aliquot of MA (1st block *DP*=50, 98% in 2 h, M_n= 4500 g.mol^{-1}, *Đ* = 1.10) with the molecular weight distribution shifting to higher molecular weight with a reduction in dispersity (*Đ* ~ 1.03) (Figure 5.5a, Section 5.4.4, Figure 5.12). When a second acrylic monomer, ethylene glycol methyl ether acrylate (EGA), was selected for the one pot block copolymerisation with PMA a well-defined PMA_{50}-*b*-$PEGA_{50}$ diblock copolymer was obtained as indicated by SEC

($Đ$ ~ 1.10) and ^{1}H NMR (98% conversion). The reverse one pot block copolymerisation, utilising $PEGA_{50}$ this time as the macroinitiator was also investigated. Pleasingly, the final block copolymer $PEGA_{50}$-*b*-PMA_{50} was attained within 5 h presenting narrow MWDs ($Đ$ ~ 1.17) at near-quantitative conversion (97%). Thus, in all cases well-defined block copolymers were obtained in very high yield without the need for a macroinitiator purification step (Figure 5.5b,c, Section 5.4.4, Figure 5.12).

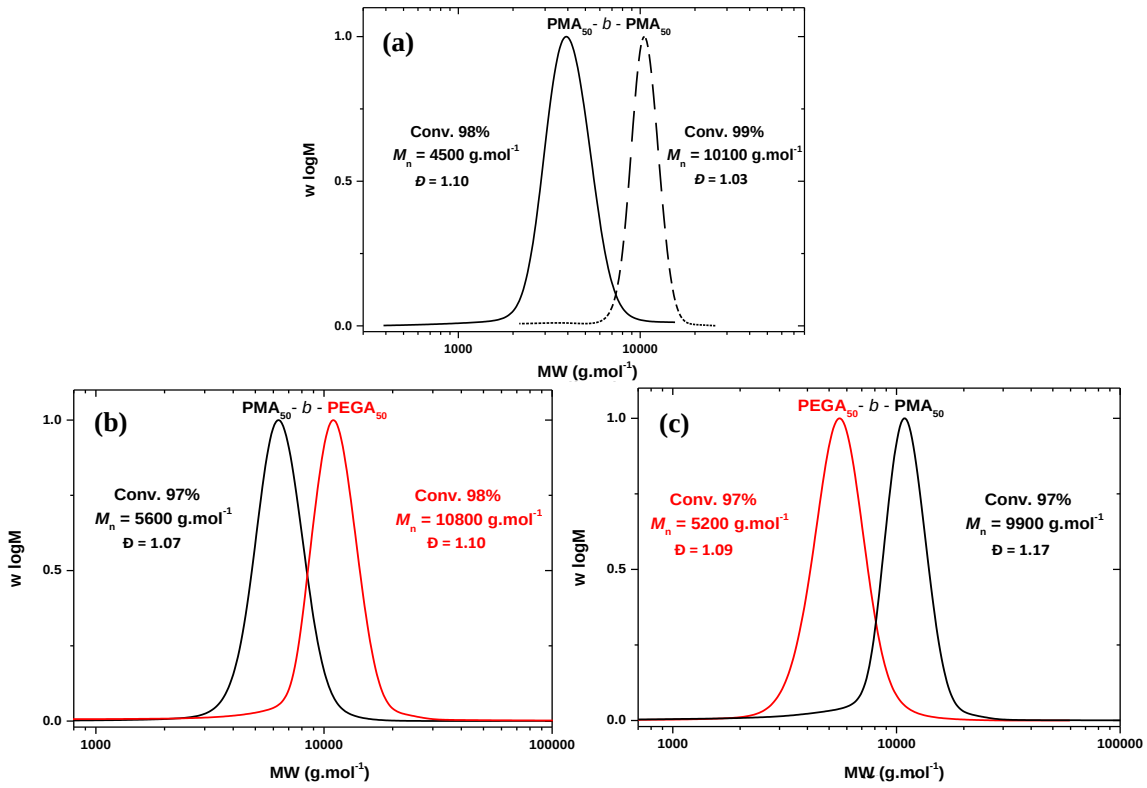

Figure 5.5: *In situ* chain extension and block copolymerisations from a PMA (a),(b) or (c)a PEGA macroinitiator. Initial conditions: [EBiB] : [[Cu(Me_6-Tren)(O_2CH)](ClO_4)] = [1] : [0.08] in DMSO 50% *v/v*.

The possibility of temporal control was also investigated *via* intermittent "light"-"dark" cycles for alternating 20 min periods (polymerisation under dark

conditions resulted in no conversion over a period of 48 h) (Table 5.1). In order to explore this possibility, our reaction mixture was exposed to UV irradiation for 20 min, which resulted in approximately 48% conversion. Subsequently a "dark" 20 min period was followed (black box, Section 5.4.4, Figure 5.13) in which no polymerisation was detected as evidenced by ^{1}H NMR. Exposing the reaction mixture for another 20 min turned the polymerisation back "on", restoring the original rate of polymerisation. These "on"-"off" cycles were repeated several times for a total exposure time of 80 min with the final conversion (92%) and dispersity (*Đ* ~ 1.10) being comparable with the standard polymerisation under uninterrupted UV irradiation (Section 5.4.4, Figure 5.14). To the best of our knowledge this is the first photo-induced copper mediated system that demonstrates complete temporal control as the removal of the light source stops the polymerisation immediately and no conversion is observed during the dark period. In previously reported systems[2, 40, 46, 50-52] the rate of polymerisation was significantly reduced but not completely prohibited.

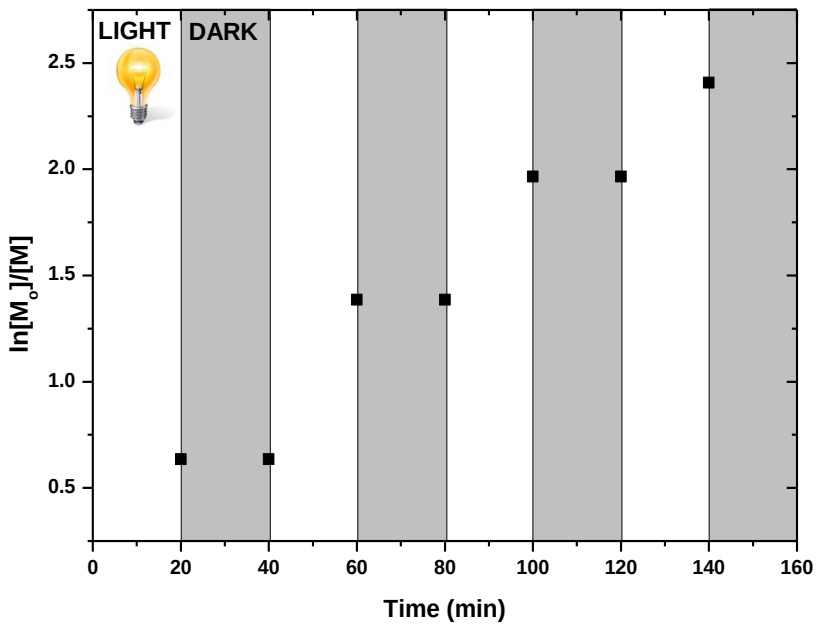

Figure 5.6: Evidence of temporal control *via* consecutive light and dark exposure. Initial conditions: [MA] : [EBiB] : [[Cu(Me_6-Tren)(O_2CH)](ClO_4)] = [50] : [1] : [0.08] in DMSO 50% *v/v*.

A further positive aspect of the [Cu(Me_6-Tren)(O_2CH)](ClO_4) complex is that even after a 6 month period, the complex is stable and subsequent polymerisation proceeded in a very similar manner, preserving the fast reaction rates (low dispersity, high end-group fidelity and thus indicating that the activity of the complex was retained. Typically, *N*-containing ligands have to be kept in ampules under strictly deoxygenated conditions (under inert atmosphere) at low temperatures (*e.g.* fridge). Even traces amount of oxygen can eventually result in oxidative degradation of the amines[32] which is visible due to a colour change (Figure 5.7). On the contrary, this complex remained stable for more than 6 months upon standing in a fumehood in a non-degassed vial and under natural (visible) light exposure (Figure 5.7).

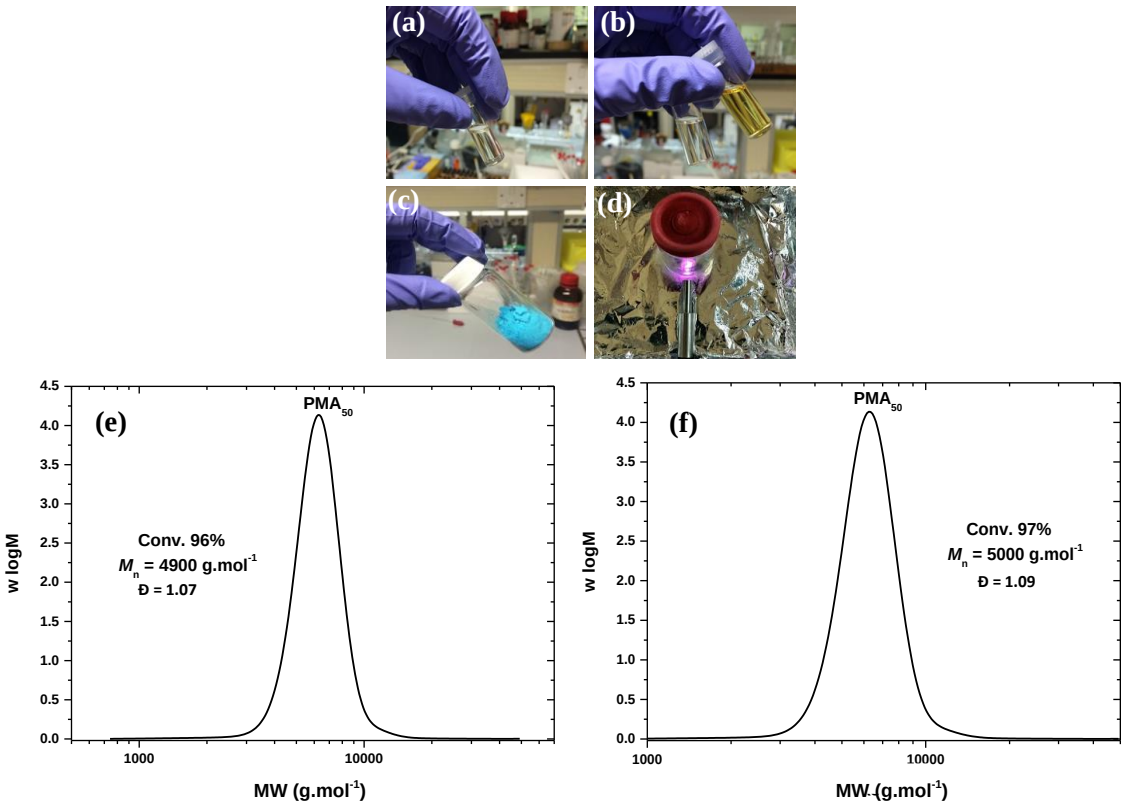

Figure 5.7: (a) Freshly distilled Me_6-Tren, (b) freshly distilled Me_6-Tren (left) *vs* degraded Me_6-Tren (right) after 1 month stored under nitrogen in the fridge, (c) [Cu(Me_6-Tren)(O_2CH)](ClO_4) stable after 6 months of exposure in light/air/ambient temperature, (d) reaction vial under UV irradiation in a homemade dark box, (e) and (f) SEC analysis of PMA utilising the complex before and after 6 months of its synthesis respectively. Initial conditions: [MA] : [EBiB] : [Cu(Me_6-Tren)(O_2CH)](ClO_4) = [50] : [1] : [0.08] in DMSO 50% *v/v*.

In order to gain a mechanistic insight, UV-Vis spectroscopy measurements were performed, after exposing the complex to UV irradiation for 2 h, mimicking the polymerisation conditions. A decrease in the characteristic absorbance (λ_{max} ~ 870 nm) was observed suggesting a significant reduction of Cu(II) (Figure 5.8). In order to further investigate the role of formate as a reducing agent, a series of experiments were performed adding sodium formate (HCO_2Na) to the standard catalyst/ligand combination (Table 5.2, Section 5.4.4 Figures 5.15). Previously, we have shown that [$CuBr_2$]:[Me_6-Tren] = [1]:[1] failed to catalyse the polymerisation under UV irradiation[40]. However, addition of 1 equiv. of HCO_2Na resulted in a well-defined polymer ($Đ$ ~ 1.12) in 2 h (80% conv.) while addition of 1 equiv. of NaBr resulted in no polymerisation, excluding a simple salt effect. In addition, a [1]:[1] mixture of copper formate (($HCO_2)_2Cu$) and Me_6-Tren also activates the catalyst ($Đ$ ~ 1.19). These data suggest that formate[53] or an excess of tertiary amines[40, 50, 54] are both capable of reducing the photo-activated [Cu(II)(Me_6-Tren)] and thus producing the active catalyst.

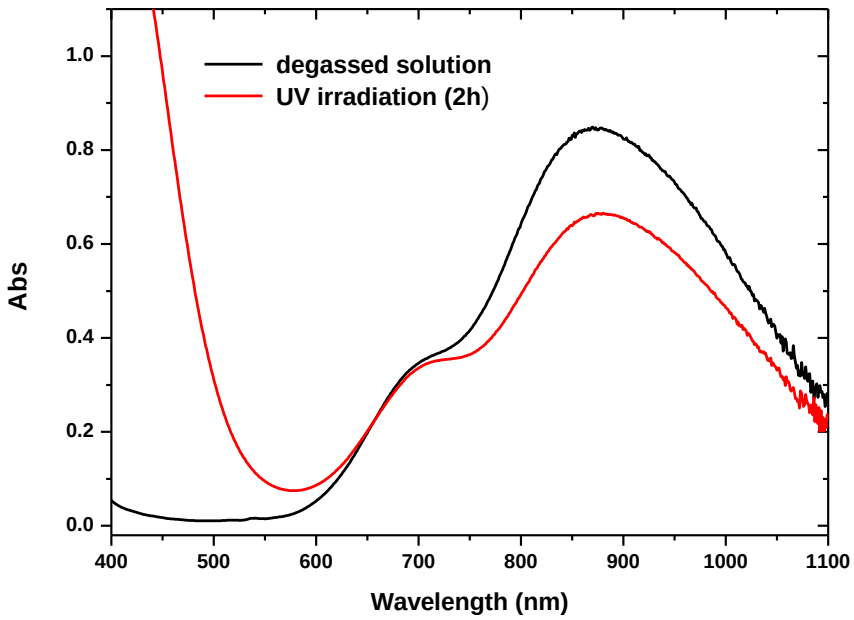

Figure 5.8: Monitoring effect of UV irradiation on [Cu(Me_6-Tren)(O_2CH)](ClO_4) as a function of time by UV−vis spectroscopy.

Table 5.2: Series of control experiments to investigate the mechanism.

Entry	Conditions	Conv. (%)	$M_{n,th}$ (g.mol^{-1})	$M_{n,SEC}$ (g.mol^{-1})	$Đ$
1	[$CuBr_2$]:[L]	-	-	-	-
2	[$CuBr_2$]:2[L]	94	4200	4300	1.10
3	[$CuBr_2$]:[L]:[HCO_2Na]	85	3800	3800	1.12
4	[$CuBr_2$]:[L]:[NaBr]	-	-	-	-
5	[$(O_2CH)_2Cu$]:[L]:[-]	95	4300	5100	1.19

5.3 Conclusions

In summary, a pre-formed discrete complex [Cu(Me_6-Tren)(O_2CH)](ClO_4) has been utilised for the first time for the photo-polymerisation of acrylates presenting excellent degrees of control, as exemplified by the low dispersities ($Đ$ ~ 1.10), high end-group fidelity (~ 99%) and the near-quantitative conversions within 2 h (> 95%). The efficiency of this complex in combination with the facile and convenient storage potential provides for a new, simple and versatile polymerisation protocol.

5.4 Experimental

5.4.1 Materials and Methods

All materials were purchased from Sigma Aldrich or Fischer Scientific unless otherwise stated. $CuBr_2$ and EBiB were used as received. All monomers were passed through a basic Al_2O_3 chromatographic column prior to use. Me_6-Tren was synthesised according to previously reported literature.[55]

5.4.2 Instrumentation

^{1}H NMR spectra were recorded on Bruker DPX-300 or DPX-400 spectrometers in $CDCl_3$ unless otherwise stated. Chemical shifts are given in ppm downfield from the internal standard tetramethylsilane. Size exclusion chromatography (SEC) measurements were conducted using an Agilent 1260 SEC-MDS fitted with differential refractive index (DRI), light scattering (LS) and viscometry (VS) detectors equipped with 2 × PLgel 5 mm mixed-D columns (300 × 7.5 mm), 1 × PLgel 5 mm guard column (50 × 7.5 mm) and autosampler. Narrow linear poly(methyl methacrylate) standards in the range of 200 to 1.0 × 10^6 g.mol^{-1} were used to calibrate the system. All samples were passed through 0.45 μm PTFE filter before analysis. The mobile phase was chloroform with 2% triethylamine eluent at a flow rate of 1.0 mL/min. SEC data was analysed using Cirrus v3.3 software with calibration curves produced using Varian Polymer laboratories Easi-Vials linear poly(methyl methacrylate) standards (200-4.7 × 10^5 g.mol^{-1}). MALDI-ToF mass spectrometry was conducted using a Bruker Daltonics Ultraflex II MALDI-ToF mass spectrometer, equipped with a nitrogen laser delivering 2 ns laser pulses at 337 nm with positive ion ToF detection performed using an accelerating voltage of 25 kV. Solutions in tetrahydrofuran (50 μL) of trans-2-[3-(4-tert-butylphenyl)-2-methyl-2-propylidene] malonitrile (DCTB) as a matrix (saturated solution), sodium iodide as cationisation agent (1.0 mg/mL) and sample (1.0 mg/mL) were mixed, and 0.7 μL of the mixture was applied to the target plate. Spectra were recorded in reflector mode calibrating PEG-Me 1100 kDa. UV/Vis spectra were recorded on Agilent Technologies Cary 60 UV-Vis spectrophotometer in the range

of 200-1100 nm using a cuvette with 10 mm path length. The source of UV light was an OmniCure® S2000 spot UV curing lamp system, 200W (λ_{max} ~ 320-390nm).

5.4.3 General procedure

Appropriate amounts of EBiB (1 equiv.), MA (*DP* equiv.), [Cu(Me_6-Tren)(O_2CH)](ClO_4) (0.08 equiv.) and DMSO (50% *v/v*) were placed in a polymerisation flask, which was equipped with a magnetic stir bar and fitted with a rubber septum. The reaction mixture was degassed *via* bubbling with nitrogen for 20 min. The polymerisation was allowed to proceed for 2 h under irradiation at λ ~ 320-390 nm. Samples were taken periodically for conversion and molecular weight analyses. The polymerisation mixture was initially dissolved in THF and then passed through a small basic Al_2O_3 chromatographic column to remove the copper salts. The resulting solution was precipitated in methanol.

5.4.4 Additional characterisation

Figure 5.9: Typical set up for photo-induced polymerisation.

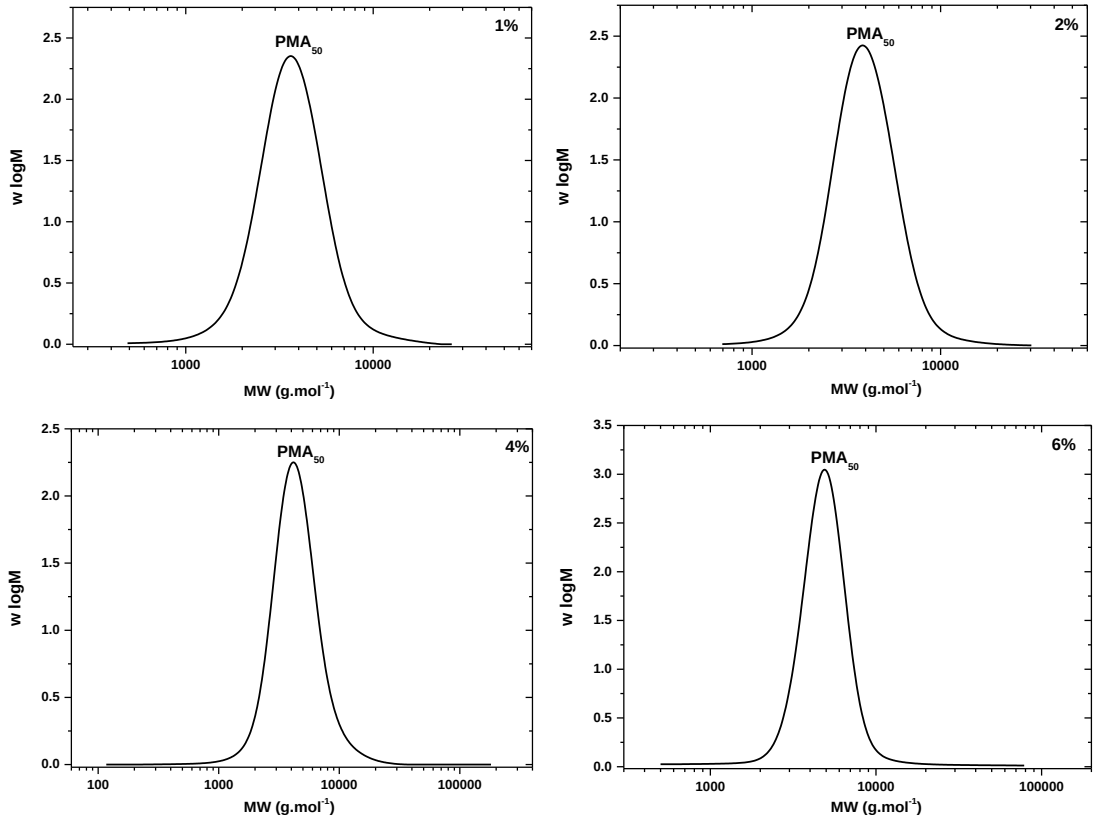

Figure 5.10: SEC analysis of the photo-induced polymerisation of PMA utilising 1%, 2%, 4% and 6% of the [Cu(Me_6-Tren)(O_2CH)](ClO_4) in DMSO 50% *v/v*.

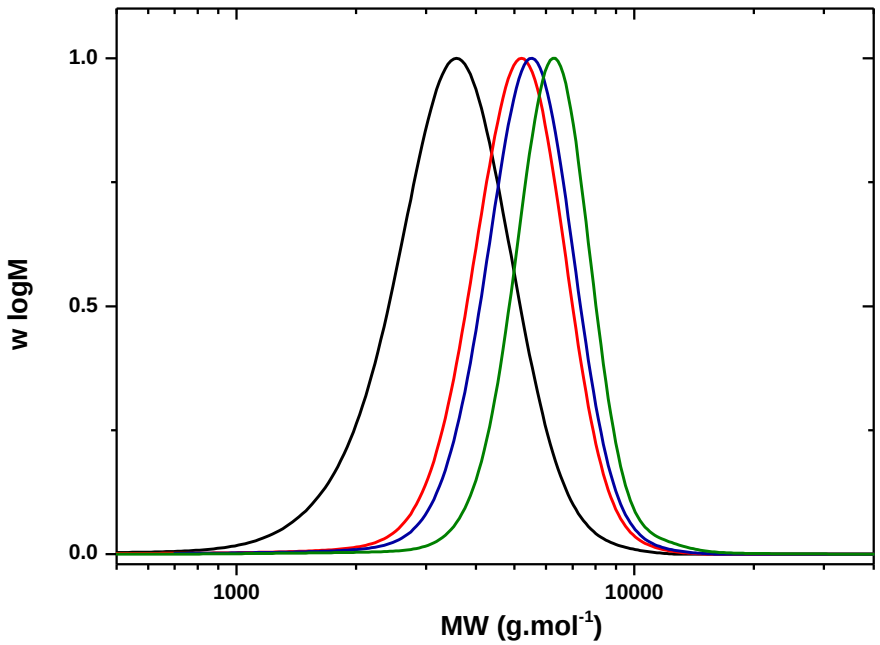

Figure 5.11: SEC analysis for the kinetic experiment under UV irradiation.

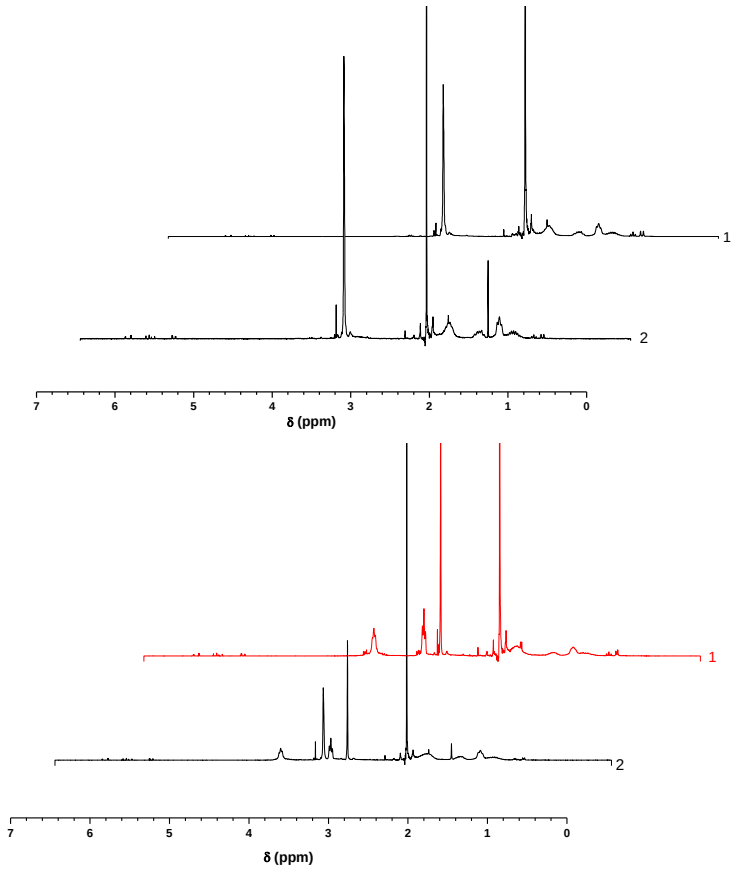

Figure 5.12: ^{1}H NMR of the *in situ* chain extension from a PMA_{50} macrointitiator (up) and (down) $PEGA_{50}$-*b*-PMA_{50} prepared by sequential addition of MA to a $PEGA_{50}$ macroinitiator. Initial conditions: [MA] : [EBiB] : [[Cu(Me_6-Tren)(O_2CH)](ClO_4)] = [50] : [1] : [0.08] in DMSO 50:50 *v/v* monomer/solvent.

Figure 5.13: Typical set up for polymerisation under dark conditions.

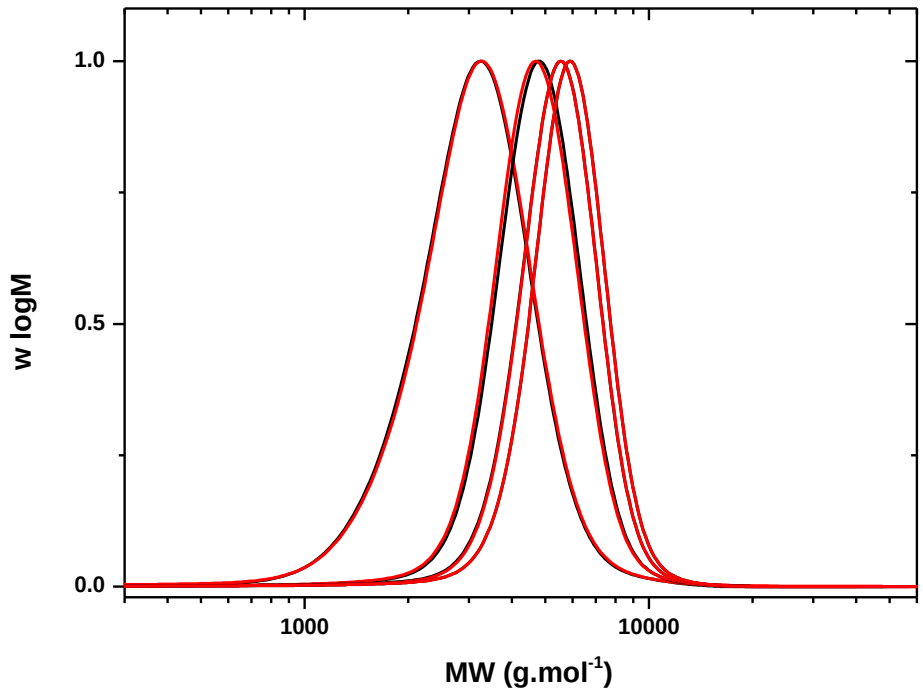

Figure 5.14: SEC analysis of temporal control *via* consecutive light and dark exposure. [MA] : [EBiB] : [[Cu(Me_6-Tren)(O_2CH)](ClO_4)] = [50] : [1] : [0.08].

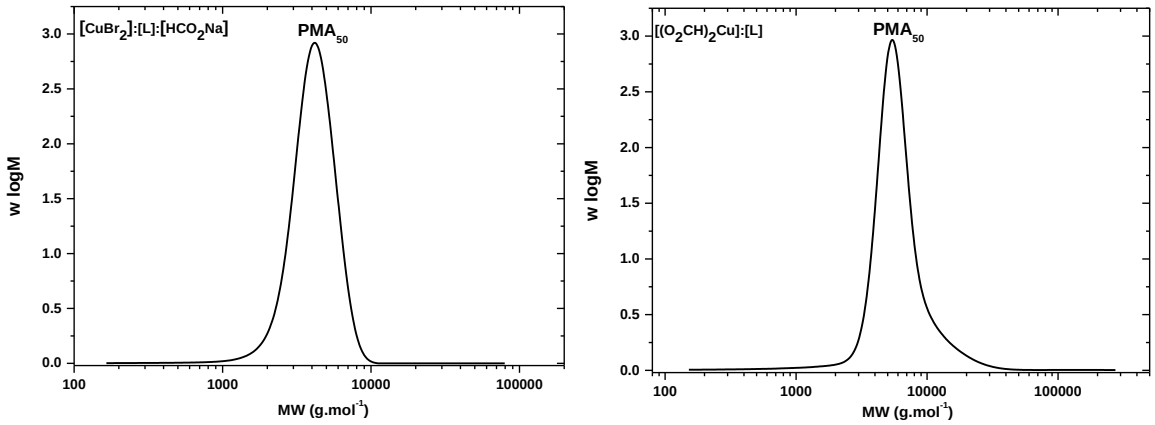

Figure 5.15: SEC analysis of PMA obtained from UV experiment: [MA] : [EBiB] : [$CuBr_2$] : [Me_6-Tren] : [HCOONa] = [50] : [1] : [0.02] : [0.02] : [0.02] (left) and [MA]: [EBiB]: [$(O_2CH)_2Cu$] : [Me_6-Tren] = [50] : [1] : [0.02] : [0.02] (right) in DMSO 50% *v/v*.

5.5 References

1. G. Gody, T. Maschmeyer, P. B. Zetterlund and S. Perrier, *Nat Commun*, 2013, **4**.

2. A. Anastasaki, V. Nikolaou, G. S. Pappas, Q. Zhang, C. Wan, P. Wilson, T. P. Davis, M. R. Whittaker and D. M. Haddleton, *Chem. Sci.*, 2014, **5**, 3536-3542.

3. J.-S. Wang and K. Matyjaszewski, *J. Am. Chem. Soc.*, 1995, **117**, 5614-5615.

4. M. Kato, M. Kamigaito, M. Sawamoto and T. Higashimura, *Macromolecules*, 1995, **28**, 1721-1723.

5. A. Anastasaki, V. Nikolaou, G. Nurumbetov, P. Wilson, K. Kempe, J. F. Quinn, T. P. Davis, M. R. Whittaker and D. M. Haddleton, *Chem. Rev.*, 2015.

6. V. Percec, T. Guliashvili, J. S. Ladislaw, A. Wistrand, A. Stjerndahl, M. J. Sienkowska, M. J. Monteiro and S. Sahoo, *J. Am. Chem. Soc.*, 2006, **128**, 14156-14165.

7. B. M. Rosen and V. Percec, *Chem. Rev.*, 2009, **109**, 5069-5119.

8. H. Fischer, *Chem. Rev.*, 2001, **101**, 3581-3610.

9. H. Fischer, *J. Polym. Sci. Part A: Polym. Chem.*, 1999, **37**, 1885-1901.

10. G. Lligadas and V. Percec, *J. Polym. Sci. Part A: Polym. Chem.*, 2008, **46**, 6880-6895.

11. B. M. Rosen, X. Jiang, C. J. Wilson, N. H. Nguyen, M. J. Monteiro and V. Percec, *J. Polym. Sci. Part A: Polym. Chem.*, 2009, **47**, 5606-5628.

12. Q. Zhang, P. Wilson, Z. Li, R. McHale, J. Godfrey, A. Anastasaki, C. Waldron and D. M. Haddleton, *J. Am. Chem. Soc.*, 2013, **135**, 7355-7363.

13. H. Zhang, B. Klumperman, W. Ming, H. Fischer and R. van der Linde, *Macromolecules*, 2001, **34**, 6169-6173.

14. K. Matyjaszewski, M. Wei, J. Xia and S. G. Gaynor, *Macromol. Chem. Phys.*, 1998, **199**, 2289-2292.

15. A. Anastasaki, C. Waldron, P. Wilson, C. Boyer, P. B. Zetterlund, M. R. Whittaker and D. Haddleton, *ACS Macro Lett.*, 2013, **2**, 896-900.

16. A. H. Soeriyadi, C. Boyer, F. Nyström, P. B. Zetterlund and M. R. Whittaker, *J. Am. Chem. Soc.*, 2011, **133**, 11128-11131.

17. V. Nikolaou, A. Anastasaki, F. Alsubaie, A. Simula, D. Fox and D. Haddleton, *Polym. Chem.*, 2015, **6**, 3581-3585.

18. A. Simakova, S. E. Averick, D. Konkolewicz and K. Matyjaszewski, *Macromolecules*, 2012, **45**, 6371-6379.

19. W. Tang and K. Matyjaszewski, *Macromolecules*, 2006, **39**, 4953-4959.

20. W. Tang, Y. Kwak, W. Braunecker, N. V. Tsarevsky, M. L. Coote and K. Matyjaszewski, *J. Am. Chem. Soc.*, 2008, **130**, 10702-10713.

21. A. Simula, V. Nikolaou, F. Alsubaie, A. Anastasaki and D. M. Haddleton, *Polym. Chem.*, 2015, **6**, 5940-5950.

22. N. H. Nguyen, X. Jiang, S. Fleischmann, B. M. Rosen and V. Percec, *J. Polym. Sci. Part A: Polym. Chem.*, 2009, **47**, 5629-5638.

23. A. Anastasaki, C. Waldron, P. Wilson, R. McHale and D. M. Haddleton, *Polym. Chem.*, 2013, **4**, 2672-2675.

24. N. H. Nguyen, M. E. Levere and V. Percec, *J. Polym. Sci. Part A: Polym. Chem.*, 2012, **50**, 35-46.

25. A. Anastasaki, A. J. Haddleton, Q. Zhang, A. Simula, M. Droesbeke, P. Wilson and D. M. Haddleton, *Macromol. Rapid Commun.*, 2014, **35**, 965-970.

26. A. Simula, V. Nikolaou, A. Anastasaki, F. Alsubaie, G. Nurumbetov, P. Wilson, K. Kempe and D. M. Haddleton, *Polym. Chem.*, 2015, **6**, 2226-2233.

27. N. H. Nguyen and V. Percec, *J. Polym. Sci. Part A: Polym. Chem.*, 2010, **48**, 5109-5119.

28. N. H. Nguyen and V. Percec, *J. Polym. Sci. Part A: Polym. Chem.*, 2011, **49**, 4241-4252.

29. A. Anastasaki, C. Waldron, V. Nikolaou, P. Wilson, R. McHale, T. Smith and D. M. Haddleton, *Polym. Chem.*, 2013, **4**, 4113-4119.

30. S. R. Samanta, A. Anastasaki, C. Waldron, D. M. Haddleton and V. Percec, *Polym. Chem.*, 2013, **4**, 5555-5562.

31. N. H. Nguyen, B. M. Rosen, G. Lligadas and V. Percec, *Macromolecules*, 2009, **42**, 2379-2386.

32. A. L. Aleksandrov, *B. Acad. Sci. USSR Ch.*, 1980, **29**, 1740-1744.

33. K. Min, H. Gao and K. Matyjaszewski, *J. Am. Chem. Soc.*, 2005, **127**, 3825-3830.

34. K. Matyjaszewski, W. Jakubowski, K. Min, W. Tang, J. Huang, W. A. Braunecker and N. V. Tsarevsky, *Proc. Natl. Acad. Sci. U.S.A.*, 2006, **103**, 15309-15314.

35. F. A. Leibfarth, K. M. Mattson, B. P. Fors, H. A. Collins and C. J. Hawker, *Angew. Chem., Int. Ed.*, 2013, **52**, 199-210.

36. B. P. Fors and C. J. Hawker, *Angew. Chem., Int. Ed.*, 2012, **51**, 8850-8853.

37. N. J. Treat, B. P. Fors, J. W. Kramer, M. Christianson, C.-Y. Chiu, J. R. d. Alaniz and C. J. Hawker, *ACS Macro Lett.*, 2014, **3**, 580-584.

38. M. A. Tasdelen, M. Uygun and Y. Yagci, *Macromol. Chem. Phys.*, 2010, **211**, 2271-2275.

39. Y. Yagci, S. Jockusch and N. J. Turro, *Macromolecules*, 2010, **43**, 6245-6260.

40. A. Anastasaki, V. Nikolaou, Q. Zhang, J. Burns, S. R. Samanta, C. Waldron, A. J. Haddleton, R. McHale, D. Fox, V. Percec, P. Wilson and D. M. Haddleton, *J. Am. Chem. Soc.*, 2013, **136**, 1141-1149.

41. A. Anastasaki, V. Nikolaou, A. Simula, J. Godfrey, M. Li, G. Nurumbetov, P. Wilson and D. M. Haddleton, *Macromolecules*, 2014, **47**, 3852-3859.

42. A. Anastasaki, V. Nikolaou, N. W. McCaul, A. Simula, J. Godfrey, C. Waldron, P. Wilson, K. Kempe and D. M. Haddleton, *Macromolecules*, 2015, **48**, 1404-1411.

43. E. Frick, A. Anastasaki, D. M. Haddleton and C. Barner-Kowollik, *J. Am. Chem. Soc.*, 2015, 137, 6889-6896.

44. J. Xu, K. Jung, A. Atme, S. Shanmugam and C. Boyer, *J. Am. Chem. Soc.*, 2014, **136**, 5508-5519.

45. J. Xu, A. Atme, A. F. Marques Martins, K. Jung and C. Boyer, *Polym. Chem.*, 2014, **5**, 3321-3325.

46. Y.-M. Chuang, A. Ethirajan and T. Junkers, *ACS Macro Lett.*, 2014, **3**, 732-737.

47. J. Vandenbergh, G. Reekmans, P. Adriaensens and T. Junkers, *Chem. Sci.*, 2015, **6**, 5753-5761.

48. J. A. Burns, C. Houben, A. Anastasaki, C. Waldron, A. A. Lapkin and D. M. Haddleton, *Polym. Chem.*, 2013, **4**, 4809-4813.

49. M. J. Scott, C. A. Goddard and R. H. Holm, *Inorg. Chem.*, 1996, **35**, 2558-2567.

50. T. G. Ribelli, D. Konkolewicz, S. Bernhard and K. Matyjaszewski, *J. Am. Chem. Soc.*, 2014, **136**, 13303-13312.

51. D. Konkolewicz, K. Schröder, J. Buback, S. Bernhard and K. Matyjaszewski, *ACS Macro Lett.*, 2012, **1**, 1219-1223.

52. B. Wenn, M. Conradi, A. D. Carreiras, D. M. Haddleton and T. Junkers, *Polym. Chem.*, 2014, **5**, 3053-3060.

53. S. Yamazaki, S. Iwai, J. Yano and H. Taniguchi, *J. Phys. Chem. A*, 2001, **105**, 11285-11290.

54. H. Tang, M. Radosz and Y. Shen, *Polymer Preprints*, 2006, **47**, 156.

55. M. Ciampolini and N. Nardi, *Inorg. Chem.*, 1966, **5**, 41-44.

Chapter 6

Discrete copper(II)/formate complexes as catalytic precursors for photo-induced reversible deactivation polymerisation

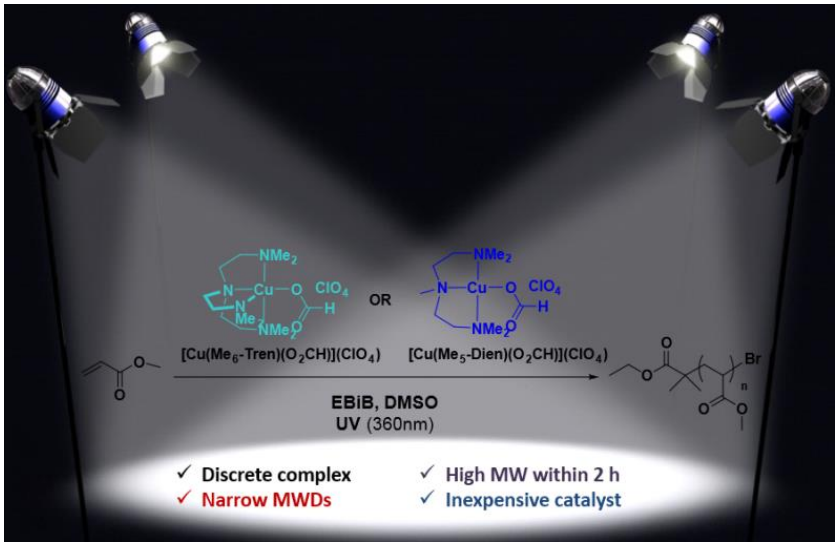

Traditional copper-mediated RDRP techniques have to employ various components (e.g. type of ligand, type and form of catalyst, additional deactivation species etc.) in order to achieve good control over the MWDs. In the previous chapter, a discrete copper(II) formate/Me_6-Tren complex was utilised as a precursor catalyst for the polymerisation of acrylates. In the present chapter, we expand the scope of this novel complex by investigating the compatibility with various solvents and a series of both hydrophilic and hydrophobic acrylic monomers. In all cases, narrow MWDs were attained (typically < 1.19), even when the polymerisation was encouraged to reach quantitative or near-quantitative conversions (>95%). High molecular weight polymers were also targeted achieving poly(MA) with a final dispersity of 1.12 within 2 h (M_n ~ 120000 g.mol^{-1}). As Me_6-Tren is relatively expensive to purchase, an additional complex was also synthesised, where PMDETA was incorporated in the coordination sphere of the copper(II) complex. Narrow MWDs, high monomer conversion and good spatiotemporal control could be achieved with the new complex, demonstrating that it could be an efficient and cheaper alternative to obtain well-defined poly(acrylates) and poly(methacrylates).

6.1 Introduction

In the previous chapter, a discrete copper(II) formate/Me_6-Tren complex was utilised to catalyse the polymerisation of acrylates.[1] Good spatiotemporal control and narrow MWDs were demonstrated when methyl acrylate (MA) was used as a model monomer. However, different monomer structures were not tested and only relatively low molecular weights were targeted (up to M_n ~ 16000 g.mol^{-1}). In addition, DMSO was the only solvent employed, perhaps limiting the applicability of this complex. More importantly, the Me_6-Tren which is incorporated in the coordination sphere of the complex is expensive to purchase, and as such it would be of great interest to replace it with a less expensive ligand, without compromising the features of the initial complex (*e.g.* narrow MWDs, near-quantitative conversions, good spatiotemporal control *etc.*).

This present chapter describes an expansion of the scope of the [Cu(Me_6-Tren)(O_2CH)](ClO_4) complex. Different solvents have been investigated including acetonitrile (MeCN), *N*,*N*-dimethylformamide (DMF), methanol (MeOH), 2-propanol (IPA), toluene, 2,2,2-trifluoroethanol (TFE), water and mixtures thereof. Note that pure water was found to exhibit poor control over the MWDs. This variety of solvents, allowed access to the polymerisation of a large diversity of acrylates including functional and hydrophilic acrylates (2-hydroxyethyl acrylate (HEA), hydroxypropyl acrylate (HPA), poly(ethylene glycol) methyl ether acrylate (PEGA) and solketal acrylate (SA)), hydrophobic acrylates (butyl acrylate (*n*-BA), *tert*-butyl acrylate (*t*-BA), lauryl acrylate (LA), octadecyl acrylate (ODA)) and thermoresponsive acrylates (*e.g.* di(ethylene glycol) diacrylate (DEGEEA)). Narrow MWDs even at quantitative or near-quantitative conversions were obtained in most

cases highlighting the versatility of the approach. Importantly, higher molecular weight polymers could also be attained (M_n ~ 120000 g.mol^{-1}) within 2 h of reaction time. Finally, a second complex was synthesised, where PMDETA (1 ml ~ £0.28) was used to replaced Me_6-Tren (1ml ~ £115) as the ligand to afford a less expensive alternative. The use of such simple and inexpensive catalysts, paves the way for using copper mediated processes in industrial level.

6.2 Results and Discussion

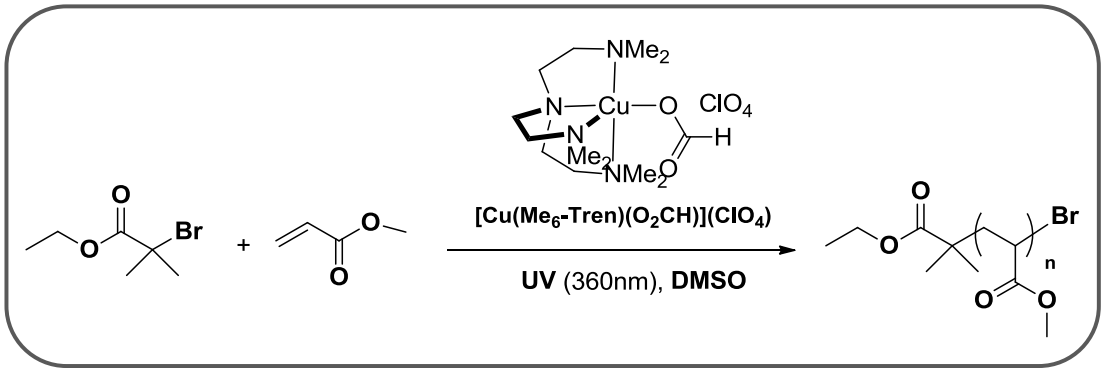

Scheme 6.1: Photo-induced polymerisation of MA, utilising [Cu(Me_6-Tren)(O_2CH)](ClO_4) as the precursor catalyst.

In order to assess the compatibility of the [Cu(Me_6-Tren)(O_2CH)](ClO_4) complex with various solvents, methyl acrylate was used as the monomer (MA) utilising previously optimised conditions ([I]:[M]:[complex]=[1]:[50]:[0.08]) (Scheme 6.1).[1] MeCN and DMF were tested giving rise to well-defined polymers with good agreement between theoretical and experimental values and narrow MWDs ($Đ$ ~ 1.09 for both solvents) (Figure 6.1a,b). However, the polymerisation rates were slower than in the case of DMSO (~ 4 h to reach >95% conversion as opposed to 2 h for the DMSO system) (Table 6.1).

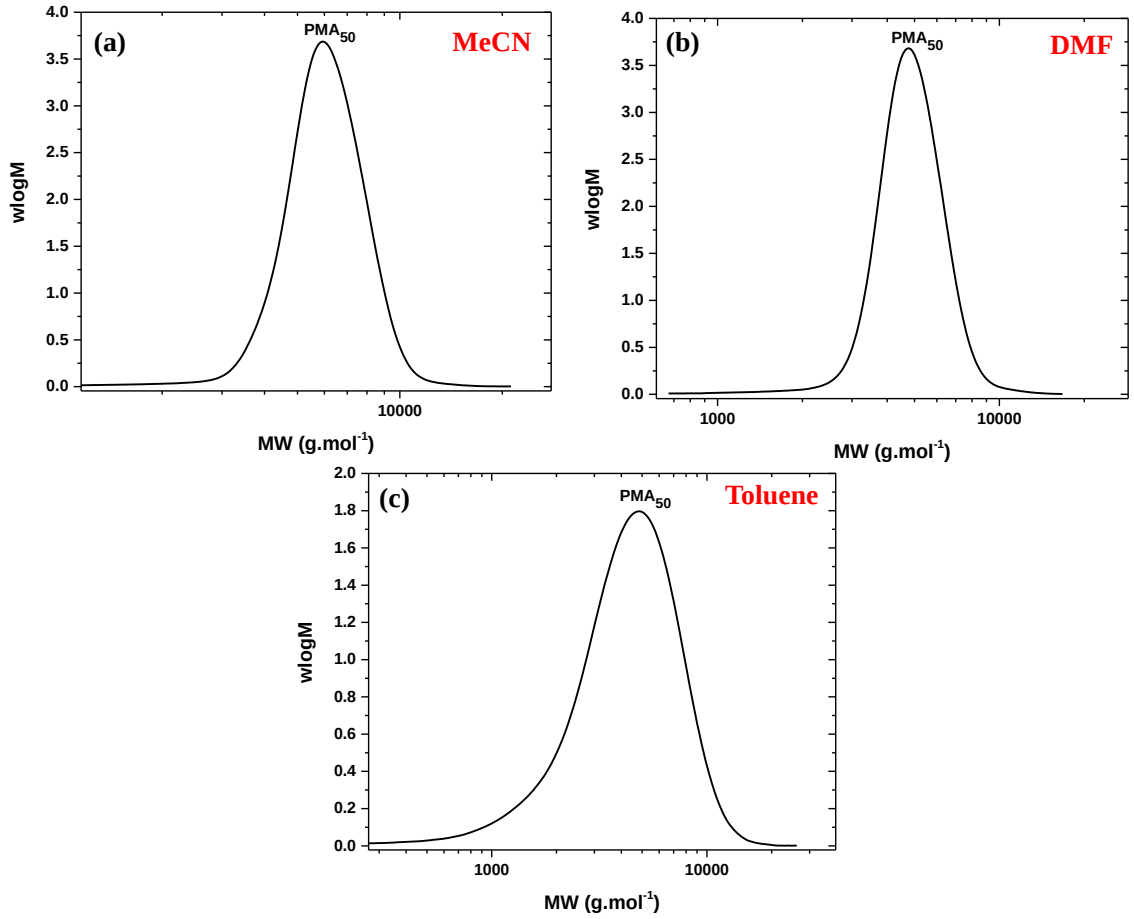

Figure 6.1: Molecular weight distribution of PMA synthesised *via* photo-induced polymerisation. Initial conditions [MA]:[EBiB]:[[Cu(Me_6-Tren)(O_2CH)](ClO_4)] = [50]:[1]:[0.08], (a) MeCN, (b) DMF and (c) Toluene, 50% *v/v*.

Alcoholic solvents were also found to be compatible with this complex, with MeOH and IPA furnishing very high conversions within 6 h, without compromising the control over the MWDs (*Đ* ~ 1.09 and *Đ* ~1.20 for MeOH and IPA respectively) (Table 6.1, Figure 6.2a,b). TFE was also tested as fluorinated solvents have shown that can be utilised for the polymerisation of a large diversity of monomers with both hydrophobic and hydrophilic moieties (*Đ* ~ 1.08) (Table 6.1, Figure 6.2c).[2-5] In order to facilitate the polymerisation of more hydrophobic monomers, toluene was also studied. Relatively fast polymerisation rates could be achieved with NMR

confirming >98% conversion within 4 h, albeit a much higher dispersity was attained ($Đ$ ~ 1.42), suggesting poor control over the polymerisation and inefficient deactivation. This could be attributed to the limited solubility of [Cu(Me_6-Tren)(O_2CH)](ClO_4) in toluene at ambient temperature, which is consistent with previously reported data (Table 6.1, Figure 6.1c).[6] However, addition of a small amount of MeOH ([MeOH]:[Toluene]=[1]:[4]) resulted in a significant reduction of the dispersity value, which resembled the dispersities obtained in MeOH ($Đ$ ~ 1.09), perhaps due to enhanced solubility of the copper complex (Table 6.1, Figure 6.2d).

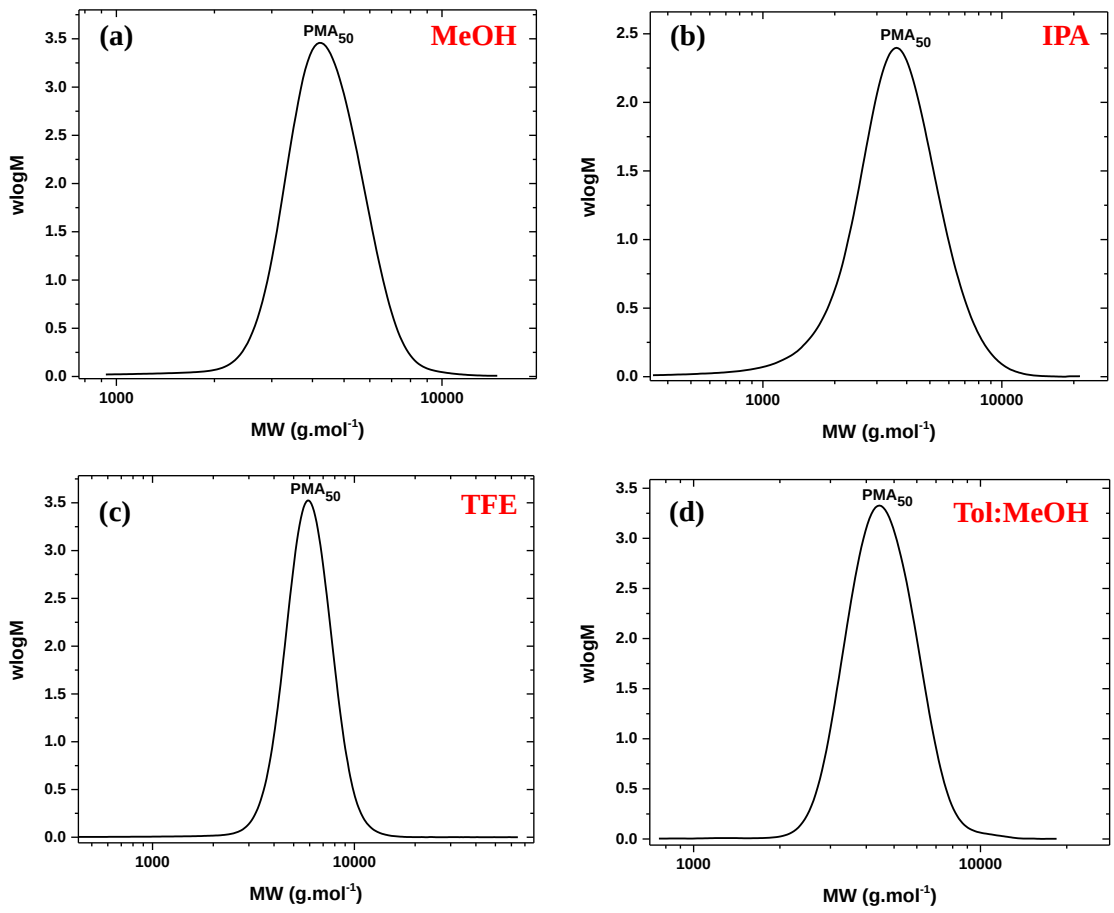

Figure 6.2: Molecular weight distribution of PMA synthesised *via* photo-induced polymerisation utilising alcohols and mixtures thereof. Initial conditions

[MA]:[EBiB]:[[Cu(Me_6-Tren)(O_2CH)](ClO_4)] = [50]:[1]:[0.08], (a) MeOH, (b) IPA, (c) TFE and (d) [Toluene]:[MeOH]= [4]:[1], 50% *v/v*.

Table 6.1: Solvent compatibility study for the photo-induced polymerisation of MA utilising [Cu(Me_6-Tren)(O_2CH)](ClO_4) as the precursor catalyst.

Solvent	Monomer	t (h)	Conv. (%)	$M_{n,th}$ (g.mol^{-1})	$M_{n,SEC}$ (g.mol^{-1})	$Đ$
DMSO[1]	**MA** ***DP* = 50**	2	97	4400	5100	1.07
MeCN		4	96	4300	5600	1.09
DMF		4	95	4300	4600	1.09
MeOH		6	96	4300	4200	1.09
IPA		6	92	4100	3200	1.20
TFE		2	96	4300	5500	1.08
Toluene		4	98	4400	3300	1.42
Tol : MeOH		6	97	4400	4300	1.09

Finally, water was also employed as the solvent. As MA is not soluble in aqueous media, PEGA was selected as an alternative monomer. Under the selected conditions, the aqueous polymerisation of PEGA presented near-quantitative conversion in 2 h (~ 98% by NMR), although broad MWDs were attained ($Đ$ ~ 1.47) suggested limited control over the polymerisation (Table 6.2, Figure 6.3a). In order to facilitate a direct comparison, the polymerisation of PEGA in DMSO was also conducted. Although the polymerisation rates were comparable, achieving also near-quantitative conversion within 2 h, the dispersity was significantly improved ($Đ$ ~ 1.13) suggesting that the solvent (water) was responsible for the loss of control (Table 6.2, Figure 6.3b, Section 6.4.4, Figure 6.8). We postulate that this is due to the inefficient reduction of Cu(II) in aqueous media under the studied conditions. However, for applications where water is desirable, mixtures with any of the aforementioned solvents could be alternatively employed.

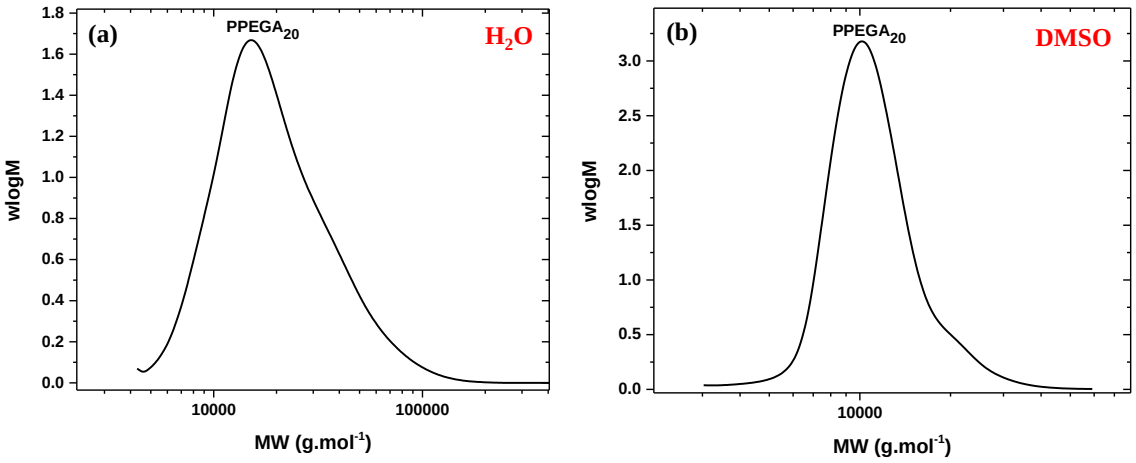

Figure 6.3: Molecular weight distribution of PPEGA synthesised *via* photo-induced polymerisation in (a) pure water and (b) DMSO, 50% *v/v*. Initial conditions [PEGA]:[EBiB]:[[Cu(Me_6-Tren)(O_2CH)](ClO_4)] = [20]:[1]:[0.08].

In an attempt to further expand the scope of this photo-mediated system and include additional monomer structures, *n*-BA was polymerised in DMSO as the solvent under the following reaction conditions: [I]:[*n*-BA]:[complex]=[1]:[50]:[0.08]). Very high conversion (>98%) could be achieved in 4 h with SEC revealing a symmetrical, monomodal molecular weight distribution with low dispersity ($Đ$ ~ 1.18) (Table 6.2, Section 6.4.4, Figure 6.9). This slightly higher dispersity (in comparison with MA) was attributed to the heterogeneity of the system as *n*-BA phase separates under the selected conditions (solvent/monomer).[7-9] As it was shown earlier, DMF was also found to be compatible with this polymerisation protocol and as such, it was chosen as an alternative solvent since it would maintain full solubility of the monomer and polymer throughout the polymerisation. Interestingly, the polymerisation under homogeneous conditions proceeded in a more controlled manner and an observed reduction in the dispersity was evident ($Đ$ ~ 1.07) (Table 6.2, Section 6.4.4, Figure 6.10). Under identical

conditions, the polymerisation of *t*-BA was also attempted in DMSO. However, a gel-like polymer was reproducibly observed within 2 h with broad MWDs attained by SEC ($Đ$ > 6) (Table 6.2, Section 6.4.4, Figure 6.11). Conversely, when DMF was chosen as the solvent the control over the MWD was restored and low dispersity was attained ($Đ$ ~ 1.09) suggesting that maintaining the solubility of all components is crucial to mediate this polymerisation (Table 6.2, Section 6.4.4, Figure 6.12).

Hydrophilic monomers were also polymerised in DMSO, including HEA and HPA with good agreement between theoretical and experimental values and relatively narrow MWDs (Table 6.2, Section 6.4.4, Figures 6.13 & 6.14). Monomers synthesised in our laboratory were also subjected to these polymerisation conditions, such as SA, demonstrating fast polymerisation rates (95% in 2 h) and low dispersity ($Đ$ ~ 1.09) (Table 6.2, Figure 6.15). Pleasingly, DEGEEA also afforded a controlled polymerisation yielding well-defined materials with narrow MWDs ($Đ$ ~ 1.15) (Table 6.2, Figure 6.16). The controlled photo-induced polymerisation of increasingly hydrophobic acrylates was also demonstrated. As LA is insoluble in DMSO and other polar solvents, a mixture of toluene/methanol was selected to facilitate solubility of the monomer, polymer and catalyst. Under these conditions, well-controlled polymers could be obtained, albeit slower polymerisation rates were observed (~ 12 h). Nevertheless, low dispersities were attained even when the reaction was pushed to reach quantitative or near-quantitative levels ($Đ$ ~ 1.10) (Table 6.2, Section 6.4.4, Figure 6.17). Similarly, ODA was also polymerised by changing the solvent from toluene/methanol to toluene/IPA in order to facilitate the solubility of this longer alkyl chain acrylate. Again ^{1}H NMR confirmed high conversions (~ 90%) and SEC revealed symmetrical traces without any obvious low

or high molecular weight shoulders (Table 6.2, Section 6.4.4, Figure 6.18). Although different families of monomers were also tested, including MMA and styrene, broad MWDs and poor conversion was attained respectively (Table 6.2, Section 6.4.4, Figure 6.19), while the inclusion of additional NaBr gave rise to 0% conversion, even when the reaction was left to proceed overnight.

Table 6.2: Monomer compatibility study for the photo-induced polymerisation of MA utilising [Cu(Me_6-Tren)(O_2CH)](ClO_4) as the precursor catalyst.

Monomer	Solvent	*DP*	t (h)	Conv. (%)	$M_{n,th}$ (g.mol^{-1})	$M_{n,SEC}$ (g.mol^{-1})	*Đ*
***n*-BA**	*DMSO*	50	4	98	6500	9200	1.18
	DMF		4	95	6300	6600	1.07
***t*-BA**	*DMSO*		2	93	6100	7400	6.40
	DMF		4	99	6600	8300	1.09
PEGA	*DMSO*	20	2	98	9600	10400	1.13
	H_2O		2	98	9600	10000	1.47
DEGEEA	*DMSO*		6	99	3000	3000	1.15
HEA	*DMSO*		6	95	2400	2800	1.18
HPA	*DMSO*		6	99	2800	3000	1.32
ODA	*Tol:IPA*	50	12	90	14800	9900	1.13
LA	*Tol:MeOH*		12	98	11900	9100	1.10
SA	*DMSO*		2	95	9000	8000	1.09
MMA	*DMSO*		10	27	1400	3400	2.10
MMA[a]	*DMSO*		20	0	-	-	-
Sty	*Tol:MeOH*		6	10	540	-	-

[a]1equiv. of NaBr in respect to the complex.

Higher molecular weight polymers were also targeted, as an attempt to further explore the potential of this novel compound. For this reason, a range of polymerisations were conducted targeting various degrees of polymerisation (*DP* = 400 - 3200). For *DP* = 400 ([I]:[MA]:[complex]=[1]:[400]:[0.08]), high conversion (~ 95% by ^{1}H NMR) and narrow MWDs (*Đ* ~ 1.10) were attained in 2 h with good correlation between the theoretical and experimental molecular weights (Table 6.3,

Figure 6.4). Similar results were obtained when *DP* = 800 was subsequently targeted (*Đ* ~ 1.10, 95% conversion in 2 h) and a final M_n of 67000 g.mol^{-1} was evident as shown by SEC (Table 6.3, Figure 6.4). However, when identical conditions were applied for the synthesis of even higher MW polymers (*DP* = 1600) the polymerisation rate was decreased reaching a final conversion of 86% after 14 h (Table 6.3, Section 6.4.4, Figure 6.20). In order to circumvent this, the complex concentration was increased to 0.16 equiv. with respect to initiator ([I]:[MA]:[complex]=[1]:[1600]:[0.16]), which lead to a remarkable increase on the rate yielding well-controlled polymers with M_n ~ 120000 g.mol^{-1} and *Đ* ~ 1.12 (Table 6.3, Figure 6.4). Interestingly the same conditions led to uncontrolled polymers when a *DP*= 3200 was targeted (bimodal SEC peak). A similar scenario was evident (bimodal SEC peaks were observed) even when higher concentrations of copper complexes were utilised (0.32 equiv. with respect to initiator) suggesting that the limitations of the system had been reached. Although when a small amount of NaBr was externally added at the beginning of the polymerisation (1 equiv. with respect to the complex) higher molecular weight polymers could be attained, a low molecular weight shoulder was still visible by SEC, showing unavoidable premature termination under the conditions employed (M_n ~ 160000 g.mol^{-1}, 85% conversion) (Table 3, Section 6.4.4, Figures 6.20).

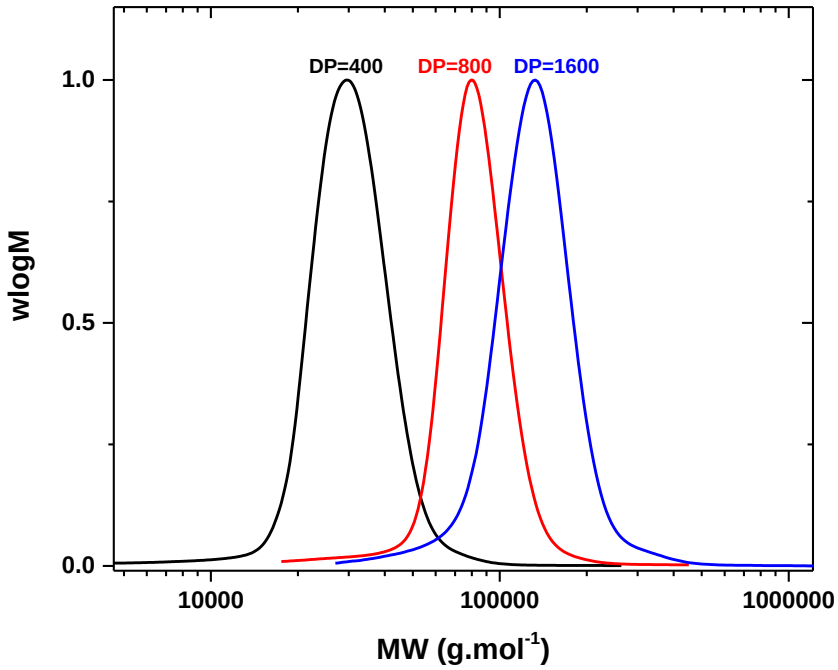

Figure 6.4: High molecular weight poly(MA) synthesised *via* photo-induced polymerisation utilising [Cu(Me$_6$-Tren)(O$_2$CH)](ClO$_4$) as the precursor catalyst.

Table 6.3: Synthesis of high molecular weight poly(MA) *via* photo-induced polymerisation utilising [Cu(Me$_6$-Tren)(O$_2$CH)](ClO$_4$) or [Cu(Me$_5$-Dien)(O$_2$CH)](ClO$_4$) as the precursor catalyst.

Complex		*DP*	t (h)	Conv. (%)	$M_{n,SEC}$ (g.mol^{-1})	*Đ*
Methyl Acrylate	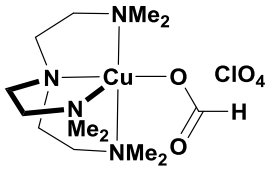	400	2	95	28800	1.10
		800	2	95	67000	1.10
		1600	6	90	94000	1.10
		1600[a]	2	95	120000	1.12
		3200[a]	12	94	110000	1.35
		3200[b]	4	95	110000	1.18
		3200[c]	6	85	160000	1.13
	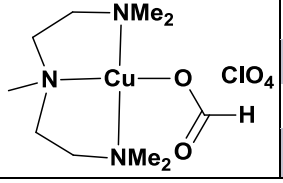	200	10	99	20000	1.13
		800	10	88	50000	1.38
		800[a]	10	95	60000	1.20
		1600[a]	10	70	69000	1.60

[a]0.16 equiv. and [b]0.32 equiv. of the complex, [c]1 equiv. NaBr was added in the solution.

As Me_6-Tren is a relatively expensive ligand (~ £115/ml), an additional strategy was also employed to provide a cost effective alternative, where PMDETA replaced Me_6-Tren as the ligand in the complex. The $[Cu(Me_5\text{-Dien})(O_2CH)](ClO_4)$ complex was synthesised according to a literature procedure[10] and subsequently used for the polymerisation of MA. Although slower polymerisation rates were obtained (95% in 5 h), the control over the MWD was not compromised with SEC showing low dispersities ($Đ$ ~ 1.18) (Table 6.4, Figure 6.5a). In order to probe the versatility of the complex, EGA was also polymerised in DMF, yielding high conversions and low dispersities and thus demonstrating the potential of this complex to be used as a less expensive and efficient alternative (Table 6.4, Figure 6.5b).

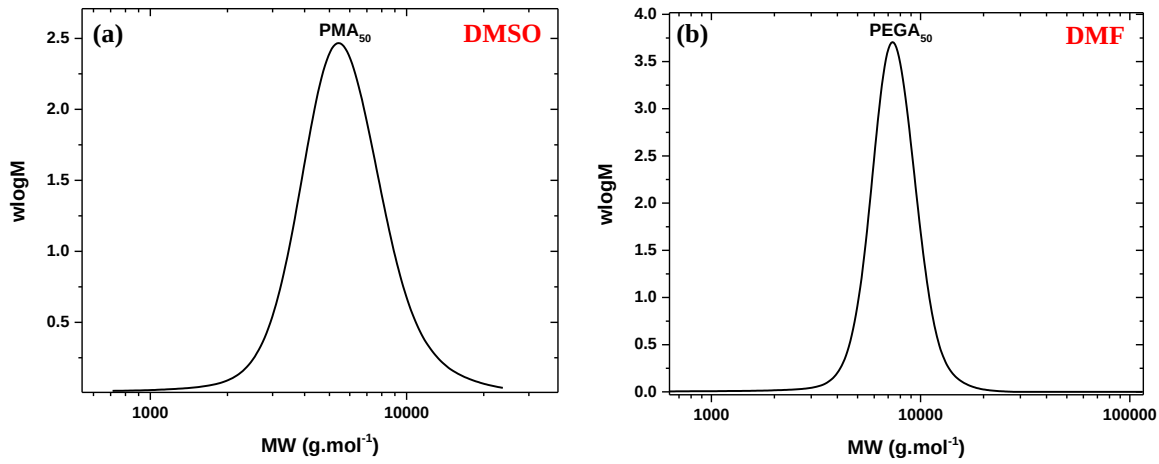

Figure 6.5: Molecular weight distribution of: (a) PMA synthesised *via* photo-induced polymerisation. Initial conditions [MA]:[EBiB]:[$[Cu(Me_5\text{-Dien})(O_2CH)](ClO_4)$] = [50]:[1]:[0.08], DMSO 50% *v/v* and (b) PEGA synthesised *via* photo-induced polymerisation. Initial conditions [EGA]:[EBiB]:[$[Cu(Me_5\text{-Dien})(O_2CH)](ClO_4)$] = [50]:[1]:[0.08], DMF 50% *v/v*.

Higher molecular weight polymers (DP = 800) could also be attained, although $Đ$ < 1.20 could be achieved only with the use of additional NaBr (Table

6.3, Figure 6.6a,b, Section 6.4.4, Figure 6.21). The polymerisation of MMA was also attempted, showing higher conversion and better control over the molecular weight distribution in comparison with the Me_6-Tren complex, although the dispersities were still high for a controlled polymerisation ($Đ$ ~ 1.50) (Table 6.4, Section 6.4.4, Figure 6.22). This issue was circumvented by adding 1 equiv. of NaBr with respect to the complex, giving rise to well-defined poly(MMA) with $Đ$ ~ 1.25 (Table 6.4, Section 6.4.4, Figure 6.22).

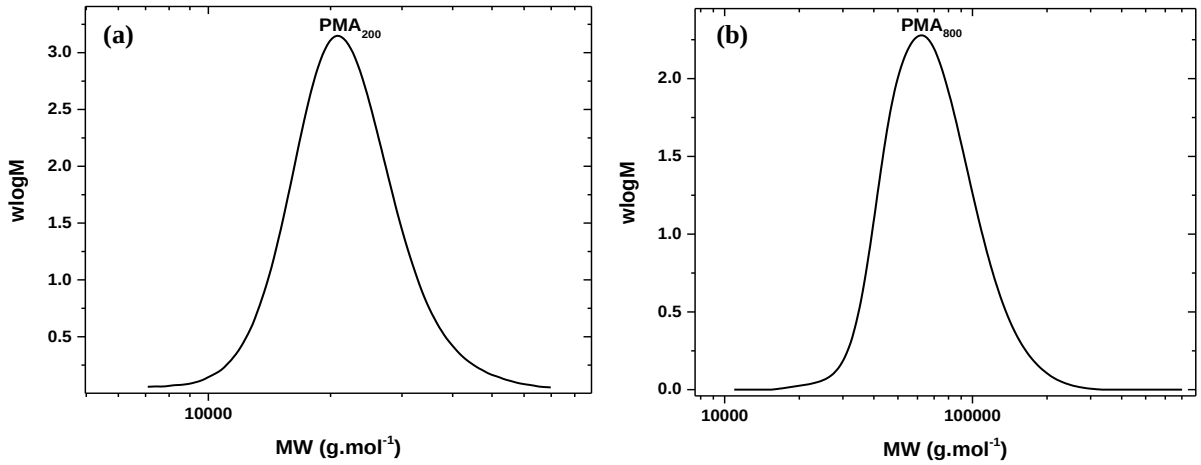

Figure 6.6: Molecular weight distribution of PMA synthesised *via* photo-induced polymerisation. Initial conditions: (a) [MA]:[EBiB]:[[Cu(Me_5-Dien)(O_2CH)](ClO_4)] = [200]:[1]:[0.08] and (b) [MA]:[EBiB]:[[Cu(Me_5-Dien)(O_2CH)](ClO_4)] = [800]:[1]:[0.16], DMSO 50% *v/v*.

Table 6.4: Synthesis of various poly((meth)acrylates) *via* photo-induced polymerisation utilising [Cu(Me_5-Dien)(O_2CH)](ClO_4) as the precursor catalyst.

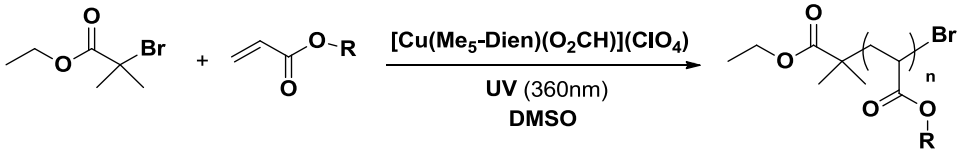

Monomer	*DP*	Solvent	t (h)	Conv. (%)	$M_{n,th}$ (g.mol^{-1})	$M_{n,SEC}$ (g.mol^{-1})	*Đ*
MA	50	*DMSO*	5	95	4300	5000	1.18
MMA			6	80	4100	7600	1.50
MMA[a]			6	73	3800	6300	1.25
EGA		*DMF*	5	95	6500	6400	1.10

[a]1 equiv. of NaBr in respect to the complex was added.

In order to further explore the potential of this complex, the possibility of "on/off" temporal control was also investigated throughout the polymerisation. Intermittent "light/dark" cycles for alternating periods were conducted, where the polymerisation mixture was initially exposed under UV irradiation for 45 min, achieving 36% of conversion. A "dark" period of a further 45 min was followed in which no polymerisation was observed by either ^{1}H NMR or SEC. Upon re-exposure of the mixture to UV irradiation switched the polymerisation back "on" and approximately 58% conversion was attained in an additional 1 h (Figure 6.7, Section 6.4.4, Figure 6.23). These cycles were repeated several times (with no or minimal polymerization (1-2%) observed during the dark periods), demonstrating not only the necessity of photo exposure at an appropriate wavelength for the polymerisation to commence but also the potential of utilising spatiotemporal control for future applications.

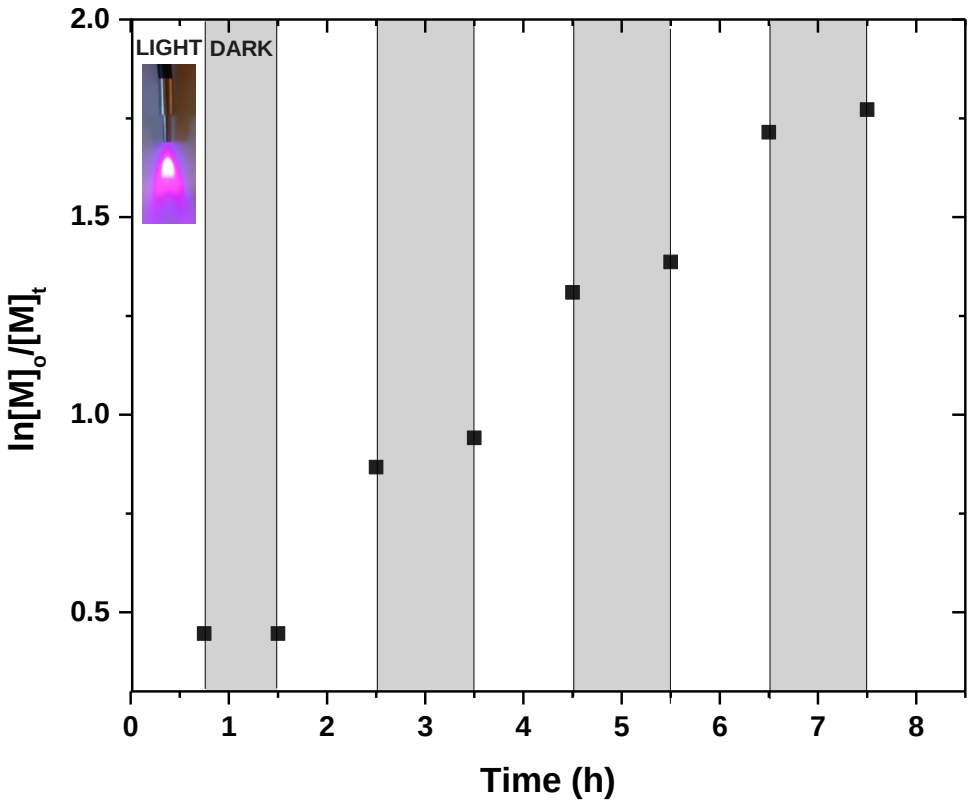

Figure 6.7: Evidence of temporal control *via* concecutive light and dark exposure. Initial conditions: [MA] : [I] : [[Cu(Me_5-Dien)(O_2CH)](ClO_4)] = [50] : [1] : [0.08] in DMSO 50% *v/v*.

6.3 Conclusions

In summary, the employment of two discrete copper complexes, namely [Cu(Me_6-Tren)(O_2CH)](ClO_4) and [Cu(Me_5-Dien)(O_2CH)](ClO_4) for the controlled polymerisation of acrylates and methacrylates is presented. For the case of [Cu(Me_6-Tren)(O_2CH)](ClO_4), different solvents were investigated such as MeCN, DMF, MeOH, IPA, toluene, TFE, water and mixtures thereof. Functional and hydrophilic acrylates (*e.g.* HEA, HPA, PEGA and SA), hydrophobic acrylates (*e.g. n*-BA, *t*-BA, LA and ODA) and thermoresponsive acrylates (*e.g.* DEGEEA) were successfully polymerised yielding narrow MWDs even at very high conversions and high

molecular weight polymers in a matter of 2 h (M_n ~ 120000 g.mol^{-1}, $Đ$ ~ 1.12). [Cu(Me$_5$-Dien)(O$_2$CH)](ClO$_4$) was also synthesised and employed for the controlled polymerisation of acrylates as an inexpensive alternative yielding well-defined polymers with narrow MWDs. Importantly, the incorporation of PMDETA in the coordination sphere of the complex afforded the polymerisation of methacrylates in addition to the polymerisation of acrylates allowing access to a wider range of materials. Spatiotemporal control was also demonstrated highlighting the potential of simple and cost effective complexes to be used for copper mediated processes in numerous applications, including synthesis of these materials in an industrial level.

6.4 Experimental

6.4.1 Materials and Methods

All materials were purchased from Sigma Aldrich or Fischer Scientific and used as received unless otherwise stated. All monomers were passed through a basic Al_2O_3 chromatographic column prior to use. Cu(Me$_6$-Tren)(O$_2$CH)](ClO$_4$) and Cu(Me$_5$-Dien)(O$_2$CH)](ClO$_4$) were synthesised according to previously reported literature. [10]

6.4.2 Instrumentation

^{1}H NMR spectra were recorded on Bruker DPX-300 or DPX-400 spectrometers in $CDCl_3$ unless otherwise stated. Chemical shifts are given in ppm downfield from the internal standard tetramethylsilane. Size exclusion chromatography (SEC) measurements were conducted using an Agilent 1260 SEC-

MDS fitted with differential refractive index (DRI), light scattering (LS) and viscometry (VS) detectors equipped with 2 × PLgel 5 mm mixed-D columns (300 × 7.5 mm), 1 × PLgel 5 mm guard column (50 × 7.5 mm) and autosampler. Narrow linear poly(methyl methacrylate) standards in the range of 200 to 1.0×10^6 g.mol^{-1} were used to calibrate the system. All samples were passed through 0.45 μm PTFE filter before analysis. The mobile phase was chloroform with 2% triethylamine eluent at a flow rate of 1.0 mL/min. SEC data was analysed using Cirrus v3.3 software with calibration curves produced using Varian Polymer laboratories Easi-Vials linear poly(methyl methacrylate) standards (200 - 4.7×10^5 g.mol^{-1}). The source of UV light was an OmniCure® S2000 spot UV curing lamp system, 200W (λ_{max} ~ 320-390 nm).

6.4.3 General procedures

Appropriate amounts of EBiB (1 equiv.), monomer (*DP* equiv.), [Cu(Me$_6$-Tren)(O$_2$CH)](ClO$_4$) or [Cu(Me$_5$-Dien)(O$_2$CH)](ClO$_4$) (0.08 equiv.) and solvent (50% *v/v* in respect to the monomer) were placed in a polymerisation flask, which was equipped with a magnetic stir bar and fitted with a rubber septum. The reaction mixture was degassed *via* bubbling with nitrogen for 20 min. The polymerisation was allowed to proceed for 2 h under irradiation at λ ~ 320-390 nm. Samples were taken periodically for conversion and molecular weight analyses. The polymerisation mixture was initially dissolved in THF and then passed through a small basic Al_2O_3 chromatographic column to remove the copper salts.

6.4.4 Additional Characterisation

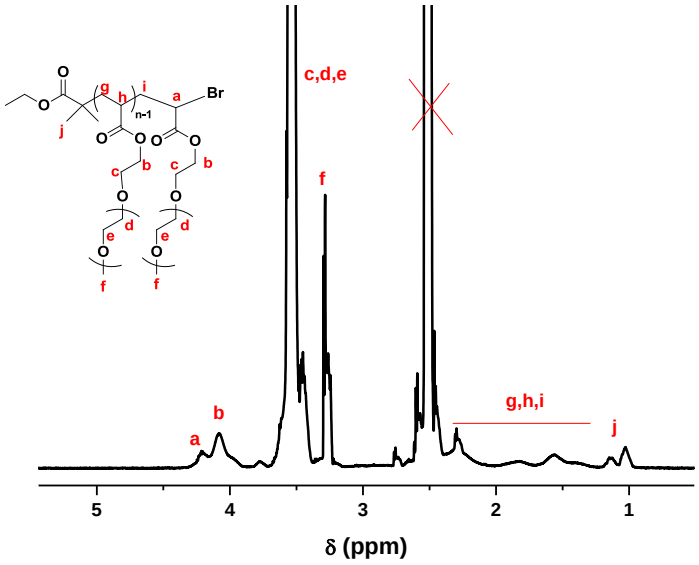

Figure 6.8: ^{1}H NMR of PPEGA synthesised *via* photo-induced polymerisation. Initial conditions [PEGA]:[EBiB]:[[Cu(Me$_6$-Tren)(O$_2$CH)](ClO$_4$)] = [20]:[1]:[0.08], DMSO 50% *v/v*.

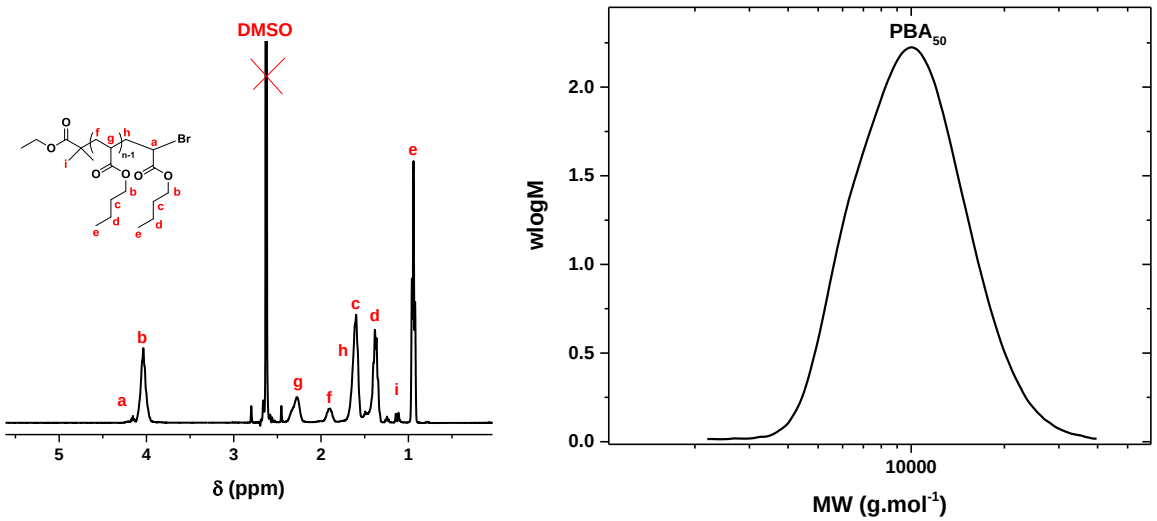

Figure 6.9: ^{1}H NMR (left) and MWD (right) of PBA synthesised *via* photo-induced polymerisation. Initial conditions [*n*-BA]:[EBiB]:[[Cu(Me$_6$-Tren)(O$_2$CH)](ClO$_4$)] = [50]:[1]:[0.08], DMSO 50% *v/v*.

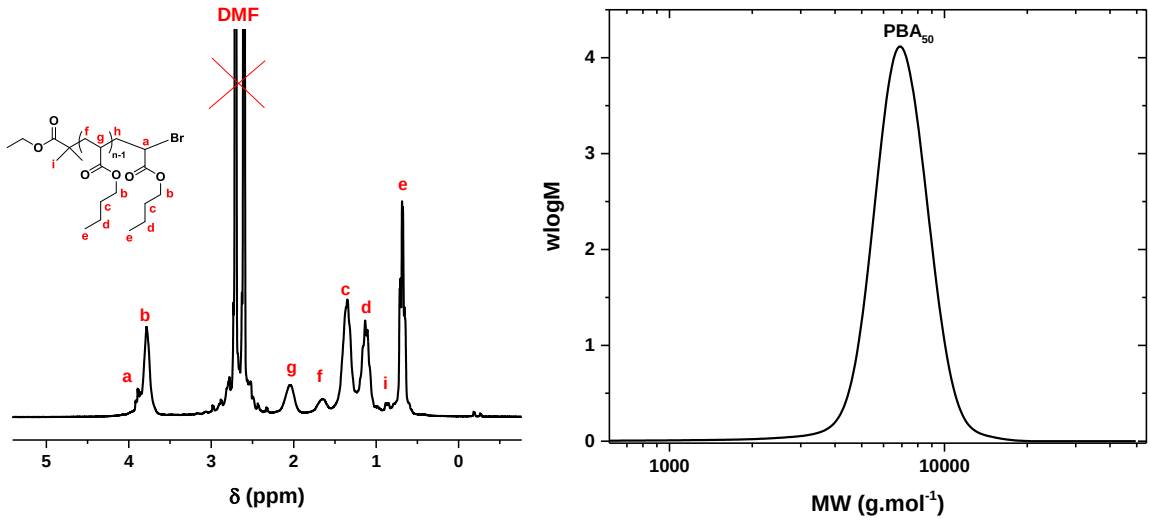

Figure 6.10: ^{1}H NMR (left) and MWD (right) of PBA synthesised *via* photo-induced polymerisation. Initial conditions [*n*-BA]:[EBiB]:[[Cu(Me$_6$-Tren)(O$_2$CH)](ClO$_4$)] = [50]:[1]:[0.08], DMF 50% *v/v*.

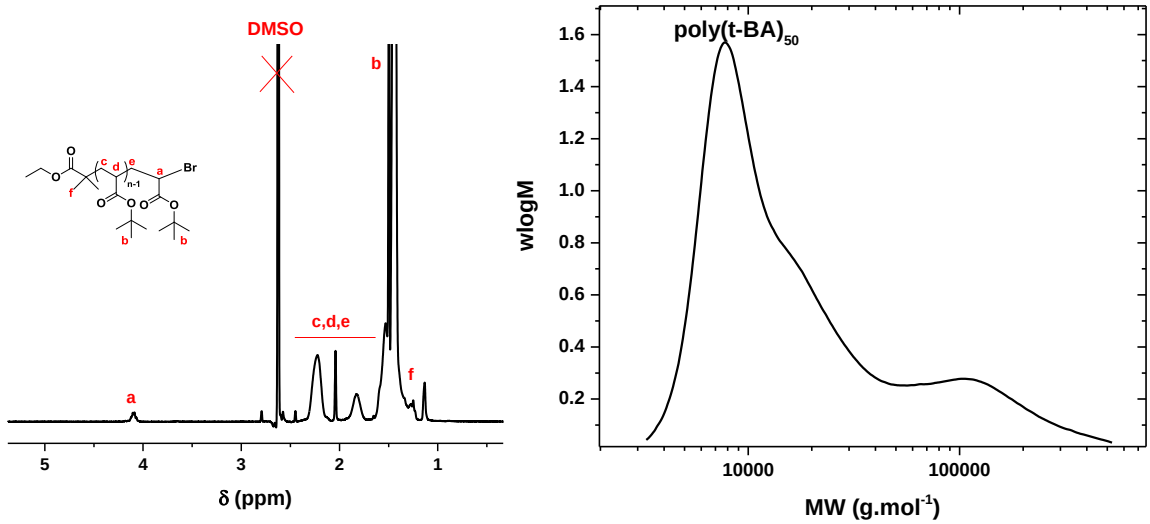

Figure 6.11: ^{1}H NMR (left) and MWD (right) of poly(*t*-BA) synthesised *via* photo-induced polymerisation. Initial conditions [*t*-BA]:[EBiB]:[[Cu(Me$_6$-Tren)(O$_2$CH)](ClO$_4$)] = [20]:[1]:[0.08], DMSO 50% *v/v*.

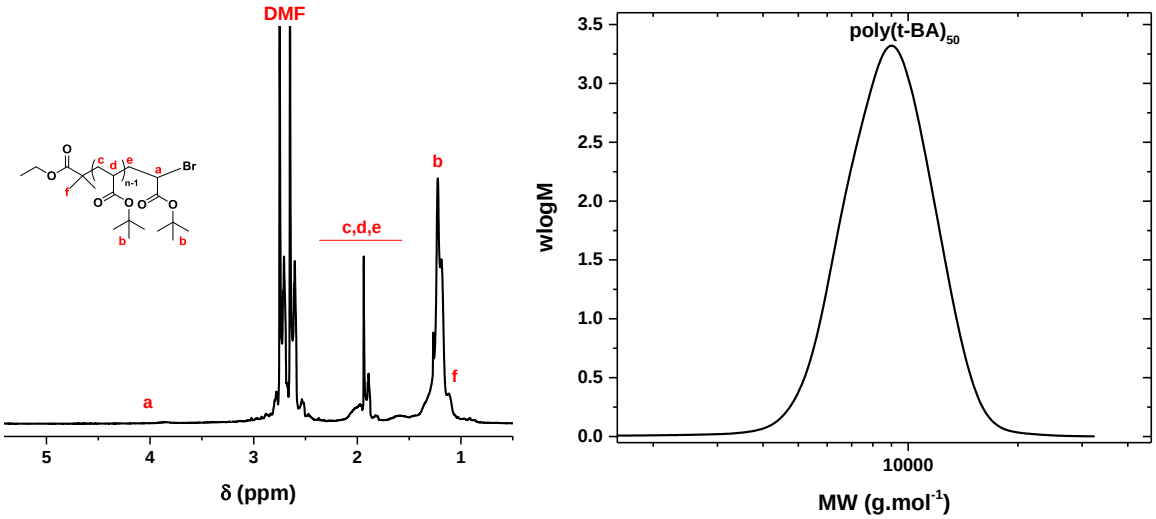

Figure 6.12: ^{1}H NMR (left) and MWD (right) of poly(*t*-BA) synthesised *via* photo-induced polymerisation. Initial conditions [*t*-BA]:[EBiB]:[[Cu(Me$_6$-Tren)(O$_2$CH)](ClO$_4$)] = [50]:[1]:[0.08], DMF 50% *v/v*.

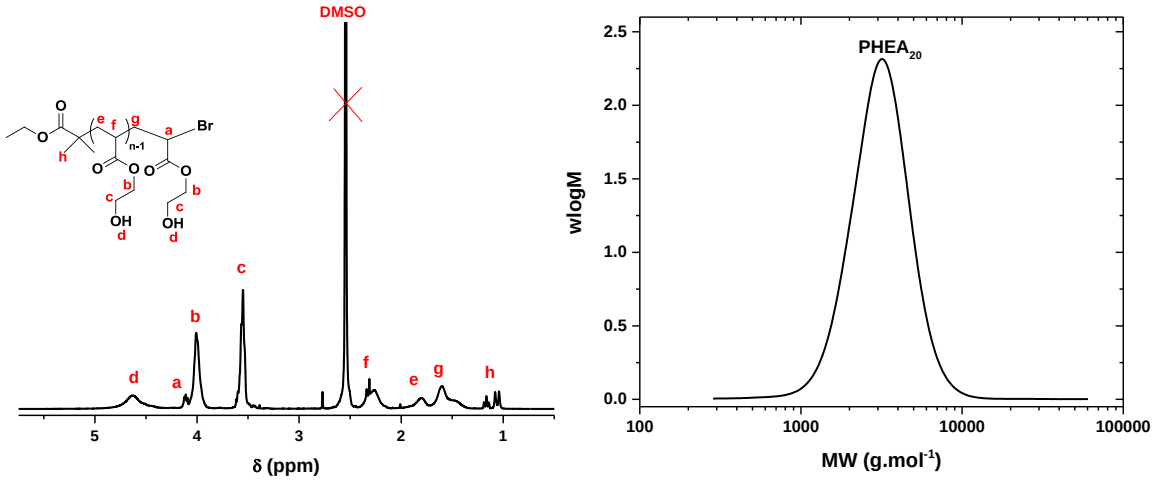

Figure 6.13: ^{1}H NMR (left) and MWD (right) of PHEA synthesised *via* photo-induced polymerisation. Initial conditions [HEA]:[EBiB]:[[Cu(Me$_6$-Tren)(O$_2$CH)](ClO$_4$)] = [50]:[1]:[0.08], DMSO 50% *v/v*.

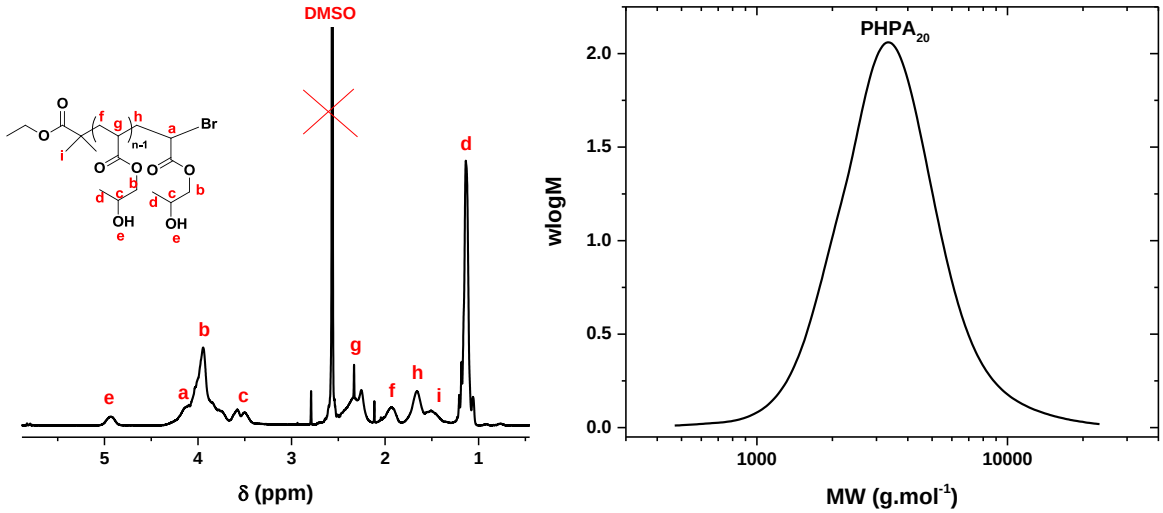

Figure 6.14: ^{1}H NMR (left) and MWD (right) of PHPA synthesised *via* photo-induced polymerisation. Initial conditions [HPA]:[EBiB]:[[Cu(Me$_6$-Tren)(O$_2$CH)](ClO$_4$)] = [20]:[1]:[0.08], DMSO 50% *v/v*.

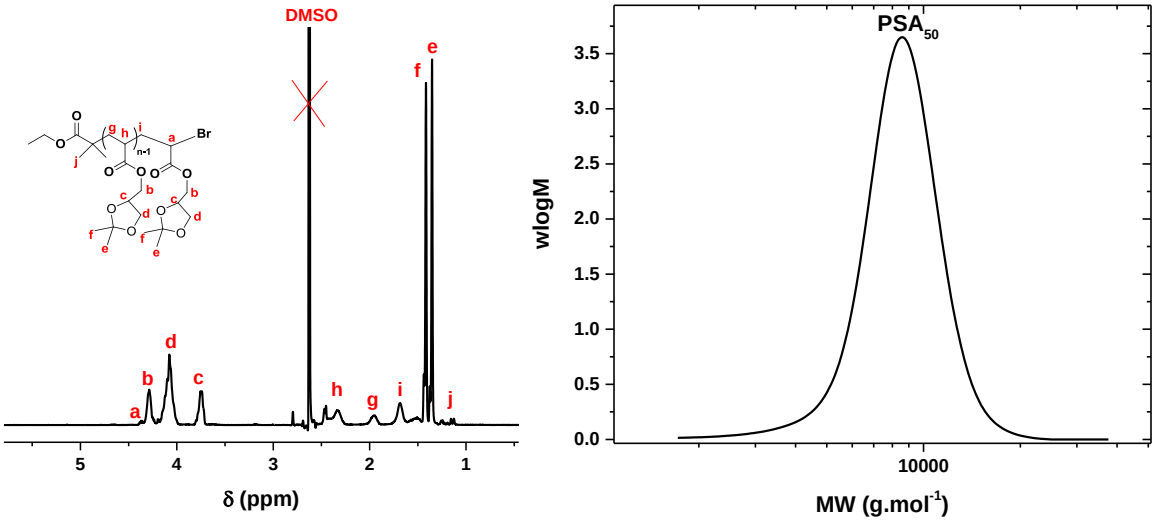

Figure 6.15: ^{1}H NMR (left) and MWD (right) of PSA synthesised *via* photo-induced polymerisation. Initial conditions [SA]:[EBiB]:[[Cu(Me$_6$-Tren)(O$_2$CH)](ClO$_4$)] = [50]:[1]:[0.08], DMSO 50% *v/v*.

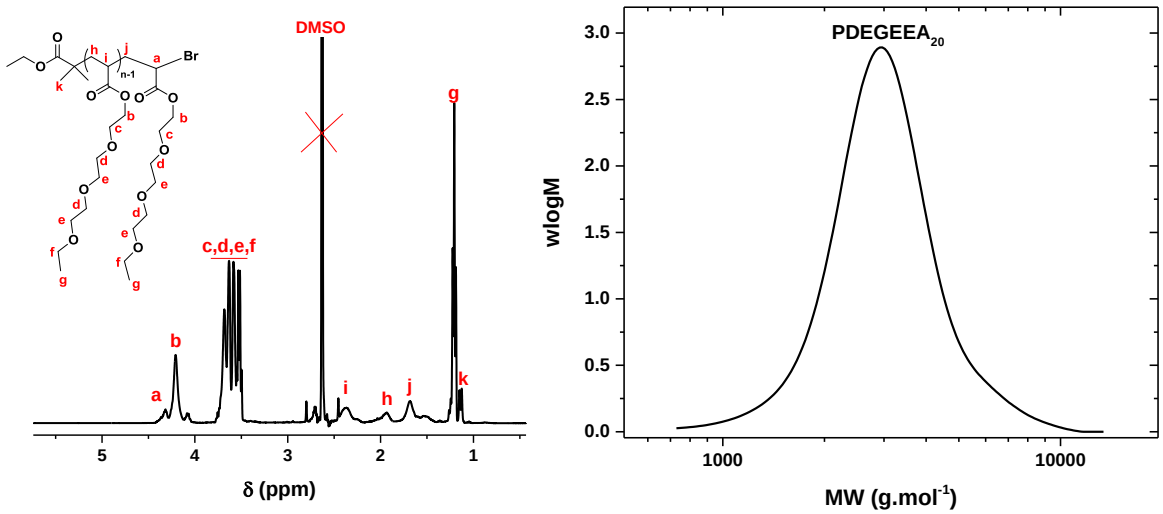

Figure 6.16: ^{1}H NMR (left) and MWD (right) of PDEGEEA synthesised *via* photo-induced polymerisation. Initial conditions [DEGEEA]:[EBiB]:[[Cu(Me_6-Tren)(O_2CH)](ClO_4)] = [50]:[1]:[0.08], DMSO 50% *v/v*.

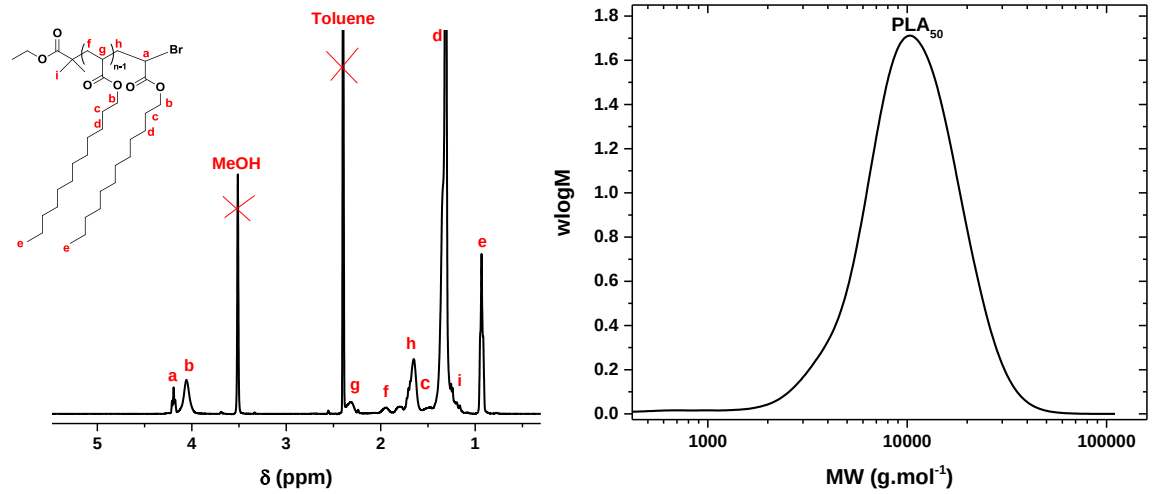

Figure 6.17: ^{1}H NMR (left) and MWD (right) of PLA synthesised *via* photo-induced polymerisation. Initial conditions [LA]:[EBiB]:[[Cu(Me_6-Tren)(O_2CH)](ClO_4)] = [50]:[1]:[0.08], [Toluene]:[MeOH] = [4]:[1] 50% *v/v*.

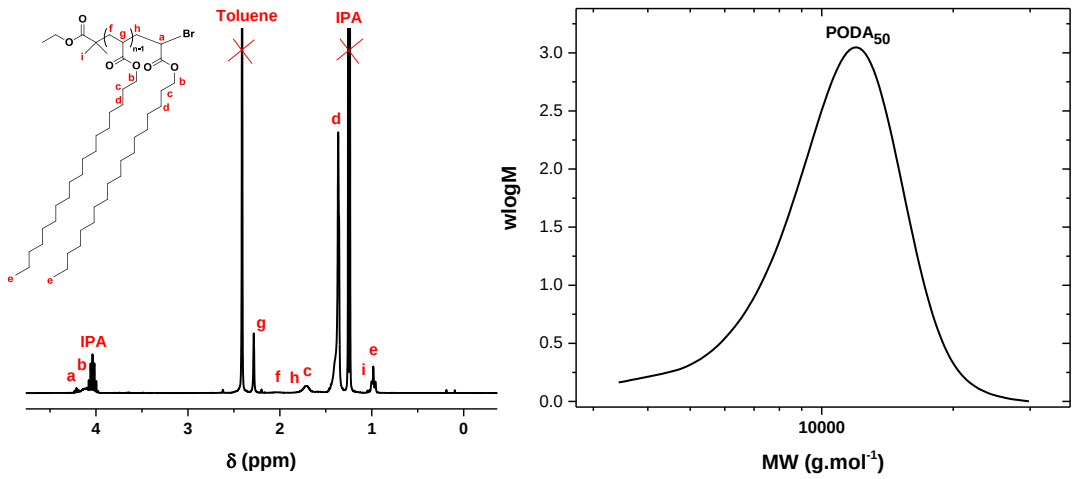

Figure 6.18: ^{1}H NMR (left) and MWD (right) of PODA synthesised *via* photo-induced polymerisation. Initial conditions [ODA]:[EBiB]:[[Cu(Me_6-Tren)(O_2CH)](ClO_4)] = [50]:[1]:[0.08], [Toluene]:[IPA] = [4]:[1] 50% *v/v*.

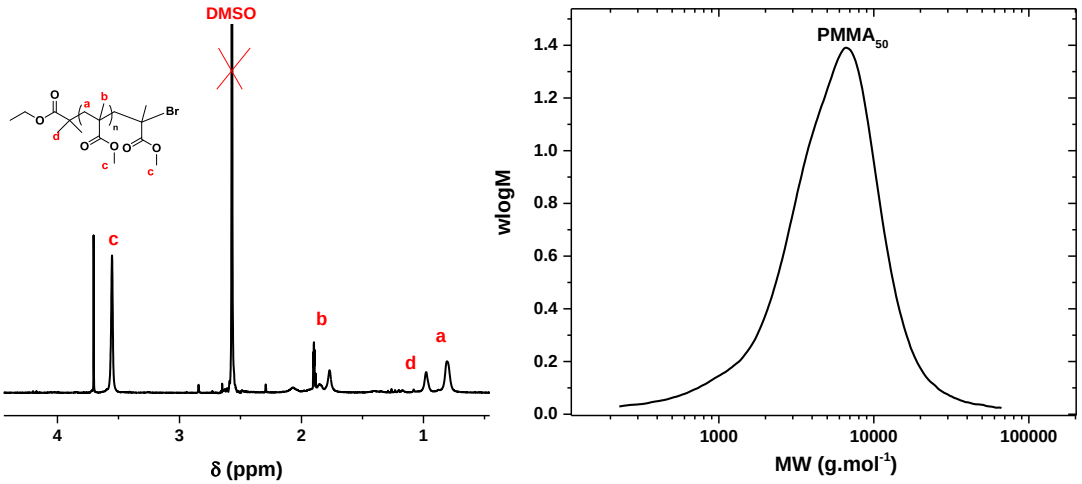

Figure 6.19: ^{1}H NMR (left) and MWD (right) of PMMA synthesised *via* photo-induced polymerisation. Initial conditions [MMA]:[EBiB]:[[Cu(Me_6-Tren)(O_2CH)](ClO_4)] = [50]:[1]:[0.08], DMSO 50% *v/v*.

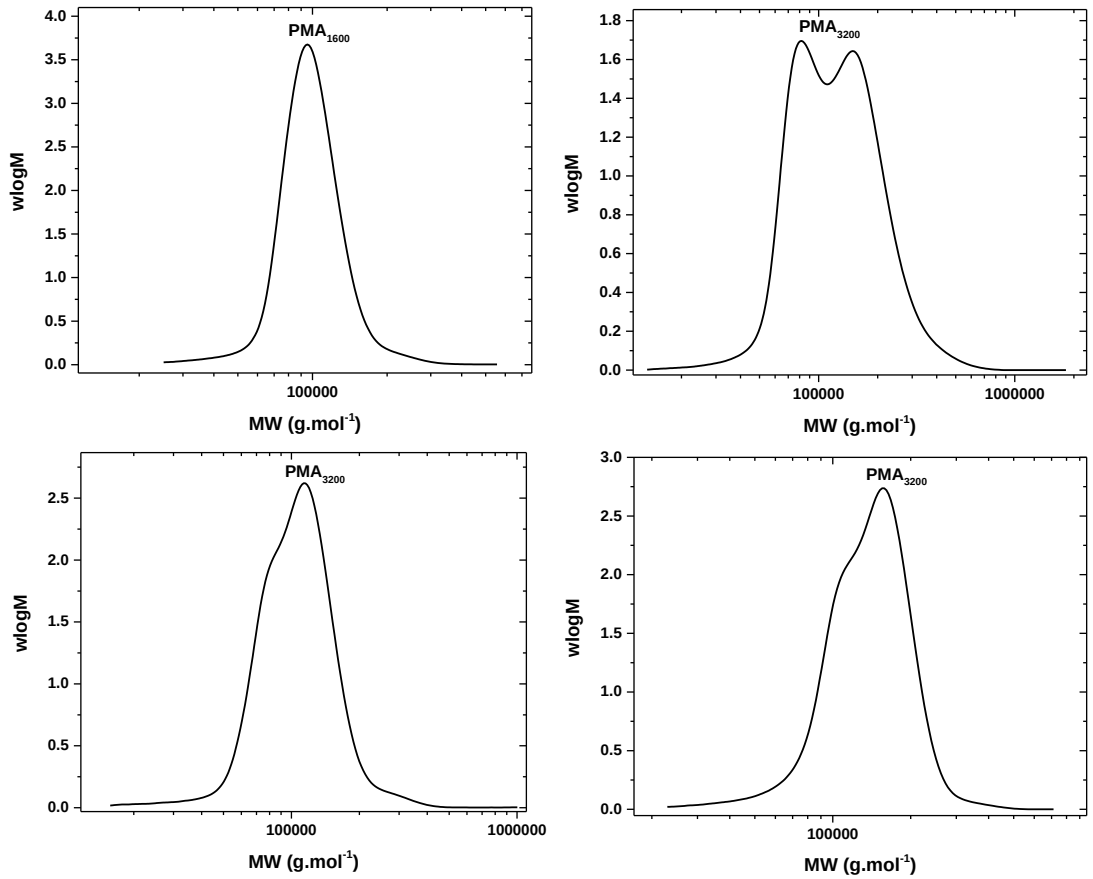

Figure 6.20: MWDs of PMA synthesised *via* photo-induced polymerisation. Initial conditions: [MA]:[EBiB]:[[Cu(Me_6-Tren)(O_2CH)](ClO_4)] = [1600]:[1]:[0.08] (up-left), [MA]:[EBiB]:[[Cu(Me_6-Tren)(O_2CH)](ClO_4)] = [3200]:[1]:[0.16] (up-right), [MA]:[EBiB]:[[Cu(Me_6-Tren)(O_2CH)](ClO_4)] = [3200]:[1]:[0.32] (down-left), [MA]:[EBiB]:[[Cu(Me_6-Tren)(O_2CH)](ClO_4)]:[NaBr] = [3200]:[1]:[0.32]:[0.32] (down-right) in DMSO 50% *v/v*.

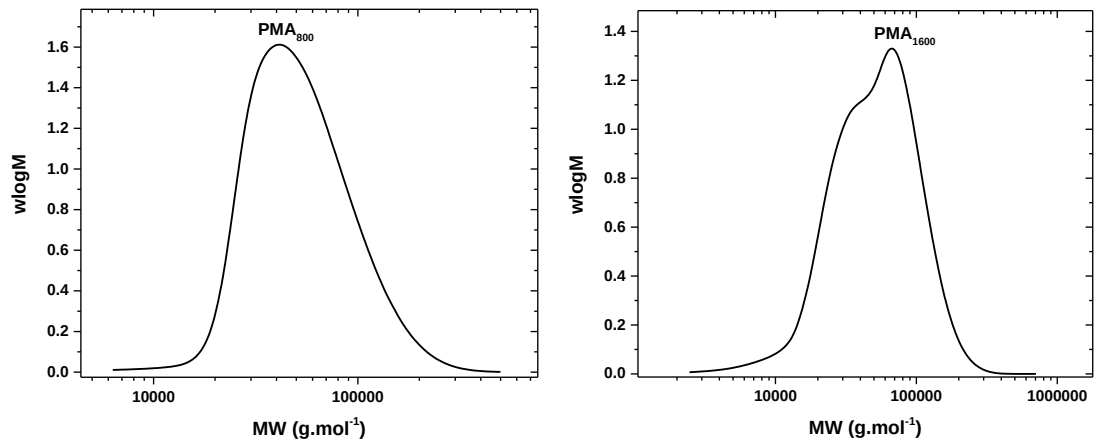

Figure 6.21: MWDs of PMA synthesised *via* photo-induced polymerisation. Initial conditions [MA]:[EBiB]:[[Cu(Me_5-Dien)(O_2CH)](ClO_4)] = [800]:[1]:[0.08] (left),

[MA]:[EBiB]:[[Cu(Me_5-Dien)(O_2CH)](ClO_4)] = [1600]:[1]:[0.16] (right), in DMSO 50% *v/v*.

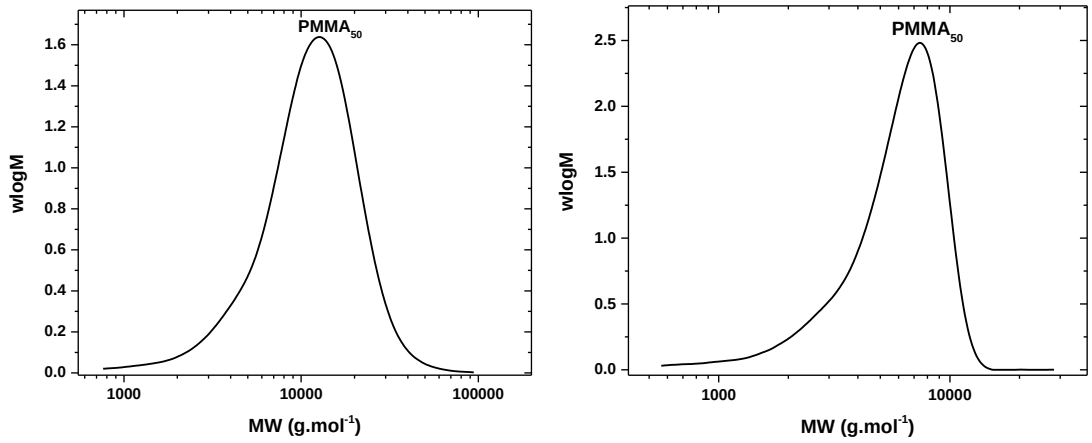

Figure 6.22: MWDs of PMMA synthesised *via* photo-induced polymerisation. Initial conditions: [MMA]:[EBiB]:[[Cu(Me_5-Dien)(O_2CH)](ClO_4)] = [50]:[1]:[0.08] (left), [MMA]:[EBiB]:[[Cu(Me_5-Dien)(O_2CH)](ClO_4)]:[NaBr] = [50]:[1]:[0.08]:[0.08] (right), in DMSO 50% *v/v*.

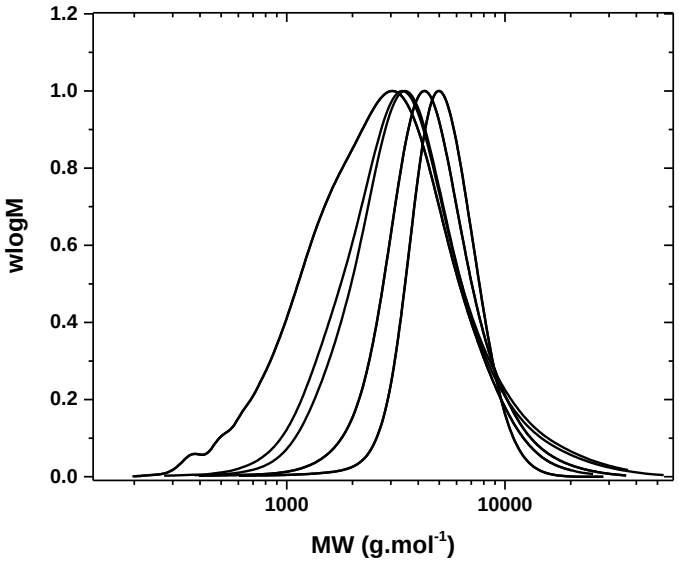

Figure 6.23: MWDs for the concecutive light and dark exposures. Initial conditions: [MA]:[I]:[[Cu(Me_5-Dien)(O_2CH)](ClO_4)] = [50]:[1]:[0.08] in DMSO 50% *v/v*.

6.5 References

1. A. Anastasaki, V. Nikolaou, F. Brandford-Adams, G. Nurumbetov, Q. Zhang, G. J. Clarkson, D. J. Fox, P. Wilson, K. Kempe and D. M. Haddleton, *Chem. Commun.*, 2015, **51**, 5626-5629.

2. S. R. Samanta, M. E. Levere and V. Percec, *Polym. Chem.*, 2013, **4**, 3212-3224.

3. S. R. Samanta, A. Anastasaki, C. Waldron, D. M. Haddleton and V. Percec, *Polym. Chem.*, 2013, **4**, 5555-5562.

4. S. R. Samanta, H.-J. Sun, A. Anastasaki, D. M. Haddleton and V. Percec, *Polym. Chem.*, 2014, **5**, 89-95.

5. S. R. Samanta, A. Anastasaki, C. Waldron, D. M. Haddleton and V. Percec, *Polym. Chem.*, 2013, **4**, 5563-5569.

6. A. Anastasaki, V. Nikolaou, A. Simula, J. Godfrey, M. Li, G. Nurumbetov, P. Wilson and D. M. Haddleton, *Macromolecules*, 2014, **47**, 3852-3859.

7. C. Boyer, A. Atme, C. Waldron, A. Anastasaki, P. Wilson, P. B. Zetterlund, D. Haddleton and M. R. Whittaker, *Polym. Chem.*, 2013, **4**, 106-112.

8. C. Waldron, A. Anastasaki, R. McHale, P. Wilson, Z. Li, T. Smith and D. M. Haddleton, *Polym. Chem.*, 2014, **5**, 892-898.

9. A. Anastasaki, C. Waldron, V. Nikolaou, P. Wilson, R. McHale, T. Smith and D. M. Haddleton, *Polym. Chem.*, 2013, **4**, 4113-4119.

10. M. J. Scott, C. A. Goddard and R. H. Holm, *Inorg. Chem.*, 1996, **35**, 2558-2567.

Chapter 7

Synthesis of well-defined polyelectrolytes and functional double hydrophilic block copolymers *via* Cu(0)-mediated RDRP in aqueous media

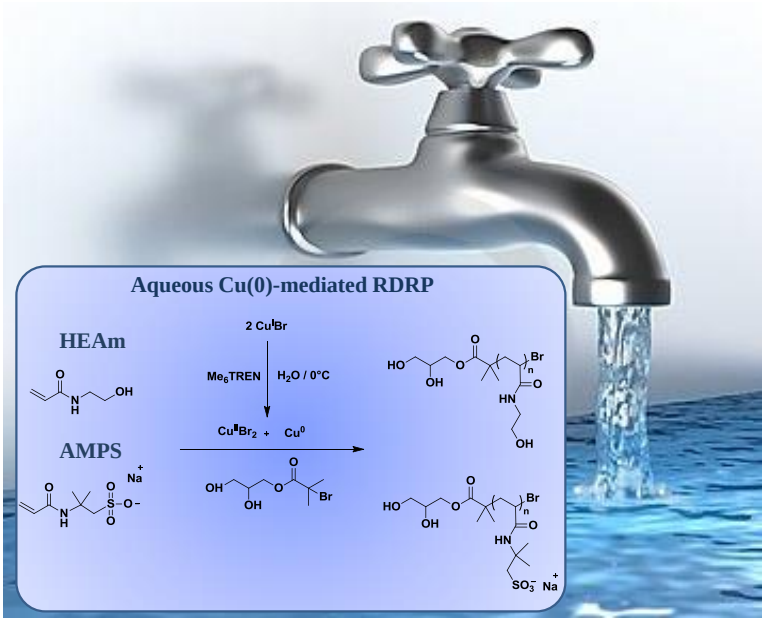

In this chapter, the Cu(0)-mediated RDRP of N-hydroxyethyl acrylamide (HEAm) and 2-acrylamido-2-methylpropane sulfonic acid (AMPS) in aqueous media is reported under a range of reaction conditions. Near-quantitative conversion could be attained in as low as 3 min and a range of chain lengths (DP = 10-640) has been targeted, exhibiting low dispersity values and good agreement between theoretical and experimental values. Remarkably, equally well-defined materials were obtained when DP=1280 was targeted, yielding polymers with high conversions (97%, M_n ~ 180000 g.mol^{-1}) and narrow MWDs (Đ=1.25). The aqueous Cu(0)-mediated RDRP of AMPS was subsequently conducted, resulting in well-defined polymers (Đ ~ 1.16-1.29) in short time scales while first order kinetics confirmed the living nature of the system. Double hydrophilic, thermoresponsive acrylamide and acrylic block copolymers could also be obtained in a quantitative manner within a few minutes, highlighting aqueous Cu(0) mediated RDRP as a robust protocol to obtain functional materials, without the need to purify the macroinitiators or compromise the final dispersity.

7.1 Introduction

In the previous chapter it was noted that the photo-induced polymerisation is problematic under purely aqueous conditions which is in line with previously reported data.[1] In addition acrylamides cannot be polymerised with this polymerisation protocol giving rise to 0% conversion. Therefore an alternative technique needs to be employed for the controlled polymerisation of acrylamides. Acrylamides are very interesting monomers and they find use in a variety of biomedical and industrial applications including tissue engineering, drug delivery, viscosity modifiers, precipitation and flocculation agents for waste water treatment, oil recovery and cosmetics.[2-4] In addition, both ionic and non-ionic water soluble polyacrylamides have attracted considerable interest the last decades due to their extensive applications in hydrogels, adhesives and emulsion coatings.[5-7]

AMPS is a reactive, hydrophilic, sulfonic acid acrylic monomer typically used to modify the chemical properties of a wide range of anionic polymers. Importantly, the presence of the sulfonate group not only enhances the hydrophilicity and acidic character but also dissociates completely over different pH values, indicating that AMPS is a strong electrolyte.[8, 9] Due to its hydrolytic and thermal stability in combination with its high polarity, water solubility and inhibition of divalent cation precipitation, an increasing attention has recently been received around the controlled polymerisation of AMPS.[10-13] RAFT has dominated the work in controlled aqueous polymerisation of AMPS with Sumerlin and co-workers reporting narrow MWDs (~1.20) in a range of targeted molecular weights.[14] In this work, the conversion was relatively moderate (65 - 88%) while the polymerisations required 4-6 h in order to reach their maximum values. ATRP has also been

employed to control the polymerisation of AMPS, low dispersities were achieved only in aqueous/organic mixtures as ATRP of acrylamides in purely aqueous media remains problematic.[15]

N-Hydroxyethyl acrylamide (HEAm) is an interesting hydrophilic acrylamide monomer which contains a primary hydroxyl group that has been used extensively in industrial and biological applications, either directly or after modification post polymerisation.[16-19] Novel materials exhibiting antifouling properties and thermoresponsive behaviour were obtained when block copolymers of HEAm with various monomers were synthesised.[20-23] Hence, the controlled polymerisation of this monomer has also attracted considerable attention with Narumi *et al*. utilising ATRP in ethanol/water mixtures at ambient temperature. Although narrow MWDs were obtained, only relatively low molecular weight polymers were synthesised (highest M_n ~ 12000 g.mol^{-1}), limiting the applications where higher molecular weight polymers are desirable.[24] In addition, conversions remained moderate in all cases (26 - 80%) and *in situ* chain extensions and block (co)polymerisations were not reported.

In 2013 Haddleton and co-workers introduced a facile approach for conducting TMM-RDRP in water (often referred to as aqueous SET-LRP[25-27] or Cu(0)-mediated RDRP).[28] The key step in this approach is the full disproportionation of the CuBr/L in water prior to the addition of a deoxygenated solution of monomer and initiator; it is very important for this to occur prior to monomer addition. The ratio of [ligand] relative to [monomer] is important with effective polymerisation occurring with [L]:[CuBr] = 1. This differentiates the approach from other reported work where (1) disproportionation occurs in the presence of 18% monomer does not go to completion prior to the addition of initiator and subsequent initiator addition

allows for further oxidation of CuBr and (2) a high excess of ligand is used, typically 6:1 with respect to CuBr and computer simulations using ratios as high as 20:1.[29] Excess ligand supresses disproportionation due to being part of the equilibrium, dilution of water with organic solvents/monomers dramatically reduces the equilibrium constant for disproportionation[30] and the monomer can also act as an alternative ligand stabilising CuBr especially as it is present in a large excess relative to the *N*-donor ligand. The fast disproportionation of the CuBr/L complex forming Cu(0) and $CuBr_2$/L deactivating species led to the controlled polymerisation of various hydrophilic monomers, including (meth)acrylates[31-36], (meth)acrylamides[37-41] and glycomonomers reporting low dispersities and high end-group fidelity as evident by *in situ* chain extensions.[28, 42] To further illustrate the versatility of the system and its tolerance towards impurities the polymerisation also proceeded in the presence of phosphonate buffer,[28] blood serum[43] and various alcoholic media[44] resulting in equally well-defined materials.

In this chapter the polymerisation of HEAm and AMPS in aqueous media is exploited utilising aqueous Cu(0)- mediated RDRP.[28]A wide range of molecular weights have been targeted for both monomers and the end-group fidelity was exemplified by *in situ* chain extensions and block copolymerisation, without further purification steps prior to the addition of the second aliquot in both cases. The homopolymerisation of HEAm proceeded in a controlled manner ($Đ$ = 1.12) within 3 minutes at 0^oC as evidenced by kinetic experiments. High molecular weight poly(HEAm) up to 180000 $g.mol^{-1}$ has been synthesised, maintaining narrow MWDs ($Đ$ = 1.25). For the case of AMPS, full monomer conversions (>99%) were obtained in < 30 min at 0^oC while maintaining low dispersities ($Đ$ ~ 1.22) up to M_n ~ 30000 $g.mol^{-1}$. Block copolymerisation of AMPS with both acrylate (PEGA) and

acrylamide monomers (HEAm and NIPAm) has also been realised furnishing well-defined materials as evidenced by nuclear magnetic resonance (NMR), size exclusion chromatography (SEC) and dynamic light scattering (DLS) analyses.

7.2 Results and Discussion

Initially, the homopolymerisation of HEAm was investigated utilising previously optimised conditions targeting a *DP*=10: [HEAm]:[I]:[CuBr]:[Me_6-Tren] = [10]:[1]:[0.4]:[0.4].[28, 37] CuBr was added directly to a deoxygenated aqueous solution of Me_6-Tren in water and was allowed to disproportionate for 15 min prior to polymerisation to ensure the rapid and quantitative formation of Cu(0) and the [$CuBr_2$/Me_6-Tren] complex. A deoxygenated solution of monomer and initiator in water was prepared separately at the same time. Polymerisation commenced upon addition of the aforementioned mixture to the deoxygenated catalyst solution at 0^{o}C. ^{1}H NMR analysis of the resulting polymer confirmed full monomer conversion in less than 3 min and SEC analysis revealed a mono-modal peak distribution with narrow MWDs ($Đ$ = 1.16) highlighting the controlled nature of the system (Figure 7.1, Table 7.1).

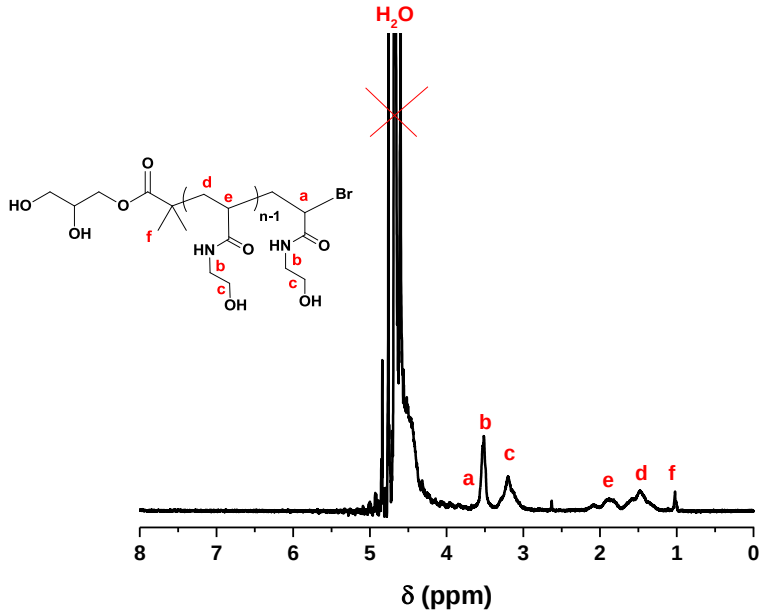

Figure 7.1: ^{1}H NMR spectrum of poly(HEAm)$_{20}$ utilising aqueous Cu(0)-mediated RDRP. Initial conditions: [HEAm]:[I]:[CuBr]:[Me$_6$-Tren] = [20]:[1]:[0.4]:[0.4] in 4 mL H_2O at 0^{o}C.

The first order kinetic plot showed $\ln[M]_0/[M]_t$ increasing linearly with time showing a constant radical concentration and the rate of polymerisation to be first order in monomer concentration (Figure 7.2). Pleasingly, near-quantitative conversion (>99%) could be attained in < 3 min, demonstrating the speed of the polymerisation without compromising the control over the MWDs which remained as narrow as 1.15 (Section 7.4.4, Figure 7.10). It should be noted that the data points used for the kinetic plots are derived from 2 identical experiments at different time points. Initially, regular sampling was attempted in one batch, however, cessation of the polymerisation was observed after the first four samples had been taken. It was hypothesised that multiple samples could perhaps disturb the polymerisation equilibrium as due to the heterogeneous nature of the system leading to random amounts of Cu(0) being removed from the reaction upon each sampling. Indeed,

reducing the number of samples to 3 per reaction, gave rise to consistent results and the polymerisation reached full monomer conversion.

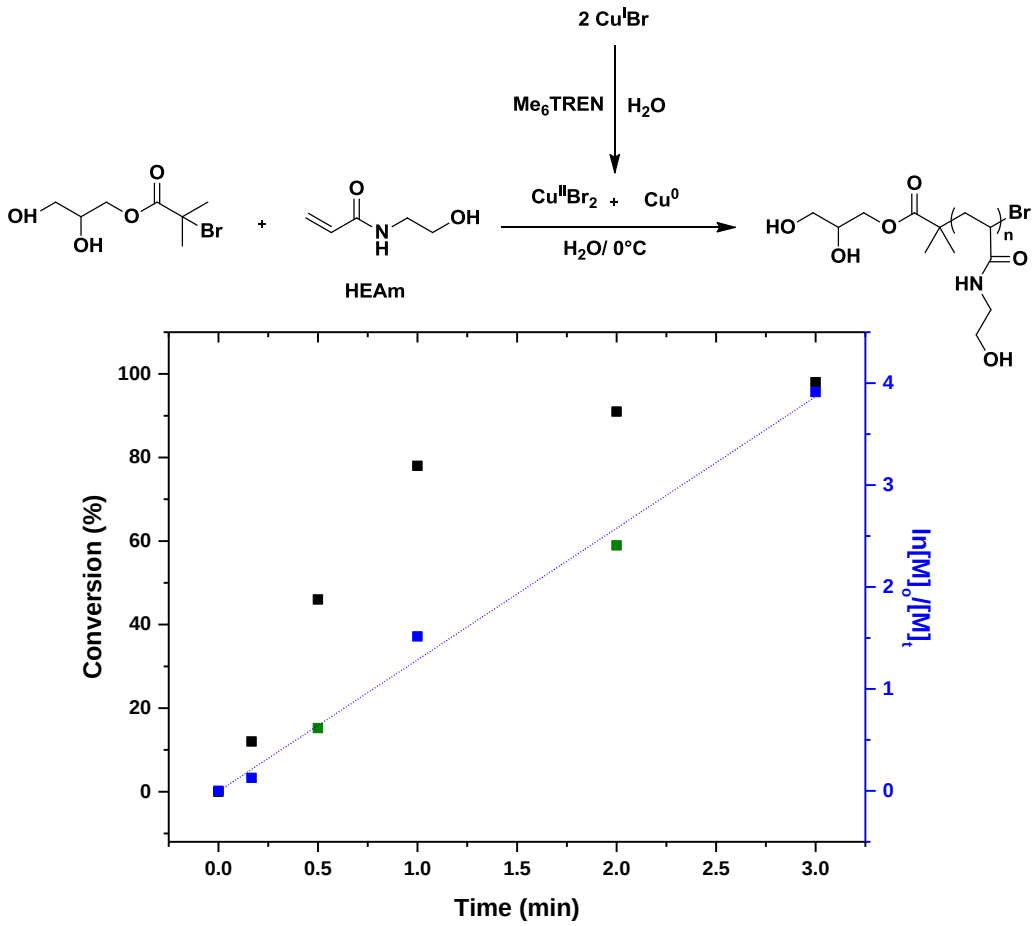

Figure 7.2: Kinetic data for the aqueous Cu(0)-mediated RDRP of HEAm (blue and green data points represent samples from two identical batches).

Subsequently, the same ratio ([CuBr]:[Me_6-Tren] = [1]:[1]) was used to target higher degrees of polymerisation poly(HEAm), (*DP* = 20 & 40), resulting in equally well-defined polymers (99%, *Đ* ~ 1.17 and 100%, *Đ* ~ 1.18 respectively) within minutes (Figure 7.3, Table 7.1). Conversely, when *DP*=80 was targeted, a higher dispersity was observed (*Đ* > 1.37) for the final product, suggesting inefficient deactivation throughout the polymerisation (Figure 7.4a, Table 7.1).

Previous literature studies have reported that the ideal catalyst loading relies upon the targeted *DP* and by carefully tuning the [CuBr]:[Me_6-Tren] ratio, both an acceptable reaction time and control can be attained. Therefore, the ratio was initially modified to [I]:[CuBr]:[Me_6-Tren] = [1]:[0.8]:[0.4], assuming that a higher concentration of CuBr would provide a higher amount of [Cu(Me_6-Tren)Br_2] during disproportionation, which would control the deactivation step more efficiently. Although, as expected, the dispersity value was significantly improved ($Đ$ = 1.17 *vs.* $Đ$ = 1.35), a decrease in the polymerisation rate was also observed with a maximum conversion of 90% achieved, even when the polymerisation was left to proceed overnight (Figure 7.4b, Table 7.1). However, full monomer conversion is a requirement for the *in situ* chain extensions and block copolymerisations. Therefore, a higher concentration of ligand was employed relative to CuBr ([I]:[CuBr]:[Me_6-Tren] = [1]:[0.8]:[0.6]) resulting in 99% conversion in 15 min, with M_n = 18600 g.mol^{-1} while the low dispersity was maintained ($Đ$ = 1.16) (Figure 7.3, Table 7.1).

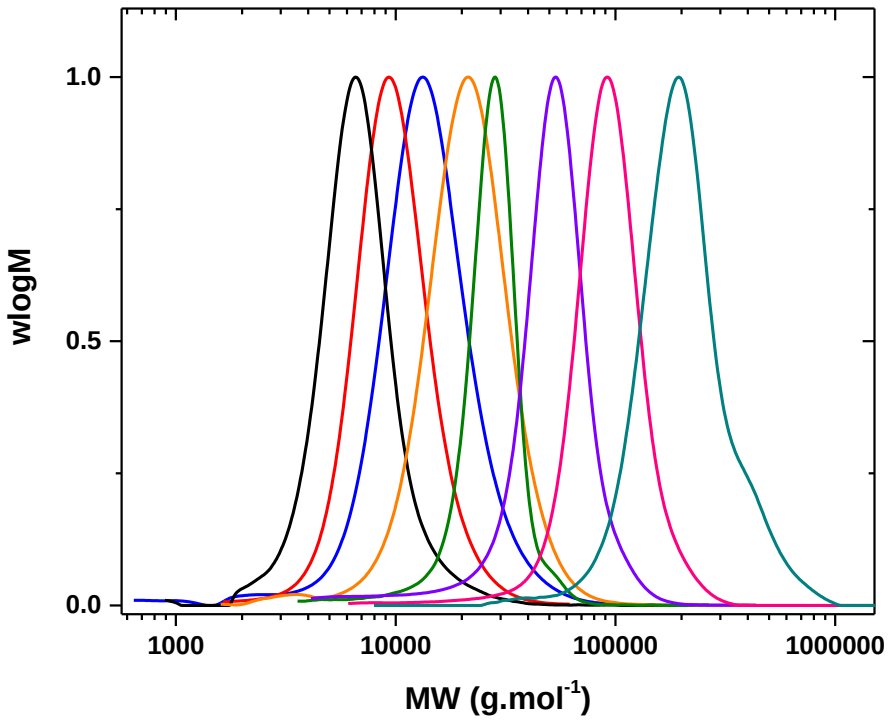

Figure 7.3: SEC analysis of poly(HEAm) of various *DP* = (10-1280) prepared by Cu(0)-mediated RDRP in pure water.

Similar issues were confronted during the polymerisation of poly(HEAm)$_{160}$. When the previously optimised conditions were employed, the polymerisation proceeded in a relatively uncontrolled manner (98%, M_n = 26000 g.mol^{-1}, $Đ$ = 1.30) (Figure 7.4c, Table 7.1). Further optimisation of the catalytic ratio ([I]:[CuBr]:[Me$_6$-Tren] = [1]:[1.6]:[1]) gave rise to poly(HEAm) with the desired high conversion (>99%) and narrow MWDs (~ 1.09) (Figure 7.3, Table 7.1). Identical conditions were subsequently applied for even higher degrees of polymerisation (*DP* = 320 & 640). Pleasingly, near-quantitative conversions (~ 98%) and narrow MWDs (~ 1.15) were obtained in both cases within 15 min, demonstrating the robustness of the system to obtain well-defined high molecular weight polymers (M_n~ 90000 g.mol^{-1}) in short time scales (Figure 7.3, Table 7.1).

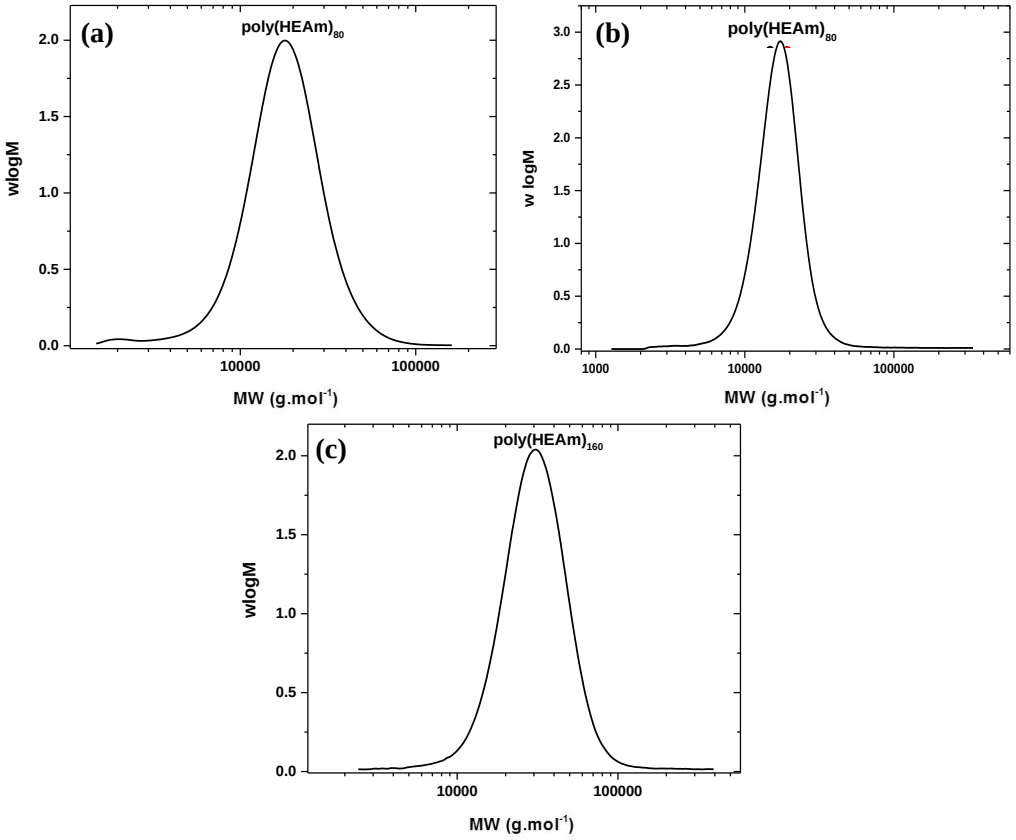

Figure 7.4: SEC analysis for the synthesis of poly(HEAm)$_{80}$ and poly(HEAm)$_{160}$ utilising aqueous Cu(0)-mediated RDRP. Initial conditions: (a) [HEAm]:[I]:[CuBr]:[Me$_6$-Tren] = [80]:[1]:[0.4]:[0.4] in 4 mL H_2O at 0^{o}C, (b) [HEAm]:[I]:[CuBr]:[Me$_6$-Tren] = [80]:[1]:[0.8]:[0.4] in 4 mL H_2O at 0^{o}C and (c) [HEAm]:[I]:[CuBr]:[Me$_6$-Tren] = [160]:[1]:[0.8]:[0.6] in 4 mL H_2O at 0^{o}C.

In order to further probe the potential of the technique in maintaining control for even higher molecular weights, *DP* = 1280 was also attempted. Utilising the previously optimised conditions for *DP* = 320 and 640, a gel was evident within 2 min, which could not be further analysed *via* either SEC or NMR due to insolubility. This gel formation indicates poor control over the MWDs and high dispersities, suggesting for once more inefficient deactivation. Hence, a higher catalyst ratio ([I]:[CuBr]:[Me$_6$-Tren] = [1]:[2]:[1.2]) was employed resulting in a well-controlled polymerisation, even at near-quantitative monomer conversion (~ 97%) with a final

M_n = 180000 g.mol^{-1} and a dispersity equal to 1.25 (Figure 7.3, Table 7.1). However, it should be noted that for such high molecular weight polymer, longer reaction times were required (12 h to reach 97% and 2 h to reach 70%) and SEC analysis revealed a tailing in high molecular weight, most likely due to termination events. Further attempts to diminish or reduce this shoulder proved unsuccessful and resulted in loss of control and/or gel formation revealing the limitation of this system (data not shown).

Table 7.1: Synthesis of poly(HEAm) with various *DP via* aqueous Cu(0)-mediated RDRP.

DP	**Ratio [I]:[Cu]:[L]**	**Time (min)**	**Conversion (%)**	$M_{n,SEC}$ **(g.mol^{-1})**	***Đ***
10	[1]:[0.4]:[0.4]	3	99	4600	1.16
20	[1]:[0.4]:[0.4]	15	99	8700	1.17
40	[1]:[0.4]:[0.4]	15	100	12000	1.18
80	[1]:[0.4]:[0.4]	15	100	14700	1.37
80	[1]:[0.8]:[0.4]	15	90	15200	1.17
80	[1]:[0.8]:[0.6]	15	99	18600	1.16
160	[1]:[0.8]:[0.6]	15	98	26000	1.30
160	[1]:[1.6]:[1]	15	100	26000	1.09
320	[1]:[1.6]:[1]	15	98	48000	1.15
640	[1]:[1.6]:[1]	30	98	89000	1.14
1280	[1]:[1.6]:[1]	2	-	GEL	-
1280	[1]:[2]:[1.2]	12 h	97	180000	1.25

Previous reports highlighted the difficulty to maintain the high end-group fidelity under purely aqueous conditions due to hydrolysis of the terminal bromide.[39] Thus, in order to assess the livingness of the resultant polymers *in situ* chain extension was attempted. When full monomer conversion was obtained for the poly(HEAm)$_{10}$ homopolymer (after 3 min, 100% conversion, M_n = 4500 g.mol^{-1}, *Đ*=1.08), a second aliquot of HEAm was added and full conversion was attained in

30 min (100% conversion, M_n = 7200 g.mol^{-1}, $Đ$=1.09) without the need for any purification steps prior to the second monomer addition. SEC analysis revealed a shift to higher molecular weights and the absence of any visible tailing at high or low molecular weights, demonstrating high end-group functionality (Figure 7.5). This high end-group fidelity was further exemplified by the synthesis of double hydrophilic diblock copolymers. Among stimuli responsive polymers, thermo-responsive are the most widely applied with poly(NIPAm) being the most common representative as it shows a sharp phase transition at approximately 32^{o}C in aqueous solution. Hence, NIPAm was employed as the second monomer for the synthesis of block copolymers furnishing poly(HEAm)$_{80}$-*b*-poly(NIPAm)$_{40}$. ^{1}H NMR confirmed that near-quantitative conversions (>99%) were attained within each block and SEC analysis revealed a clear MW shift maintaining a narrow MWD ($Đ$ ~ 1.18) (Figure 7.5). Cloud point measurements for the resultant block copolymer were also carried out, however no cloud point temperature (T_{cp}) could be observed. This is most likely due to the hydrophilic nature of HEAm that increases the T_{cp} of the diblock beyond 90 ^{o}C and our detection limits.[36]

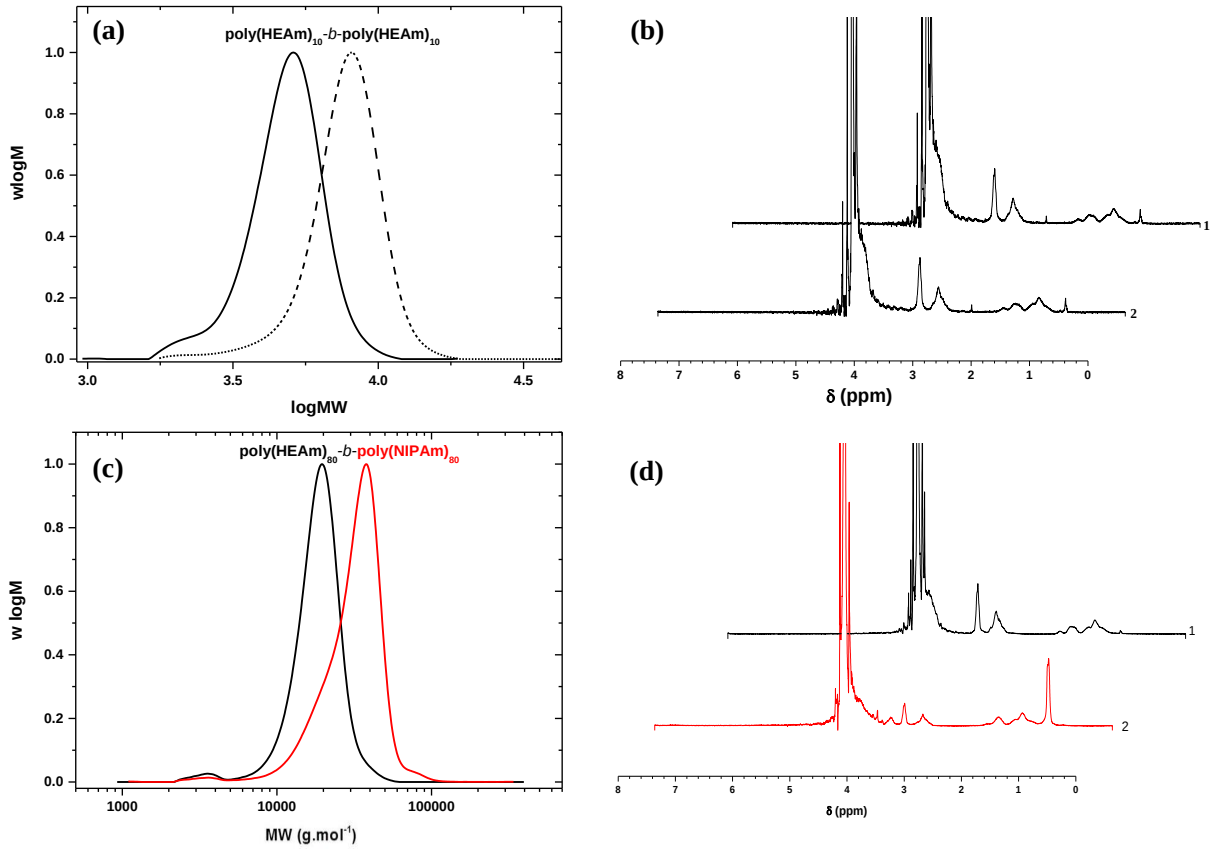

Figure 7.5: SEC and ^{1}H NMR analysis for the *in situ* (a), (b) chain extension and (c), (b) block copolymerisation from a poly(HEAm)$_{10}$ macroinitiator utilising aqueous Cu(0)-mediated RDRP. Initial conditions for the *in situ* chain extension: [HEAm]:[I]:[CuBr]:[Me$_6$-Tren] = [10]:[1]:[0.4]:[0.4]. Chain extension achieved upon addition of an aliquot of HEAm (10 equiv.) in H_2O (2 mL). Initial conditions for the in situ block copolymerisation [HEAm]:[I]:[CuBr]:[Me$_6$-Tren] = [80]:[1]:[0.8]:[0.6]. Chain extension achieved upon addition of an aliquot of HEAm (80 equiv.) in H_2O (2 mL).

In a similar vein with HEAm, the polymerisation of AMPS was also performed by aqueous Cu(0)-mediated RDRP. The sodium form of AMPS (sodium salt solution 50 wt. % in H_2O) was utilised to avoid problems of low pH protonation of the ligand and potential catalyst deactivation. The successful synthesis of poly(AMPS)$_{20}$ was confirmed by both NMR and SEC analyses when previously optimised conditions were employed ([AMPS]:[I]:[CuBr]:[Me$_6$-Tren] = [20]:[1]:[0.4]:[0.4]). ^{1}H NMR confirmed full monomer conversion in 30 min as

indicated by the disappearance of the vinyl signals between 5.5 and 6.5 ppm and aqueous SEC characterisation showed a symmetrical, mono-modal MWD ($Đ$ ~ 1.16) for the obtained polymer (Figure 7.6, Table 7.2). Kinetic analysis revealed a linear increase of $\ln([M]_0/[M]_t)$ *vs* time further supporting the living nature of the system (Figure 7.7). It should be noted that longer reaction times were required for the polymerisation of AMPS in comparison with HEAm. Likewise, an equally well-defined polymer (100%, M_n = 23500 g.mol^{-1}, $Đ$ = 1.20) was prepared when DP = 40 was targeted under similar conditions to DP = 20 ([CuBr]:[Me_6-Tren] = [1]:[1]) (Figure 7.8, Table 7.2).

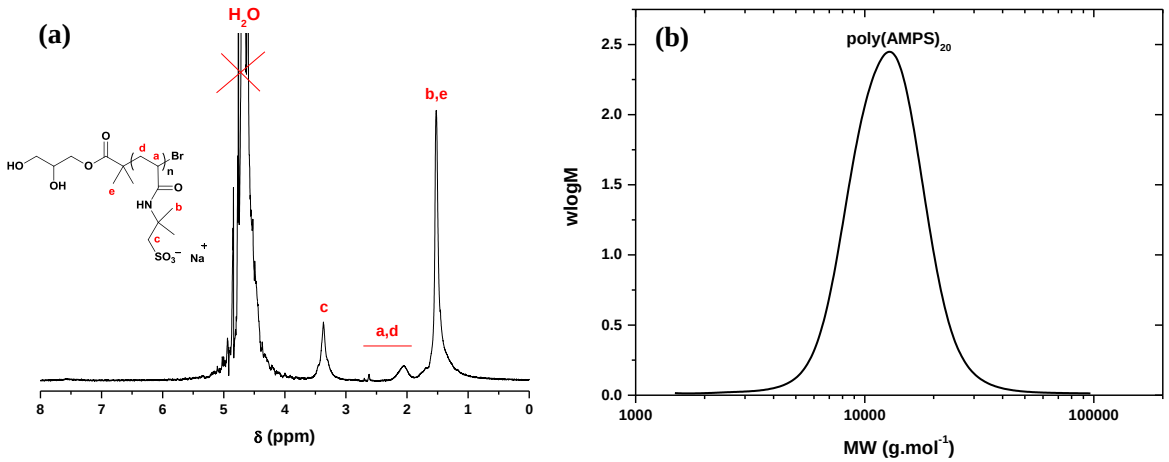

Figure 7.6: ^{1}H NMR and SEC analysis of poly(AMPS)$_{20}$ utilising aqueous Cu(0)-mediated RDRP. Initial conditions: [AMPS]:[I]:[CuBr]:[Me_6-Tren] = [20]:[1]:[0.4]:[0.4] in 4 mL H_2O at 0^{o}C.

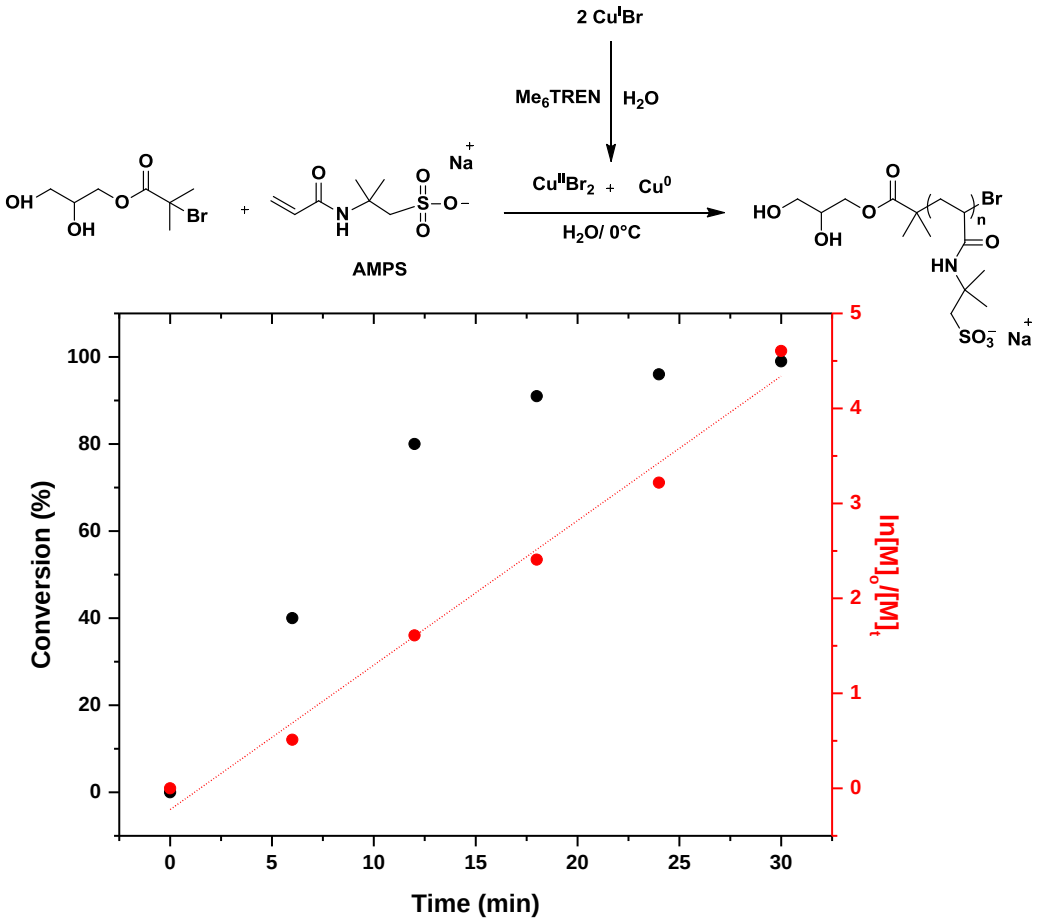

Figure 7.7: Kinetic data for the aqueous Cu(0)-mediated RDRP of AMPS.

Previously reported literature indicates slow polymerisation rates and limited conversions when higher molecular weight poly(AMPS) were synthesised in purely aqueous solutions. Encouraged by our initial findings for HEAm, higher molecular weight poly(AMPS) was subsequently targeted as an attempt to explore the limitations of the system for this monomer. The synthesis of polymer with a targeted *DP* = 80 was initially assessed by employing a previously optimised catalyst ratio, [CuBr]:[Me_6-Tren] = [2]:[1]. The polymerisation reached high conversion (>99%) in 30 min, having a final dispersity of ~ 1.30 was obtained, demonstrating the controlled polymerisation of this monomer up to M_n ~ 30000 g.mol^{-1} (Figure 7.8, Table 7.2). However, the polymerisation with *DP*=160 proved problematic under

these conditions, furnishing polymers with broad MWDs ($Đ$ > 2.00). Further attempts to rectify these issues proved fruitless even when the catalytic ratio was increased to [I]:[CuBr]:[Me_6-Tren] = [1]:[1.6]:[1] resulting in materials with high dispersities (M_n = 42000 g.mol^{-1}, $Đ$ = 1.70) (Figures 7.8, Table 7.2).

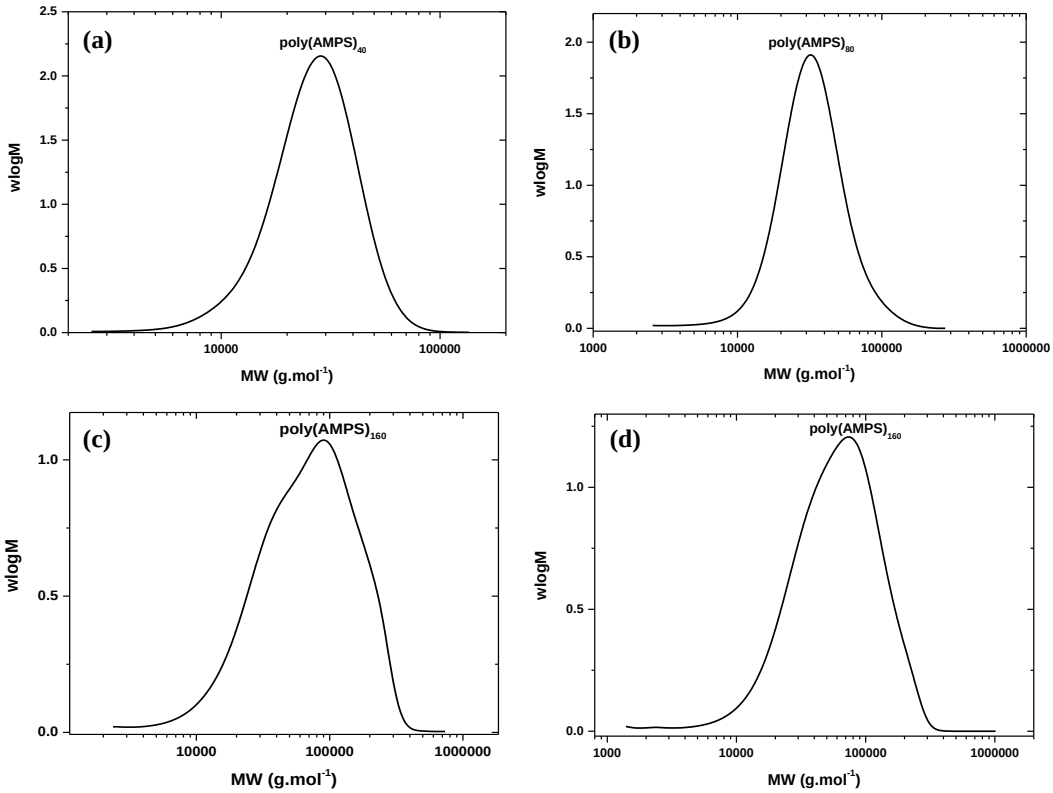

Figure 7.8: SEC analysis for the synthesis of poly(AMPS) utilising aqueous Cu(0)-mediated RDRP. Initial conditions: (a) [AMPS]:[I]:[CuBr]:[Me_6-Tren] = [40]:[1]:[0.4]:[0.4], (b) [AMPS]:[I]:[CuBr]:[Me_6-Tren] = [80]:[1]:[0.8]:[0.4], (c) [AMPS]:[I]:[CuBr]:[Me_6-Tren] = [160]:[1]:[0.8]:[0.4] and (d) [AMPS]:[I]:[CuBr]:[Me_6-Tren] = [160]:[1]:[1.6]:[1] in 4 mL H_2O at 0^{o}C.

Table 7.2: Synthesis of poly(AMPS) with various *DP via* aqueous Cu(0)-mediated RDRP.

DP	Ratio [I]:[Cu]:[L]	Time (min)	Conversion (%)	$M_{n,SEC}$ (g.mol^{-1})	*Đ*
20	[1]:[0.4]:[0.4]	30	100	11500	1.16
40	[1]:[0.4]:[0.4]	30	100	23500	1.20
80	[1]:[0.8]:[0.4]	30	100	29700	1.30
160	[1]:[0.8]:[0.4]	30	100	43000	2.00
160	[1]:[1.6]:[1]	30	100	42000	1.70

Sequential monomer additions to block copolymers were also carried out. The synthesis of poly(AMPS)$_{20}$-*b*-poly(AMPS)$_{20}$ was successful within 30 min after the addition of a second aliquot of AMPS without the need to purify the macroinitiator. SEC analysis revealed a clear shift in higher molecular weight retaining the initial low dispersity (>99%, *Đ* = 1.20) and highlighting the high end-group fidelity of the polymer at this molecular weight (Table 7.3, Figure 7.9a, Section 7.4.4, Figure 7.11). Well-defined block copolymers of AMPS with both acrylamides (HEAm and NIPAm) and acrylate monomers (PPEGA) were also synthesised. ^{1}H NMR revealed quantitative conversions (>99%) within an hour with the MWDs to remain narrow (*Đ* ~ 1.20) in all cases (Table 7.3, Figure 7.9b & c, Section 7.4.4, Figures 7.12 & 7.13). Finally, NIPAm was also utilised as the second monomer for the synthesis of poly(AMPS)$_{20}$-*b*-poly(NIPAm)$_{20}$. Under these reaction conditions, poly(AMPS) was obtained at full conversion within 30 min with a dispersity of 1.17 (Table 7.3, Section 7.4.4, Figure 7.14 & 7.15). However, the SEC analysis of the final polymer was not possible due to insolubility of the diblock copolymer in either DMF or aqueous eluents (instrument performs above 30^{o}C). DLS was employed for further characterisation of the diblock, showing one single particle distribution with low dispersities (Table 7.3, Section 7.4.4, Figure 7.16).

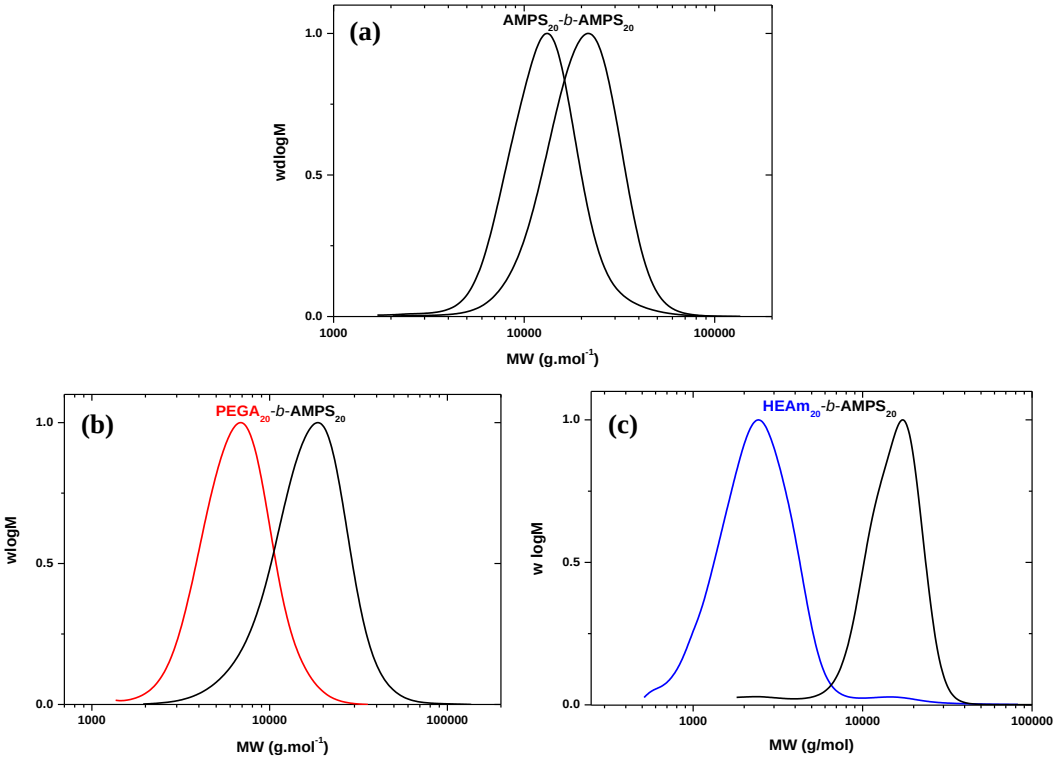

Figure 7.9: (a) *In situ* chain extension and (b), (c) block copolymerisations of AMPS with a variety of acrylic monomers *via* Cu(0)-mediated RDRP. Initial conditions: [M]:[I]:[CuBr]:[Me_6-Tren] = [20]:[1]:[0.4]:[0.4]. Chain extension achieved upon addition of an aliquot of the second (20 equiv.) in H_2O (2 mL).

Table 7.3: Synthesis of block copolymers containing AMPS.

	Cycle	Time (min)	Conversion (%)	$M_{n,SEC}$ (g.mol^{-1})	$Đ$
In situ **Chain Extension**	**AMPS**	30	> 99	11600	1.21
	AMPS	30	> 99	18000	1.21
Block (Co)polymerisations	**PEGA**	30	100	5800	1.24
	AMPS	30	100	14100	1.30
	HEAm	30	100	2500	1.29
	AMPS	30	100	14000	1.15
	AMPS	30	100	11000	1.17
	NIPAm	30	100	-	0.077*

* Obtained by DLS in DMF/H_2O (90% *v/v*) at 25°C.

7.3 Conclusions

In summary, utilising aqueous Cu(0)-mediated RDRP and the pre-disproportionation of CuBr in water allows for the synthesis of well-defined poly(AMPS) and poly(HEAm) with relatively high molecular weights and very low dispersities. Under optimised conditions, narrow MWDs could be obtained within a few minutes at ambient temperatures with a range of targeted molecular weights, including the synthesis of high molecular weight poly(HEAm) up to M_n ~ 180000 g.mol^{-1}. Kinetic studies in both cases confirmed the living nature of the polymerisations and verified full monomer conversion in a matter of minutes. High end-group fidelity was exemplified by *in situ* chain extensions and block (co)polymers *via* sequential monomer addition with both acrylamide and acrylate monomers, yielding well-defined hydrophilic materials without compromising the final dispersities.

7.4 Experimental

7.4.1 Materials and Methods

All chemicals were purchased from Sigma-Aldrich or Fischer Scientific unless otherwise stated. The water soluble initiator (I) 2, 3-dihydroxypropyl 2-bromo-2-methylpropanoate (WSI) was prepared as reported in the literature.[45] Me_6-Tren was synthesised according to literature procedures and stored under nitrogen prior to use.[46] CuBr, was sequentially washed with acetic acid and ethanol and dried under vacuum. Copper wire (diameter = 0.25 mm) was pre-treated by washing in hydrochloric acid or hydrazine for 30 min and rinsed thoroughly with MiliQ water, dried under nitrogen and used immediately.

7.4.2 Instrumentation

^{1}H NMR spectra were recorded on Bruker DPX-300 and DPX-400 spectrometers using deuterated solvents obtained from Sigma-Aldrich. Size-exclusion chromatography (SEC) was conducted on Varian 390-LC system using DMF as the mobile phase (5 mM NH_4BF_4) at 50 ˚C, equipped with refractive index, UV and viscometry detectors, 2 × PLgel 5 mm mixed-D columns (300 × 7.5 mm), 1 × PLgel 5 mm guard column (50 × 7.5 mm) and autosampler. Commercial narrow linear poly (methyl methacrylate) standards in range of 200 to 1.0 × 10^6 g.mol^{-1} were used to calibrate this system. All samples were passed through 0.45 μm PTFE filter before analysis. Aqueous SEC traces were obtained on a PL-GPC50 system using a buffer (0.1M $NaNO_3$, pH 7.4) eluent at 30°C, equipped with a refractive index detector, two PLaquagel-OH 30 (300 × 7.5 mm), PLaquagel guard (50 × 7.5 mm) and autosampler. Narrow linear poly(ethylene oxide) standards in range of 200 to 1.3 × 10^5 g.mol^{-1} were used to calibrate the system. All samples were passed through 0.22μm PTFE filter before analysis. Dynamic light scattering (DLS) experiments were carried out at 25°C on a MALVERN Zetasizer instrument (backscattering angle 173°C) using a quartz cuvette with 1 cm path length.

7.4.3 General procedures

To a Schlenk tube fitted with a magnetic stirring bar and a rubber septum, H_2O (2 mL) and Me_6-Tren (0.4 equiv.) were added and the mixture was bubbled with nitrogen for 15 min. CuBr (0.4 equiv.) was then carefully added under slight positive pressure of nitrogen to protect the *in situ* generated Cu(0) powder from possible side oxidation reaction. The mixture immediately became blue ([Cu(Me_6-

Tren)]Br_2) and a precipitate (Cu(0)) was observed. A separate vial fitted with a rubber septum and magnetic stirring bar was charged with WSI (60 mg), monomer (*DP* equiv.) and H_2O (2 mL). The mixture was left to stir until complete dissolution of the monomer and was deoxygenated with nitrogen for 10 minutes. The solution was then cannulated into the Schlenk tube and the reaction was left to proceed at 0°C.

For the *in situ* chain extensions/ block copolymerisations, an aliquot of a deoxygenated monomer solution (*DP*, equiv.), in H_2O (2 mL) was added *via* a nitrogen-purged syringe and again the solution was allowed to polymerise at 0°C.

7.4.4 Additional Characterisation

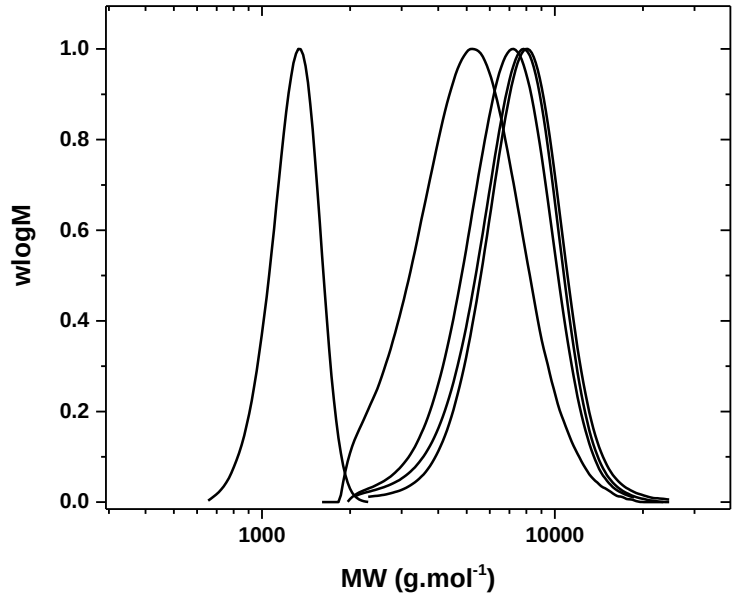

Figure 7.10: SEC analysis showing the molecular weight evolution during the kinetic experiment of the aqueous Cu(0)-mediated RDRP of HEAm.

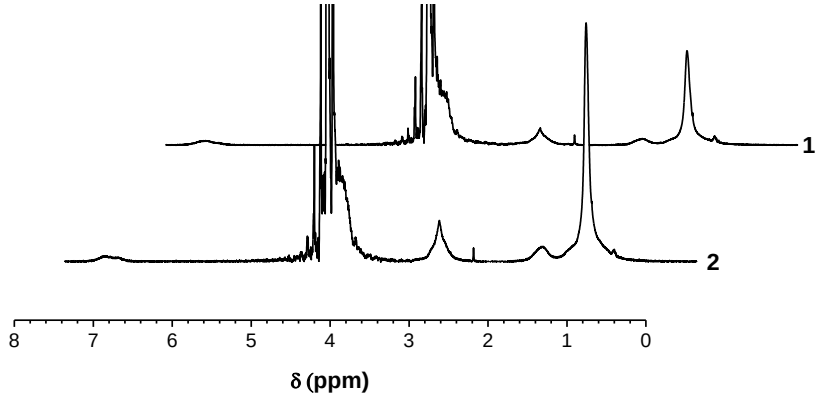

Figure 7.11: ^{1}H NMR analysis for the *in situ* chain extension from a poly(AMPS)$_{20}$ macroinitiator utilising aqueous Cu(0)-mediated RDRP. Initial conditions: [AMPS]:[I]:[CuBr]:[Me$_6$-Tren] = [20]:[1]:[0.4]:[0.4]. Chain extension achieved upon addition of an aliquot of AMPS (20 equiv.) in H_2O (2 mL).

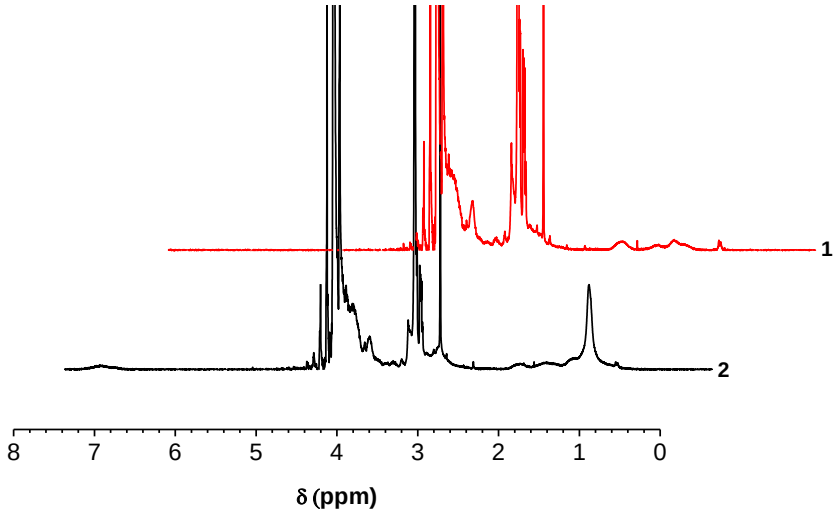

Figure 7.12: ^{1}H NMR analysis for the *in situ* chain extension from a PPEGA$_{20}$ macroinitiator utilising aqueous Cu(0)-mediated RDRP. Initial conditions: [PEGA]:[I]:[CuBr]:[Me$_6$-Tren] = [20]:[1]:[0.4]:[0.4]. Chain extension achieved upon addition of an aliquot of AMPS (20 equiv.) in H_2O (2 mL).

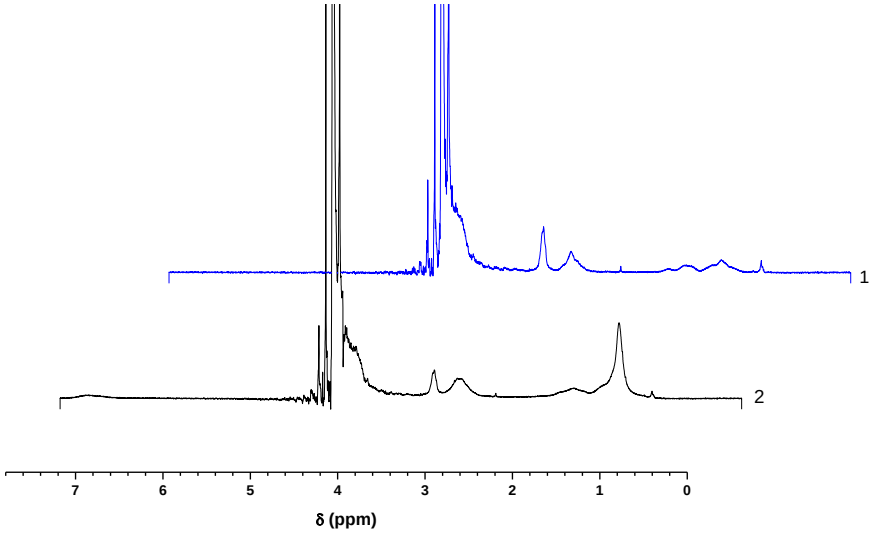

Figure 7.13: ^{1}H NMR analysis for the *in situ* chain extension from a poly(HEAm)$_{20}$ macroinitiator utilising aqueous Cu(0)-mediated RDRP. Initial conditions: [HEAm]:[I]:[CuBr]:[Me$_6$-Tren] = [20]:[1]:[0.4]:[0.4]. Chain extension achieved upon addition of an aliquot of AMPS (20 equiv.) in H_2O (2 mL).

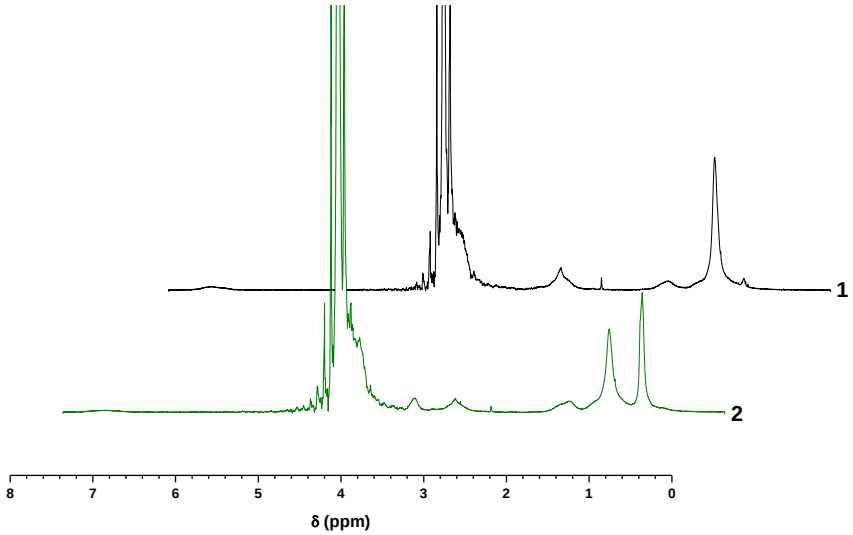

Figure 7.14: ^{1}H NMR analysis for the *in situ* block copolymerisation from a poly(AMPS)$_{20}$ macroinitiator utilising aqueous Cu(0)-mediated RDRP. Initial conditions: [AMPS]:[I]:[CuBr]:[Me$_6$-Tren] = [20]:[1]:[0.4]:[0.4]. Chain extension achieved upon addition of an aliquot of NIPAm (20 equiv.) in H_2O (2 mL).

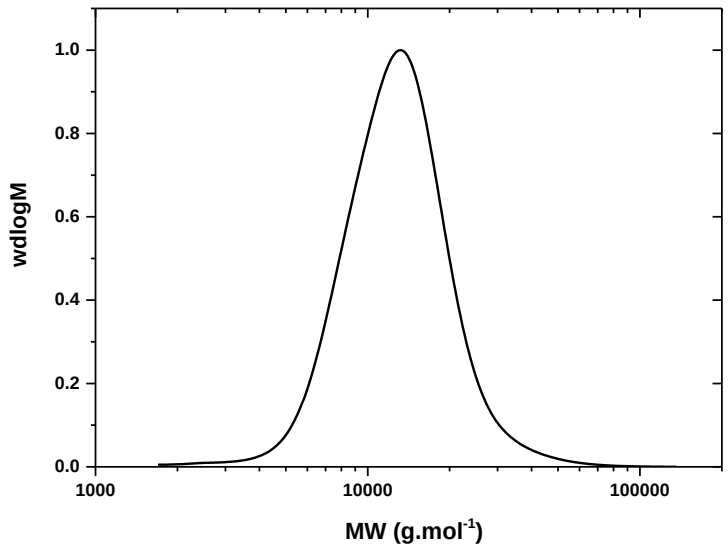

Figure 7.15: SEC analysis for the poly(AMPS)$_{20}$ macroinitiator utilising aqueous Cu(0)-mediated RDRP. Initial conditions: [AMPS]:[I]:[CuBr]:[Me$_6$-Tren] = [20]:[1]:[0.4]:[0.4].

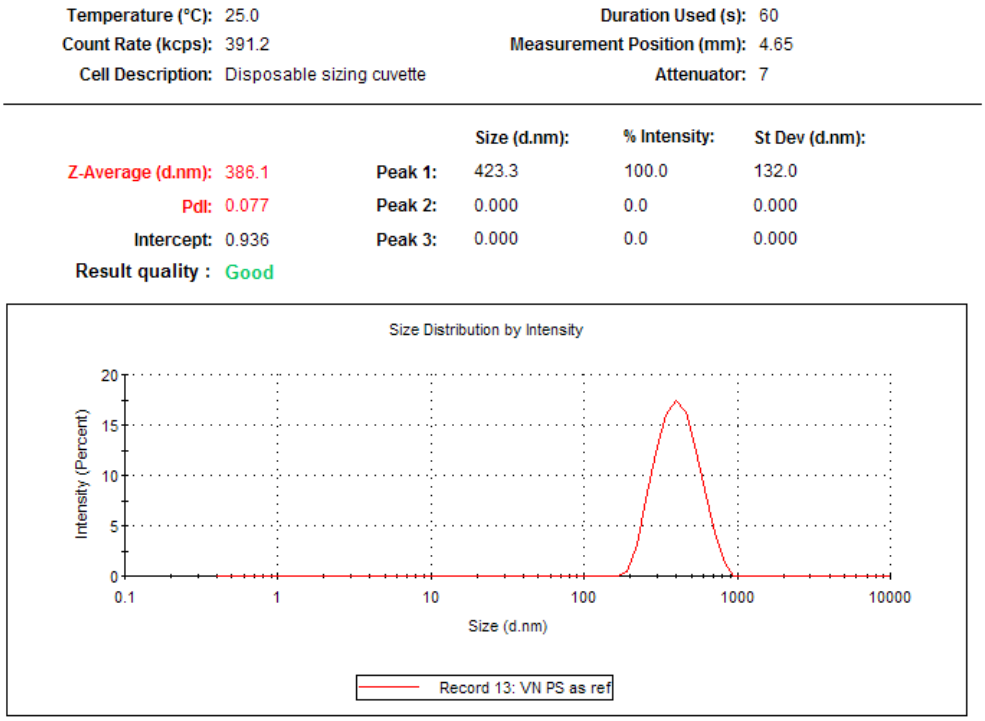

Figure 7.16: Particle size and size distribution of poly(AMPS)$_{20}$-*b*-poly(NIPAm)$_{20}$ at 25^{o}C *via* DLS (1 g/ml solution in DMF/H$_2$O 90% *v/v*).

7.5 References

1. A. Anastasaki, V. Nikolaou, A. Simula, J. Godfrey, M. Li, G. Nurumbetov, P. Wilson and D. M. Haddleton, *Macromolecules*, 2014, **47**, 3852-3859.

2. W. Gu, Z. Jia, N. P. Truong, I. Prasadam, Y. Xiao and M. J. Monteiro, *Biomacromolecules*, 2013, **14**, 3386-3389.

3. M. J. Caulfield, G. G. Qiao and D. H. Solomon, *Chem. Rev.*, 2002, **102**, 3067-3084.

4. T. Marshall and K. M. Williams, *Electrophoresis*, 1991, **12**, 461-471.

5. L. P. Krul', T. A. Ivanova, L. B. Yakimtsova and E. V. Grinyuk, *Russ. J. App. Chem.*, 2005, **78**, 839-842.

6. H. Kaşgöz, S. Özgümüş and M. Orbay, *Polymer*, 2003, **44**, 1785-1793.

7. E. C. Muniz and G. Geuskens, *Macromolecules*, 2001, **34**, 4480-4484.

8. J. Travas-Sejdic and A. Easteal, *J. Appl. Polym. Sci.*, 2000, **75**, 619-628.

9. D. Melekaslan and O. Okay, *Polymer*, 2000, **41**, 5737-5747.

10. F. Maggi, S. Ciccarelli, M. Diociaiuti, S. Casciardi and G. Masci, *Biomacromolecules*, 2011, **12**, 3499-3507.

11. R. Fei, J. T. George, J. Park, A. K. Means and M. A. Grunlan, *Soft Matter*, 2013, **9**, 2912-2919.

12. G. Masci, M. Diociaiuti and V. Crescenzi, *J. Polym. Sci. Part A: Polym. Chem.*, 2008, **46**, 4830-4842.

13. S.-I. Yusa, M. Shibata, M. Noborizato and P. Bahadur, *J. Dispersion Sci. Technol.*, 2011, **33**, 287-292.

14. B. S. Sumerlin, M. S. Donovan, Y. Mitsukami, A. B. Lowe and C. L. McCormick, *Macromolecules*, 2001, **34**, 6561-6564.

15. G. Masci, L. Giacomelli and V. Crescenzi, *J. Polym. Sci. Part A: Polym. Chem.*, 2005, **43**, 4446-4454.

16. E. Simò-Alfonso, C. Gelfi, M. Lucisano and P. G. Righetti, *J. Chromatogr. A*, 1996, **756**, 255-261.

17. M. N. Albarghouthi, B. A. Buchholz, P. J. Huiberts, T. M. Stein and A. E. Barron, *Electrophoresis*, 2002, **23**, 1429-1440.

18. M. N. Albarghouthi, T. M. Stein and A. E. Barron, *Electrophoresis*, 2003, **24**, 1166-1175.

19. T. Tanigami, H. Iwata and T. Mori, *J. Appl. Polym. Sci.*, 2007, **103**, 2788-2796.

20. N. P. Truong, M. V. Dussert, M. R. Whittaker, J. F. Quinn and T. P. Davis, *Polym. Chem.*, 2015, **6**, 3865-3874.

21. C. Zhao, Q. Chen, K. Patel, L. Li, X. Li, Q. Wang, G. Zhang and J. Zheng, *Soft Matter*, 2012, **8**, 7848-7857.

22. G. Fundueanu, M. Constantin, I. Asmarandei, S. Bucatariu, V. Harabagiu, P. Ascenzi and B. C. Simionescu, *Eur. J. Pharm. Biopharm.*, 2013, **85**, 614-623.

23. C. Zhao, K. Patel, L. M. Aichinger, Z. Liu, R. Hu, H. Chen, X. Li, L. Li, G. Zhang, Y. Chang and J. Zheng, *RSC Advances*, 2013, **3**, 19991-20000.

24. A. Narumi, Y. Chen, M. Sone, K. Fuchise, R. Sakai, T. Satoh, Q. Duan, S. Kawaguchi and T. Kakuchi, *Macromol. Chem. Phys.*, 2009, **210**, 349-358.

25. V. Percec, T. Guliashvili, J. S. Ladislaw, A. Wistrand, A. Stjerndahl, M. J. Sienkowska, M. J. Monteiro and S. Sahoo, *J. Am. Chem. Soc.*, 2006, **128**, 14156-14165.

26. B. M. Rosen and V. Percec, *Chem. Rev.*, 2009, **109**, 5069-5119.

27. A. Anastasaki, V. Nikolaou, G. Nurumbetov, P. Wilson, K. Kempe, J. F. Quinn, T. P. Davis, M. R. Whittaker and D. M. Haddleton, *Chem. Rev.*, 2015.

28. Q. Zhang, P. Wilson, Z. Li, R. McHale, J. Godfrey, A. Anastasaki, C. Waldron and D. M. Haddleton, *J. Am. Chem. Soc.*, 2013, **135**, 7355-7363.

29. D. Konkolewicz, Y. Wang, P. Krys, M. Zhong, A. A. Isse, A. Gennaro and K. Matyjaszewski, *Polym. Chem.*, 2014, **5**, 4396-4417.

30. F. Alsubaie, A. Anastasaki, V. Nikolaou, A. Simula, G. Nurumbetov, P. Wilson, K. Kempe and D. M. Haddleton, *Macromolecules*, 2015, **48**, 5517-5525.

31. S. R. Samanta, V. Nikolaou, S. Keller, M. J. Monteiro, D. A. Wilson, D. M. Haddleton and V. Percec, *Polym. Chem.*, 2015, **6**, 2084-2097.

32. A. Simula, V. Nikolaou, F. Alsubaie, A. Anastasaki and D. M. Haddleton, *Polym. Chem.*, 2015, **6**, 5940-5950.

33. N. H. Nguyen, X. Leng, H.-J. Sun and V. Percec, *J. Polym. Sci. Part A: Polym. Chem.*, 2013, **51**, 3110-3122.

34. N. H. Nguyen, J. Kulis, H.-J. Sun, Z. Jia, B. van Beusekom, M. E. Levere, D. A. Wilson, M. J. Monteiro and V. Percec, *Polym. Chem.*, 2013, **4**, 144-155.

35. P. Wilson, A. Anastasaki, M. R. Owen, K. Kempe, D. M. Haddleton, S. K. Mann, A. P. R. Johnston, J. F. Quinn, M. R. Whittaker, P. J. Hogg and T. P. Davis, *J. Am. Chem. Soc.*, 2015, **137**,4215-4222.

36. A. Simula, V. Nikolaou, A. Anastasaki, F. Alsubaie, G. Nurumbetov, P. Wilson, K. Kempe and D. M. Haddleton, *Polym. Chem.*, 2015, **6**, 2226-2233.

37. A. Anastasaki, A. J. Haddleton, Q. Zhang, A. Simula, M. Droesbeke, P. Wilson and D. M. Haddleton, *Macromol. Rapid Commun.*, 2014, **35**, 965-970.

38. W. Ding, C. Lv, Y. Sun, X. Liu, T. Yu, G. Qu and H. Luan, *J. Polym. Sci. Part A: Polym. Chem.*, 2011, **49**, 432-440.

39. F. Alsubaie, A. Anastasaki, P. Wilson and D. M. Haddleton, *Polym. Chem.*, 2015, **6**, 5940-5950.

40. N. H. Nguyen, C. Rodriguez-Emmenegger, E. Brynda, Z. Sedlakova and V. Percec, *Polym. Chem.*, 2013, **4**, 2424-2427.

41. M. Vorobii, A. de los Santos Pereira, O. Pop-Georgievski, N. Y. Kostina, C. Rodriguez-Emmenegger and V. Percec, *Polym. Chem.*, 2015, **6**, 4210-4220.

42. Q. Zhang, P. Wilson, A. Anastasaki, R. McHale and D. M. Haddleton, *ACS Macro Lett.*, 2014, **3**, 491-495.

43. Q. Zhang, Z. Li, P. Wilson and D. M. Haddleton, *Chem. Commun.*, 2013, **49**, 6608-6610.

44. C. Waldron, Q. Zhang, Z. Li, V. Nikolaou, G. Nurumbetov, J. Godfrey, R. McHale, G. Yilmaz, R. K. Randev, M. Girault, K. McEwan, D. M. Haddleton, M. Droesbeke, A. J. Haddleton, P. Wilson, A. Simula, J. Collins, D. J. Lloyd, J. A. Burns, C. Summers, C. Houben, A. Anastasaki, M. Li, C. R. Becer, J. K. Ki*via*ho and N. Risangud, *Polym. Chem.*, 2014, **5**, 57-61.

45. S. Perrier, S. P. Armes, X. S. Wang, F. Malet and D. M. Haddleton, *J. Polym. Sci. Part A: Polym. Chem.*, 2001, **39**, 1696-1707.

46. M. Ciampolini and N. Nardi, *Inorg. Chem.*, 1966, **5**, 41-44.

Synthesis of semifluorinated block copolymers *via* Cu(II)-mediated photo-induced RDRP on a multigram scale: Industrial applications & future perspectives

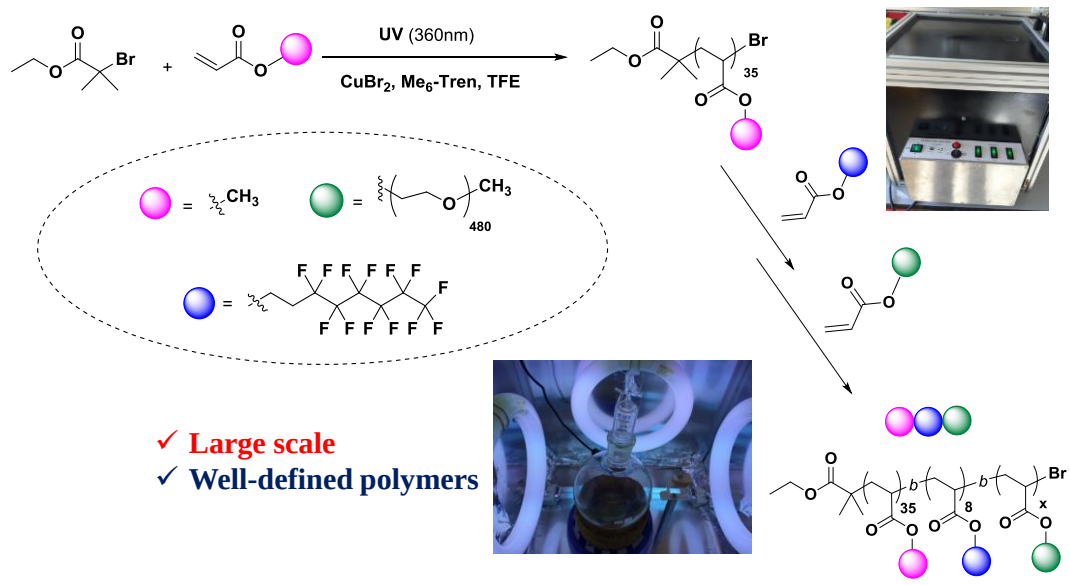

✓ **Large scale**
✓ **Well-defined polymers**

8.1 Introduction

Sequence specific polymers are of interest for diverse applications as they allow for the precise control of functional group location relative to a surface and can incorporate various functionalities along the polymer backbone. Specifically semifluorinated block copolymers possess unique properties allowing for excellent phase separation including very low surface energy, oil/water repellence and therefore they can be utilised in various applications (*e.g.* surfactants for polyurethane foams, antifouling coatings *etc.*).[1]

Various polymerisation protocols have been employed for the synthesis of semifluorinated block copolymers including cationic,[2] anionic[3] and RDRP.[1, 4] Previous studies have already shown that the Cu(II)-mediated photo-induced system offers a versatile and inexpensive platform for the preparation of high-order multiblock functional materials with additional applications arising from the precise spatiotemporal "on/off" control and resolution when desired.[5, 6] In previous chapters it has been shown that both mono and bi-functional initiators have been employed for their synthesis comprising of four alternating acrylic monomer sequences. Remarkable degree of control was obtained in all cases with quantitative or near-quantitative conversions achieved between the iterative monomer additions.

Lubrizol as sponsors of this work had a request for a sequence specific semifluorinated triblock copolymer for use as a modifier for a thermoplastic elastomer polyurethane. They had carried out work on a statistical ter-copolymer used as an additive in extrusion of the thermoplastic elastomer. The low molecular weight ter-polymer had been shown to end up at the surface resulting in reduced protein fouling of catheters made by this process. The hypothesis put to us that block

copolymers to similar overall composition should migrate more efficiently and that all polymers should be able to contribute to this effect. Thus we utilised the photo-induced system in an attempt to improve the performance.The main focus of this chapter is to describe these initial studies for the synthesis of semifluorinated triblock copolymers in a range of compositions and to set the scene for future work. It is noted that this is an ongoing project funded from the Lubrizol Corporation, the applications of which will not be further discussed. Nevertheless, the optimised conditions to facilate the synthesis of these complex and demanding structures will be developed and identified, including the screening of various solvents and the synthesis of the materials on a multigram scale (100-200 g), capable to afford subsequent industrial testing.

8.2 Initial Results

Initially, 2,2,2-trifluoroethyl acrylate (TFEA) was employed as a model monomer to test the compatibility of this monomeric family with the Cu-mediated photo-induced system. Utilising previously optimised conditions (initial feed [EBiB]:[$CuBr_2$]:[Me_6-Tren]=[1]:[0.02]:[0.12]) the synthesis of the triblock copolymer (PMA_{20}-*b*-$PTFEA_{20}$-*b*-$PPEGA_{10}$) was attempted. The PMA block was obtained at full conversion within 10 h with a dispersity of 1.12. Upon addition of the second monomer (TFEA) in DMSO (2 : 1 *v/v*), high monomer conversion was also attained within 12 h with the SEC analysis to revealing a clear shift to higher molecular weights confirming the successful chain extension. The same process was repeated for the addition of the final monomer (PEGA) yielding the desired triblock copolymer. Although longer reaction times were required to reach full monomer

conversion in the final cycle, >99% in 24 h, the low dispersity was maintained (*Đ* ~ 1.16) (Table 8.1, Figure 8.1).

Table 8.1: Characterisation data for the synthesis of the triblock copolymer in DMSO Initial conditions: [MA]:[EBiB]:[$CuBr_2$]:[Me_6-Tren] = [20]:[1]:[0.02]:[0.12].

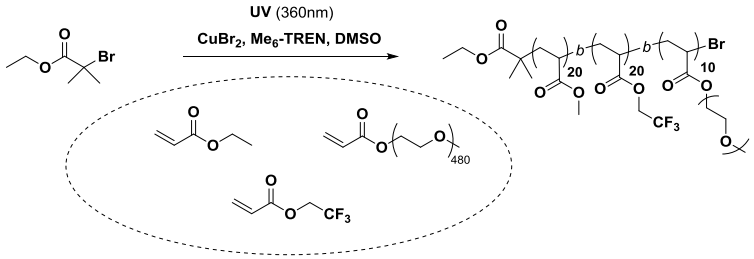

Triblock composition	Time (h)	Conv. (%)	$M_{n,th}$ (g.mol^{-1})	$M_{n,SEC}$ (g.mol^{-1})	*Đ*
PMA_{20}	8	100	2000	2400	1.12
PMA_{20}-*b*-$PTFEA_{20}$	17	98	4900	5000	1.18
PMA_{20}-*b*-$PTFEA_{20}$-*b*-$PPEGA_{10}$	24	99	9700	14000	1.16

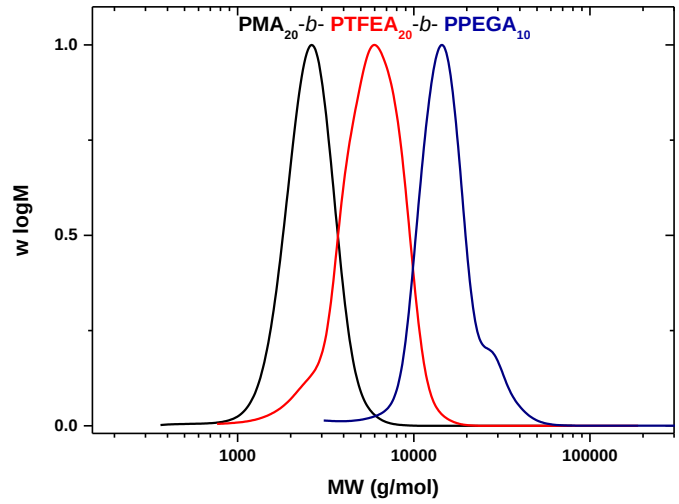

Figure 8.1: SEC analysis for successive cycles during synthesis of the triblock copolymer in DMSO. Initial conditions: [MA]:[EBiB]:[$CuBr_2$]:[Me_6-Tren] = [20]:[1]:[0.02]:[0.12].

Encouraged by this successful synthesis of the triblock copolymer utilising TFEA, we subsequently employed the same procedure for the polymerisation of

PFOA. However, since the monomer was not soluble in the typical solvent employed (DMSO), a short solvent screening was conducted to find an alternative choice. Homopolymerisation of PFOA was attempted in a range of solvents including DMF, TFE and mixtures of toluene with MeOH and IPA which have already proved to be compatible with this system.[7] Among all the solvents tested, TFE was found to be the only one to solubilise both the monomer and the polymer whilst in all other cases the polymer was precipitated during the reaction. Nevertheless, since the aim of this work is not the homopolymerisation of PFOA but the synthesis of triblock copolymers that bear this moiety, the use of alternative solvents (*e.g.* DMF) is possible just by tuning the length of the other two blocks (MA, PEGA) which make the technique more attractive for applications where the use of fluorinated solvents is undesirable. However for simplicity, TFE was utilised for all the polymers presented in this work to avoid precipitation issues.

The synthesis of the PMA_{25}-*b*-$PPFOA_8$-*b*-$PPEGA_{10}$ employing TFE was investigated. Despite the inclusion of a long chain semifluorinated monomer the dispersity of the final polymer was not compromised and remained low ($Đ$ = 1.12) achieving at the same time quantitative conversions in each monomer addition (> 99%). In an attempt to further demonstrate the versatility of the technique an altered sequence was also endeavoured (PMA_{25}-*b*-$PPEGA_{10}$-$PPFOA_8$). Positioning of the fluorinated groups in the middle of a chain as opposed to chain ends have been reported to result in changes in the conformation of the chain.[8] Equally well-defined polymers were obtained presenting narrow MWD (> 99%, $Đ$ = 1.18) and good agreement between theoretical and experimental molecular weights in a total of 24 h (Table 8.2, Figure 8.2).

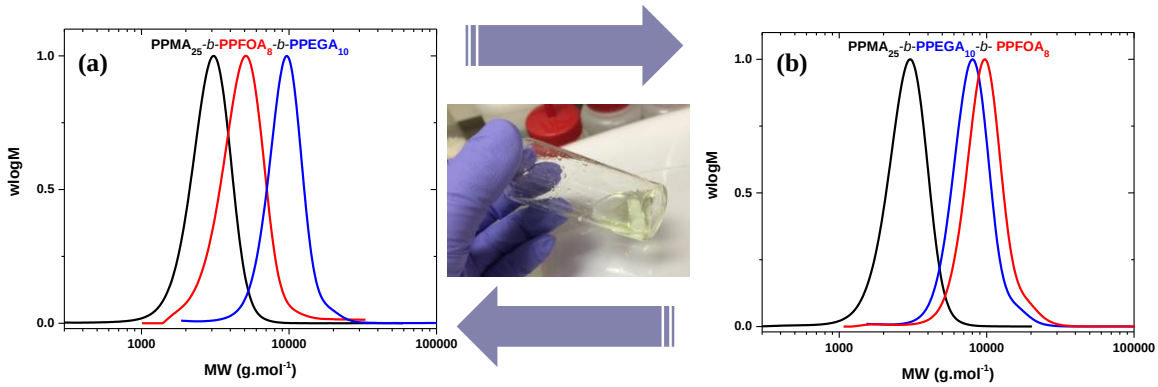

Figure 8.2: SEC analysis for the successive cycles during synthesis of (a) PMA_{25}-*b*-$PPFOA_8$-*b*-$PPEGA_{10}$ and (b) PMA_{25}-*b*-$PPEGA_{10}$-$PPFOA_8$. Initial feed [MA]:[EBiB]:[$CuBr_2$]:[Me_6-Tren] = [25]:[1]:[0.02]:[0.12] in TFE.

Table 8.2: Characterisation data for the synthesis of the triblock copolymers in TFE.

Triblock copolymer	Time (h)	Conv. (%)	$M_{n,th}$ (g.mol^{-1})	$M_{n,SEC}$ (g.mol^{-1})	$Đ$
PMA_{25}-*b*-$PPFOA_8$-*b*-$PPEGA_{10}$	10	99	2300	2700	1.12
	12	99	4600	4500	1.18
	24	99	9400	8800	1.12
PMA_{25}-*b*- $PPEGA_{10}$-*b*- $PPFOA_8$	10	100	2300	2700	1.16
	12	99	7100	7300	1.16
	24	100	9400	9200	1.18

Finally, different compositions of the desired triblock copolymer PMA_{35}-*b*-$PPFOA_8$-*b*-$PPEGA_x$ were targeted varying the hydrophilic part (PEG) of the block from *DP*=5 to *DP*=14. It should be noted that the synthesis was conducted in large scales (100 - 200 g) in a homemade UV box to facilitate industrial testing (Figure 8.3). Nevertheless, narrow MWDs (~1.16) along with high conversions (>95%) were observed during each iterative monomer addition as indicated by ^{1}H NMR and SEC analyses (Table 8.3, Figure 8.4, Section 8.4.4 Tables 8.4-8.6, Figures 8.5 & 8.6).

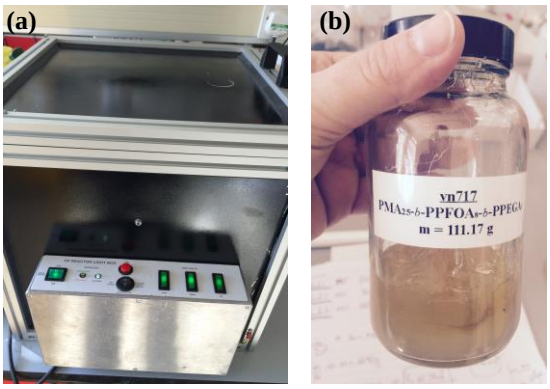

Figure 8.3: (a) UV homemade light box utilised and (b) synthesised triblock copolymer in a large scale.

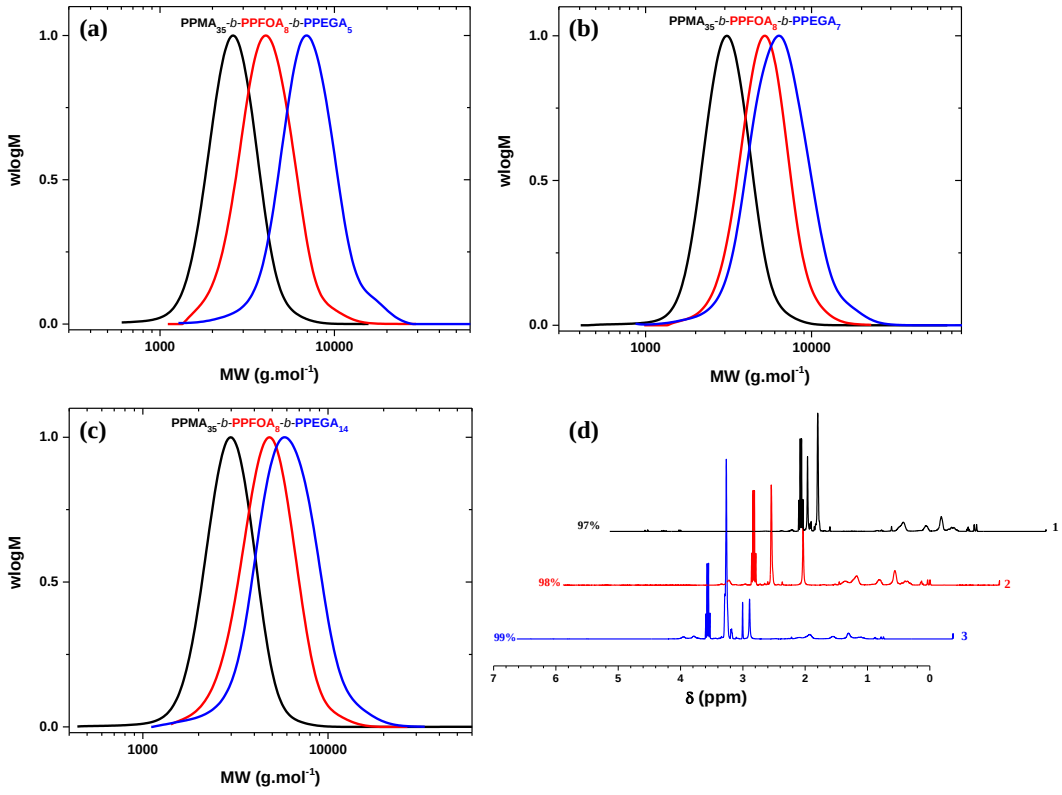

Figure 8.4: SEC analysis of the synthesis of (a) PMA_{35}-*b*-$PPFOA_8$-*b*-$PPEGA_5$, (b) PMA_{35}-*b*-$PPFOA_8$-*b*-$PPEGA_7$ and (c),(d) SEC analysis and ^1H NMR of PMA_{35}-*b*-$PPFOA_8$-*b*-$PPEGA_{14}$.

Table 8.3: Characterisation data for the final cycle of the various triblock copolymers.

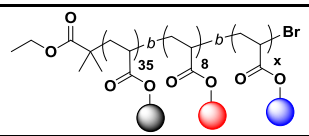	**Time (h)**	**Conv. (%)**	$M_{n,th}$ **(g.mol^{-1})**	$M_{n,NMR}$ **(g.mol^{-1})**	$M_{n,SEC}$ **(g.mol^{-1})**	$Đ$
x= 5	24	99	8700	8700	7000	1.18
x=7	24	98	9500	9200	6300	1.18
x=14	24	99	12900	11600	6600	1.16

8.3 Conclusions & future work

This chapter is an ongoing work in collaboration with the Lubrizol Corporation and therefore only a few initial findings are presented and discussed. Further characterisations and initial testing for the synthesised triblock copolymers are currently carried out in the Lubrizol site. Moreover statistical block copolymers and blends of these monomers need to be synthesised and tested to explore the importance of the controlled sequence. However, it was already manifested that the Cu(II)-mediated photo-induced RDRP system can be employed for the synthesis of multiblock copolymers bearing both hydrophilic and hydrophobic moieties giving access to a wide range of applications thus paving the way for the synthesis of "smart" materials.

8.4 Experimental

8.4.1 Materials and Methods

All materials were purchased from Sigma Aldrich or Du Pont unless otherwise stated. $CuBr_2$ and EBiB were used as received. PFOA was provided from Lubrizol and was passed through a basic Al_2O_3 chromatography column prior to use. Me_6-Tren was synthesised according to previously reported literature.

8.4.2 Instrumentation

^1H NMR spectra were recorded on Bruker DPX-250 or DPX-300 spectrometers using deuterated chloroform ($CDCl_3$) obtained from Aldrich. Chemical shifts are given in ppm downfield from the internal standard tetramethylsilane. Size exclusion chromatography (SEC) measurements were conducted using an Agilent 1260 SEC-MDS fitted with differential refractive index (DRI), light scattering (LS) and viscometry (VS) detectors equipped with 2 × PLgel 5 mm mixed-D columns (300 × 7.5 mm), 1 × PLgel 5 mm guard column (50 × 7.5 mm) and autosampler. Narrow linear poly(methyl methacrylate) standards in range of 200 to 1.0×10^6 $g.mol^{-1}$ were used to calibrate the system. All samples were passed through a 0.45 μm PTFE filter before analysis. The mobile phase was chloroform with 2% triethylamine eluent at a flow rate of 1.0 mL/min. SEC data was analysed using Cirrus v3.3 software with calibration curves produced using Varian Polymer laboratories Easi-Vials linear poly(methyl methacrylate) standards (200-4.7×10^5 $g.mol^{-1}$). The source of UV light was a homemade UV light box (λ_{max} ~ 360 nm) equipped with four 9W bulbs.

8.4.3 General procedures

Filtered monomer (*DP* equiv.), EBiB (1 equiv.), $CuBr_2$ (0.02 equiv.), Me_6-Tren (0.12 equiv.) and solvent (1:1 in respect to the monomer) were added to a septum-sealed vial and degassed by purging with nitrogen for 15 min. Polymerisation commenced upon addition of the degassed reaction mixture to the UV lamp. Samples were taken periodically and conversions were measured using ^{1}H NMR and SEC analysis. For the iterative chain extensions, an aliquot of a degassed monomer (*DP* equiv.), in solvent (50% *v/v*) was added *via* a nitrogen-purged syringe and again the solution was allowed to polymerise in the lamp. Purification was achieved *via* dialysis against water or methanol (depending on the hydrophilic chain length) and the final polymer was obtained after freeze drying.

8.4.4 Additional characterisation

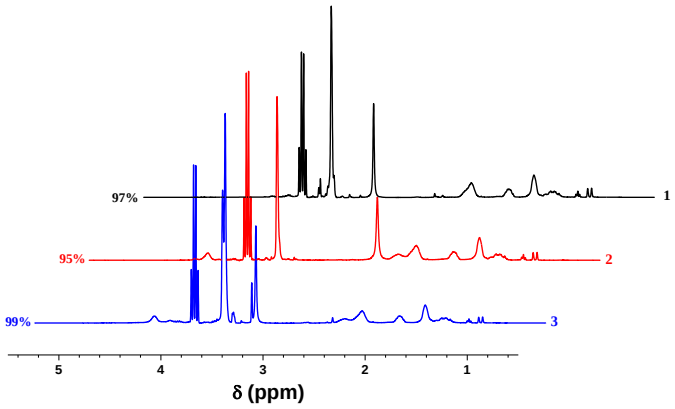

Figure 8.5: ^{1}H NMR for the monomer conversion for each cycle during the synthesis of the triblock copolymer PMA_{35}-*b*-$PPFOAA_8$-*b*-$PPEGA_5$.

Table 8.4: Characterisation data for the triblock copolymer PMA_{35}-*b*-$PPFOAA_8$-*b*-$PPEGA_5$.

Triblock composition	Time (h)	Conv. (%)	$M_{n,th}$ (g.mol^{-1})	$M_{n,SEC}$ (g.mol^{-1})	$Đ$
PMA_{35}	10	97	3100	2800	1.10
PMA_{35}-*b*-$PPFOA_8$	14	95	6400	4400	1.14
PMA_{35}-*b*-$PPFOAA_8$-*b*-$PPEGA_5$	24	99	8700	7000	1.18

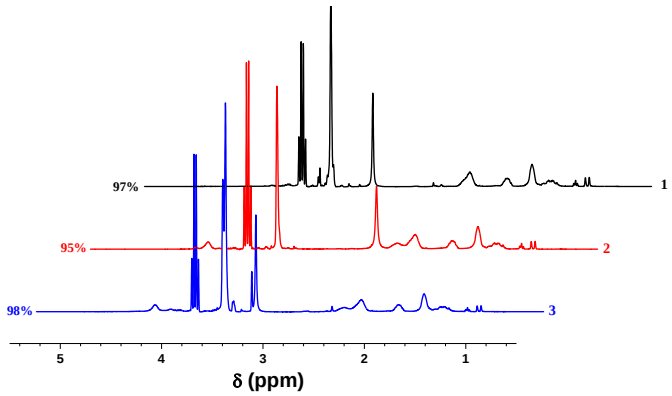

Figure 8.6: ^{1}H NMR for the monomer conversion for each cycle during the synthesis of the triblock copolymer PMA_{35}-*b*-$PPFOAA_8$-*b*-$PPEGA_7$.

Table 8.5: Characterisation data for the triblock copolymer PMA_{35}-*b*-$PPFOAA_8$-*b*-$PPEGA_7$.

Triblock composition	Time (h)	Conv. (%)	$M_{n,th}$ (g.mol^{-1})	$M_{n,SEC}$ (g.mol^{-1})	$Đ$
PMA_{35}	10	97	3100	3100	1.12
PMA_{35}-*b*-$PPFOA_8$	14	95	6100	4800	1.13
PMA_{35}-*b*-$PPFOAA_8$-*b*-$PPEGA_7$	24	98	9500	6300	1.18

Table 8.6: Characterisation data for the triblock copolymer PMA_{35}-*b*-$PPFOAA_8$-*b*-$PPEGA_{14}$.

Triblock composition	Time (h)	Conv. (%)	$M_{n,th}$ (g.mol^{-1})	$M_{n,SEC}$ (g.mol^{-1})	$Đ$
PMA_{35}	10	97	3100	2400	1.11
PMA_{35}-*b*-$PPFOA_8$	14	98	6300	3800	1.14
PMA_{35}-*b*-$PPFOAA_8$-*b*-$PPEGA_{14}$	24	99	12900	6600	1.16

8.5 References

1. K. T. Lim, M. Y. Lee, M. J. Moon, G. D. Lee, S.-S. Hong, J. L. Dickson and K. P. Johnston, *Polymer*, 2002, **43**, 7043-7049.

2. V. Percec and M. Lee, *J. Macromol. Sci. Pure Appl. Chem.*, 1992, **29**, 723-740.

3. D. R. Iyengar, S. M. Perutz, C.-A. Dai, C. K. Ober and E. J. Kramer, *Macromolecules*, 1996, **29**, 1229-1234.

4. D. E. Betts, T. Johnson, D. LeRoux and J. M. DeSimone, *ACS Symp. Ser.*, 1998, **685**, 418-432.

5. A. Anastasaki, V. Nikolaou, G. S. Pappas, Q. Zhang, C. Wan, P. Wilson, T. P. Davis, M. R. Whittaker and D. M. Haddleton, *Chem. Sci.*, 2014, **5**, 3536-3542.

6. A. Anastasaki, V. Nikolaou, N. W. McCaul, A. Simula, J. Godfrey, C. Waldron, P. Wilson, K. Kempe and D. M. Haddleton, *Macromolecules*, 2015, **48**, 1404-1411.

7. A. Anastasaki, V. Nikolaou, A. Simula, J. Godfrey, M. Li, G. Nurumbetov, P. Wilson and D. M. Haddleton, *Macromolecules*, 2014, **47**, 3852-3859.

8. W. van Zoelen, R. N. Zuckermann and R. A. Segalman, *Macromolecules*, 2012, **45**, 7072-7082.

Chapter 9

Conclusions & Outlook

The main focus of this thesis was to expand the scope of the newly developed copper-mediated photo-induced RDRP system. The synthesis of *α,ω*-telechelic multiblock copolymers was initially attempted utilising a wide range of bi-functional initiators and acrylic monomers. When low temperatures were employed (15 °C), well-defined tricosablock copolymer ($Đ$ = 1.18, M_n = 9500 g.mol^{-1}, DP ~ 2 per block) and a high molecular weight undecablock copolymer ($Đ$ = 1.22, M_n = 150000 g.mol^{-1}) were obtained which represent the highest number of blocks and the highest molecular weight multiblock respectively to date.

The compatibility of this system with ILs as solvents and a non-toxic food supplement as the catalyst were also investigated presenting good control over the MWDs and high end-group fidelity, as evidenced by both ^{1}H NMR and MALDI-ToF-MS analysis. Specifically, ILs presented fast polymerisation rates, attaining quantitative conversions (> 98%) in 30 min or less. Moreover, the combination of ppm concentrations of catalyst *via* this photo-induced polymerisation protocol with the recyclability of the IL/catalyst solution significantly contributes to the reduction of polymerisation cost and thus paves the way for the inexpensive synthesis of well-defined materials.

Importantly, the main limitations of this technique were highlighted and a novel discrete complex that incorporates both catalyst and ligand was synthesised to circumvent the aforementioned issues demonstrating excellent degrees of control, as

exemplified by the low dispersities ($Đ$ ~ 1.10), high end-group fidelity (~ 99%) and the near-quantitative conversions within 2 h (> 95%). Additionally the scope of this protocol was subsequently expanded to include a range of hydrophilic, hydrophobic and functional acrylates along with various solvents and solvent mixtures. Importantly, an alternative complex that contained PMDETA as the ligand was also synthesised highlighting the potential of simple and cost effective complexes to be used for copper mediated processes in numerous applications, including synthesis of these materials in an industrial level.

Since the light system proved to be incompatible with acrylamides, aqueous Cu(0)-mediated RDRP was employed for their controlled polymerisation. Specifically, the polymerisation of HEAm and AMPS in aqueous media was exploited and a wide range of molecular weights have been targeted for both monomers and the end-group fidelity was exemplified by *in situ* chain extensions and block copolymerisation, without further purification steps prior to the addition of the second aliquot in both cases.

Finally, the synthesis of semifluorinated triblock copolymers utilising the photo-induced RDRP was described. Only a few initial studies were demonstrated including solvent screening and the synthesis of these materials on a multigram scale and more results are yet to come. Nevertheless, well-defined polymers with potential applications capable to afford subsequent industrial testing were synthesised by this protocol.

The current status of the art for copper mediated RDRP allows for the synthesis of well-defined poly(acrylates) and poly(acrylamides) with excellent end-group fidelity capable of undergoing multiple chain extensions. However, similar

end-group fidelity for poly(methacrylates) has not yet demonstrated and significantly slower polymerisation rates are reported, highlighting the direction of future studies. In addition, further research should be conducted to investigate the effect of sequence-controlled polymers in both materials and biological applications.